

**Advancing hydrological modeling for understanding drought dynamics in the Ebro river basin. The role of Land Surface Models in coupled natural-human systems**

**Omar Cenobio Cruz**

<http://hdl.handle.net/10803/689450>

Data de defensa: 21-11-2023

**ADVERTIMENT.** L'accés als continguts d'aquesta tesi queda condicionat a l'acceptació de les condicions d'ús establertes per la següent llicència Creative Commons: [Llicència CC Reconeixement - NoComercial \(by-nc\)](#)

**ADVERTENCIA.** El acceso a los contenidos de esta tesis queda condicionado a la aceptación de las condiciones de uso establecidas por la siguiente licencia Creative Commons: [Licencia CC Atribución - NoComercial \(by-nc\)](#)

**WARNING.** The access to the contents of this doctoral thesis it is limited to the acceptance of the use conditions set by the following Creative Commons license: [License CC Attribution - NonCommercial \(by-nc\)](#)

## DOCTORAL THESIS

Title	Advancing hydrological modeling for understanding drought dynamics in the Ebro river basin. The role of Land Surface Models in coupled natural-human systems.
Presented by	Omar Cenobio Cruz
Centre	Ebro Observatory University Institute
Department	Geophysics
Directed by	Dr. Pere Quintana Seguí Dr. Luis Garrote

This Ph.D. research was made possible through the financial support of the HUMID project (CGL2017-85687-R, AEI/FEDER, UE), the predoctoral grant PRE2018-085027 (AEI/FSE), and the IDEWA project (PRIMA PCI2020-112043 / AEI / 10.13039/501100011033).

---

*Water does not resist. Water flows. When you plunge your hand into it, all you feel is a caress. Water is not a solid wall; it will not stop you. But water always goes where it wants to go, and nothing, in the end, can stand against it. Water is patient. Dripping water wears away a stone. Remember that my child. Remember you are half water. If you can't go through an obstacle, go around it. Water does.*

*M. Atwood, The Penelopiad*

---

---

---

---

## Abstract

Droughts are a complex and multidimensional phenomenon described in simple terms as sustained periods of water deficit compared to normal conditions. While global in nature, their most severe consequences are observed in arid or semi-arid regions, such as the Iberian Peninsula. However, these hydrological extremes are not solely driven by natural processes. Human activities, including dam construction, groundwater abstractions, and irrigation practices, have significantly altered the natural water flow, leading to the current era being labeled the Anthropocene. This highlights the critical importance of water resources management in regions already facing variable and limited water availability. Consequently, there is a growing need for methodologies that accurately represent the hydrological response of basins in coupled natural-human systems, especially during low flow periods, to effectively manage water resources.

Modeling is an adequate tool used in water management to address the challenges of managing scarce water resources and mitigating the impacts of climate change on the water cycle. In this research, various approaches are applied to improve hydrological simulations using the physically based and spatially distributed hydrometeorological platform SASER (SAFRAN-SURFEX-Eaudyssée-Rapid). These approaches aim to enhance the representation of hydrological processes, particularly for low flows, and incorporate human water management considerations.

This document presents two interrelated works. First, improvements have been implemented in the SASER model in order to improve its performance. Second, a dam model has been implemented, which is forced by both observations and the SASER model to study the impacts of dams in droughts. This work has been implemented in an area encompassing the Pyrenean domain, including the Ebro basin, basins flowing to the Bay of Biscay, the Catalan and some Languedocian basins, and the Adour-Garonne basins, but these methodologies can be applied anywhere.

Adequate input-forcing data with appropriate spatial and temporal resolution are essential for obtaining accurate and reliable results from Land Surface Models (LSMs). To this end, a novel linear correction method in precipitation forcing that leverages regional climate model (RCM) data was introduced. By utilizing a weekly correction window, the method better captures the temporal variability and patterns in precipitation, resulting in a more realistic portrayal of precipitation events in statistical terms. The impact on simulated runoff aligns with expectations, while changes in drainage and evapotranspiration are influenced by various factors, including climate regime and response in wet climates.

Additionally, the default SASER model exhibited a negative bias in low flows, which is problematic in drought studies. The cause of this bias in the low flows is the lack of a groundwater scheme in the SASER model. The inclusion of a conceptual reservoir scheme to regulate drainage improved streamflow simulation, as evidenced by positive values in performance metrics. The implementation of the reservoir scheme was straightforward and effectively enhanced the

---

---

representation of low flows without compromising high flows. Moreover, a regionalization approach was implemented, allowing the integration of the conceptual reservoir as an external module in SURFEX. This approach facilitated the establishment of parameter relationships with climate and physiographic variables using a genetic algorithm, enabling the consideration of within-catchment variability across the study area. While the reservoir lacks a physical basis, it successfully links the new parameters with physical variables, striking a favorable balance between distributed modeling and physical representation. Furthermore, the regionalization approach extends the applicability of the reservoir beyond natural systems, encompassing both natural and human-influenced basins.

To incorporate human water management in the study, the area irrigated by the *Canal de Aragón y Cataluña* was chosen as a case study to apply a prototype dam module. This has been used in combination with the new SURFEX irrigation scheme, which allows us to estimate actual demands. This approach combines a reservoir operation model and the SURFEX irrigation scheme, accurately capturing drought dynamics. The new module effectively simulates storage and outflows, demonstrating good agreement with reference data. Furthermore, SURFEX's new irrigation scheme captures interannual water demand variability, leading to an improved representation of the system, allowing us to go further than the usual “climatological” demand tables used in such studies. The study reveals that human influences exacerbate hydrological drought but alleviate agronomical drought. Hydrological drought characteristics lengthen, and the timing of peak hydrological drought events shifts under human influences. Irrigation impacts both hydrological and agronomical droughts, emphasizing the need to consider these factors in drought management strategies. These findings enhance our understanding of the complex interactions between human activities, water resources, and drought dynamics.

In conclusion, this research significantly advances the representation of hydrological processes in a LSM-based model in a semi-arid region, sensitive to droughts, through the incorporation of various approaches and the development of a module to integrate the human factor. The improvements achieved in precipitation representation and hydrological modeling provide valuable insights into the complex dynamics of hydrological response and drought, encompassing both natural and anthropogenic influences. This work is a first step towards the integration of human influences, such as irrigation and reservoir operation, into the SASER platform, opening up new possibilities for studying drought dynamics and developing improved strategies for drought assessment and management in coupled natural-human systems.

---

## Resumen

Las sequías son un fenómeno complejo y multidimensional descrito en términos sencillos como periodos sostenidos de déficit hídrico en comparación con las condiciones normales. Aunque de carácter global, sus consecuencias más graves se observan en regiones áridas o semiáridas, como la Península Ibérica. Sin embargo, estos extremos hidrológicos no se deben únicamente a procesos naturales. Las actividades humanas, como la construcción de presas, las extracciones de aguas subterráneas y las prácticas de regadío, han alterado significativamente el flujo natural del agua, lo que ha llevado a la era actual a denominarse Antropoceno. Esto pone de relieve la importancia crítica de la gestión de los recursos hídricos en regiones que ya se enfrentan a una disponibilidad de agua variable y limitada. En consecuencia, existe una creciente necesidad de metodologías que representen con precisión la respuesta hidrológica de las cuencas en sistemas naturales-humanos acoplados, especialmente durante los periodos de caudales bajos, para gestionar eficazmente los recursos hídricos.

La modelización es una herramienta adecuada utilizada en la gestión del agua para afrontar los retos de gestionar unos recursos hídricos escasos y mitigar los impactos del cambio climático en el ciclo del agua. En esta investigación se aplican varios enfoques para mejorar las simulaciones hidrológicas utilizando la plataforma hidrometeorológica SASER (SAFRAN-SURFEX-Eaudyssée-Rapid), de base física y distribuida espacialmente. Estos enfoques tienen por objeto mejorar la representación de los procesos hidrológicos, en particular para los caudales bajos, e incorporar consideraciones relativas a la gestión humana del agua.

Este documento presenta dos trabajos interrelacionados. En primer lugar, se han introducido mejoras en el modelo SASER para mejorar su comportamiento. En segundo lugar, se ha implementado un modelo de presas, forzado tanto por las observaciones como por el modelo SASER, para estudiar los impactos de las presas en las sequías. Este trabajo se ha llevado a cabo en una zona que abarca el dominio pirenaico, incluyendo la cuenca del Ebro, las cuencas que fluyen hacia el Golfo de Vizcaya, las cuencas catalanas y algunas languedocianas, y las cuencas Adour-Garonne, pero estas metodologías pueden aplicarse en cualquier lugar.

Para obtener resultados precisos y fiables de los modelos de superficie terrestre (LSM, en inglés) es esencial disponer de datos de forzamiento de entrada adecuados con una resolución espacial y temporal apropiada. Con este fin, se ha introducido un nuevo método de corrección lineal del forzamiento de las precipitaciones que aprovecha los datos de los modelos climáticos regionales (RCM). Al utilizar una ventana de corrección semanal, el método capta mejor la variabilidad temporal y los patrones de precipitación, lo que resulta en una representación más realista de los eventos de precipitación en términos estadísticos. El impacto en la escorrentía simulada se ajusta a las expectativas, mientras que los cambios en el drenaje y la evapotranspiración están influidos por diversos factores, entre ellos el régimen climático y la respuesta en climas húmedos.

Además, el modelo SASER por defecto presentaba un sesgo negativo en los caudales bajos, lo que resulta problemático en los estudios sobre la sequía. La causa de este sesgo en los caudales bajos es la falta de un esquema de aguas subterráneas en el modelo SASER. La inclusión de un



---

esquema conceptual de embalses para regular el drenaje mejoró la simulación de los caudales, como demuestran los valores positivos en las métricas de rendimiento. La aplicación del esquema de embalses fue sencilla y mejoró eficazmente la representación de los caudales bajos sin comprometer los caudales altos. Además, se aplicó un enfoque de regionalización que permitió la integración del embalse conceptual como módulo externo en SURFEX. Este enfoque facilitó el establecimiento de relaciones entre los parámetros y las variables climáticas y fisiográficas mediante un algoritmo genético, lo que permitió tener en cuenta la variabilidad dentro de la cuenca en toda la zona de estudio. Aunque el embalse carece de una base física, vincula con éxito los nuevos parámetros con variables físicas, logrando un equilibrio favorable entre la modelización distribuida y la representación física. Además, el enfoque de regionalización amplía la aplicabilidad del embalse más allá de los sistemas naturales, abarcando tanto las cuencas naturales como las influenciadas por el hombre.

Para incorporar la gestión humana del agua en el estudio, se eligió la zona regada por el *Canal de Aragón y Cataluña* como caso de estudio para aplicar un módulo prototipo de presa. Éste se ha utilizado en combinación con el nuevo esquema de riego SURFEX, que permite estimar las demandas reales. Este enfoque combina un modelo de explotación de embalses y el esquema de riego SURFEX, capturando con precisión la dinámica de la sequía. El nuevo módulo simula eficazmente el almacenamiento y los flujos de salida, demostrando una buena concordancia con los datos de referencia. Además, el nuevo esquema de riego de SURFEX capta la variabilidad interanual de la demanda de agua, lo que da lugar a una representación mejorada del sistema, permitiéndonos ir más allá de las habituales tablas "climatológicas" de demanda utilizadas en este tipo de estudios. El estudio revela que las influencias humanas agravan la sequía hidrológica, pero alivian la agronómica. Las características de la sequía hidrológica se alargan y el momento de los picos de sequía hidrológica cambian bajo la influencia humana. El regadío influye tanto en la sequía hidrológica como en la agronómica, lo que subraya la necesidad de tener en cuenta estos factores en las estrategias de gestión de la sequía. Estos resultados mejoran nuestra comprensión de las complejas interacciones entre las actividades humanas, los recursos hídricos y la dinámica de la sequía.

En conclusión, esta investigación avanza significativamente la representación de los procesos hidrológicos en un modelo basado en LSM en una región semiárida, sensible a las sequías, mediante la incorporación de varios enfoques y el desarrollo de un módulo para integrar el factor humano. Las mejoras logradas en la representación de las precipitaciones y en la modelización hidrológica aportan valiosos conocimientos sobre la compleja dinámica de la respuesta hidrológica y la sequía, abarcando tanto las influencias naturales como las antropogénicas. Este trabajo es un primer paso hacia la integración de las influencias humanas, como el regadío y la explotación de embalses, en la plataforma SASER, lo que abre nuevas posibilidades para estudiar la dinámica de la sequía y desarrollar estrategias mejoradas de evaluación y gestión de la sequía en sistemas naturales-humanos acoplados.

---

## Resum

Les sequeres són un fenomen complex i multidimensional descrit en termes senzills com a períodes sostinguts de dèficit hídric en comparació amb les condicions normals. Encara que de caràcter global, les seves conseqüències més greus s'observen a regions àrides o semiàrides, com la península Ibèrica. No obstant això, aquests extrems hidrològics no es deuen únicament a processos naturals. Les activitats humanes, com la construcció de preses, les extraccions d'aigües subterrànies i les pràctiques de regadiu, han alterat significativament el flux natural de l'aigua, cosa que ha fet que l'era actual s'anomeni Antropocè. Això posa en relleu la importància crítica de la gestió dels recursos hídrics a regions que ja s'enfronten a una disponibilitat d'aigua variable i limitada. En conseqüència, hi ha una creixent necessitat de metodologies que representin amb precisió la resposta hidrològica de les conques en sistemes naturals-humans acoblats, especialment durant els períodes de baix cabal, per gestionar eficaçment els recursos hídrics.

La modelització és una eina adequada utilitzada en la gestió de l'aigua per afrontar els reptes de gestionar uns recursos hídrics escassos i mitigar els impactes del canvi climàtic en el cicle de l'aigua. En aquesta investigació s'apliquen diversos enfocaments per millorar les simulacions hidrològiques emprant la plataforma hidrometeorològica SASER (SAFRAN-SURFEX-Eaudyssée-Rapid), de base física i distribuïda espacialment. Aquests enfocaments tenen per objecte millorar la representació dels processos hidrològics, en particular per als cabals baixos, i incorporar-hi consideracions relatives a la gestió humana de l'aigua.

Aquest document presenta dos treballs interrelacionats. En primer lloc, s'han introduït millores al model SASER per augmentar-ne el rendiment. En segon lloc, s'ha implementat un model de preses, forçat tant per les observacions com pel model SASER, per estudiar els impactes de les preses a les sequeres. Aquest treball s'ha dut a terme en una zona que abasta el domini pirinenc, incloent-hi la conca de l'Ebre, les conques que flueixen cap al Golf de Biscaia, les conques catalanes, algunes llenguadocianes, i les conques de l'Adur-Garona, però aquestes metodologies poden aplicar-se a qualsevol regió.

Per obtenir resultats precisos i fiables dels models de superfície terrestre (Land Surface Model, LSM) és essencial disposar de dades de forçament d'entrada adequades amb una resolució espacial i temporal apropiada. A aquest efecte, s'ha introduït un nou mètode de correcció lineal del forçament de les precipitacions que aprofita les dades dels models climàtics regionals (MCR). En utilitzar una finestra de correcció setmanal, el mètode capta millor la variabilitat temporal i els patrons de precipitació, cosa que resulta en una representació més realista dels esdeveniments de precipitació en termes estadístics. L'impacte en l'escorriment simulat s'ajusta a les expectatives, mentre que els canvis en el drenatge i l'evapotranspiració estan influïts per diversos factors, com ara el règim climàtic i la resposta en climes humits.

A més, el model SASER per defecte presentava un biaix negatiu als cabals baixos, cosa que resulta problemàtica en els estudis sobre la sequera. La causa dels cabals baixos és la manca d'un esquema d'aigües subterrànies al model SASER. La inclusió d'un esquema conceptual d'embassaments per regular el drenatge va millorar la simulació dels cabals, com demostren els valors positius a les

---

mètriques de rendiment. L'aplicació de l'esquema d'embassaments va ser senzilla i va millorar eficaçment la representació dels cabals baixos sense comprometre els cabals alts. A més, es va aplicar un enfocament de regionalització que va permetre la integració de l'embassament conceptual com a mòdul extern a SURFEX. Aquest enfocament va facilitar l'establiment de relacions entre els paràmetres i les variables climàtiques i fisiogràfiques mitjançant un algorisme genètic, fet que va permetre tenir en compte la variabilitat dins de la conca a tota la zona d'estudi. Tot i que l'embassament no té una base física, vincula amb èxit els nous paràmetres amb variables físiques, aconseguint un equilibri favorable entre la modelització distribuïda i la representació física. A més, l'enfocament de regionalització amplia l'aplicabilitat de l'embassament més enllà dels sistemes naturals, i abasta tant les conques naturals com les influenciades per l'home.

Per incorporar la gestió humana de l'aigua a l'estudi, es va triar la zona regada pel Canal d'Aragó i Catalunya com a cas d'estudi per aplicar un mòdul prototip de presa. Aquest ha estat utilitzat en combinació amb el nou esquema de reg de SURFEX, que permet estimar les demandes reals. Aquest enfocament combina un model d'explotació d'embassaments i l'esquema de reg de SURFEX, capturant amb precisió la dinàmica de la sequera. El nou mòdul simula eficaçment l'emmagatzematge i els fluxos de sortida i demostra una bona concordança amb les dades de referència. A més, el nou esquema de reg de SURFEX capta la variabilitat interanual de la demanda d'aigua, cosa que dona lloc a una representació millorada del sistema, permetent anar més enllà de les habituals taules de demanda "climatològiques" emprades en aquest tipus d'estudis. L'estudi revela que les influències humanes agreugen la sequera hidrològica, però alleugen l'agrònica. Les característiques de la sequera hidrològica s'allarguen i el moment dels pics de sequera hidrològica es desplaça sota la influència humana. El regadiu influeix tant en la sequera hidrològica com en l'agrònica, cosa que subratlla la necessitat de tenir en compte aquests factors en les estratègies de gestió de la sequera. Aquests resultats milloren la nostra comprensió de les complexes interaccions entre les activitats humanes, els recursos hídrics i la dinàmica de la sequera.

En conclusió, aquesta investigació avança significativament la representació dels processos hidrològics en un model basat en LSM en una regió semiàrida sensible a les sequeres mitjançant la incorporació de diversos enfocaments i el desenvolupament d'un mòdul per integrar el factor humà. Les millores aconseguïdes en la representació de les precipitacions i en la modelització hidrològica aporten valuosos coneixements sobre la complexa dinàmica de la resposta hidrològica i la sequera, abastant tant les influències naturals com les antropogèniques. Aquest treball és un primer pas cap a la integració de les influències humanes, com el regadiu i l'explotació d'embassaments, a la plataforma SASER, fet que obre noves possibilitats per estudiar la dinàmica de la sequera i desenvolupar estratègies millorades d'avaluació i gestió de la sequera en sistemes naturals-humans acoblats.

---

## Acknowledgments

I would like to extend my deepest gratitude to *Dr. Pere Quintana-Seguí* for the opportunity to embark on this Ph.D. journey. For his exceptional mentorship, profound knowledge, unwavering dedication, and continuous inspiration throughout my Ph.D. journey. His invaluable guidance has been instrumental in shaping my growth as a scientific researcher. Likewise, I am sincerely thankful to *Dr. Luis Garrote* for his exceptional contributions, wise advice, and invaluable suggestions, which have significantly enriched the quality of my work. I am profoundly grateful for inviting me to UPM in Madrid. Both thanks for helping me in tackling seemingly unsolvable problems.

To *Dra. Anaïs Barella-Ortiz*, my office-mate and source of inspiration, I am immensely grateful for the transformative experiences we shared. Your enthusiasm, kindness, and motivation have guided me through challenges, both in my research and personal life. I would like to express my heartfelt appreciation to *Dr. Boone* and *Dr. Artinyan* for their priceless support, particularly during the early stages of my Ph.D. Additionally, I extend my gratitude to all the researchers who have contributed to my scientific career, enriching my knowledge and skills along the way.

*Jaime* and *Victoria*, thank you for the experiences we shared during those initial months together. To the members of the *OE family* and all the people I encountered on this journey -*Jacopo, Marie, Roger, and Judith*- I am deeply grateful for our connections and shared experiences. *Héctor* and *Edgar* thanks for those first and unexpected days off across Spain in 2020.

My sincere appreciation goes out to the entire *UPM community* for creating an exceptional environment during my stay in Madrid. Especially, I would like to express my deepest gratitude to *Araceli* and *Sandro* for their warm welcome, hospitality, and contagious enthusiasm. Those shared moments over coffee provided not only a much-needed break but also offered an opportunity to exchange ideas and perspectives. Thank you for your friendship and for making my time at UPM truly unforgettable. *Lorenzo*, your guidance in the city and your unique perspective of Madrid have left a lasting impact on me. Thank you.

To my *II-UNAM family* (Mexico), your advice and steadfast support mean the world to me. Thank you for making me feel connected.

*Alejandra, Talisia, and Stephanie*, I extend my deepest gratitude for being my unwavering support network. Even from a distance, you have been a guiding light during moments of confusion and doubt, helping me rediscover my path. Your constant presence and encouragement have played an integral role in my personal and professional growth. I am profoundly thankful for your friendship and support.

I wish to acknowledge my family. To my incredible mother, *Emilia*, I am profoundly thankful for your unwavering strength and support. You have taught me the importance of perseverance and have been a constant source of inspiration in my life. Your presence has guided me through every challenge, and I am forever grateful for your love and guidance.

Finally, a heartfelt tribute to all my loved ones in Mexico. Though you are no longer physically present, your memories reside deep within my heart, beating with love.

---

---

# Contents

<b>Abstract</b> .....	<b>v</b>
<b>Acknowledgments</b> .....	<b>xi</b>
<b>1. Introduction</b> .....	<b>1</b>
1.1. Background .....	1
1.1.1. Drought and water management in the Mediterranean region.....	2
1.1.2. The role of Land Surface Models in understanding drought .....	3
1.2. Motivation.....	4
1.2.1. Research subject and objectives .....	4
1.2.2. Structure of the thesis .....	4
<b>2. State-of-the-art</b> .....	<b>5</b>
2.1. Drought as part of the water cycle.....	5
2.1.1. Drought definition and propagation.....	7
2.1.2. The impacts of drought (a global phenomenon).....	10
2.1.2.1. Drought (and water management) in the Mediterranean region .....	11
2.1.3. The need for effective drought assessment.....	12
2.2. Modeling the water cycle and drought.....	13
2.2.1. Background.....	14
2.2.2. Addressing the complexities in low-flow modeling.....	15
2.2.3. The application of LSMs for drought assessment .....	16
2.3. The current state of the LSMs.....	17
2.3.1. Overview of the Land Surface Models.....	17
2.3.2. The structure and components .....	18
2.3.2.1. The key processes involved .....	20
2.3.3. Main limitations and uncertainties.....	21
2.4. Recent Advances in the LSMs .....	22
2.4.1. Advances in model complexity .....	23
2.4.2. The use of remote sensing in LSMs .....	24
2.4.3. Progress of LSMs in the modeling of the Mediterranean region.....	25
2.4.4. Incorporation of the human dimension into LSMs.....	26
<b>3. Area of study and materials</b> .....	<b>29</b>
3.1. Study area.....	29
3.1.1. The Pyrenean Domain .....	29
3.1.2. Description of the Ebro basin .....	31
3.1.2.1. Exposure to drought.....	31
3.1.3. Canal de Aragón y Cataluña (CAyC) .....	32
3.2. Data .....	33
3.2.1. Precipitation data .....	33
3.2.1.1. Observational data .....	33

---

---

3.2.1.2. High-resolution RCM simulation: CNRM-ALADIN63 .....	35
3.2.2. Hydrological data .....	35
3.2.2.1. Observed streamflow data.....	35
3.2.2.2. SIMPA model (reference).....	36
3.2.3. Physiographic data.....	36
3.2.3.1. ESDAC database.....	37
3.2.4. Information on anthropogenic influences.....	37
3.3. The SASER hydrometeorological modeling chain .....	39
3.3.1. SAFRAN .....	39
3.3.2. SURFEX.....	39
3.3.2.1. Irrigation scheme in SURFEX .....	40
3.3.3. Eaudyssée-RAPID .....	41
3.3.4. Limitations of the SASER model .....	42
<b>4. Methodological framework .....</b>	<b>43</b>
4.1. Pathway to improve the hydrologic modeling in the SASER model .....	43
4.2. Improvements in the SASER modeling chain.....	45
4.2.1. Improvement to precipitation in SAFRAN forcing .....	45
4.2.2. Attempts to improve inner model parameters.....	45
4.2.3. Improvement of low-flow simulation in the SURFEX model.....	46
4.2.4. Adding human water management to the SASER model.....	46
4.2.5. Criteria for evaluation of model performance .....	47
4.2.5.1. Precipitation forcing.....	47
4.2.5.2. Hydrological information.....	48
<b>5. Improvement of the precipitation forcing.....</b>	<b>51</b>
5.1. Introduction .....	51
5.2. Study area and data .....	53
5.3. Methodology .....	53
5.3.1. Correction Method.....	53
5.3.1.1. Assessment of the corrected precipitation .....	54
5.3.2. Assessment the impact on hydrological variables .....	55
5.4. Results .....	56
5.4.1. Improvement of precipitation intensities .....	56
5.4.2. Impact on the water balance components.....	62
5.4.2.1. Impact on intense events.....	62
5.4.2.2. Long-term water budget.....	64
5.5. Discussion .....	67
5.6. Conclusions .....	69
<b>6. Improvements in the SASER modeling chain .....</b>	<b>71</b>
6.1. Introduction .....	71
6.2. Early attempts aimed at improving inner model parametrization .....	72
6.2.1. Calibration of the <i>runoff b</i> parameter .....	72
6.2.2. Attempts to improve the soil information database .....	75
6.3. Improvement of low flows simulation .....	76

---

---

6.3.1. Study area and data.....	77
6.3.2. Methodology.....	77
6.3.2.1. Conceptual reservoir .....	79
6.3.2.2. Calibration procedure for reservoir parameters .....	80
6.3.2.3. Regionalization approach.....	81
6.3.2.4. Low flow indices.....	83
6.3.3. Results .....	84
6.3.3.1. Evaluation of the model including the reservoir with calibrated parameters..	85
6.3.3.2. Evaluation of the regionalization approach .....	88
6.3.3.3. Computing natural streamflow with the improved model .....	91
6.3.3.4. Evaluation of low-flows indices .....	95
6.3.3.5. Comparison with a reference model .....	96
6.4. Discussion .....	97
6.4.1. Attempt to improve inner parametrization.....	97
6.4.2. Improvement on low flows representation .....	98
6.5. Conclusions.....	100
<b>7. Water management and drought.....</b>	<b>103</b>
7.1. Introduction .....	103
7.2. Case study and data.....	105
7.3. Methodology .....	105
7.3.1. Reservoir operation scheme.....	107
7.3.1.1. Description of the WAAPA model .....	107
7.3.1.2. Model input data .....	108
7.3.1.3. Model configuration.....	109
7.3.1.4. Evaluation criteria.....	110
7.3.2. Irrigation water demands .....	110
7.3.3. Drought analysis .....	111
7.3.3.1. Threshold level method.....	112
7.3.3.2. Calculation procedure .....	114
7.3.3.3. Drought characteristics .....	115
7.3.3.4. Quantifying the human influence.....	116
7.4. Application of the methodology to the CAyC.....	116
7.4.1. Irrigations demands from SURFEX-LSM.....	116
7.4.2. Performance of the reservoir operation scheme .....	117
7.4.3. Identifying drought events and analysis .....	120
7.4.3.1. Barasona case study .....	120
7.4.3.2. Santa Ana case study .....	124
7.4.4. Human influence on drought events.....	128
7.5. Discussion .....	131
7.6. Conclusions.....	133
<b>8. Conclusions and further work .....</b>	<b>135</b>
8.1. Scientific framework synthesis .....	136
8.2. Conclusions.....	137
8.3. Implications and recommendations.....	139

---



---

8.4. Perspectives and further research .....	140
<b>Appendix A. Attempts to improve internal model parameters of the SASER model .</b>	<b>143</b>
A.1. Runoff generation scheme.....	143
A.1.1. Background.....	143
A.1.2. Calibration of the parameter b .....	144
A.1.3. Finding a relationship between runoff b and IDPR .....	146
A.2. Improvement of Soil Information .....	151
A.2.1. Background.....	151
A.2.2. Search for an improved soil depth database .....	152
<b>Appendix B. Results of the reservoir scheme using different inputs .....</b>	<b>155</b>
B.1. Estimation volume – area curves.....	155
B.2. Reservoir simulation plots.....	157
B.3. Drought analysis using standardized indices.....	165
<b>References .....</b>	<b>169</b>
<b>List of figures .....</b>	<b>205</b>
<b>List of tables.....</b>	<b>213</b>

---

# 1. Introduction

## 1.1. Background

Water is an essential resource, but its availability is limited and varies. The movement and transformation of water within and between Earth's surface, atmosphere, and oceans are known as the water cycle or hydrological cycle. Water flows and stocks on the earth's surface play a vital role in shaping human and environmental systems. Additionally, water and its movement can lead to potential hazards such as floods and droughts. These hydrological extremes have significant impacts on society and the environment across the globe (Wilhite et al., 2007).

Floods and droughts, which are part of the complex water cycle, occur in diverse geographies and climates. As a result, society is exposed to these hydrological hazards, which can also be influenced by human activities (Van Loon et al., 2016). To manage these variations, our societies have developed hydraulic infrastructure such as dams. These structures allow for water storage during wet seasons or melting periods in snow-dominated areas, which can then be released during high-demand dry periods.

In this context, the water cycle is not solely driven by natural processes; human interactions have significantly altered it, leading to the era being labeled the Anthropocene (Van Loon et al., 2016; Di Baldassarre et al., 2017). Anthropogenic factors such as river diversion, dam construction, groundwater abstractions, and irrigation practices have disrupted the natural flow of water (Nilsson et al., 2005), causing changes in its storage and movement.

Moreover, in some regions of the world (e.g. southern Europe and West Africa), droughts have experienced a trend toward more intense and longer effects in the last decades (Seneviratne et al., 2012; Prudhomme et al., 2014; Zhao & Dai, 2015). Additionally, climate change and growing water demand exert additional stress on water resource systems (Bates et al., 2008; Wanders & Wada, 2015). As a result, droughts have garnered increasing attention.

However, defining drought universally is challenging since it is a complex and multidimensional phenomenon. In simple terms, drought can be described as an extreme climate event characterized by a sustained period of water deficit compared to normal conditions. Traditionally, drought is categorized into different types depending on the variable it affects (Wilhite, 2000; Mishra & Singh, 2010).

While precipitation deficits naturally propagate through the interconnected components of the water cycle (Van Loon, 2015; Zhang et al., 2022), drought cannot be considered solely a natural phenomenon in human-dominated environments. Water scarcity resulting from human activities and drought are interconnected processes that need to be examined together (Van Loon et al., 2016). Human activities play a significant role in the development of drought and thus in the underlying processes and must be considered in current drought research (AghaKouchak et al.,

---

2021). Understanding the complex interplay between natural and anthropogenic drivers is essential for effective water management and sustainable development, especially as water resources face increasing pressure.

### **1.1.1. Drought and water management in the Mediterranean region**

Droughts, a global phenomenon, exhibit their most severe consequences in arid or semi-arid regions. These areas face the challenge of meeting water demands that often surpass the available natural resources, necessitating the reliance on hydraulic infrastructure for adaptation to semiarid conditions and drought events. Consequently, drought impacts have significant implications on agriculture, ecosystems, and human health (Schwabe et al., 2013, 2015).

The Mediterranean region is characterized by a dry summer season and a pronounced annual precipitation cycle, with limited or no rainfall during summer. This inherent climate pattern renders the region highly vulnerable to droughts, making it one of the most exposed areas to socioeconomic drought impacts (Seneviratne et al., 2012). Previous studies have documented severe drought events in the Mediterranean region (Vicente-Serrano, 2006; Tejedor et al., 2017), including the Iberian Peninsula (García-Herrera et al., 2007; Belo-Pereira et al., 2011; Andrade & Belo-Pereira, 2015; Coll et al., 2017; Páscoa et al., 2017, 2021) resulting in adverse environmental, agricultural, and economic consequences (Hoerling et al., 2012; Vicente-Serrano et al., 2014; Blauhut et al., 2015). And more specifically, in Spain, comprehensive assessments of extreme drought events have been conducted, spanning different historical periods (Domínguez-Castro et al., 2012; García-Valdecasas Ojeda et al., 2017; González-Hidalgo et al., 2018).

The combination of the arid and semi-arid climate, high population density, heavy reliance on agriculture, and already limited water resources creates significant pressure on water supplies in the Mediterranean region. Consequently, effective drought management in this area poses unique challenges. The uneven distribution of water resources further complicates water resources management, contributing to the complexity of the situation.

Furthermore, climate change projections indicate a drier and warmer Mediterranean region (Bates et al., 2008; Seneviratne et al., 2012; Trambly et al., 2020), accompanied by an increase in drought occurrences. Studies investigating streamflow trends have shown negative trends, resulting in decreased streamflow in the southern and eastern regions of Europe, while generally positive trends have been observed in the western and northern regions (Stahl et al., 2010, 2011). Thus, changes in drought patterns are also anticipated. However, significant uncertainties persist due to the intricate interrelationships among drought impacts on ecosystems, agriculture, water resources, and other sectors, further compounded by the complexity of the phenomenon.

Therefore, the research topic of understanding and studying drought and its underlying processes in the Mediterranean region is important. Valuable insights can be gained by unraveling the mechanisms that drive drought in the Mediterranean, such as the interplay between climate patterns, land surface processes, and human activities. This understanding informs the design and implementation of effective drought management strategies (Iglesias et al., 2007, 2012; Garrote et al., 2016).

This highlights the importance of water resources management in areas where water availability is already highly variable and limited, at seasonal and annual scales (e.g., the Iberian Peninsula).

Furthermore, it reinforces the necessity to apply methodologies to reproduce more appropriately the hydrological response of the basins, especially during low flow periods, to provide decision-makers with tools to efficiently manage water resources.

### **1.1.2. The role of Land Surface Models in understanding drought**

In recent years, the use of models in water management has increased to address the growing need for managing scarce water resources and mitigating the impacts of climate change on the water cycle (Vörösmarty et al., 2015; Döll et al., 2016). The recognition of the interconnectedness between water flows, economic factors, and institutions has led to the development of models that transcend the boundaries of stand-alone hydrological models (Alcamo et al., 2008). Among these models, Land Surface Models (LSMs) have emerged as valuable tools for large-scale hydrological modeling and predicting extreme events.

LSMs are numerical models that simulate the exchange of water, energy, and carbon between the Earth's surface and the atmosphere. Significant advancements have been made in recent years to improve their representation of the water cycle (Clark et al., 2015; Blyth et al., 2021), incorporating more realistic descriptions of physical processes. They now encompass a wide range of processes, including soil moisture dynamics, hydrological processes, vegetation dynamics, and biogeochemical cycles (Lawrence et al., 2019).

LSMs are particularly suitable for studying drought due to their ability to simulate the processes associated with drought propagation throughout the system (Vidal et al., 2010). This makes them valuable for investigating the causes and mechanisms underlying drought events. Numerous studies have demonstrated the enhanced analysis of the hydrological cycle, particularly droughts, through the use of LSMs (Lehner et al., 2006; Vidal et al., 2010; Prudhomme et al., 2011; Van Loon et al., 2012; Mo & Lettenmaier, 2014; Xia et al., 2014; Quintana-Seguí et al., 2020).

While LSMs have predominantly focused on natural processes, it is essential to consider the significant impact of human activities on water flows and storage on the Earth's land surface (Vörösmarty & Sahagian, 2000; Rost et al., 2008; Sterling et al., 2013). Current generation models often have limited representations of human factors and struggle to capture the complexity of interactions between human and natural processes (Pokhrel et al., 2016; Wada et al., 2017). Incorporating human activities into global LSMs remains a significant challenge that needs to be addressed.

A comprehensive understanding of freshwater systems and improved water resource management can be achieved by advancing the representation of human impacts in LSMs and thus, improving their integration into global models. Addressing these challenges will enable more accurate simulations and predictions, facilitating informed decision-making for sustainable water management in the face of changing environmental conditions.

## 1.2. Motivation

The utilization of comprehensive models known as Land Surface Models (LSMs) is on the rise as they aim to encompass various aspects of the Earth's system (Vörösmarty et al., 2015; Döll et al., 2016). These models require parameterization of all physical processes and the definition of boundary and initial conditions, demanding a substantial amount of information. While LSMs offer a high level of detail, they have inherent limitations that impede the understanding of hydrological processes and hinder attribution studies. Therefore, there is a need for improvements in both the parametrization and process representations of these models (Clark et al., 2015; Fisher & Koven, 2020). Consequently, it is crucial to develop comprehensive simulations that capture the complex dynamics of hydrological response, considering both natural and anthropogenic influences within LSMs. Such advancements will enable the development of improved strategies for drought assessment and management in a coupled natural-human system.

### 1.2.1. Research subject and objectives

The thesis aims to enhance comprehension of drought in Spain by utilizing physical modeling, with a specific focus on the impact of human activity. Additionally, the research seeks to supply valuable information for informed decision-making.

- I. Improve different aspects of the SASER modeling chain in order to improve streamflow simulation.
- II. Simulating the main reservoirs of the Ebro basin in conjunction with the SASER model and studying the impacts of water management on the (anthropic) drought.
- III. Analysis of drought in an irrigated area using the tools developed in the project.

### 1.2.2. Structure of the thesis

This thesis is structured as follows. After this introductory chapter, an overview of the current state-of-the-art for the reader is presented in Chapter 2. The study area, general data, and the model used throughout this thesis are introduced in Chapter 3.

In Chapter 4, a methodological framework is presented, which describes the pathway followed in this thesis to improve different aspects of the SASER model. Additionally, the different approaches employed in this research are briefly explained.

In Chapters 5 and 6, the different efforts to improve the hydrologic modeling in the SASER model are explained, focusing on the improvements in precipitation forcing and the enhancement streamflow simulation, in particular low-flow simulation, respectively.

In Chapter 7, a new module, externally incorporated, to simulate human water management (reservoir operation scheme) is introduced in the SASER modeling chain.

Finally, a synthesis of this research is summarized in Chapter 8. In this final chapter, the relevance of the research outcomes to the general objective is evaluated. Moreover, examines the implications for the scientific field and drought management and provides guides for future research.

---

## 2.State-of-the-art

### 2.1. Drought as part of the water cycle

Water is a vital resource that plays a crucial role in supporting ecosystems and sustaining human societies. The movement and transformation of water within and between Earth's surface, atmosphere, and oceans, is known as the water cycle or hydrological cycle. It is a fundamental component of the Earth's climate system that describes the exchange and transformation of water between the atmosphere, land, and oceans. This process is mainly driven by solar radiation, wind, and temperature gradients.

Water flows and stocks on the earth's surface play a vital role in shaping human and environmental systems. In addition, water and its movement also raise potential hazards such as floods and droughts. Both floods and drought, hydrological extremes, are part of the complex water cycle and occur in diverse geographies and climates. These hydrological extremes have significant impacts on society and the environment across the globe (Wilhite, 2000; Wilhite et al., 2007). The immediate and visible impacts of floods often receive more attention. Conversely, droughts, also known as "the creeping phenomenon" (Mishra & Singh, 2011), pose a significant and widespread threat to societies globally. Among the different forms of drought, flash droughts emerge as a concern due to their rapid onset and intensified nature. These events, characterized by a sudden and severe decline in soil moisture and the abrupt manifestation of drought conditions, can have profound implications on many socioeconomic sectors, particularly agriculture (Christian et al., 2019, 2023). Unlike floods, droughts typically occur over a much larger spatial and temporal scale, affecting extensive areas for months or even years and causing severe impacts on many economic sectors (Tallaksen & Van Lanen, 2004; Sheffield et al., 2012; Stahl et al., 2016). As a result, there has been a growing focus on this phenomenon in recent years.

Therefore, understanding the water cycle and its interaction with these hydrological extremes, especially with drought, is essential for predicting, managing, and adapting to the current and future challenges of water resources sustainability and resilience.

Moreover, the water cycle is not only driven by natural processes, human interactions have also significantly altered the natural water cycle, leading to the era being labeled the Anthropocene (Van Loon et al., 2016; Di Baldassarre et al., 2017). Anthropogenic factors such as river diversion, dam construction, hydroelectricity generation, municipal uses, and agricultural irrigation have disrupted the natural flow of water, causing changes in its storage and movement. Although much research has been done in recent years on the interaction between natural and human drivers, a unified and comprehensive diagram illustrating these interactions had not been developed until 2022, **Figure 2-1**. This diagram provided by the United States Geological Survey (USGS) depicts the present-day global water cycle with a focus on the major human activities that impact the water flow and storage at the global scale.

---

These interactions between natural and anthropogenic drivers can cause alterations in the quantity, quality, and timing of water availability, leading to significant impacts on humans and ecosystems. Hence, understanding the complex interplay between these drivers is essential for effective water management and sustainable development under the increasing pressure on water resources.

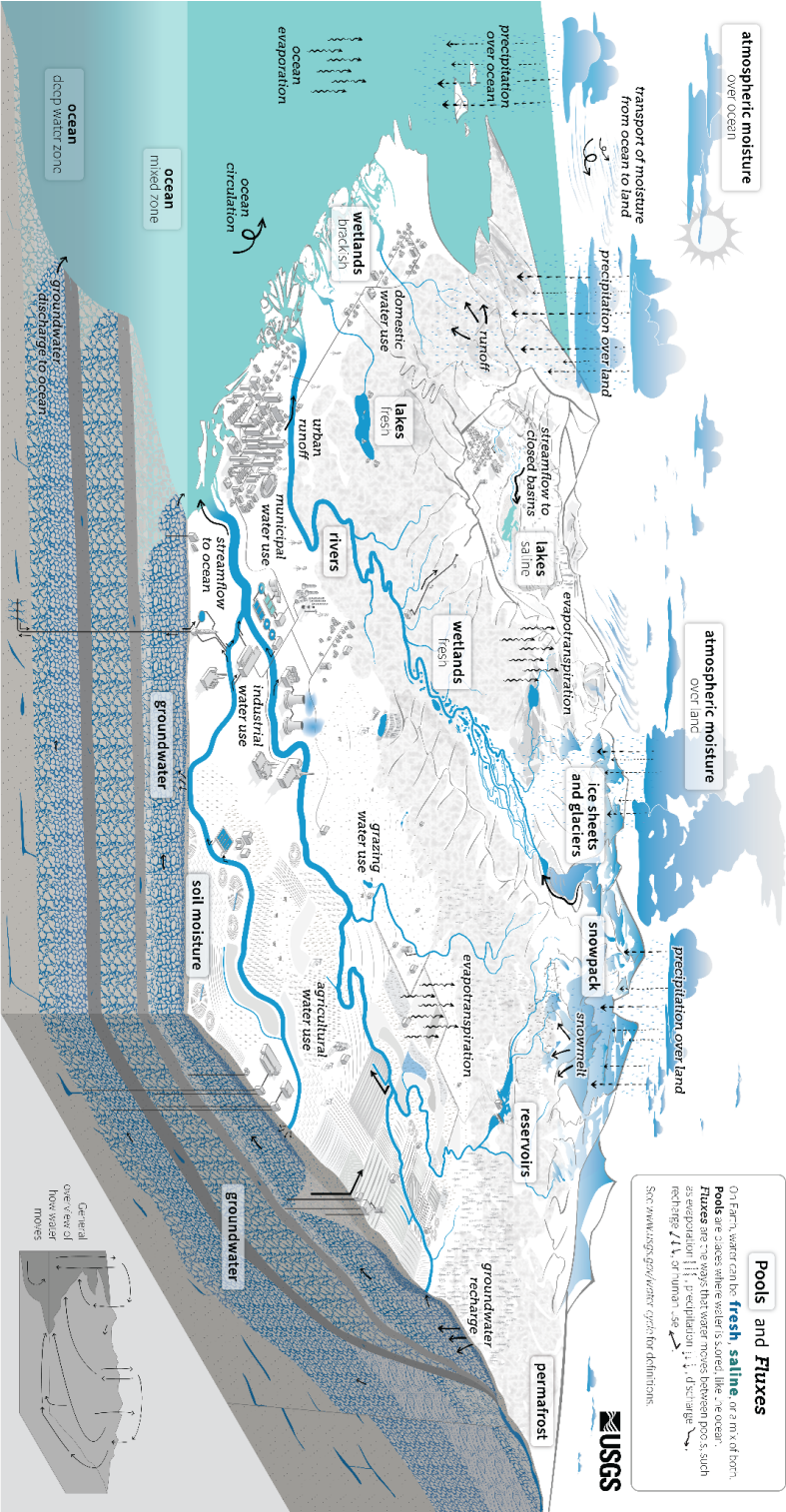


Figure 2-1 Diagram of the water cycle considering human components.

### 2.1.1. Drought definition and propagation

Drought is a complex and multidimensional phenomenon that leads to a lack of a universal definition that can be applied across all regions and contexts. As a result, several definitions have been proposed in scientific literature and operational practice, some definitions can be found in (Dracup et al., 1980a; Wilhite & Glantz, 1985; Mishra & Singh, 2010; Dai, 2011). Hence, finding an appropriate definition of drought represents the first challenge to address, and thus may hinder its accurate assessment, monitoring, and management.

In a simple and general way, drought can be defined as an extreme climate event characterized by a sustained period of water deficit compared with normal conditions. By their nature droughts can persist for extended periods, ranging from months to years or even decades. Its worldwide and spatial and temporal characteristics depend on the region. However, it is important to regard that “normal” conditions depend on the water use and therefore, the drought definition strongly depends on the objective of the study.

Traditionally drought is usually categorized into different types (Mishra & Singh, 2010), depending on which variable affects it, Figure 2-2. Extensive drought indices can be found in (Dracup et al., 1980a; Wilhite, 2000; Keyantash & Dracup, 2002; Mishra & Singh, 2010; Dai, 2011; Sheffield & Wood, 2012). Here, an exhaustive review of the available drought indices is not provided. Instead, a select set of widely-utilized indices is focused on to characterize the meteorological, agricultural, and hydrological drought.

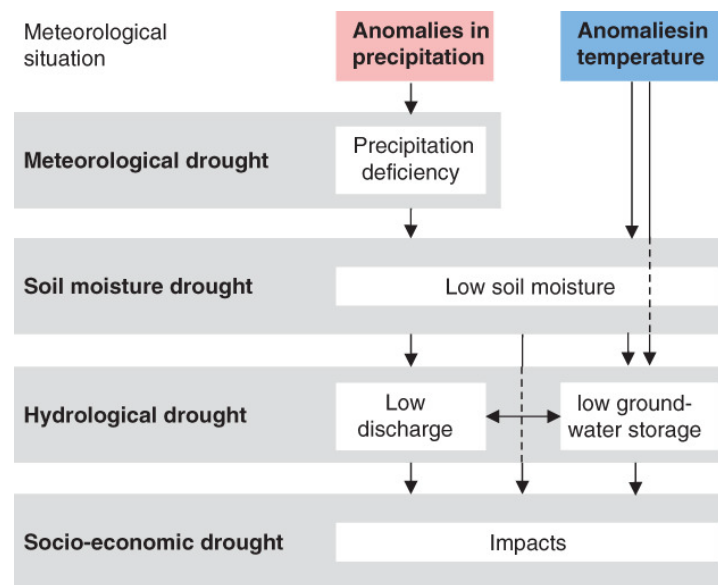


Figure 2-2 Schematic representation of drought categories and their development (Van Loon, 2015).

Meteorological drought refers to a prolonged period characterized by an extended period of below-average precipitation. Meteorological drought is usually identified through the use of standardized precipitation indices (SPI, McKee et al., 1993), which calculate the amount of precipitation that falls in a given period relative to the long-term average for the same period. SPI is a flexible index that can be calculated for different time scales, from a few weeks to several years, and can be used to assess the severity and duration of a drought event. The main benefit of the SPI is that it allows to compare drought status across climates. The main limitation of this index is that precipitation is the only variable considered for calculation. For calculation, long-



term records of precipitation are required. In addition, fitting a probability distribution within SPI calculation is necessary, which has an important impact on its results (Mishra & Singh, 2011). Comprehensive frameworks for calculating standardized indices, both univariate and multivariate, in a nonparametric manner have been also developed (Farahmand & Aghakouchak, 2015). Since precipitation is not the only driver of the meteorological drought, other indices considered are the Standardized Precipitation and Evapotranspiration Index (SPEI; Vicente-Serrano et al., 2010) and the Palmer Drought Severity Index (PDSI; Palmer, 1965), which consider the evapotranspiration and soil moisture on their calculation, respectively. Nevertheless, it is imperative to understand that these indices are not without their drawbacks and may not always offer an optimal solution. The choice of index depends on the particular type of drought being analyzed and the specific needs and preferences of the user. Furthermore, it is important to note that the SPEI inherits the challenges associated with the SPI, while also introducing additional complexities in estimating evapotranspiration.

Agricultural drought occurs when there is a soil moisture deficit caused by low precipitation and/or high evapotranspiration, which affects crop growth and productivity. This type of drought is primarily measured using indicators such as crop yield, plant stress, and soil moisture content. The formulation of SPI can be extended to other variables, such as soil moisture. The Standardized Soil Moisture Index (SSMI) uses a similar approach that SPI (Sheffield et al., 2004). The PDSI is primarily considered a meteorological drought index but can also serve as an agricultural drought index. Other indices are the Soil Moisture Drought Index (SMDI) and the Evapotranspiration Deficit Index (ETDI) developed by (Narasimhan & Srinivasan, 2005).

Hydrological drought is related to a negative anomaly (below-normal level) in water availability in rivers, lakes, and groundwater systems. The most commonly used variable to characterize this drought type is streamflow due to its widely available measured data and easily simulated, but piezometers are also often used in areas where groundwater plays an important role. The Standardized Runoff Index (SRI; Shukla & Wood, 2008) is calculated similarly to the Standardized Precipitation Index (SPI), with the difference that SRI uses streamflow data instead of precipitation data. The Surface Water Supply Index (SWSI; Shafer & Dezman, 1982), provides a single value for each basin on a monthly scale throughout the year. The index is derived from the cumulative probability distributions of snow course, precipitation, reservoir, and streamflow data. Similarly, piezometric data can also be standardized (Bloomfield & Marchant, 2013).

The impacts of such drought events extend beyond the natural environment and have significant consequences for society and the economy. Referred to as socio-economic drought when water resource systems are not able to meet the water demands of society and the adverse effects on various sectors (Apurv et al., 2017; AghaKouchak et al., 2021).

Under natural conditions, the precipitation deficits transmit through the interconnected components of the water cycle, including soil, surface runoff, and groundwater as shown in **Figure 2-2**, thus giving rise to what is known as drought propagation (Van Loon, 2015; Zhang et al., 2022). In their research, Gaona et al. (2022) suggest that the complexity of drought propagation in semi-arid regions is amplified by the interplay of factors such as soil moisture and evaporation. Nevertheless, in human-dominated environments, drought cannot be considered solely a natural phenomenon; just as water scarcity (unbalance between available water and demands) resulting from human activities cannot be considered a separate and independent process from drought (Van Loon et al., 2016). Indeed, human activities play an important role in the development of drought (**Figure 2-3**), which needs to be accounted for in the current research on drought (AghaKouchak et al., 2021).

### Anthropogenic Drought

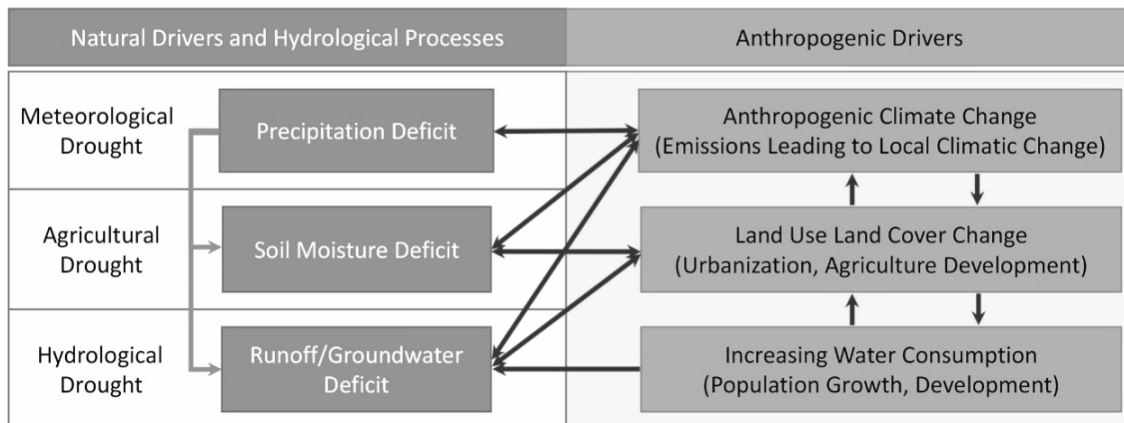


Figure 2-3 Schematic representation of natural and human-induced drivers and their corresponding interactions (AghaKouchak et al., 2021).

Recent studies argued that both natural and human processes have to be considered in drought definitions and analysis frameworks (Nazemi & Wheeler, 2015a; Van Loon et al., 2016; Di Baldassarre et al., 2017; AghaKouchak et al., 2021). Human activities can modify the propagation of drought, amplifying its effects or even triggering drought events in the absence of natural drivers. Van Loon et al. (2016) have proposed to group natural drought types into “climate-induced” droughts and “human-induced” droughts to those based on human drivers. This distinction can be helpful in research focused on attributing the causes of drought.

Table 2-1 Nature and causes of the different phenomena related to water availability (adapted from Pereira et al., 2002).

Regime	Nature produced	Human-induced
<b>Permanent</b>	Aridity	Desertification
<b>Temporary</b>	Drought	Water scarcity

Moreover, aridity, desertification, and water scarcity are all complex concepts that are closely intertwined with drought, however, understanding the differences between these concepts is crucial to addressing the challenges related to water resources. Aridity and desertification describe climatic and environmental conditions and refer to long-time scales (Table 2-1). Desertification is the process of land degradation resulting from various factors, including human activities and climate change. Whereas drought is a temporary phenomenon, and water scarcity is due to insufficient water resources to meet the demands of the population or ecosystem. To sum up, aridity is caused by a change in the mean status of the hydro-system and drought is an extreme event.

### 2.1.2. The impacts of drought (a global phenomenon)

Drought has been a recurring natural disaster throughout human history. It is important to note that the most severe drought events in recent history have occurred across all continents in recent decades, and some of these events have had far-reaching and long-lasting consequences. However, in contemporary times, the impact of droughts has been notably intensified, primarily attributable to a confluence of two contributing factors: firstly, the reliance on water-dependent economies and increasingly growing population, and secondly, the influence of climate change. It is essential to elucidate that the aim of this section does not entail an exhaustive enumeration of the multifaceted effects of drought; rather, it endeavors to provide a comprehensive understanding of the wide-ranging drought impacts.

The risk of droughts has increased since the late 1970s, attributed to global warming causing higher temperatures and increased drying (Dai et al., 2004; Zou et al., 2005). India is among the most vulnerable drought-prone countries in the world, studies have shown that the occurrence of drought is more prevalent in the upper regions of a basin, resulting in an increased risk of water shortages in these areas compared to the lower parts of the basin (Pandey et al., 2008).

For instance, North America has been experiencing severe droughts with a longer duration and wider extent (Wilhite & Hayes, 1998), causing substantial economic and environmental damages. Hence, droughts have been identified as the costliest natural disasters, in terms of economic losses, to strike the United States (Cook et al., 2007). Similarly, Europe has witnessed droughts in several countries with significant consequences on agriculture, hydrology, and water management (Hisdal et al., 2001; Stahl, 2001; Blauhut et al., 2015). Over the last three decades, Europe has experienced numerous severe drought events (Bradford, 2000). More recently, in 2008, the Iberian Peninsula faced a multiyear drought reducing groundwater levels and reservoir storage (Andreu et al., 2009)

Australia has also suffered from frequent and severe droughts, which have severely affected its agricultural productivity and water supply the “Millennium” drought had significant impacts on Southern and Eastern Australia, and is considered to be one of the most severe droughts experienced in the region (Murphy & Timbal, 2008). In Africa, droughts are recurrent and often lead to widespread famine, poverty, and migration. In 2011 drought in the Horn of Africa had devastating consequences (Viste et al., 2013).

In Asia, droughts have affected many countries, leading to severe water scarcity and affecting millions of people. In northern China, frequent severe droughts from 1997, 1999 to 2002 resulted in major economic and societal losses, causing water shortages, and dust storms in both rural and urban areas (Zou et al., 2005).

These recent drought events are not exhaustive but serve as a reminder of the devastating impacts that drought can have on societies, economies, and the environment; and evidence that drought is a worldwide and recurrent phenomenon. It is, therefore, crucial to have a thorough understanding of the impacts of drought to develop effective drought management strategies to mitigate its adverse effects on both the environment and society.

---

### 2.1.2.1. Drought (and water management) in the Mediterranean region

While droughts are a global phenomenon, their most severe consequences tend to occur in arid or semi-arid areas, where the availability of water is already limited. For example, semiarid environments are characterized by low water availability because the mean annual potential evapotranspiration is 2 to 5 times greater than the mean annual precipitation (Ponce et al., 2000; Stahl & Hisdal, 2004). In these regions, the water demand often exceeds the natural availability and societies depend on hydraulic infrastructure to adapt to semiarid conditions and droughts. As a result, droughts in semiarid regions can have a substantial impact on agriculture, ecosystems, and human health (Schwabe et al., 2013).

The dry summer season and marked annual precipitation cycle with little to no rainfall during summer, are inherent to the Mediterranean region. Additionally, the Mediterranean basin is a region particularly vulnerable to droughts. This region is considered one of the most exposed areas to the socioeconomic impacts of droughts, as highlighted by Seneviratne et al. (2012). As a result, effective drought management in this region is particularly challenging. Indeed, several studies have documented severe drought events in the last century (Vicente-Serrano, 2006; Sousa et al., 2011; Vicente-Serrano et al., 2014; Spinoni et al., 2015; Tejedor et al., 2017; Russo et al., 2019). Moreover, the Iberian Peninsula has been tackled by increased severity of droughts over the past few decades (García-Herrera et al., 2007; Belo-Pereira et al., 2011; Andrade & Belo-Pereira, 2015; Coll et al., 2017; Páscoa et al., 2017, 2021), with adverse environmental, agricultural, and economic impacts (Vicente-Serrano et al., 2011, 2014; Gouveia et al., 2012; Hoerling et al., 2012; Blauhut et al., 2015).

In the context of Spain, Domínguez-Castro et al. (2012) conducted a comprehensive assessment of extreme drought events spanning the period from 1750 to 1850. Furthermore, González-Hidalgo et al. (2018) presented a descriptive analysis focusing on more recent decades to shed light on drought events. Another study by García-Valdecasas Ojeda et al. (2017) specifically aimed to evaluate the effectiveness of the WRF model in detecting droughts within Spain.

In the Mediterranean region, the different types of drought and their impacts are strongly interrelated, making drought a complex phenomenon, further compounding the challenges of effective drought management. The arid and semi-arid climate of the region, combined with its high population density, heavy reliance on agriculture, and already limited water resources, has resulted in significant pressure on water supplies (Tramblay et al., 2020). In addition, intense water regulation exists to meet the needs of irrigation and drinking water needs. For instance, López-Moreno et al. (2009) highlight the complex nature of water management in the Tagus River basin due to seasonal streamflow regimes and severe changes in droughts caused by the exploitation of the Alcántara reservoir. Additionally, there are competing interests for water resources in the region, such as irrigation, drinking water, ecosystem conservation, and other uses.

The Mediterranean region faces a complex challenge when it comes to water resources management, due to the irregular distribution of water resources (Iglesias et al., 2007, 2012; Garrote et al., 2016). This region has historically experienced a high frequency of conflicts related to water use, leading to a need for intensive control of water resources to meet various water demands (Monreal & Amelin, 2010). To address the heterogeneity of water resources, different measures have been implemented at the national level. For example, water supply infrastructures have been constructed or upgraded to meet irrigation demands and ensure adequate public water

supply. However, the presence of reservoirs has been found to could be contributing to the aggravation of streamflow drought downstream (Van Loon et al., 2022). In Spain, for instance, Batalla et al. (2004) analyze the hydrological alterations caused by dams in the Ebro River basin.

Moreover, climate change predictions suggest a dryer and warmer Mediterranean area (Bates et al., 2008; Seneviratne et al., 2012) with increased droughts. Some studies have investigated trends in streamflow and found negative trends, resulting in lower streamflow in southern and eastern regions of Europe, while western and northern regions experience generally positive trends (Stahl et al., 2010, 2012). Therefore, changes in drought are also expected. More recently, Trambly et al. (2020) reported that the Mediterranean basin is projected to experience more frequent and severe droughts under future climate change scenarios, Figure 2-4. By 2100, it is estimated that the frequency of droughts in the region could increase by up to 40%. Finally, according to Gu et al. (2020), the Mediterranean region is one of the most vulnerable areas to the socioeconomic impacts of droughts, and this vulnerability is expected to worsen in the next years

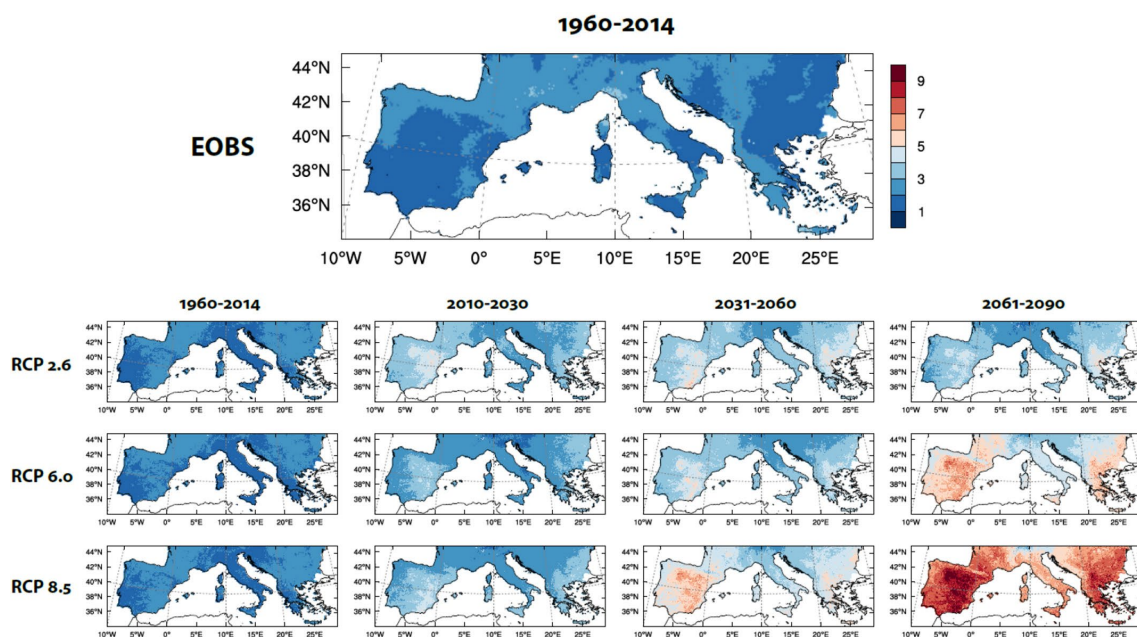


Figure 2-4 Drought duration from historical observations (E-OBS) during the period 1960–2014 and with RCP 2.6, 6.0, and 8.5 for three periods: near future (2010–2030), mid-century (2031–2060), and end of the century (2061–2090) for the Mediterranean region (Trambly et al., 2020).

In addition, projections from various model experiments indicate that future climate change scenarios will likely exacerbate the frequency and severity of droughts in this region (Trambly et al., 2020). However, significant uncertainties remain, given the complexity of the phenomenon and the intricate interrelationships among its impacts on ecosystems, agriculture, water resources, and other sectors. Therefore, it involves a significant obstacle in assessing and managing drought effectively in the Mediterranean basin.

### 2.1.3. The need for effective drought assessment

The complex nature of drought and its potential impact on various sectors, in both natural and human systems, have made it a topic of interest to a wide range of scientists. Consequently, a wide range of approaches have been developed to study drought, each with its advantages and

limitations. They vary from statistical methods to modern remote sensing and modeling techniques (Mishra & Singh, 2011).

Statistical analysis-based approaches serve as valuable tools for understanding the interconnections between various types of drought and characterizing their propagation. The statistical analysis offers several advantages in drought assessment. It is a relatively straightforward approach that can be applied to various datasets, including precipitation and streamflow. These methods provide quantitative measures and indices that help in quantifying the severity and duration of droughts. However, it is essential to acknowledge the limitations of statistical analysis in fully characterizing drought propagation. These approaches are not suitable to capture the underlying physical processes that drive drought dynamics. Furthermore, statistical analysis may not explicitly account for the complex interactions between climatic, hydrological, and human factors that influence drought occurrence and impacts.

Conversely, modeling approaches have been employed for studying drought propagation. To understand the process that leads to drought, the Land Surface Models (LSMs) offer a physically-based approach and thus they allow us to assess drought impacts and interactions on different variables through the water cycle. The use of LSMs in drought research has several advantages, including their ability to incorporate various land surface characteristics including human influences, their flexibility in modeling different land use types, and their ability to be applied across different spatial and temporal scales. But they do have important limitations such as uncertainties in input data and challenges in capturing the complex interactions between various factors influencing droughts.

Overall, a combination of both approaches provides a comprehensive understanding of drought propagation, taking into account both statistical relationships and physical processes. Moreover, advances in remote sensing and data availability have expanded our ability to study drought, but uncertainties remain (Aghakouchak et al., 2015; Gaona et al., 2022).

Despite extensive research on various aspects of drought, there is a significant gap in effectively communicating the results to decision-makers (Thompson et al., 2013). Moreover, (Thompson et al., 2013; Verburg et al., 2016) reinforce the necessity to develop a framework that takes into account the interactions between hydrology and other sub-systems such as vegetation, land use, and anthropogenic uses. For example, Iglesias et al. (2007) present a proactive approach to mitigate the impacts of droughts in the Mediterranean region. Instead of relying on crisis management, their framework emphasizes preparedness and risk reduction. Thus, the objective of these insight frameworks can aid in developing strategies to mitigate its effects on society and the environment in the Anthropocene (Verburg et al., 2016). Nevertheless, developing such systems is challenging due to the inherent uncertainties associated with climate models and the complex nature of the drought phenomenon.

## **2.2. Modeling the water cycle and drought**

Water movement and storage in the Earth's systems have a significant impact on water availability for both humans and ecosystems. This relationship can lead to natural hazards, such as floods and droughts. Likewise, with the increasing demand for water resources and the growing threat of droughts, it is essential to monitor and understand the behavior of the water cycle in various

climatic conditions. Hence, modeling the water cycle, and understanding underlying processes, is a crucial area of research in hydrology.

Modeling is an essential tool in hydrology that enables the simulation and prediction of the complex dynamics of the water cycle. Hydrological research has traditionally focused on understanding the precipitation-runoff process, evaporation, surface water-groundwater interactions, and water supply and demand in basins. However, recent studies have treated the water cycle as a more integrated system. As a result, comprehensive studies of water systems have become increasingly popular and have led to the development of various sub-disciplines, such as eco-hydrology (Acreman, 2001; Hannah et al., 2004; Wood et al., 2008) and socio-hydrology (Di Baldassarre et al., 2013, 2015; Ross & Chang, 2020).

The use of land surface models (LSMs) in hydrological studies has experienced a notable upswing in recent times. These models have proven to be indispensable tools for investigating the intricate dynamics between the land surface and the water cycle in comparison with the classical hydrological models (Vidal et al., 2010). By simulating various physical processes, such as evapotranspiration, soil moisture dynamics, and runoff generation, LSMs offer a comprehensive understanding of water fluxes and storage within the land surface. This enhanced understanding enables us to accurately assess water availability, study the impacts of climate change on hydrological systems, and devise effective strategies for sustainable water management.

### **2.2.1. Background**

Modeling the hydrological cycle, at different scales, both temporal and spatial is essential to understand natural (and human-induced) water flows. Hence, a variety of models have been developed for spatial scales that range from a small catchment to the global scale; and for temporal scales that range from the intense precipitation event (and subsequently peak flow) to climate scales. Of course, both spatial and temporal scales are not independent and models for larger domains tend to focus on longer time scales. Hydrological models vary in complexity from simple conceptual models with a few parameters that represent the movement of water through a catchment using simplified equations, to complex physically-based models that simulate the physical processes involved in the water and energy cycles. The choice of model type depends on the research question, the scale of analysis, and the available data.

The recognition of the “global water system” has emerged as a significant paradigm in the field of hydrology, emphasizing the interdependencies between water flows and other interconnected systems, including economic and institutional factors (Alcamo et al., 2008). In response to this, there has been a growing effort to develop models and associated processes that enable simulations that transcend the boundaries of stand-alone hydrological models. This facilitates a more comprehensive understanding of the complex interactions within the water system. By incorporating the physical relationships, these integrated models strive to provide a holistic representation of the global water cycle and its implications for sustainable water management strategies.

Therefore, process descriptions are becoming more physically based resulting in the physically-based models that provide a most detailed representation of the water cycle. Thus, Land Surface Models (LSMs), initially created to aid in atmospheric and climate modeling purposes, emerged and are used for large-scale hydrological modeling and prediction of extreme events. The LSMs simulate both water and energy balances at the land surface. Additionally, the LSMs often

represent the soil with a higher vertical resolution and represent evapotranspiration and other processes (such as snowmelt) less conceptually than the hydrological models. Nevertheless, LSMs do not simulate, or do roughly, the impact of human water use, and even they often lack a lateral routing and groundwater representation. The latter results in poor simulation of river discharge during the summer season, making it subject to improvement (Stahl et al., 2011; Gudmundsson, Tallaksen, et al., 2012).

The use of models in water management has increased in recent years, driven by the need to manage increasingly scarce water resources and mitigate the impacts of climate change on the water cycle (Vörösmarty et al., 2015; Döll et al., 2016). However, model uncertainty remains a major challenge in hydrological modeling, and efforts to improve model accuracy and reduce uncertainty are ongoing areas of research in hydrology (Sood & Smakhtin, 2015). However, the complexities of hydrological systems heavily influenced by humans make this task difficult.

### **2.2.2. Addressing the complexities in low-flow modeling**

Despite the numerous models to simulate natural (and human) flows, most of them are optimized to simulate peak flows, and thus, low flows are often not well reproduced by these models (Smakhtin et al., 1998; Lehner et al., 2006; Kumar et al., 2010). Modeling low flows through hydrological models is still a challenging task due to the complexity of low-flow generation processes (Smakhtin, 2001; Staudinger et al., 2011). Low flows are generally controlled by subsurface storage and the slow response of groundwater systems. Therefore, capturing the low flow regime requires models that accurately simulate groundwater and surface water interactions. This is often one of the main weak points of the LSM community.

In recent years, attempts have been developed to improve low-flow modeling in established models, some of them are discussed in section 6.3. The level of complexity often depends on the availability of data and the research questions being addressed. Furthermore, as Clark et al. (2008) point out, the choice of the model structure is just as crucial as the choice of model parameters. The model structure determines the type of hydrological processes that can be represented and the level of detail in the model's parameterization. A suitable model structure will depend on the specific characteristics of the hydrological system under study, including its geology, topography, and climate. Each model has a very different model structure and parametrizations, and therefore very different responses, which the choice cannot be made easily (Staudinger et al., 2011; Van Loon et al., 2012).

In the context of low-flow modeling, incorporating groundwater schemes into the simulations is a complex task that involves a detailed knowledge of the hydrogeological characteristics of groundwater systems that can accurately represent the complex interactions between surface water and groundwater (Habets et al., 2008; Vergnes et al., 2012). Furthermore, hydrological and hydrogeological communities have limited the exchange of ideas, methodologies, and data, impeding holistic approaches to water resource management. However, in recent years, there has been a growing recognition of the need for integrated hydrological and hydrogeological modeling to address water-related challenges effectively.

In addition, low-flow modeling has been a topic of concern in recent years, especially in simulating drought propagation processes. It has been observed that models fail to accurately simulate some of these processes, indicating a strong coupling between precipitation and runoff generation (Van Loon et al., 2012; Quintana-Seguí et al., 2020). Such immediate reaction of



runoff to precipitation, which does not occur in some regions, such as arid or semi-arid, nor in catchments with significant storage capacity. These difficulties suggest the need for improved simulation of processes related to storage in large-scale models.

Moreover, model outputs are frequently evaluated based on how accurately they can replicate the shape of a hydrograph and the corresponding flood peaks and volumes. While these criteria are essential, they do not necessarily indicate the accuracy of low-flow simulations. In this context, it is crucial to use other evaluation criteria that provide insight into the model's performance in the low-flow domain (Smakhtin et al., 1998; Staudinger et al., 2011)

### **2.2.3. The application of LSMs for drought assessment**

Low flow conditions and drought exhibit a close interconnection in the field of hydrology, as they are integral components of the natural water cycle. Low flows are encompassed within the concept of hydrological droughts, however, hydrological droughts, in a broader sense, encompass several factors beyond low flows (Smakhtin, 2001; Van Loon, 2015). Despite their distinctive characteristics, both droughts and low flows encounter similar modeling challenges, highlighting their interconnected nature and the importance of studying and understanding them together.

Droughts are a serious problem that affects many regions of the world, with significant economic, social, and environmental impacts, as previously discussed. Hence, the analysis of the hydrological cycle, particularly droughts, has been greatly enhanced by the utilization of Land Surface Models (Lehner et al., 2006; Vidal et al., 2010; Prudhomme et al., 2011; Van Loon et al., 2012; Mo & Lettenmaier, 2014; Xia et al., 2014).

In recent years, LSMs which simulate the energy balance between vegetation, soil, and atmosphere, have emerged as an important tool for assessing and monitoring drought conditions (Sheffield et al., 2014; Wood et al., 2015). Moreover, due to their physical nature, LSMs simulate a majority of the processes associated with the propagation of drought throughout the system (Vidal et al., 2010). Therefore, they are well-suited for studying drought-related processes. In addition, LSMs are crucial components of drought prediction systems (Wood et al., 2015; Thober et al., 2015).

One of the key advantages of LSMs for drought assessment is that provide a comprehensive and accurate picture of the current system conditions. This is particularly important in regions where data are limited or unreliable, and where traditional methods of drought assessment, such as the standardized precipitation index (SPI), may not provide a complete or accurate assessment of drought severity. However, it should be acknowledged that LSMs are susceptible to uncertainties in the forcing data as well as the model structure. In their study, Quintana-Seguí et al. (2020) found that the duration of drought propagation, from precipitation to soil moisture and streamflow, is significantly influenced by the LSM model structure

The LSMs also provide a useful framework for investigating the underlying causes and mechanisms of drought. LSMs can identify the relative contributions of different factors, such as changes in the main hydrological variables (evapotranspiration, soil moisture, and runoff) to the onset as well as the persistence of drought. In a recent study, Gaona et al. (2022) identified critical feedback for both antecedent and subsequent drought conditions with a fundamental role of evapotranspiration in the relationship between rainfall and soil moisture. It also further underlines

the importance of analyzing drought at a weekly scale, to better identify the quick self-intensifying and mitigating drought mechanisms, which are relevant for drought monitoring in semi-arid areas.

Barella-Ortiz & Quintana-Seguí (2019) evaluated the accuracy of drought representation through the use of regional climate models (RCMs). Their findings indicate that RCMs can enhance the representation of meteorological drought, which is a crucial aspect of drought characterization. However, uncertainties are also identified in RCMs' ability to accurately capture soil moisture and hydrological drought, as well as the propagation of drought.

Another instance where LSMs have been applied to study drought is (Crow et al., 2012). They examined the effectiveness of different land surface models (LSMs) in agricultural drought monitoring. Their research revealed that when globally averaged across the entire annual cycle, LSMs have limited impact on the accuracy of agricultural drought monitoring systems, however, these models can provide significant added value (ranging from 5% to 15% in relative terms) during specific points along the seasonal cycle.

Overall, LSMs represent a powerful and flexible tool for drought assessment and management, with the potential to improve our understanding of the causes and impacts of drought, and to support more effective and sustainable water resource management practices (Hao et al., 2014; Nijssen et al., 2014).

## 2.3. The current state of the LSMs

Land surface models (LSMs) are numerical models that simulate fluxes of water, energy, and carbon between the earth's surface and the atmosphere. In recent years, significant progress has been made in the development of these models for simulating the water cycle (Blyth et al., 2021). These models have become increasingly sophisticated over time, incorporating more realistic representations of the physical and biogeochemical processes that govern land surface dynamics and thus the influence on the water cycle. This section provides a general overview of the advancements in LSM to understand the water cycle, as well as the limitation and further improvements. Additionally, a description of the current challenges of these models to represent the human-natural system is presented.

### 2.3.1. Overview of the Land Surface Models

LSMs were initially created to aid in atmospheric and climate modeling purposes, however, land surface processes and their impacts themselves have gained relevance in recent years. Over time, LSMs have undergone significant improvements, incorporating a multitude of processes that impact the dynamics of land-atmosphere interactions, Figure 2-5. From their initial simple biophysical configurations (Sellers et al., 1986), they have evolved to include representations of a range of processes, such as soil moisture dynamics, hydrological processes, vegetation dynamics, and biogeochemical cycles (Lawrence et al., 2019) until human land management (Döll et al., 2016; Wada et al., 2017).

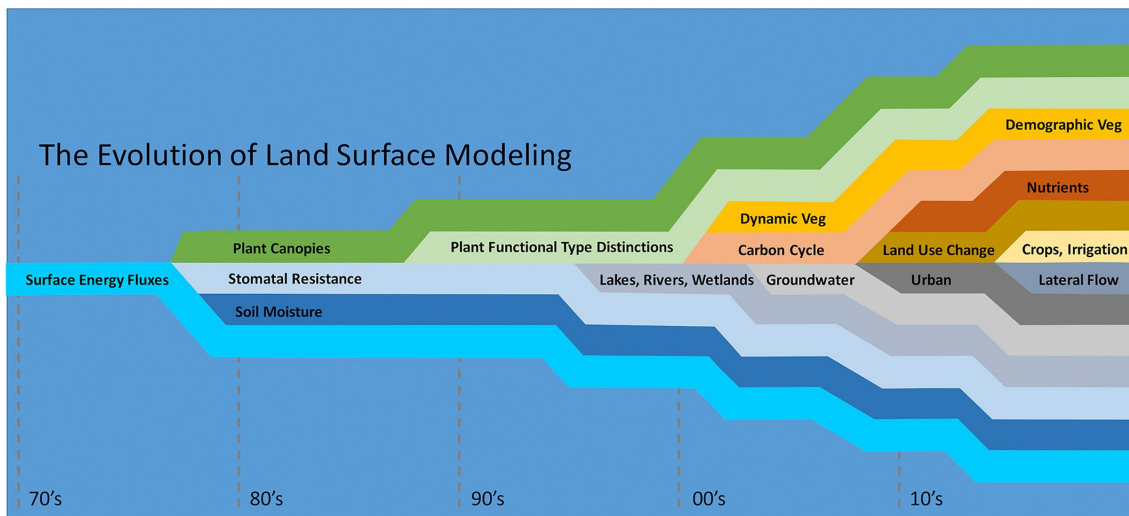


Figure 2-5 Chronological overview of the development of land surface models (Fisher & Koven, 2020).

LSMs may be coupled with atmospheric models (online) or can be run offline, forced, for instance, by a gridded dataset of atmospheric observations. Online simulations include the feedback between the land surface and the atmosphere, which is physically more realistic, but they inherit the biases of the atmospheric model. In the offline case, the surface energy and water balance are simulated without explicit feedback to the atmosphere, but if the forcing dataset is based on observations, the atmospheric forcing will have fewer biases. Offline simulations have proven to be crucial in hydrology research, as they allow for the isolation and examination of individual land surface processes. By separating the land surface model from the atmospheric model, offline simulations can provide more accurate and precise estimates of water and energy fluxes, soil moisture dynamics, and other hydrological variables, despite the missing explicit feedback.

### 2.3.2. The structure and components

While LSMs are complex models that incorporate numerous processes and mechanisms, this subsection aims to provide an understanding of the different components that make up these models. As such, it does not delve into each mechanism's intricate details but offers a simplified overview of the main elements. Wood et al. (2011), Lawrence et al. (2019), Decharme et al. (2019), and Blyth et al. (2021) provide an extensive review of the state-of-the-art of LSMs. The structure of the LSM models could be grouped into (i) vegetation and canopy representation, (ii) soil physics, (iii) water bodies and hydrology, and (iv) land and water use, as depicted in Figure 2-6.

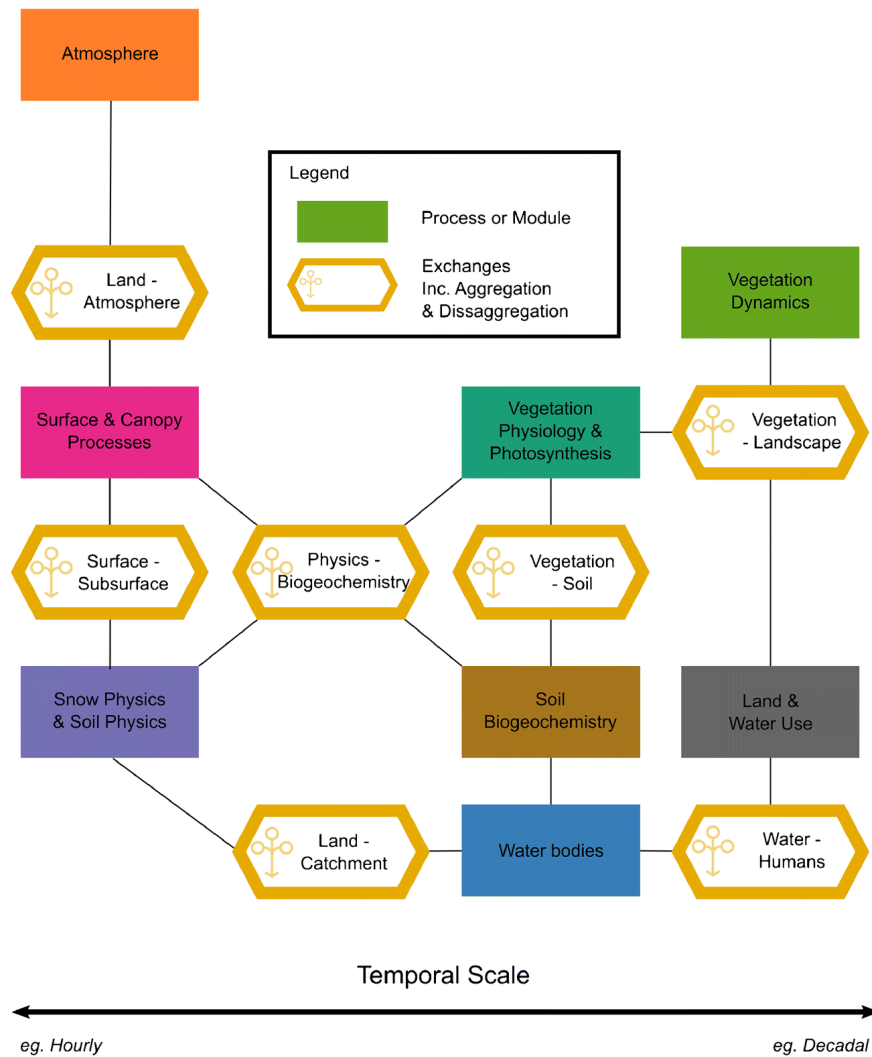


Figure 2-6 Schematic representation of the LSMs' components and their exchanges between them (Blyth et al., 2021).

The vegetation and canopy components of LSMs simulate the exchange of energy, water, and carbon between the land surface and the atmosphere. Canopy models incorporate various physical, chemical, and biological processes to describe the behavior of vegetation. These models typically rely on remote sensing data and assume a uniform distribution of leaves within the canopy.

As an example of advancements in the field, (Calvet et al., 1998) added an interactive vegetation algorithm to ISBA (Noilhan & Planton, 1989) -SVAT (soil-vegetation-atmosphere transfer) scheme, called ISBA-A-gs. More recently, research conducted by Boone et al. (2017) and Napoly et al. (2017) has played a crucial role in enhancing our understanding of vegetation dynamics within the SURFEX (Surface Externalisée, in French) platform (Masson et al., 2013). Boone et al. (2017) focused on the development of an explicit representation of vegetation, called the ISBA multi-energy balance (MEB). Similarly, Napoly et al. (2017) conducted an in-depth evaluation of this explicit vegetation representation for local-scale forest sites in France.

The soil component of LSMs plays a crucial role in stimulating energy and water transfer vertically through the soil. Soil models incorporate various physical, chemical, and biological processes to describe the behavior of soil, including soil water balance, soil temperature, and soil

nutrient cycling. These models can vary in complexity depending on the research question and available data. Whereas the hydrology component simulates the movement and storage of water through the land surface, including surface runoff, infiltration, and groundwater recharge. At the simplest level, bucket models can be used to simulate the water balance by dividing the land surface into a few water storage compartments, such as soil moisture and surface water.

The land and water use component in LSMs is an important component that captures the impact of human activities on the land surface and water cycle. This component represents the management of land and water resources by humans, including various agricultural practices, land-use changes, irrigation schemes, reservoir operations, and groundwater withdrawal.

Finally, the structure and configuration of LSMs can vary widely depending on the components included in the model. This flexibility allows for LSMs to be tailored to specific research questions or applications, and to capture the complexity of land-atmosphere interactions at different scales. For example, some LSMs may include only the bare minimum of components necessary to simulate surface fluxes of energy and water, such as a simple vegetation model and a soil water balance model. On the other hand, more advanced LSMs can incorporate additional components such as the carbon cycle, nutrient cycling, and vegetation dynamics. These models are typically more complex and computationally intensive but can provide more accurate simulations of ecosystem processes and feedback to the Earth system.

### **2.3.2.1. The key processes involved**

The LSMs use a combination of physical laws and empirical relationships to represent these complex processes in a simplified way that can be used for weather and climate prediction. For example, to represent canopy processes LSMs model the interactions between vegetation and the atmosphere, throughout photosynthesis, transpiration, and carbon uptake (Sellers et al., 1996; Wang & Leuning, 1998). More detailed canopy models aim to capture these interactions by simulating the physiological processes of individual leaves (Bonan et al., 2014).

The ISBA scheme within the SURFEX platform has made significant strides in recent years, leading to important developments in the field. One notable advancement is the introduction of the ISBA-A-gs model, which represents a breakthrough in simulating the combined processes of photosynthesis and stomatal conductance, as well as the response of leaf transpiration to atmospheric carbon dioxide concentration (Calvet et al., 2004, 2008; Gibelin et al., 2006; Albergel et al., 2010). Precipitation undergoes various processes once it reaches the land surface. It can either infiltrate through the soil matrix and get stored or be lost through evapotranspiration or drainage. If the precipitation accumulates on the soil surface, it can evaporate, or in the case of sloped terrain or saturated soil, it can lead to surface runoff. To simulate these complex water exchanges between the surface and soil, most LSMs use the TOPMODEL basis (Beven & Kirkby, 1979; Todini, 1996), which considers the spatial distribution of contributing areas to simulate the movement of water through the landscape. In recent years, LSMs have incorporated deeper soil layers into their models (Miguez-Macho et al., 2007) and improved organic soil representation (Lawrence & Slater, 2008). This has enhanced the soil's thermal and hydrologic dynamics on longer timescales (Lawrence & Slater, 2008) and has enabled a better representation of soil carbon processes.

Water movement on the surface plays a critical role in the terrestrial water cycle, as it determines the timing and magnitude of flows to the oceans. To accurately estimate these flows, it is

necessary to incorporate a routing scheme into LSMs (Lohmann et al., 1996; Oki et al., 1999). Traditionally, routing schemes have been developed to estimate runoff without considering the interaction between energy and water balance. However, recent studies have shown that water flows can have a significant impact on the energy balance. For instance, Fan et al. (2013) demonstrated that groundwater can alter the energy balance in the Iberian region. As a result, there has been a growing interest in including groundwater models in LSMs to better capture the interactions between water and energy (Miguez-Macho et al., 2007; Miguez-Macho & Fan, 2012). Several attempts have been made to develop groundwater models that can be incorporated into LSMs, such as those proposed by de Graaf et al. (2015, 2019). By incorporating groundwater models, LSMs can more accurately represent the complex feedback between water and energy in the terrestrial system, leading to improved predictions of future hydrological and climate conditions.

Water management practices have significantly altered the natural water flows and storage in the hydrological systems due to human activities such as land management, water abstractions, and the construction of dams. Agricultural irrigation, for example, has a considerable impact on the energy balance of a region. Many LSMs have incorporated irrigation schemes, in which water is artificially supplied rather than sourced from reservoirs or surface water bodies, that trigger irrigation when soil water drops below a certain threshold (Sacks et al., 2009). This approach can be used to investigate how increased evaporation due to irrigation influences local and regional weather and climate (Sorooshian et al., 2012; Tuinenburg et al., 2014). However, to obtain a comprehensive understanding of human intervention in hydrological systems, models must consider various processes such as water withdrawal from surface and groundwater sources, and reservoir operations (Pokhrel et al., 2016; Calvin & Bond-Lamberty, 2018; Yokohata et al., 2020). Incorporating these processes in LSMs enables more realistic simulations of human-induced impacts on the hydrological system and provides a complete picture of the water and energy balance of a region.

### **2.3.3. Main limitations and uncertainties**

The current generation of LSMs now includes representations of sub-grid variability, vegetation dynamics, and soil heterogeneity, which have significantly improved our ability to capture the spatial and temporal dynamics of the water cycle. Improving the exchanges between the land and atmosphere is crucial to increasing the complexity of component models in LSMs. The exchange must respond to both the temporal and spatial scale of the atmosphere model and urban land surfaces must also be better represented to address the increasing need for finer-scale modeling for human health and well-being.

The largest limitation in present LSMs is sub-grid heterogeneity (Ament & Simmer, 2006; De Vrese & Hagemann, 2016). For instance, most models use a single set of soil data that may not be adequate for all regions. To improve the representation of soil properties, it may be important to include the changes in soil properties with time (Wang & Feddema, 2020). Incorporating detailed process understanding into LSMs for catchment and smaller scales is a recent development, and it is important to capture how the flow and storage of water across a landscape are regulated by fine-scale topographic features (Wood et al., 2011; Fan et al., 2019).

Detailed sourcing data to describe human-influenced environments is a major challenge for developing global-scale models that include these human processes. Additionally, including other quantities such as the impact on the temperature of river water or the use of agricultural fertilizers

(Bussi et al., 2016) is important when addressing water resources. Although some models include detailed descriptions of water management activities, they often rely on the prescription of simple operating rules (Hanasaki et al., 2018). Future developments will need to better represent the optimal management of complex catchments while considering economic and social impacts.

The uncertainty in LSM parameters can arise from a variety of sources, including input data (Döll & Fiedler, 2008; Biemans et al., 2009), simplified model structures, and the complexity of land surface processes (Walker et al., 2018). Many of the parameters used in LSMs are also site-specific and can vary across different regions or vegetation types, which can further complicate parameter estimation and lead to uncertainty in model predictions (Samaniego et al., 2010). For example, Samaniego et al. (2013) demonstrated that parametric uncertainty of simulated soil moisture plays a strong spatiotemporal variability in drought characteristics. Weihermüller et al. (2021) showed that the parameterization of soil hydraulic properties in LSMs introduces notable variability in the simulated fluxes. Hence, the accuracy of LSM predictions for future scenarios is limited by the uncertainty in model parameters or inputs and the ability of the models to capture the full complexity of land-atmosphere interactions under changing conditions.

Furthermore, one of the critical problems is quantifying the role of humans in the Earth System. Linking LSMs with integrated models that capture feedback between climate, food, water, and land-use are necessary to address this (Yokohata et al., 2020). This will enable future LSMs to address key societal and scientific questions related to ecosystem resilience under a range of environmental and anthropogenic pressures.

## 2.4. Recent Advances in the LSMs

LSMs were initially developed to provide physical boundary conditions for atmospheric and climate models, particularly to represent the influences of the land in meteorological processes (Fisher & Koven, 2020). Later the aims and applications of LSMs have expanded considerably. By simulating the behavior of land surface processes, such as water cycling and biogeochemical cycling, LSMs offer a means to assess the impacts of future climate scenarios, especially under global warming (Cox et al., 2000). Additionally, the integration of anthropogenic factors, such as irrigation or water abstractions, into LSMs has gained significant attention in the scientific community to better understand the different impacts that human activities have on modifying the land surface and water cycle (Lawrence et al., 2012; Boysen et al., 2014; Pongratz et al., 2018; Yue et al., 2018).

The incorporation of process representations into LSMs is accelerating due to the needs of diverse user communities, including hydrologists, ecologists, atmospheric scientists, and crop modelers. These communities have increasingly recognized the importance of accurately representing land surface processes and their impacts on the broader Earth system, thus making LSM an interdisciplinary tool.

In recent years, LSMs play a critical role to inform decision-making related to natural resource management, such as water availability and crop production, and provide critical insights into the vulnerabilities and resilience of ecological and societal systems to events such as floods and droughts. As a result, the LSMs have become an increasingly important tool for understanding and investigating the complex feedback between the land surface, the atmosphere, and human activities on the Earth system.

### 2.4.1. Advances in model complexity

The continued incorporation of processes into LSMs has also increased the complexity of these models. This reflects the reality that the Earth is a complex system and that the interactions between land, atmosphere, and water systems are highly interconnected and dynamic. The inclusion of more detailed process representations within LSMs recognizes the importance of capturing the complexity of these interactions and their impacts.

Incorporating different processes in LSMs the modular approach is widely used. This approach involves dividing the models into smaller and more manageable modules, each representing a specific process or component of the land surface system. By doing so, these modules can be developed, improved, or removed independently, and then combined as needed to create a more complex and comprehensive model. The modular approach has made it easier to update or modify specific components of the model without affecting other parts. A comprehensive exploration of large-scale models utilizing a modular structure can be found in the literature, e.g. (Bierkens et al., 2015; Blyth et al., 2021). Additionally, modularization can allow for greater flexibility in terms of representing different configurations within a given model.

At lower resolutions, numerous inaccuracies in prognosis and the strong non-linearity of the land surface processes are notable (Sellers et al., 2007). To deal with this, Wood et al. (2011) described the hyper-resolution models for hydrological applications, to improve the representation of surface interactions. Later, recent LSMs implemented a gridded tile approach to take account and disaggregate the heterogeneity of various surface processes, e.g. SURFEX (Masson et al., 2013), ORCHIDEE (de Rosnay & Polcher, 1998; Guimberteau, Drapeau, et al., 2012) and JULES (Best et al., 2011) to name few. On the other hand, while early land surface models were primarily focused on representing one-dimensional processes, recent years have seen a growing emphasis on including vertical detail in model development (Clark, Nijssen, et al., 2015). This increased vertical resolution has enabled more robust comparisons between model simulations and field data. Enhancing resolution poses a significant challenge, given the intricate nature of the continental surface, the diverse range of processes operating at various time scales, the lack of accurate information, and the inherent uncertainty associated with parameters (Wood et al., 2011; Bierkens et al., 2015; Clark, Nijssen, et al., 2015).

Finally, artificial intelligence (AI) and machine learning (ML) are rapidly increasing in the water cycle and water resources analysis. Besides, the increasing availability of data and computational resources, these techniques have the potential to transform the field of water resources management and facilitate the development of more sustainable and efficient water use practices. Machine learning opens a new and promising perspective to a detailed process-level understanding where solving complex equations is computationally too expensive for a given application (Fisher & Koven, 2020). In this case, models based on machine learning approaches that have been trained on the full process representation models may allow for higher fidelity solutions than the current, purely process-driven approach used across LSMs.

In this regard, leveraging techniques such as machine learning and data mining can enhance model precision by providing more efficient and accurate methods for obtaining physiographic data and parameter estimation (Shen, 2018; Sawada, 2020; Schmidt et al., 2020). These techniques enable the analysis and processing of large volumes of geospatial data, facilitating the identification of complex patterns and relationships. By employing these techniques in enhancing physiographic representations and parameter estimation, more precise and reliable results might be obtained in



modeling the water cycle and its interactions with the environment. One of the key challenges with AI models is their lack of interpretability. Complex AI algorithms, can produce accurate predictions but provide little insight into the underlying physical processes (Schmidt et al., 2020). Thus, the interpretability of ML models should be carefully investigated to further explore understand and validate the model's outputs. Future research should focus on developing interpretable AI models, enhancing generalization capabilities, quantifying uncertainties, addressing biases, and making AI approaches computationally feasible for broader application in hydrological modeling and water resource management (Pal & Sharma, 2021).

Given the increasing emphasis on machine learning approaches and the successes of machine learning in solving problems in Earth System Models (Gentine et al., 2018; Shen, 2018) or offline hydrologic models (Bai et al., 2016; Fang et al., 2017) designing models with an emphasis on modular complexity to allow for such hybrid approaches is a crucial challenge in modeling the land surface.

### **2.4.2. The use of remote sensing in LSMs**

Recently, the use of remote sensing has provided an unprecedented opportunity to fill the spatial and temporal gaps in ground-based observations for large-scale modeling. Remote sensing has rapidly become an essential tool for land surface modeling, allowing for the observation and measurement of surface properties and processes through different scales (Overgaard et al., 2006). Additionally, advancements in data assimilation techniques have facilitated the integration of multiple sources of data, including remote sensing, to improve the representation of processes in LSMs (Reichle et al., 2004; Albergel et al., 2017).

Advancements in satellite Earth observation have significantly improved our ability to monitor various aspects of the Earth's surface covering different topics. For instance, the Tropical Rainfall Measuring Mission (TRMM) and Global Precipitation Measurement - Integrated Multi-satellitE Retrievals (GPM-IMERG) provide precipitation data, while the Shuttle Radar Topography Mission (SRTM) provides high-resolution topography data useful for global and regional water transport and groundwater modeling. Meanwhile, products such as the Moderate Resolution Imaging Spectroradiometer (MODIS), Sentinel 2, and Landsat satellites provide data on vegetation development and stress. To monitor surface soil moisture, satellites such as the Advanced Scatterometer (ASCAT), Soil Moisture and Ocean Salinity (SMOS), Soil Moisture Active Passive (SMAP), and Sentinel 1, have been launched, to name a few. These observations are used to inform and constrain the parameterization of models, which in turn improves their accuracy and predictive capabilities.

Moreover, remote sensing has also enabled a better evaluation of human activities in hydrological models (Famiglietti et al., 2015). Winsemius et al. (2009) demonstrated the use of combinations of available remote sensing products to force, calibrate, and/or validate hydrological models to increase understanding of hydrological behavior and the influence of human activities. However, satellite-derived products have inherent uncertainties and limitations, such as limited temporal coverage and significant uncertainties due to certain algorithms used to derive the desired geophysical product. Despite these limitations, the advancements in remote sensing have greatly improved our understanding and modeling of the Earth's surface and this is, in turn, helping improve LSMs.

### 2.4.3. Progress of LSMs in the modeling of the Mediterranean region

Land Surface Models (LSMs) have evolved in the last years, they were designed originally to simulate the energy and mass balances of the Earth's surface until incorporating more physical and biological processes to meet the growing demands of the research and user communities, as discussed in the previous subsections and section 2.3. In recent years, there has been a growing interest in enhancing LSMs to better capture the effects of drought in arid and semi-arid regions, with improved physics and parameterizations aimed at improving the accuracy of hydrological response in LSMs' simulations.

In this context, the SURFEX platform has undergone a significant number of improvements, showcasing advancements that have expanded its capabilities and enhanced its performance. While some of these enhancements were previously mentioned (see section 2.3.2), numerous other advancements have significantly contributed to the platform's capabilities. For instance, researchers have focused on the development of a multi-layer approach to explicitly represent sub-surface heat transfer, resulting in more accurate simulations (Boone et al., 2000; Decharme et al., 2016). Additionally, efforts have been made to refine soil hydrological processes, further enhancing the platform's representation of the water cycle (Boone et al., 2000). Furthermore, (Boone & Etchevers, 2001) dedicated research towards improving the realism of snowpack simulations within SURFEX. More recently, Guinaldo et al. (2021) introduced a novel lake mass module called MLake (Mass-Lake Model) into the river-routing model CTRIP. This addition has allowed for more comprehensive modeling of lake dynamics and their interactions. In a similar vein, Sadki et al. (2023) incorporated the DROP (Dam-Reservoir Operation) model into the ISBA-CTRIP model, specifically focusing on its implementation within Spain.

Recent other studies have been exploring ways to enhance the representation of physical processes in LSMs. For instance, Gelati et al. (2018) presented a hydrological assessment of atmospheric forcing uncertainty in the Euro-Mediterranean. They reported that atmospheric forcing uncertainty has a significant impact on hydrological processes, particularly in regions with high variability in precipitation and temperature. Leroux et al. (2018) implemented satellite-derived Surface Soil Moisture and Leaf Area Index products to improve the monitoring quality of land surface variables in the Euro-Mediterranean region and reported positive impacts. On the other hand, incorporating water vapor transfer into LSMs has been demonstrated to significantly enhance simulated soil moisture and evapotranspiration, particularly in semiarid regions (Garcia Gonzalez et al., 2012).

Although there have been advancements in the representation of physical processes in LSMs there are still challenges (section 2.3.3) in accurately capturing atmosphere-land interactions in semiarid Mediterranean environments. Hogue et al. (2005) depicted that LSMs face difficulties in accurately capturing the spatial heterogeneity of semi-arid environments, leading to significant variations in their performance across sites with similar characteristics.

In addition, the Mediterranean landscape is significantly influenced by anthropogenic processes such as reforestation and agricultural practices (including irrigation) and reservoir buildings. However, the incorporation of these anthropogenic processes within LSMs is important for regions like this, especially, since incorporating irrigation into LSMs is challenging since detecting and quantifying irrigation at a plot scale over large areas is difficult. This involves two

aspects: mapping irrigated areas and representing the physical process and impacts of irrigation, both of which present their unique challenges (Tramblay et al., 2020).

#### 2.4.4. Incorporation of the human dimension into LSMs

The Earth's hydro-climatic components are intertwined with human factors, shaping the overall functioning of the Earth's system (Pokhrel et al., 2016). The schematic framework, depicted in Figure 2-7, illustrates the intricate linkages between human influences and the Earth system, providing insights into the pathways through which human activities can influence critical processes within the hydro-climatic system.

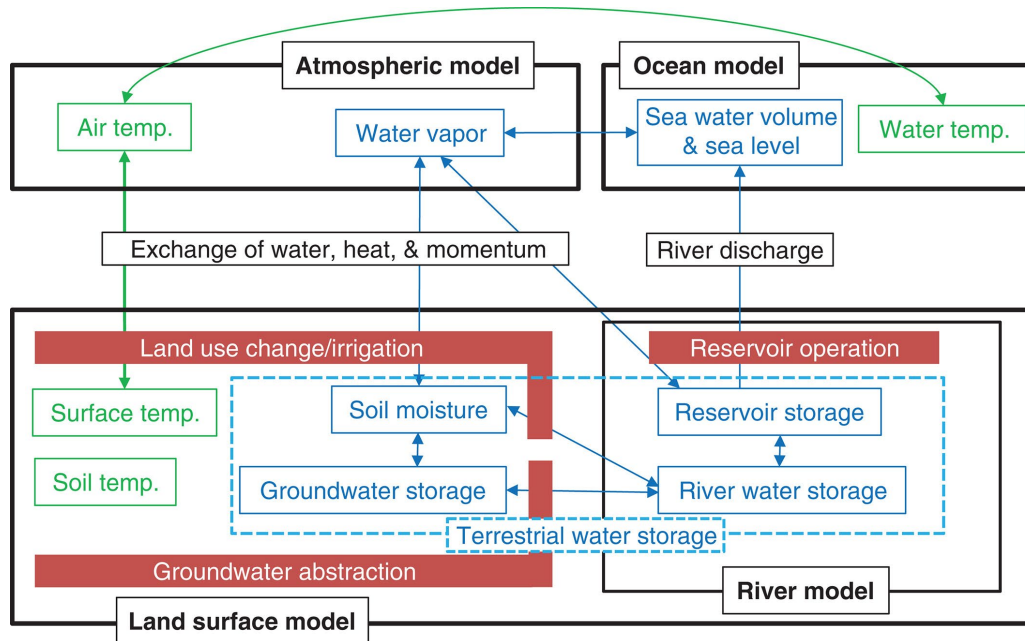


Figure 2-7 Schematic illustrating the interconnections and impact pathways between human land-water management practices and the simulated land-atmosphere-ocean processes within Earth System Models (Pokhrel et al., 2016).

Land Surface Models have focused on natural processes such as vegetation dynamics, soil moisture, and energy exchanges. Nevertheless, human activities have significantly impacted the natural water flows and storage on the land surface of the Earth (Vörösmarty & Sahagian, 2000; Rost et al., 2008; Sterling et al., 2013), highlighting the need for a comprehensive characterization of freshwater systems, as shown in Figure 2-1, that includes both their natural and human components (Oki & Kanae, 2006; Döll et al., 2016). Hence, to better understand the complex interplay between human activities and natural systems, current LSMs must incorporate anthropogenic factors into their representations, Figure 2-8.

Although LSMs have the potential to incorporate human factors, their representation in current generation models is often limited to fully capturing the complexity of their interactions with natural processes, mainly because human representations are rather simple (Pokhrel et al., 2016; Wada et al., 2017). Thus, incorporating human activities into global LSMs remains a significant challenge.

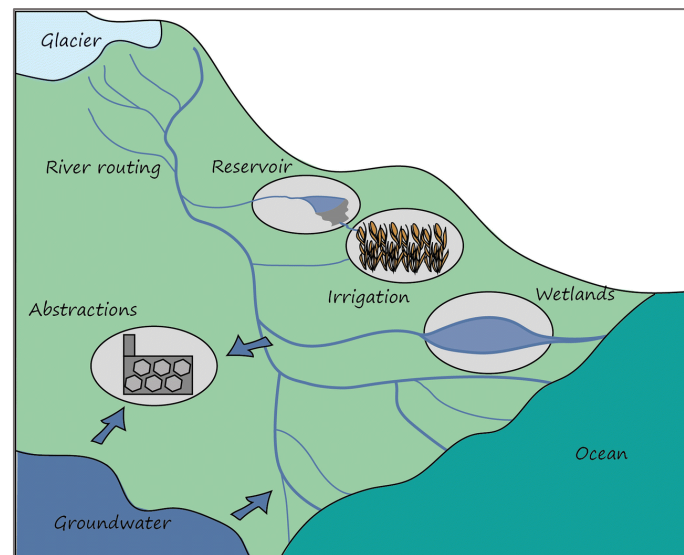


Figure 2-8 Schematic representation of exchange between water and main human systems (Blyth et al., 2021).

The goal of this section is not to delve extensively into the existing literature on human impact modeling. Instead, its purpose is to provide an overview of the current status of large-scale hydrologic modeling within the context of how humans interact with water systems, particularly regarding reservoir management and irrigation practices.

For instance, primarily advances have been focused on incorporating human activities with the main objective of assessing water resources availability and use at global to regional scales (Alcamo et al., 2003; Döll et al., 2009; Van Beek et al., 2011), and more recently progress in incorporating human land-water management into global land surface models, especially in land use change (particularly irrigation practices), reservoir operation, and groundwater (Figure 2-7).

Some examples of studies that have incorporated human-water management into their schemes. For instance, Alcamo et al. (2003) integrated a water use model and a hydrology model, both global, creating the hydrological model, Water-Global Analysis and Prognosis (WaterGAP) that provides scenarios of changes in water resources. Haddeland et al. (2006) examined the effects of reservoir operation and irrigation water withdrawal on surface water fluxes at the continental scale in the Variable Infiltration Capacity (VIC; Liang et al., 1996) model. A reservoir operation scheme was implemented in the river routing model Total Runoff Integrating Pathways (TRIP; Oki & Sud, 1998) demonstrated that reservoir operations substantially altered monthly discharge (Haddeland et al., 2006), and more recently, Sadki et al. (2023) incorporate the DROP (Dam-Reservoir Operation) model into the ISBA-CTRIP scheme. Wada et al. (2011) listed several studies focused on the assessment of water stress through global hydrological models. In addition, recent advances in the representation of human activities in hydrological models have been extensively reviewed in the literature (Döll & Siebert, 2002; Nazemi & Wheeler, 2015b, 2015a; Döll et al., 2016; Pokhrel et al., 2016; Wada et al., 2017).

An expanding body of literature has increasingly emphasized the integration of irrigation into various LSMs. For instance, Takata et al. (2003) introduced irrigation and groundwater pumping into the MATSIRO LSM, thereby examining human-induced alterations to land surface water and energy balances. de Rosnay et al. (2003) incorporated an irrigation scheme into the ORCHIDEE-LSM, investigating the regional repercussions of irrigation on the partitioning of energy,

differentiating between sensible and latent heat fluxes. [Tang et al. \(2007\)](#) integrated irrigation into the simulation of land surface hydrologic processes using a distributed biosphere hydrological model. In the case of LPJmL ([Rost et al., 2008](#)), attributed the irrigation demand to surface water and groundwater resources. [Ozdogan et al. \(2010\)](#) incorporated a satellite-derived irrigation data approach into the NOAH LSM to scrutinize the influence of irrigation on hydrologic fluxes and states within the LSM. On a global scale, [Guimberteau et al. \(2012\)](#) investigated the impact of irrigation on climate using the ORCHIDEE model, shedding light on its profound effects on the water cycle. Similarly, [Leng et al. \(2014; 2015\)](#) applied irrigation schemes across various global land surface models, including the Community Land Model (CLM), for offline applications.

In addition to these offline studies, some researchers have directly incorporated water management, particularly irrigation, into online applications. These studies aim to investigate the climate effects of irrigation and the associated feedback mechanisms within the land water cycle, e.g., ([Adegoke et al., 2003](#); [Boucher et al., 2004](#); [Lobell et al., 2009](#); [Sacks et al., 2009](#); [Saeed et al., 2009](#)).

Moreover, regional water management is a complex task, and current LSMs have limitations in accounting for dynamic irrigation water supply, flooding control, and hydropower production, which are crucial for realistic simulations of regional hydrological processes. These processes are increasingly important in the context of water scarcity and climate change. For instance, current LSMs predominantly assume optimal irrigation practices in their simulations, whereas accounting for regional deficit irrigation practices can significantly reduce water demand by up to 30% ([Döll et al., 2014](#)).

While progress has been made in recent years to incorporate human impacts into large-scale hydrological models, there are still significant gaps and challenges. It is noteworthy to emphasize that most of these models are typically designed to operate in an offline mode, meaning they simulate the water cycle on land using external climate data as input and are not coupled with global or regional climate models. Thus, the integration of these schemes in online simulations is still a challenge ([Pokhrel et al., 2016](#)).

The development of a common and standardized framework for the evaluation of the advancement of LSMs is another of the major challenges ([Döll et al., 2016](#); [Wada et al., 2017](#)). This lack leads to a wide range of models with significant differences in model parameterization and representation of biophysical processes and human land-water management. Hence, inter-comparison between different models and schemes is a relevant interest area for further development. Same mentioned in section 2.3.3, most of those limitations and challenges are also in common with the incorporation of water-human management into large-scale hydrological models.

In the face of the urgent need to understand how Earth modifications, associated with human interactions, will affect our living conditions and the ecological and hydrological systems we rely on, the LSMs mustn't be merely viewed as atmospheric boundary conditions but recognized as distinct own scientific discipline ([Fisher & Koven, 2020](#)). Finally, it is important to mention that LSM has evolved into a powerful and multidisciplinary field, with extensive applications in atmospheric science, ecology, water management, and hydrology.

---

## 3. Area of study and materials

In this section, the study area and data used in this research, together with the model applied to it, are described throughout this chapter. The study area utilized is introduced first, followed by a summary of the data and a comprehensive description of the model.

### 3.1. Study area

This study uses three study areas, which all lay within the larger domain of the Pyrenees and all surrounding basins that drain this mountain range, which is the area of study of Chapter 6, the Ebro river basin, which is the focus of Chapter 5, and, finally, the hydrological system of the Canal de Aragon and Catalonia, which is the focus of Chapter 7.

#### 3.1.1. The Pyrenean Domain

The Pyrenean domain covers the Ebro basin to the south, some basins that flow to the Bay of Biscay to the west, the Catalan and some Languedocian basins to the east, and the Adour-Garonne basins to the north as depicted in [Figure 3-1](#).

---

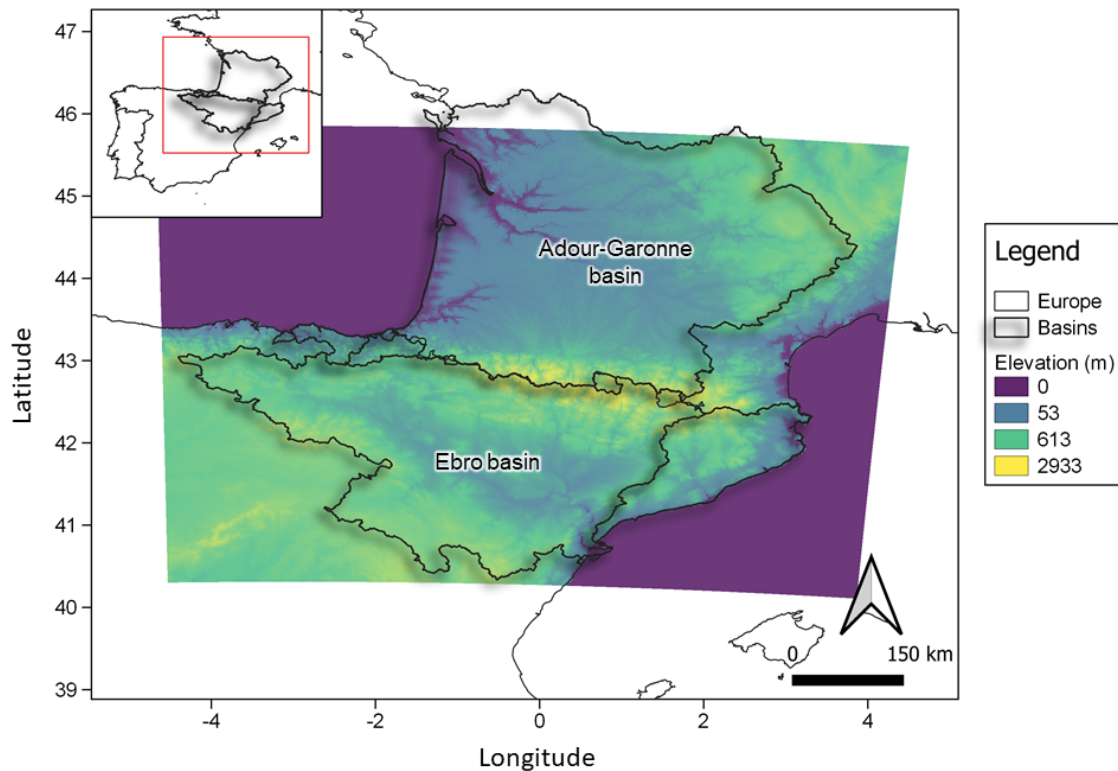


Figure 3-1 Location of the study area and domain used for simulations.

The Pyrenees are located on the isthmus of the Iberian Peninsula, between the Atlantic Ocean and the Mediterranean Sea, with a length of more than 400 km in the E-W direction and a maximum width of 150 km in its central part. The topography of the study area is very heterogeneous, as it includes the Pyrenees Mountain range, which reaches over 3000 m. at the highest points, and flat areas of the surrounding valleys, such as the Ebro Valley. The climate is predominantly influenced by Mediterranean features on its eastern side and Atlantic influences on its western side, with an alpine climate in the highest areas. Furthermore, the topography results in large spatial precipitation and temperature variability.

In the Adour-Garonne River basin, the southeastern part is dominated by the Mediterranean climate, whereas the western part is influenced by Atlantic Ocean conditions. Precipitation varies on average from 600 mm in the middle part of the basin to 2000 mm in the south part and Atlantic coast. The precipitation decreases with both the topography and the distance to the Atlantic. Seasonally, precipitation has two maxima, one in winter and a second in spring.

Similarly, on the Spanish side of the Pyrenees precipitation decreases from west to east and from north to south. Annual precipitation varies from 100 mm in the central Ebro Valley to more than 2000 mm in the highest areas. The precipitation regime is characterized by high interannual variability (López & Justribó, 2010), particularly in Mediterranean areas, most of the annual precipitation occurs during spring and autumn. However in some regions the maximum precipitation occurs during the cold season (in the Atlantic areas). In the Pyrenees and the central Ebro Valley, the summers are mainly dry (López-Moreno et al., 2008, 2011).

The Pyrenees, considered natural water towers for their surrounding basins, provide the water that satisfies the downstream demands for human and environmental needs (Immerzeel et al., 2019). The main water uses in the Adour-Garonne basin are agricultural and industrial. In the Ebro, water

demands by the agricultural sector represent 92% of the total water volume of the basin, this being the main water use in the basin (<http://www.chebro.es/guest/uso-del-agua>). This agricultural development was made possible by the construction of several dams that regulate the river flows and store water for dry periods. The large number of dams has caused major alterations in river regimes and reduced the magnitude of floods. Nevertheless, low flows were also affected, being reduced by half, on average, and by an order of magnitude in some cases, which is undesirable for ecological purposes (environmental flows) (Batalla et al., 2004). Additionally, the ever-expanding human activity, mainly irrigation, has increased the pressure on the water resources of the basin.

### **3.1.2. Description of the Ebro basin**

The Ebro River basin is located in the Iberian Peninsula, the largest basin of Mediterranean Spain with an extension of 85,534 km<sup>2</sup> (Figure 3-1). It is surrounded by a number of mountain ranges. To the north, the Pyrenees and the Cantabrian Mountain ranges shape the edge of the basin. To the south, the Iberian range marks the southern boundary of the basin. To the east, the Catalan coastal ranges extend along the Mediterranean Sea and enclose the basin from the east. The basin has a heterogeneous topography, the maximum elevation exceeds 3000 m at the peak of Aneto Mountain, and the mean elevation in the central valley is around 200 m.

Due to the location, the spatial and temporal distribution of the precipitation of the Ebro basin is complex and varied, attributable to relief and the Atlantic and Mediterranean influences, as mentioned in the previous section. The Ebro basin can experience high rainfall events, particularly during the autumn and winter months when the region is most likely to receive significant precipitation but can occur at any time of year. Overall, the combination of these weather influences on precipitation creates a unique and dynamic climate in the Ebro basin.

Moreover, the Ebro basin has a complex hydraulic infrastructure that serves various purposes, including irrigation, energy production, flood control, and navigation. The hydraulic infrastructure in the Ebro basin includes large reservoirs, dams, and canals, which are used mainly to store and distribute water for irrigation and hydropower generation purposes. This infrastructure plays a crucial role in the management of water resources in the region and contributes to its economic and social development.

#### **3.1.2.1. Exposure to drought**

The Ebro basin is an example of a Mediterranean region heavily reliant on water sources originating in mountainous areas like the Pyrenees, which face significant challenges. Several factors have converged to intensify the pressure on its water resources. The expansion of irrigation zones, the growth of industrial zones, and the development of major cities have all led to increased demands on this critical water supply, as mentioned previously. In the Ebro basin, there are 125 reservoirs. Together, they can hold about 8000 Hm<sup>3</sup>. They are mainly used to provide water for over 900,000 ha of farmland that needs irrigation, and they also help run 360 hydroelectric power plants (CHE, 2022).

One key factor that exacerbates the Ebro basin's vulnerability to drought is the complex relationship between climate fluctuations and vegetation in its headwaters (Beguiría et al., 2003; López-Moreno et al., 2008). These dynamics are the primary drivers behind the concerning reduction in river flows in the Pyrenean rivers. Furthermore, to manage water resources and



mitigate floods, numerous dams were constructed in the region. However, these dams, while serving their intended purpose, have significantly altered the natural flow of rivers (López-Moreno & García-Ruiz, 2004). Yet, this reliance on engineered structures, combined with the inherent variability of water resources, has made the basin more susceptible to drought.

An analysis of a prolonged drought period from 2005 to 2008 has shed light on the Ebro basin's vulnerability and exposure to drought. While agriculture and food production suffered the most during this extended drought, its effects rippled through various sectors. Hydropower production faced significant reductions, as well as water supplies, and recreational activities were constrained, and the overall ecosystem functioned less effectively (Pérez y Pérez & Barreiro-Hurlé, 2009; Hernandez-Mora et al., 2013). Moreover, different drought events have been reported in the literature (Linés et al., 2017, 2018). This highlights the urgent need for holistic strategies to drought management recognizing the intricate web of dependencies within the Ebro basin.

### 3.1.3. Canal de Aragón y Cataluña (CAyC)

The Canal de Aragón y Cataluña (hereafter, CAyC) is a strong, and one of the most important, irrigated areas located in the northeastern part of the Ebro basin with a size of 98,000 ha (Figure 3-2). This irrigation district is supplied by the canal with the same name (CAyC). This canal has a length of 124 km with a source point at the Barasona or Joaquín Costa Reservoir, constructed along the Ésera River. Additionally, it receives the water of the Noguera-Ribagorzana River from the Santa Ana reservoir, through the Canal de Enlace which has a 6 km longitude.

There are two defined regions within the irrigated zone: an upstream zone (54,000 ha) supplied by the Barasona reservoir and a downstream zone supplied by the Santa Ana reservoir, with 44,000 ha.

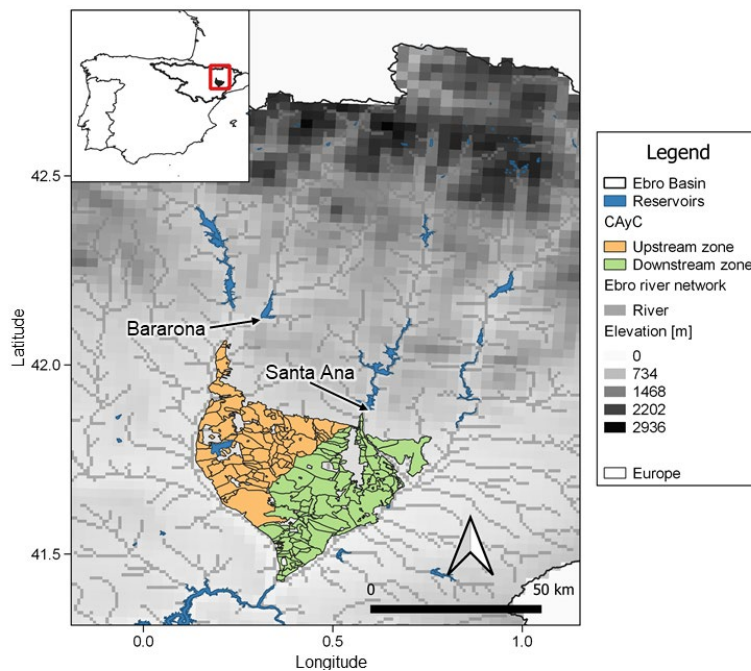


Figure 3-2. Location of the CAyC and the two reservoirs that supply this irrigated area.

The Barasona reservoir has a maximum capacity of 92 Hm<sup>3</sup>, whereas Santa Ana has 236 Hm<sup>3</sup>. In recent years, the San Salvador reservoir has been put into operation, which along with the Barasona reservoir, manages the water in the upstream zone on the CAyC. However, the San Salvador reservoir is not included in this research.

The primary crops grown in the area consist of fruit orchards, including apples, pears, peaches, and nectarines, and extensive herbaceous crops like maize, alfalfa, and barley. The region has seen an increase in wine vine cultivation, though it remains largely concentrated in certain areas.

## **3.2. Data**

For hydrological analysis, the availability of time series of different variables is required. Our region of study is rich in data. However, observational data are not always available, data quality is sometimes too low, or they include processes that are not simulated, such as human processes. Hydrological models can be employed as a solution to overcome these problems by extending data sets, simulating unobserved variables, and simulating the natural regime, however, models also require data, to be forced or for calibration and validation. In this sub-section, the meteorological and hydrological data used are described.

### **3.2.1. Precipitation data**

Here, a comprehensive overview of the precipitation data utilized, with a specific focus on Chapter 5, is provided.

#### **3.2.1.1. Observational data**

The observational data comprise 11 rainfall gauging stations with hourly precipitation records, selected from the SAIH (Automatic Hydrologic Information System, in its original acronym in Spanish) of the Ebro River basin authority (Confederación Hidrográfica del Ebro, in Spanish) (Table 3-1). The stations were chosen so that data the time series would have data during the period (2005 to 2014).

The stations are distributed over the Ebro basin, thus representing the diversity of conditions found in the basin (mountain vs valley, Atlantic vs Mediterranean). Figure 3-3 and Table 3-1 show the location and details of rainfall gauge stations used it.

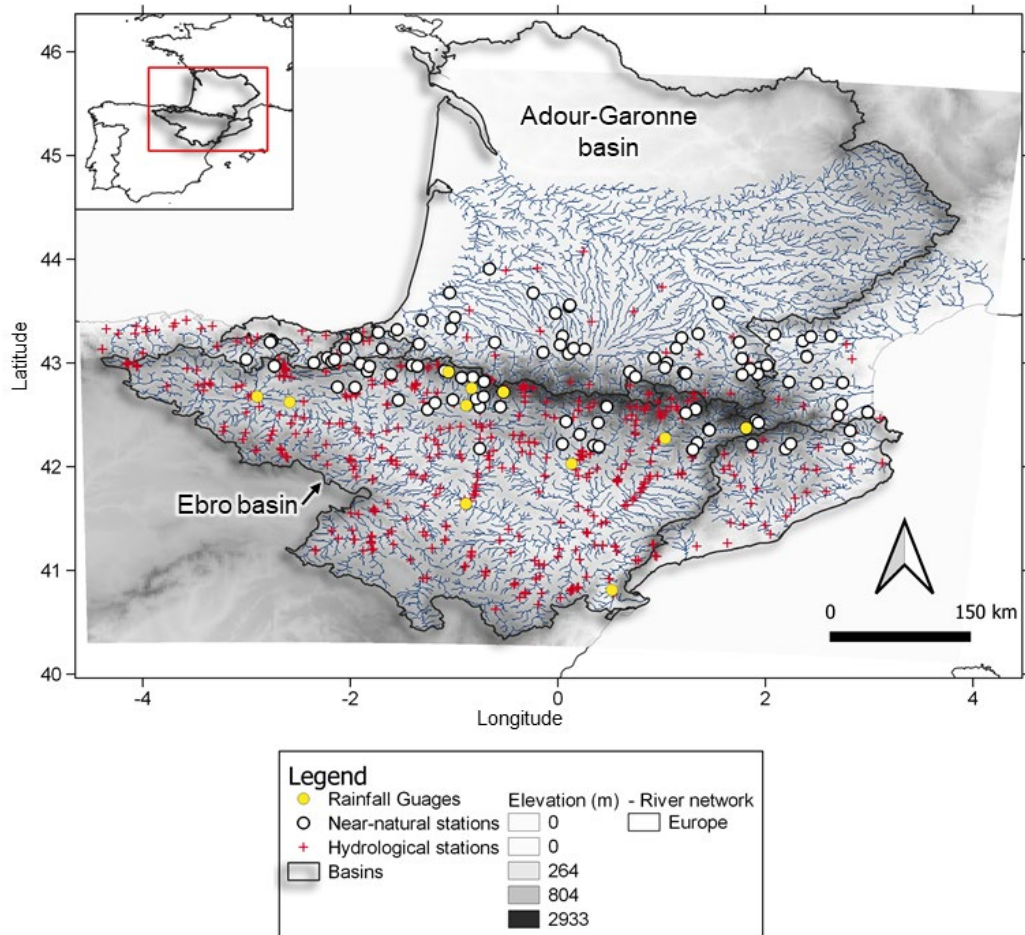


Figure 3-3 Location of the selected rain gauge stations, in yellow circles; the streamflow stations, in red; stations in black circles are defined as near-natural. The river network is depicted in blue.

Table 3-1. Location of the selected stations

ID	Station Name	Lat (°)	Lon (°)	Alt (m)	Start	End
9027	EBRO TORTOSA	40.812	0.520	25	04/06/2004	01/09/2014
9102	NOGUERA	42.275	1.034	535	01/10/1997	01/09/2014
PC04	ZARAGOZA	41.644	-0.886	215	01/01/1998	01/09/2014
9074	ZADORRA	42.677	-2.897	455.1	01/10/1997	31/12/2017
9095	VERO	42.029	0.132	320	01/10/1997	31/12/2017
9256	SEGRE	42.373	1.814	1030.6	02/07/1998	31/12/2017
9259	SALAZAR	42.914	-1.055	796	01/01/2005	31/12/2017
9271	ARAGON	42.720	-0.525	1045	01/10/1997	31/12/2017
9282	ARAGÓN EN MARTES	42.591	-0.883	544	01/01/2005	31/12/2017
P008	LAGRAN	42.623	-2.584	750.5	01/10/1997	31/12/2017
P016	ANSO	42.757	-0.832	900	01/10/1997	31/12/2017

### 3.2.1.2. High-resolution RCM simulation: CNRM-ALADIN63

The CNRM-ALADIN model, Aire Limitée Adaptation dynamique Développement InterNational, is a regional climate model (Daniel et al., 2019; Nabat et al., 2020), is used by the Centre National de Recherches Météorologiques (CNRM) as a regional climate model. This model uses a microphysical parameterization scheme to simulate the rain and snow amounts at the surface. This ALADIN simulation is driven by Era-Interim (Dee et al., 2011), which guarantees synchronicity with actual weather and is part of the EURO-CORDEX initiative, the Europe branch of the Coordinated Regional Downscaling Experiment (Jacob et al., 2014).

The CNRM-ALADIN model provides a climate simulation at a fine spatial and temporal resolution of  $0.11^\circ$  (12 km approx.) and, most importantly, a time resolution of one hour. The area covers the European domain (<http://www.euro-cordex.net/>, last access: 10/09/2022), version 6.3 is used in this study.

## 3.2.2. Hydrological data

### 3.2.2.1. Observed streamflow data

The observational streamflow database used, especially in Chapter 6, was gathered by the EFA210/16 PIRAGUA project (Zabaleta et al., 2022). It consists of daily streamflow records from the different river basin authorities that manage the water in the study area. For the analysis, a final database comprising 392 gauging stations that encompass the period between September 1979 and August 2014 (35 years) was considered, of these, 104 were selected as natural and near-natural gauging stations analyzing the data and metadata, as indicated by the Figure 3-3 with black circles. The selection was carried out following the criteria below:

1. Only stations with at least 20 years of data within the analysis period were considered.
2. Data gaps of less than 10% of the total record length (these gaps were not filled) were allowed.
3. Flows must have a natural or near-natural hydrological regime, i.e. the stations must not be downstream of important human-influenced areas (e.g., reservoirs, irrigation areas).

For calibration purposes (section 6.3.2.3), from the selection of natural stations previously done, outlet stations with series starting in 1979 and with at least 30 years of records were selected. Figure 3-4 shows the final selection, which resulted in 31 outlet stations (in total 53 sub-catchments if the nested catchments are considered).

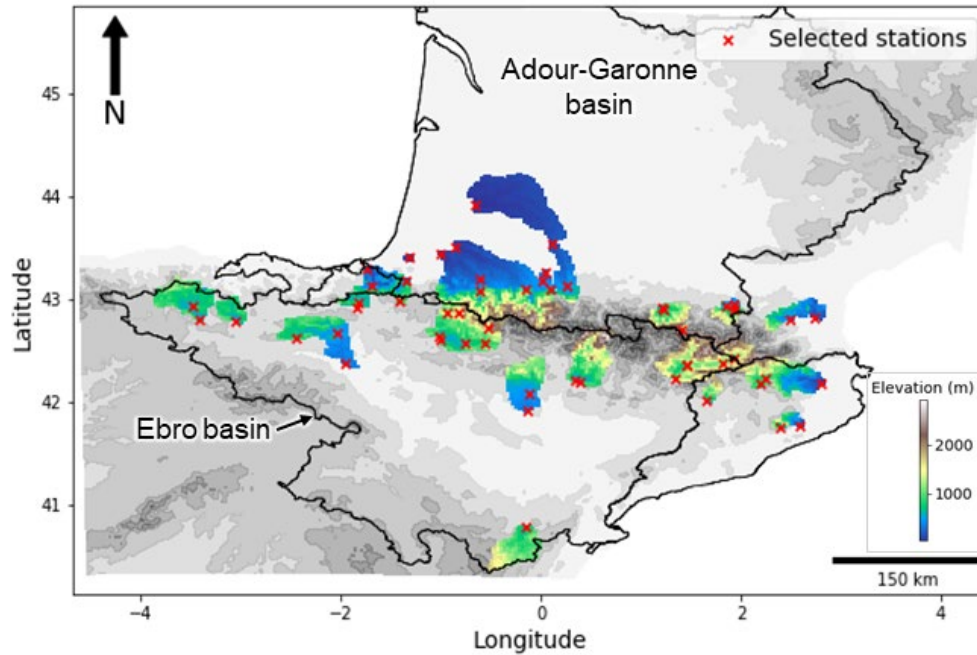


Figure 3-4 Selected outlet gauging stations of near-natural basins.

### 3.2.2.2. SIMPA model (reference)

SIMPA ("Integrated Precipitation-Streamflow Modelling System", in its original acronym in Spanish) is a conceptual and semi-distributed hydrological model developed in the Centre for Public Works Studies and Experimentation (CEDEX) in Spain (Estrela & Quintas, 1996). SIMPA simulates the natural water balance and provides information about the main hydrological variables (precipitation, evapotranspiration, streamflow) at a monthly time step. SIMPA is used by the Spanish authorities for water resources evaluation. In this research, the focus is solely placed on the streamflow data provided by SIMPA.

### 3.2.3. Physiographic data

Within this thesis (explicitly section 6.3.2.3), SURFEX's default physiographic database ECOCLIMAP II (Faroux et al., 2013) was used. It has a spatial resolution of 1 km and includes an ecosystem classification as well as a consistent set of land surface parameters.

In contrast to commonly used land cover products like Corine Land Cover and Global Land Cover, ECOCLIMAP-II has a new division of the existing classes with a better regional character obtained from the climatic environment (latitude, proximity to the sea, topography). The land cover parameters provided in this dataset include root depth, minimal stomatal resistance, albedo, and Leaf Area Index (LAI). The temporal variables are represented using a climatology (i.e. a mean annual cycle).

Additionally, the Copernicus NDVI product, which was obtained from (<https://land.copernicus.eu/global/products/ndvi>, last access 2022/06/07) was utilized.

### 3.2.3.1. ESDAC database

The European Soil Data Centre (ESDAC) was initiated in 2009 by the European Union (EU) as a project with the overarching objective of facilitating informed decision-making. ESDAC provides an invaluable repository of soil-related data and knowledge to policymakers, researchers, and diverse stakeholders. Encompassing a rich spectrum of soil-focused information, the database includes comprehensive datasets on topics ranging from soil properties and erosion to soil organic carbon, biodiversity, and contamination. ESDAC, overseen by the European Commission's Joint Research Centre is an integral component of the EU's broader commitment to promoting sustainable land management practices.

This database was employed in this research to enhance the default model's soil information is thoroughly expounded upon in Chapter 6, Section 6.2.2. This section provides a detailed exploration of how it was utilized to refine the model's representation of soil. For a comprehensive understanding of the results, we invite readers to explore Appendix A.2

### 3.2.4. Information on anthropogenic influences

In this section, a comprehensive and detailed overview of the data related to human-water management, specifically utilized in Chapter 7, is presented.

As mentioned in section 3.1.2, the Ebro basin features a hydraulic infrastructure that serves multiple purposes, such as supporting irrigation and playing a decisive role in the region's socioeconomic progress. To obtain information about reservoirs, data provided from the automatic measurement stations of the Automatic Hydrologic Information System (SAIH, in Spanish) was utilized. These stations provide information, such as storage, inflows, and releases. These data are available from <https://ceh.cedex.es/anuarioaforos/default.asp> (last access: 2022/11/30). Data from both reservoirs, Barasona (station code: 9848) and Santa Ana (station code: 9852) are available from 1944 to 2019 and from 1961 to 2019, respectively. In this study, the period from 01/09/1979 to 01/08/2014 was utilized.

The Ebro River Basin Authority (Confederación Hidrográfica del Ebro, CHE) holds the responsibility of making operational decisions regarding drought and water allocation. To establish a robust framework for these decisions, CHE spearheaded the development of a pioneering drought management plan in 2007 (CHE, 2007), setting a precedent within Europe. This plan outlines specific indicators to guide decision-making, these indicators are based for instance on the storage level of water in reservoirs and serve as the primary indicator. In addition, other river basin authorities have implemented similar management plans. Hence, the CHE defines indicators for the different areas of the basin.

In the context of this plan, the CHE identifies situations of prolonged drought (a natural situation of reduced precipitation with a consequent decrease in the water supply) and situations of temporary scarcity (problems in meeting demands due to a reduction in the available resource). For the latter, the storage volume in the corresponding reservoirs has been selected as an indicator.

The CHE establishes distinct shortfall indicators for the Ésera and Noguera-Ribagorzana river basins (CHE, 2022). The volume of water stored in the Barasona reservoir serves as the basis for

defining the short-term scarcity thresholds (*umbrales de escasez coyuntural*) specific to the Ésera River basin, as outlined in [Table 3-2](#).

Table 3-2 Thresholds of short-term scarcity for Barasona reservoir (volume stored in Hm<sup>3</sup>)

Threshold	Oct	Nov	Dec	Jan	Feb	Mar	Apr	May	Jun	Jul	Ago	Sep
<b>Prealert</b>	45.0	60.0	68.0	68.0	68.0	68.0	74.0	82.0	82.0	60.0	33.0	24.0
<b>Alert</b>	35.0	45.0	50.0	53.0	53.0	53.0	60.0	64.0	64.0	45.0	24.0	18.0
<b>Emergency</b>	24.0	30.0	36.0	42.0	42.0	42.0	45.0	50.0	50.0	36.0	18.0	14.0

Whereas, indicators for the Noguera-Ribagorzana River basin are determined by considering the cumulative reserves in the Santa Ana, Canelles, and Escales reservoirs, as depicted in [Table 3-3](#). It is worth noting that the primary purpose of the Canelles and Escales reservoirs is energy production, which is outside the scope of this research focused on irrigation. Therefore, these reservoirs are not considered in the simulation, and only the Santa Ana reservoir is included in the analysis.

In this analysis, the thresholds applied to the Santa Ana reservoir were calculated as a proportion of the total volume (sum of the capacity of the three reservoirs).

Table 3-3 Thresholds of short-term scarcity for Santa Ana, Canelles, and Escales reservoir (cumulative volume stored in Hm<sup>3</sup>)

Threshold	Oct	Nov	Dec	Jan	Feb	Mar	Apr	May	Jun	Jul	Ago	Sep
<b>Prealert</b>	428.0	442.6	460.9	492.0	530.5	551.3	572.0	591.0	588.8	528.4	464.6	438.6
<b>Alert</b>	325.6	334.4	345.4	364.0	387.1	399.6	412.1	423.4	422.1	385.9	347.6	332.0
<b>Emergency</b>	248.9	253.2	258.7	268.1	279.6	285.9	292.1	297.8	297.1	279.0	259.8	252.0

Environmental flows are defined for different areas of the Ebro basin ([CHE, 2022](#)), [Table 3-4](#) shows the ecological flows to be respected for the two rivers downstream of the respective reservoirs.

Table 3-4 Monthly environmental flows (in Hm<sup>3</sup>)

River	Oct	Nov	Dec	Jan	Feb	Mar	Apr	May	Jun	Jul	Ago	Sep
<b>Barasona</b>	1.88	1.81	1.88	1.88	1.45	1.61	1.81	2.41	2.33	1.88	1.61	1.56
<b>Santa Ana</b>	4.12	3.8	3.72	3.75	3.39	3.41	3.75	4.22	4.52	3.81	3.72	3.67

### 3.3. The SASER hydrometeorological modeling chain

The SASER (SAfran-Surfex-Eaudysee-Rapid) suite, is a distributed and physically-based hydrometeorological modeling chain consisting of three elements: a meteorological analysis system, that generates the meteorological forcing dataset from observational data; a LSM, which simulates the energy and water balance between the land surface and the atmosphere; and a routing scheme which simulates the streamflows. In this section, a brief explanation of these elements is provided.

#### 3.3.1. SAFRAN

Système d'Analyse Fournissant des Renseignements Atmosphériques à la Neige, SAFRAN, (Durand et al., 1993) is a meteorological analysis system, which was primarily for a snow model and later developed by forcing LSM models (Habets et al., 2008; Quintana-Seguí et al., 2008), that produces the meteorological gridded forcing dataset.

SAFRAN uses an optimal interpolation algorithm (Gandin, 1966) which combines in-situ observations and a first guess to analyze different screen-level meteorological variables (precipitation, temperature, relative humidity, and wind speed). For all variables, except precipitation, the analysis is performed every six hours and then the data is interpolated to the hourly time step fitting the appropriate function for each variable. To take advantage of the dense network of daily precipitation observations, SAFRAN analyzes precipitation at a daily time step. To interpolate to the hourly time step, relative humidity is used, therefore the higher the relative humidity, the higher is the precipitation. More information on the methodology used in SAFRAN can be found in (Quintana-Seguí et al., 2008).

In a Mediterranean setting, where precipitation patterns are often characterized by a high degree of spatial variability and rainfall events occurring sporadically and often at high intensities (Herrera et al., 2010), the interpolation method referred to results in precipitation distributions that are overly smooth, with very low-intensity levels, and do not accurately capture this variability. The above represents a drawback in the current SAFRAN system, especially for regions that predominate Mediterranean conditions.

SAFRAN provides hourly meteorological data which is then ingested by the LSM. The SAFRAN dataset used here is PIRAGUA\_atmos\_analysis (Quintana-Seguí et al., 2022), which was created within the EFA210/16 PIRAGUA project and corresponds to a union of the French (Quintana-Seguí et al., 2008; Vidal et al., 2010) and the Spanish (Quintana-Seguí et al., 2016, 2017) implementations of SAFRAN. It has a temporal resolution of one hour and a spatial resolution of 2.5 km, which covers the whole domain depicted in Figure 3-1.

#### 3.3.2. SURFEX

The LSM used by SASER is SURFEX (Surface Externalisée, in French) a modeling platform developed and maintained by Metéo-France (Masson et al., 2013; Le Moigne et al., 2020). In offline mode, the LSM SURFEX is driven by the SAFRAN atmospheric forcing to simulate the water transfer in the soil and surface hydrology. Figure 3-5 shows the main schemes of the modeling platform.



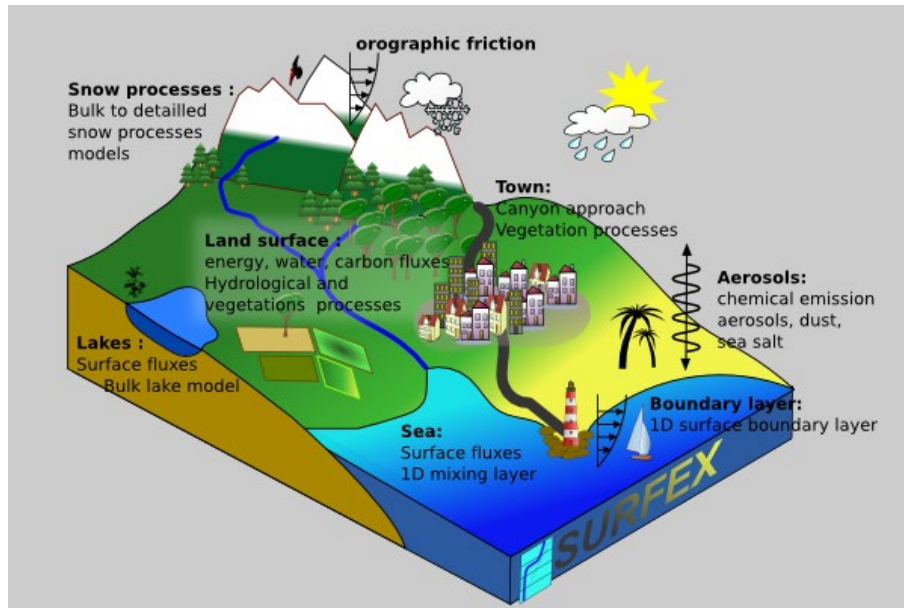


Figure 3-5 SURFEX (Surface Externalisée, in French) modeling platform (source: <http://www.umr-cnrm.fr/surfex/>).

SURFEX provides schemes for natural surfaces, urban areas, lakes, and oceans. In this research, the focus is solely placed on the natural surfaces. An integral part of the SURFEX model is the Interaction Soil-Biosphère-Atmosphère (ISBA) scheme (Noilhan & Planton, 1989; Noilhan & Mahfouf, 1996), which is used for modeling natural soils. Since the ISBA scheme is modular, different versions of ISBA have been developed, e.g. ISBA-3L (Boone et al., 1999), which includes a three-layered description of the soil; and ISBA-DIF (Boone et al., 2000; Habets et al., 2003; Decharme et al., 2011), that consider a soil multilayer diffusion scheme.

The ISBA scheme represents the land surface as a single, vertically-resolved soil column, with the vegetation and soil layers being modeled as a combined entity. This scheme describes the physical processes that occur on the land surface, including evapotranspiration, soil water balance, and heat transfer. Even though it is unable to simulate groundwater processes. In this thesis, simulations were performed using the SURFEX version 8.1 which uses the ISBA-DIF scheme.

### 3.3.2.1. Irrigation scheme in SURFEX

Irrigation is a feature that has been incorporated into many crop models, nevertheless, representation on most LSMs is not fully explicit (Verburg et al., 2016). With this in mind, a finer irrigation scheme has been recently developed (Druel et al., 2022) within the SURFEX-ISBA model, in which a detailed representation of the irrigation practices are incorporated, Figure 3-6.

In this new scheme, SURFEX v.9, three main irrigation practices (sprinkler, flood, and drip irrigation) are considered. Irrigation can be activated when soil moisture content drops (producing a limited vegetation growth) below a threshold value. The irrigation scheme takes into account soil moisture, irrigation frequency, and the amount of water applied to the crops (Druel et al., 2022). The above, allows us to estimate a realistic amount of irrigation water. In this thesis, simulations at the same spatial resolution of SAFRAN were carried out by SURFEX v.9.

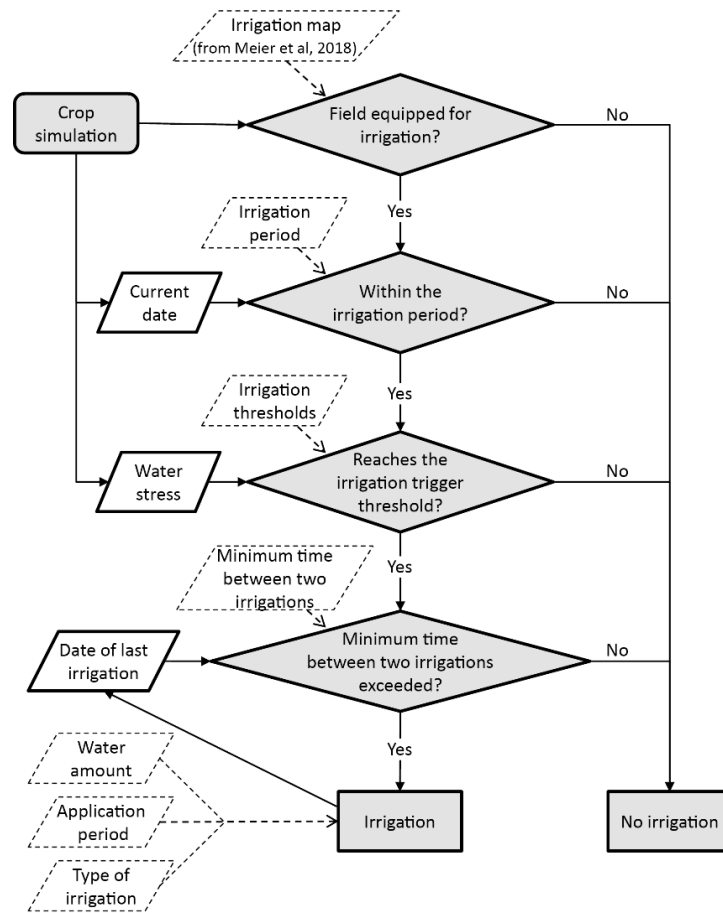


Figure 3-6 Overview of the new irrigation algorithm illustrating the sequential steps involved in its implementation (Druel et al., 2022).

### 3.3.3. Eaudyssée-RAPID

The runoff and drainage generated by SURFEX must be postprocessing to determine the water distribution on the surface, which is the reason why a routing scheme was implemented. The Routing Application for Parallel Computation of Discharge (RAPID) scheme (David et al., 2011) was chosen.

RAPID is a river network model designed to compute the river flow and estimate the discharge of water from a river basin. This model uses a matrix-based version of the Muskingum method, which allows us to calculate the flow and volume of water in all reaches of the river network, and not only in the basin outlet (David et al., 2011). To link the SURFEX's outputs with the RAPID model, the hydro-system Eaudyssée (Saleh et al., 2011; Vergnes & Habets, 2018) was used.

The Eaudyssée system, which was designed to address water resources and quality in regional scale river basins, is a suite of hydro(geo)logical models that simulate the movement of water through the soil. Four distributed modules form the core of the model and represent the major components of the terrestrial water cycle: surface, unsaturated, saturated zone (aquifer), and river network (Saleh et al., 2011).

This system has a modular design that allows for flexibility in the selection and implementation of different models and tools. This modular approach makes it possible to tailor the system to the specific needs of different regions and applications.

#### **3.3.4. Limitations of the SASER model**

Some limitations within the current SASER implementations, specifically from the SURFEX model, are that: (i) There is no lateral flow between SURFEX grid cells; (ii) there is no bidirectional interaction between the river and the alluvial aquifer; and (iii) groundwater processes are not simulated. This translates into a fast reaction between runoff and precipitation.

Another limitation of the SASER hydrometeorological modeling chain is that requires significant computational resources to run when large domains are simulated at high resolution, which can be a limiting factor for some users, especially those with limited access to high-performance computing resources.

Finally, the SASER model involves some simplifications of the real hydrological system. For example, the model may not fully capture, or do crudely, the effects of human activities, such as irrigation practices or reservoir operation, on the hydrological cycle. In addition, it is important to highlight that the irrigation scheme implemented in this study does not incorporate water conservation practices. Specifically, no direct connection has been established between the water required for irrigation and the available water in the reservoir. As a result, the irrigation water is generated independently, without considering the overall water balance or the potential scarcity of water resources.

---

## 4. Methodological framework

In this chapter, an overview of the general methodological framework utilized in this research is presented. Throughout the chapter, the different approaches used to improve the SASER-hydrometeorological modeling chain are briefly explained. This provides readers with a comprehensive understanding of the overall research methodology.

### 4.1. Pathway to improve the hydrologic modeling in the SASER model

While LSMs estimate surface state variables at high spatial and temporal resolutions, as discussed in the previous chapter. They are subjected to uncertainties in the input data to force the model, improper parameterization, and lack of or inadequate physical process representations (Clark et al., 2015). These limitations can affect the accuracy of simulations made by the LSMs. [Figure 4-1](#) presents the pathway followed to improve different aspects of the SASER modeling chain.

---

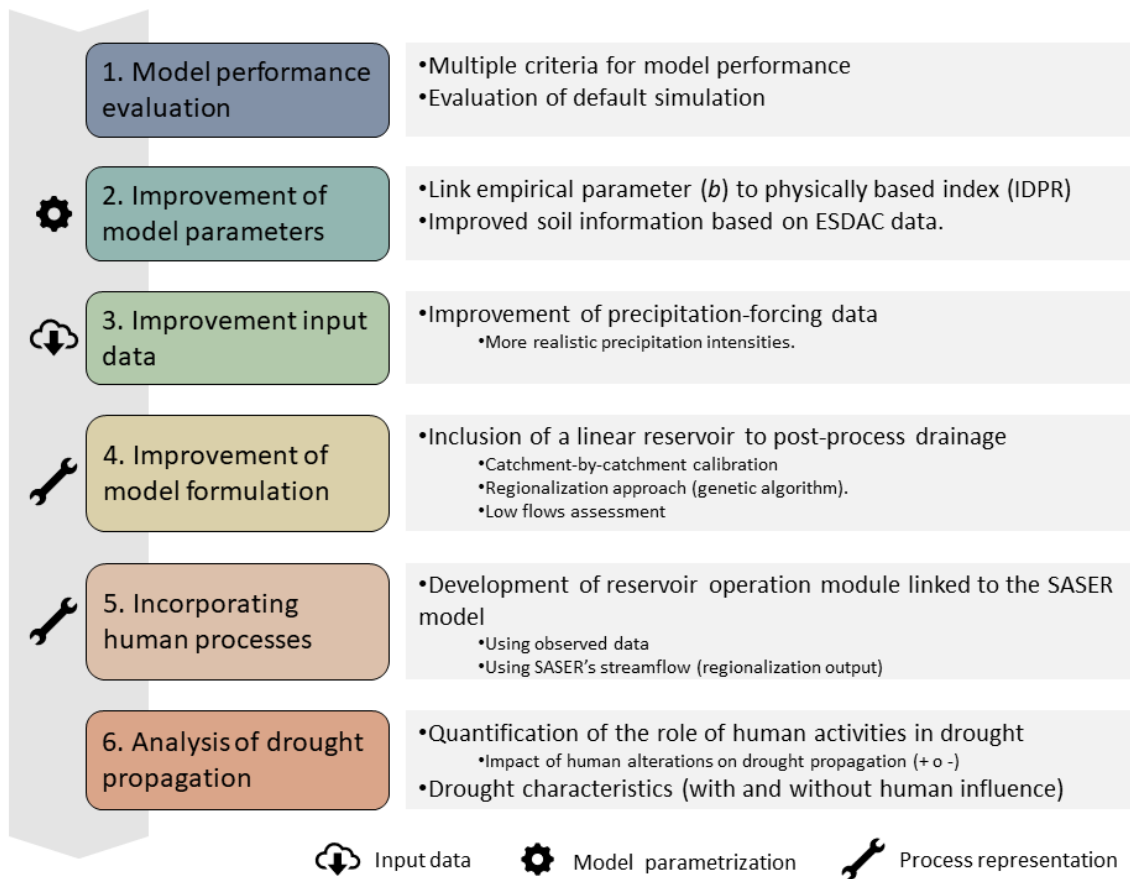


Figure 4-1 Pathway used to improve the hydrologic modeling.

In line with the significant advancements made to LSM in recent years described in section 2.1, the SASER modeling chain aims to further improve hydrologic modeling. The use of high-resolution data and remote sensing data can help to improve the initialization and constraint of the model (Wood et al., 2011), thereby increasing the accuracy of the simulated hydrologic variables. Thus, the initial focus is placed on the physical (empirical parameter dominates runoff generation) and physiographic (soil information) parametrization to improve the SURFEX-LSM model.

Another way forward to improve hydrologic modeling in LSMs is by using higher-quality forcing data. The term "forcing data" is used to denote the inputs that drive the model, including precipitation, temperature, and solar radiation. Accuracy and high temporal and spatial resolution can help to improve the realism of the hydrological response. In this sense, the hourly distribution of precipitation, as well as the corresponding intensities, in SAFRAN forcing were improved to enhance the representation of temporal precipitation patterns and their impact on runoff.

On the other hand, LSMs are not coupled to a groundwater scheme or do not directly simulate groundwater processes (which is the standard practice), thus encountering difficulties in representing the slow component of the flow, as it is often heavily influenced by underground water processes. This is observed in the case of SASER, where the representation of the slow component of the flow is challenging due to the absence of direct simulation of groundwater processes. To address this limitation and enhance the representation of the slow component of the hydrological response within SASER, a conceptual reservoir was implemented based on the

formulation derived from rainfall-runoff models. This incorporation aims to improve the simulation of low-flow conditions.

Finally, even though progress made so far in LSM, as discussed early in section 2.4.4, most of the LSMs have not yet integrated or do crudely, the impacts of human activities (e.g. irrigation, reservoir operation, withdrawal groundwater) on their formulation, which reinforces the necessity to develop models that take into account the human land-water management in LSMs (Pokhrel et al., 2016; Hanasaki et al., 2018; Pongratz et al., 2018; Boone et al., 2019; Yokohata et al., 2020). Thus, incorporating these human activities into the SASER modeling chain is essential to provide a better representation of the coupled natural-human system. Consequently, it makes it possible to analyze drought propagation in a human-modified context.

## 4.2. Improvements in the SASER modeling chain

In this section, a general description of the approaches used to improve the hydrological response of the SASER model is presented. Each modeling approach is treated in detail in the chapter in which it is used. Additionally, a section on the different metrics employed to evaluate the performance of the models included in this research is included.

### 4.2.1. Improvement to precipitation in SAFRAN forcing

Precipitation plays a vital role in the water cycle as it influences the availability of water for various purposes. This, in turn, affects the performance of Land Surface Models (LSMs) as precipitation data is the primary input for these models. Hence, the accuracy and dependability of LSM simulations depend on the quality of precipitation data used. Therefore, obtaining high-quality precipitation data is crucial for producing precise and reliable LSM simulations.

In this context, the aim is to enhance the precipitation input data for the hydrological model (Chapter 5). This is achieved by utilizing a linear correction method, which is applied to adjust the hourly precipitation distribution of SAFRAN to a more realistic distribution, obtained from the regional climate model (CNRM-ALADIN). The correction method provides a more accurate representation of the precipitation patterns in the study area.

The new precipitation dataset, with improved intensities, is then used as input to the SURFEX-LSM model to evaluate the impact on hydrological response. This effort represents a crucial step towards improving the overall performance of the hydrological model in simulating the hydrological response.

### 4.2.2. Attempts to improve inner model parameters

Our initial efforts were aimed at improving the hydrological simulation, both for low and high flow conditions, as mentioned early in this chapter. These involved (i) calibrating the internal parameters that controlled the runoff generation and (ii) enhancing the physiographic information. Despite these efforts, these attempts did not result in success (section 6.2).

The initial step involved determining the optimal value of the key empirical parameter, *runoff b* (section 6.2.1), which governs runoff generation in the model. To achieve this, a series of

simulations were performed, systematically varying the value of *runoff b*. The analysis led to the conclusion that the default value of *runoff b* (0.5) was already deemed suitable.

Subsequently, an investigation was conducted to explore the possibility of calibrating the value of *runoff b* in a distributed manner within the domain, using physical information. For this purpose, a simulation was carried out, employing *the Indice de Développement et Persistance des Réseaux* (IDPR in French, [Mardhel et al., 2021](#)). However, the simulation did not yield positive results, and no clear and direct relationship was found between the IDPR and the value of *runoff b*.

The following stage involved an attempt to improve the representation of soil information by utilizing the ESDAC database, section 6.2.2. For this purpose, simulations were performed whereby the default soil information in the SURFEX model was modified. This yielded a barely noticeable improvement in the hydrological response, adding to the uncertainty associated with the ESDAC database. Therefore, it was decided to maintain the default information of the SURFEX model.

Notwithstanding these attempts, the calibration of the internal parameters of the SURFEX model could not be improved to enhance the simulation of hydrological processes. As a result, the decision was made to maintain the default configuration and shift the focus toward investigating ways to enhance the simulation of low flows.

### 4.2.3. Improvement of low-flow simulation in the SURFEX model

In this phase, specific attention is given to the enhancement of the low flow simulation (section 6.3), considering that one of the main limitations is that the SURFEX model does not have a groundwater component (as mentioned in section 3.3.4). The choice of an approach to improve the low-flow simulation is not straightforward. In this research, a conceptual approach, common in hydrological models, to improve the representation of the slow component of the streamflow is implemented.

Two strategies were used to calibrate the new parameters associated with the conceptual reservoir added to the modeling chain: (i) a classical calibration approach (catchment-by-catchment), and (ii) a regionalization approach.

In the first one, the parameters of the conceptual reservoir model were determined on a catchment-by-catchment basis and calibrated against locally observed streamflow data, thus resulting in semi-distributed parameters. Whereas, the regionalization approach, which links physiographic information with reservoir parameters through linear equations, uses a genetic algorithm to obtain the optimized parameter set. The key benefit of it is that allows us to determine the new empirical parameter of the conceptual reservoir in basins where calibration is not possible (ungauged or human-influenced basins)

### 4.2.4. Adding human water management to the SASER model

A critical aspect of hydrological management is diagnosing and forecasting drought, particularly in regions where water is already limited. LSMs have the potential to provide valuable insights into the evolution of drought conditions, helping water managers make informed decisions ([Quintana-Seguí et al., 2020](#)). Moreover, drought is influenced by various factors, such as climate

and catchment controls, but in many regions, it is now also driven by human activities like reservoir building, irrigation, and groundwater abstraction.

With this in consideration, in Chapter 7, the focus is shifted towards assessing the impact of human activities, particularly irrigation, on the water budget and drought propagation. To achieve this, a simplified water management model was employed to simulate the reservoir operation in a human-influenced scenario, with the purpose to investigate the relationship between agricultural drought, linked to evapotranspiration, and hydrological drought in such a human-influenced environment.

Finally, to understand the drought processes, drought characteristics (duration, intensity, and timing) need to be identified, for which different approaches can be used, the choice and implementation of this approach are important as it can result in different conclusions. The threshold level method (Yevjevich, 1967; Hisdal et al., 2004; Fleig et al., 2006) was employed in this analysis, whereby a drought condition is defined when the variable falls below a specific level. This approach allows us to easily identify drought events as close to the original time series as possible and compare the changes induced by human activities.

#### 4.2.5. Criteria for evaluation of model performance

The performance of the simulated variables needs to be evaluated at different stages of this research, including the default model and each improvement approach. The model performance consists in evaluating how to correctly be reproducing observed variables (Mathevet et al., 2006). The agreement between simulated and observed variables was evaluated by different metrics and depended on each variable (precipitation, discharge, or storage). In this research, different criteria were used as an objective function for each of the variables that were simulated. Therefore, in this sub-section, the metrics used in this research are described.

##### 4.2.5.1. Precipitation forcing

In Chapter 5, our objective is to improve the distribution of hourly precipitation. Therefore, to evaluate the corrected precipitation against observations the Perkins Skill Score (PSS; Perkins et al. (2007)), which evaluates the similarity between observed and modeled frequencies was calculated

$$PSS = \sum_1^m \min(Z_1, Z_2) \quad (4.1)$$

Where  $m$  is the number of bins,  $Z_{1,2}$  are the frequencies of values from the observed and simulated data, respectively. This metric measures how well the observations and modeled frequencies coincide (De Troch et al., 2013). This score ranges from zero (no overlap) to one for a perfect match as illustrated in Figure 4-2.



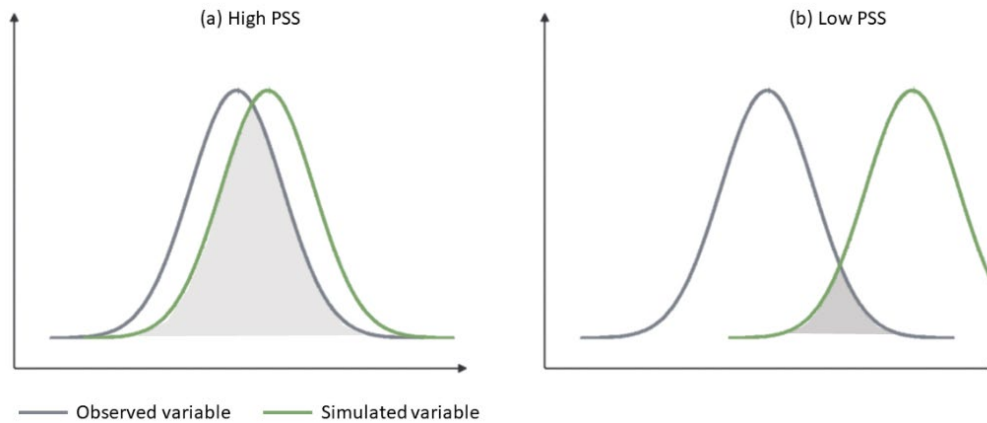


Figure 4-2 Schematic representation of Perkins Skill Score.

#### 4.2.5.2. Hydrological information

In Chapters 6 and 7 use the Kling-Gupta Efficiency, KGE (Gupta et al., 2009), a statistical measure that combines information from both correlation and bias between the modeled and observed data. The KGE ranges from 0 to 1, with a value of 1 indicating perfect agreement between the modeled and observed data. It is used to evaluate the performance of a hydrological model and thus was selected as objective function. The KGE is defined as follows:

$$KGE = 1 - \sqrt{(1 - r)^2 + (1 - \alpha)^2 + (1 - \beta)^2} \quad (4.2)$$

where  $r$  is the Pearson's correlation coefficient,  $\alpha$  is the bias component and  $\beta$  represent the ratio of discharge variance:

$$\alpha = \frac{m_s}{m_o} \text{ and } \beta = \frac{\sigma_s}{\sigma_o} \quad (4.3)$$

$m$  and  $\sigma$  represent the mean and standard deviation, respectively. Similarly, subscripts  $s$  and  $o$  represent simulated and observed discharge, respectively.

The KGE over untransformed discharge puts more weight on high flows (Garcia et al., 2017), and since this analysis is focused on low flows (Chapter 6), a root square transformation,  $KGE(Q^{1/2})$  was used. It allows balancing the weight on low and high flow without losing the physical meaning (Santos et al., 2018).

For performance metrics is important to have a benchmark to determine when the model performance is strength or not (Clark et al., 2021). The more traditional Nash-Sutcliffe (NSE) criterion (Nash & Sutcliffe, 1970) uses the average of the observations as a benchmark, this means that  $NSE > 0$  if the model performed better than the benchmark. Knoben et al. (2019), demonstrated that using the same reasoning ( $NSE > 0$ ) in the KGE criteria is not consistent. They showed that KGE values greater than -0.41 indicate an improvement over the mean flow benchmark. Therefore, a KGE value of -0.41 as the baseline value was used.

Only within the context of the genetic algorithm (section 6.3.2.3), which must evaluate the goodness of fit of each member of the population at each step, a transformation of the KGE was applies:

$$KGE_B = \frac{KGE}{2 - KGE} \quad (4.4)$$

This transformation avoids the skewed distribution of efficiencies for large samples (Mathevet et al., 2006).

In addition to calculating the KGE scores, and to evaluate how the conceptual reservoir implementation (local calibration and regionalization approach) impacted the simulated low flows, two low flow indices (the ratio  $Q_{90}/Q_{50}$  and the annual minimum monthly flow with a return period of 5 years, QMNA(5) ) were calculated (detail explained in section 6.3.2.4).



---

## 5.Improvement of the precipitation forcing<sup>1</sup>

### 5.1. Introduction

Precipitation is one of the most important components in the water cycle and climate studies, through it, water mass is transported and redistributed around the world (Kidd & Huffman, 2011; Trenberth et al., 2017). Therefore, Land Surface Models (LSMs) allow us to simulate water and energy exchanges, however, inaccuracies in precipitation forcing used in these models can lead to errors in simulated outputs, such as runoff or evapotranspiration. Thus, high-quality precipitation forcing data with the appropriate spatial and temporal resolution is a fundamental requirement for obtaining accurate and reliable results from LSMs, especially when they are used for the management of water resources (Liu et al., 2017; Sun et al., 2018).

Precipitation has a wide temporal and spatial variability worldwide, which makes it difficult to monitor. Accurate monitoring and measurement of precipitation are crucial to our well-being (Kidd & Huffman, 2011). The most common precipitation information source is ground rain gauges, which measure the depth of rainfall as it accumulates over time (Sun et al., 2018). To fully understand the variability of the precipitation, it is essential to have dense observational networks that capture such variability, specifically at fine temporal (i.e., intra-daily) and spatial, from local to global, scales. However, despite the importance of such data, observational networks fall short in terms of both spatial density and temporal resolution, as the availability of precipitation measurements at sub-daily scales is becoming increasingly limited (Kidd & Huffman, 2011; Kidd et al., 2017) making it challenging to understand intra-daily precipitation patterns and variability.

Owing to the sparse spatial coverage of observational networks, spatial interpolation methods are necessary to provide estimated precipitation over large areas (Hofstra et al., 2008; Zolina et al., 2014), resulting in gridded products, e.g. SAFRAN (Quintana-Seguí et al., 2017), Spain02 (Herrera et al., 2016), GPCC-daily (Schamm et al., 2014), GHCN-Daily (Menne et al., 2012), and the E-OBS Gridded Observation-Based Data Set (Cornes et al., 2018). Nevertheless, interpolated data is seldom representative, due to techniques used to interpolate often smooth the extreme values and affect the long-term trends. Thus, interpolated precipitation is therefore subjected to uncertainty from errors in measurements and interpolation methods, both may be associated with orography and atmospheric characteristics (Boers et al., 2016). For example, Raimonet et al.

---

<sup>1</sup> Based on: **Cenobio-Cruz, O.**, Quintana-Seguí, P., Boone, A., Le Moigne, P., & Garrote, L. (2023). Assessment of the hydrological impact of an hourly precipitation distribution correction method in the SASER modeling system. (Manuscript submitted for publication). *Journal of Hydrology X*

---

---

(2017) compared different precipitation products and showed that the choice of gridded meteorological datasets has a significant impact on the efficiency of streamflow simulations.

On the other hand, recent advances and sophisticated instruments allow us to make up for the coverage and temporal scale limitations from precipitation measurements (Sun et al., 2018) using infrared and microwave instruments, such as disdrometers and radars. The latter provides real-time spatially-distributed measurements of precipitation, although the spatial coverage of radar networks is inadequate to monitor and quantify precipitation on a global basis (Kidd & Huffman, 2011; Habib et al., 2012). Some products merge satellite and ground measurements in order to take advantage of the information provided by the different systems (Tapiador et al., 2012; Sun et al., 2018), some examples of these products include, the Climate Prediction Center morphing technique (CMORPH, Joyce et al., 2004), the Integrated Multisatellite Retrievals for Global Precipitation Measurement (IMERG, Huffman et al., 2014); the Global Satellite Mapping of Precipitation (GSMaP, Mega et al., 2014); the Climate Hazards Group Infrared Precipitation with Stations (CHIRPS, Funk et al., 2015), all of them are constrained to regions with latitudes of  $\leq 60^\circ\text{N/S}$  ( $\leq 50^\circ\text{N/S}$  for CHIRPS) and have a spatial resolution varying from  $0.04^\circ$  to  $0.25^\circ$ ; and the global coverage Multi-Source Weighted-Ensemble Precipitation (MSWEP,  $0.1^\circ$ , Beck et al., 2019).

Other sources of precipitation are models based on reanalysis (e.g. Era-Interim (Dee et al., 2011); ERA-5 (Hersbach et al., 2020); JRA25 (Onogi et al., 2007) to name a few) and Regional Climate Models (RCMs). The former provides spatially and temporally homogeneous data that encompass physical and dynamical processes which generate relatively high-quality estimations with a higher spatial resolution (Tapiador et al., 2012). Moreover, RCMs driven by reanalysis are able to simulate the internal variability of the climate system in synchrony with reality, proving the reanalysis is of enough good quality, in contrast to those driven by the Global Climate Models (GCMs). Either way, the RCMs were designed to increase the spatial resolution through a downscaling approach over a limited area domain (Giorgi et al., 1990). As a result, RCMs enable the improvement of the representation of small-scale processes that affect the precipitation (Rummukainen, 2016), even though simulated precipitation by reanalysis or RCMs often requires further processing, such as bias correction, before it can be used in different applications (Christensen et al., 2008; Teutschbein & Seibert, 2010; Themeßl et al., 2012).

The present chapter has a two-fold objective. First, to enhance the hourly representation of precipitation and its variability in the Ebro basin by incorporating data from a regional climate model to improve SAFRAN's data. To achieve this, the precipitation distribution of SAFRAN data was adjusted based on the distribution provided by a RCM, to better align it with observations. This approach is consistent with the statistical techniques applied to bias correction (Gudmundsson, Bremnes, et al., 2012; Chen et al., 2013; Lafon et al., 2013; Maraun, 2016).

Furthermore, the integration of RCMs in conjunction with Land Surface Models (LSMs) has been a widely adopted approach to improve the representation of Earth's physical processes and provide valuable insights to better understand underlying physical mechanisms (Prudhomme et al., 2014; Barella-Ortiz & Quintana-Seguí, 2019; Quintana-Seguí et al., 2020). Hence, the second objective is to evaluate the impact of the improved precipitation dataset on the hydrological simulation using the SURFEX-LSM model, by comparing the results of the simulation using the improved dataset to those of the previous simulations using the original SAFRAN dataset.

## 5.2. Study area and data

The study area, which encompasses the geographical region of interest, is described in detail in sections 3.1.1 and 3.1.2. This section provides information on the location, boundaries, and specific characteristics of the study area.

In section 3.2.1, we provide a comprehensive description of the data used in this analysis.

## 5.3. Methodology

In this section, a correction method was applied consisting of two steps: (i) hourly precipitation with very low intensity was adjusted, and (ii) the linear correction method was applied. Those steps are shown in Figure 5-1 and described in detail below.

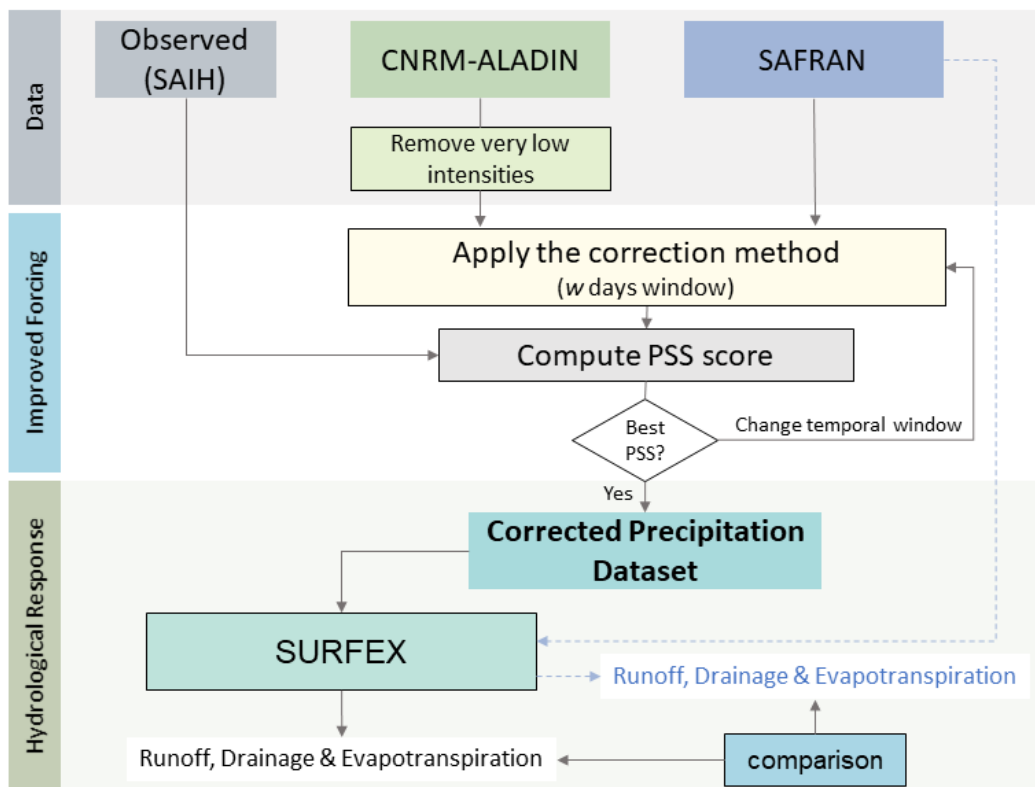


Figure 5-1 Flow chart of the methodology proposed to correct the hourly precipitation distribution and evaluate the hydrological response.

### 5.3.1. Correction Method

As a first step, simulated precipitation is corrected by removing very low intensity events. The main reason is that the drizzle effect produced by the RCM often overestimates the low intensity precipitation (Fowler et al., 2007). A static threshold between 0.01 and 1 mm d<sup>-1</sup> can be defined

to correct the precipitation, as indicated in previous studies (Piani et al., 2010; Lafon et al., 2013). Thus, a threshold was selected, which was fixed at  $1/24 \text{ mm h}^{-1}$  to be consistent with the temporal scale (24 hours), and consequently, all simulated precipitation values below this threshold were set to zero.

The hypothesis arises from the consistent negative bias in SAFRAN precipitation data, attributed to its reliance on relative humidity-based interpolation (Quintana-Seguí et al., 2008). The notable disparities between observed and modeled precipitation data, especially in complex climates like the Mediterranean (Herrera et al., 2010), suggest room for improvement. To address this, we integrate an RCM. By utilizing the RCM, we aim to notably enhance the temporal and spatial distribution of precipitation patterns, aligning them more accurately with the unique Mediterranean climate. Leveraging the RCM's capabilities, we expect to gain a more precise understanding of Mediterranean rainfall-runoff processes, thereby mitigating the negative bias in SAFRAN data and deepening our comprehension of the region's hydrological dynamics.

As a second step, a correction to the SAFRAN hourly precipitation rates was applied, to adjust their hourly distribution to the more realistic distribution provided by the RCM. As SAFRAN's precipitation is obtained from daily ground observations, we have high confidence in SAFRAN's total precipitation amounts, which are to be preserved. While RCMs perform well in non-mountainous regions, their performance is limited in areas with complex topography, as demonstrated by several studies (Rajczak et al., 2013; Isotta et al., 2014; Torma et al., 2015). Nevertheless, the precipitation temporal distribution of CNRM-ANLADIN is better than that of SAFRAN, but not necessarily the timing. Thus, a precipitation event that in reality happened at a given time, can be simulated by the model a few hours earlier or later. Thus, a time window  $w$ , which can be one or more days long, is defined in which SAFRAN's accumulated precipitation is preserved. The total precipitation is transformed to  $P_{corrected}$  according to the equation (1):

$$P(t)_{corrected} = P(t)_{ALD} \times \frac{\sum_{t=1}^w P(t)_{SAFRAN}}{\sum_{t=1}^w P(t)_{ALD}} \quad (5.1)$$

where  $P(t)$  is precipitation at time step  $t$ , in hours;  $P(t)_{ALD}$  is the CNRM-ALADIN63 precipitation data at time step  $t$ ; both in  $\text{mm h}^{-1}$ , and  $w$  is the time size of the window used to apply the correction, in days.

The previous equation was used to correct the hourly precipitation rate testing different values of  $w$  (from 1 to 7 and 14 days), to find the best window. In this step, improved precipitation data for each grid point at a spatial resolution of 2.5 km was generated.

### 5.3.1.1. Assessment of the corrected precipitation

The assessment of the methodology cannot be based on a method that requires perfect synchronicity between the time series, as this is impossible. The CNRM-ALADIN simulation will generate weather close to reality (as it has been forced by ERA-Interim at the boundaries), but it is not as close to reality as a reanalysis. Hence, our objective is to improve the distribution of hourly precipitation, while the accumulated amounts were preserved at a scale that ranges from one to a few days. Therefore, to compare the corrected product and the observations the Perkins skill score (PSS) was calculated (section 4.2.5.1).

The PSS has been calculated for hourly precipitation amounts from zero to the 99<sup>th</sup> quantile of the observations, which is used as a threshold for the calculation of the PSS. The PSS is calculated for each station separately, for different window sizes ( $w$ ) and the final value of PSS for each window size ( $w$ ) is the mean value of the 11 selected stations. The highest PSS value determines the best temporal window to correct the precipitation. Additionally, to evaluate the change of this skill score in more extreme precipitation values, the PSS for the 99.5<sup>th</sup> and 99.9<sup>th</sup> quantiles were calculated.

### 5.3.2. Assessment the impact on hydrological variables

SURFEX-LSM (SURFace EXternalisée, in French), a modeling platform developed and maintained by Météo-France (Masson et al., 2013; Le Moigne et al., 2020) that has been used to assess the hydrological response to different precipitation inputs in the current research. The ISBA (Interaction Soil-Biosphère-Atmosphère) scheme (Noilhan & Planton, 1989; Noilhan & Mahfouf, 1996) is an integral part of the SURFEX model. This scheme simulates the interactions between natural surfaces, consisting of the soil, vegetation and snow, and the atmosphere. Note that it does not simulate groundwater processes (as they are simulated by external models which can be coupled to SURFEX). In this research, SURFEX version 8.1 was used, along with the ISBA-DIF scheme, which allows for the resolution of water and heat transfer via diffusion within the soil (Decharme et al., 2011).

Precipitation plays a pivotal role, particularly in regions where flow persistence relies heavily on rainfall. Consequently, the intensity and magnitude of rainfall events constitute integral components within hydrological models (Kirkby et al., 2005; Gioia et al., 2008). The hypothesis that more intense precipitation events result in higher runoff volumes is firmly rooted in the dynamics of rainfall-runoff processes (Clark & Gedney, 2008; Price, 2011). This process occurs when the intensity of precipitation exceeds the soil's capacity for infiltration, the surplus water becomes unable to permeate the soil and, instead, swiftly traverses the land surface as runoff. This process is predominantly governed by several key factors, including soil permeability, land cover characteristics, and the antecedent moisture conditions of the soil (Price, 2011; Troch et al., 2013). Central to the hypothesis is the recognition of a direct relationship between the intensity of rainfall and the resultant volume of runoff generated

SURFEX simulations are performed using SAFRAN and the improved precipitation dataset as input. The default configuration of SURFEX uses the Variable Infiltration Capacity (VIC) to generate the sub-grid runoff, which was not modified in this research. Similarly, a comparison is made between the results obtained using the standard SAFRAN precipitation dataset and the improved dataset. Additionally, an analysis of the various components of the water balance is conducted at an hourly time step. Since a high spatial resolution SURFEX setup (such as that used herein) is computationally intensive, a subset of the data is selected for simulation purposes. This approach significantly reduces the computational burden while still yielding valuable information. Consequently, hourly simulations were performed over three years, specifically from 2011 to 2014.

The water balance analysis at the grid point scale is performed with a focus on the more intense events. For this purpose, the highest  $n$  precipitation events, with intensities exceeding  $10 \text{ mm h}^{-1}$  (WMO, 2018), were extracted and centered using a  $\pm 12$  hour time window before and after the peak. The mean hourly precipitation was then computed based on these  $n$  events. As was done for the precipitation, the values of the other variables simulated by SURFEX (surface runoff,



drainage, and evapotranspiration) were extracted, and then the mean values were computed to explore changes in the hydrological response.

## 5.4. Results

### 5.4.1. Improvement of precipitation intensities

The ability of SAFRAN to reproduce the precipitation amounts from different precipitation intensities (from 5 to 30 mm h<sup>-1</sup>) was evaluated as depicted in both panels of Figure 5-2. For lower intensities (left panel of Figure 5-2), SAFRAN reveals lower frequencies with respect to the observations, while for higher intensities, SAFRAN almost does not capture any event of the higher rainfall intensities. In other words, SAFRAN has difficulties in producing low-intensity precipitation events (between 5- and 9-mm h<sup>-1</sup>) and is practically unable to reproduce events higher than or equal to 10 mm h<sup>-1</sup>.

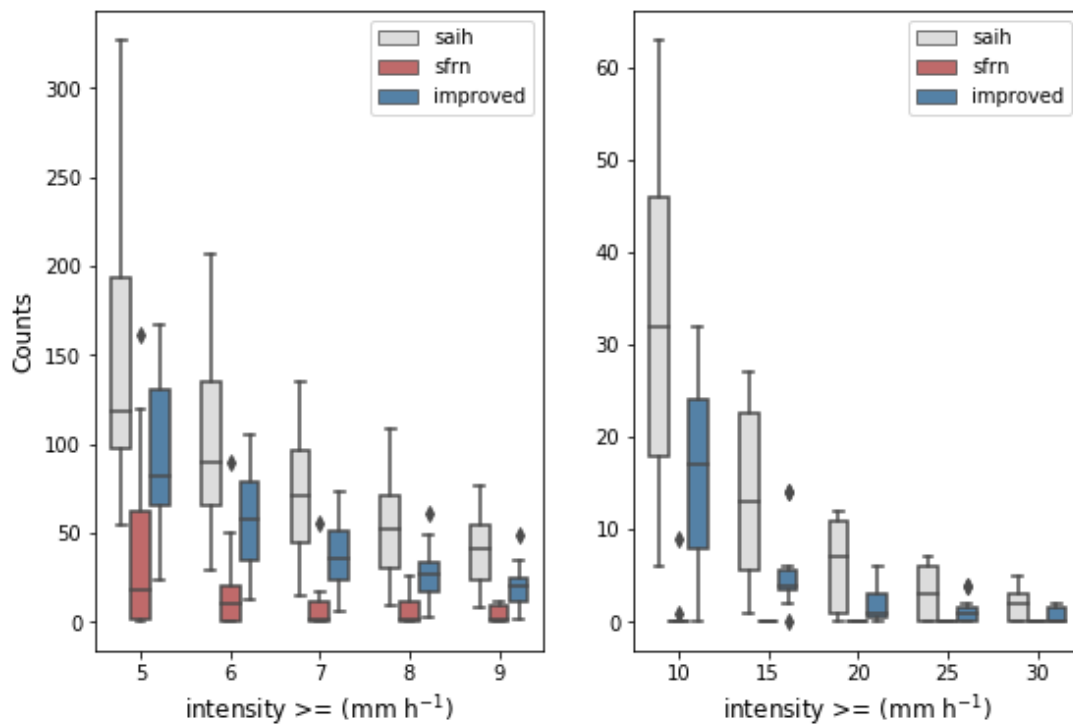


Figure 5-2 Comparison of frequency from different precipitation intensities for observed data in gray (saih), precipitation simulated by SAFRAN in red (sfrn), and corrected precipitation (7 days) in blue (corrected). The horizontal line in each box represents the median, top and bottom box edges represent the interquartile range.

To improve SAFRAN's precipitation, the determination of the optimal window size to correct precipitation intensities while preserving the accumulated rainfall of SAFRAN (which is considered reliable) is conducted as the first step. Thus, as explained earlier, the average PSS score over the 11 stations was computed, for different values of  $w$  and selected the one that maximizes the PSS, as indicated in Table 5-1. The 7-day correction shows the highest average PSS (0.86) and four stations show the highest PSS for this time step. Thus, the one-week (7 days) window size was selected. Figure 5-3 shows the time series comparison for the Ebro-Tortosa station between SAIH, SAFRAN, and improved precipitation data.

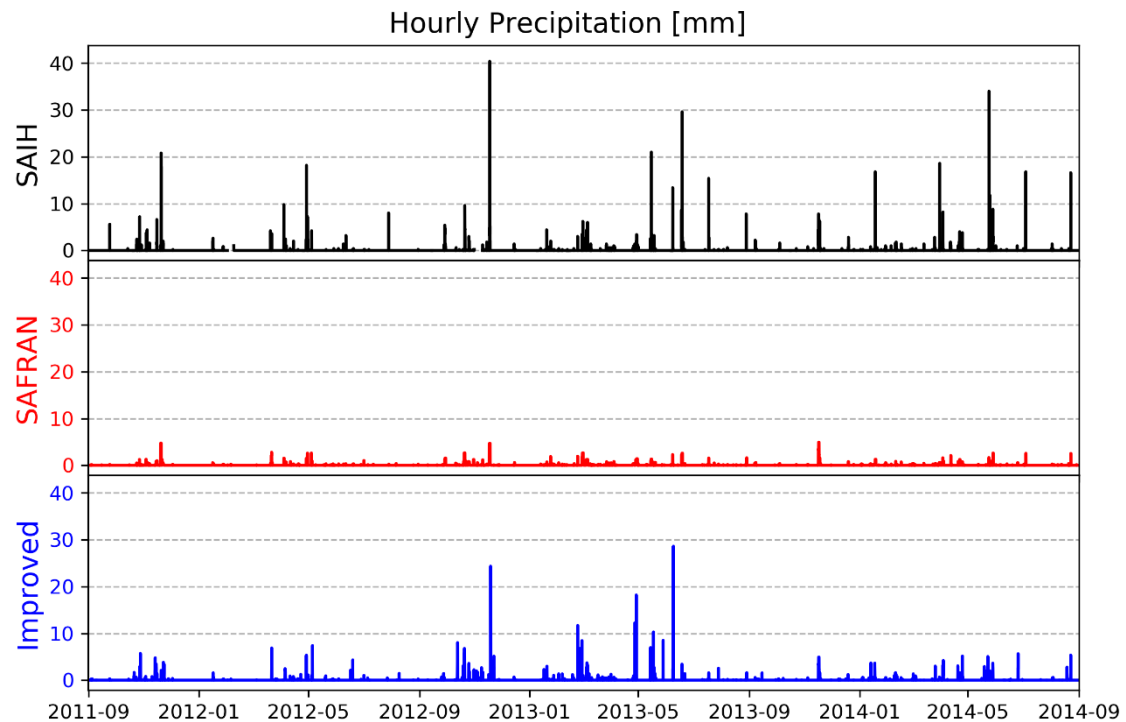


Figure 5-3 Time series comparison for the Tortosa-Ebro station (only the last 3 years for better visualization).

Figure 5-4 depicts the effect of the correction method for different window sizes ( $w$ ) for the Ebro-Tortosa station. To obtain a better representation of the extreme values, a logarithmic scale was used. It allows us to compare the relative frequency of hourly precipitation between the improved precipitation (in blue), the observed data (in black), and the simulated precipitation by SAFRAN and CNRM-ALADIN (in red and gray, respectively). Notice that the SAFRAN maximum intensity rate does not exceed  $10 \text{ mm h}^{-1}$ , which is much lower than the observed intensity rate ( $40 \text{ mm h}^{-1}$ ). It is therefore clear that SAFRAN underestimates precipitation intensities. Also, as observed, as a larger window size is employed for calculating the precipitation correction, it becomes closer to the observed data, especially for 7 and 14-day values.

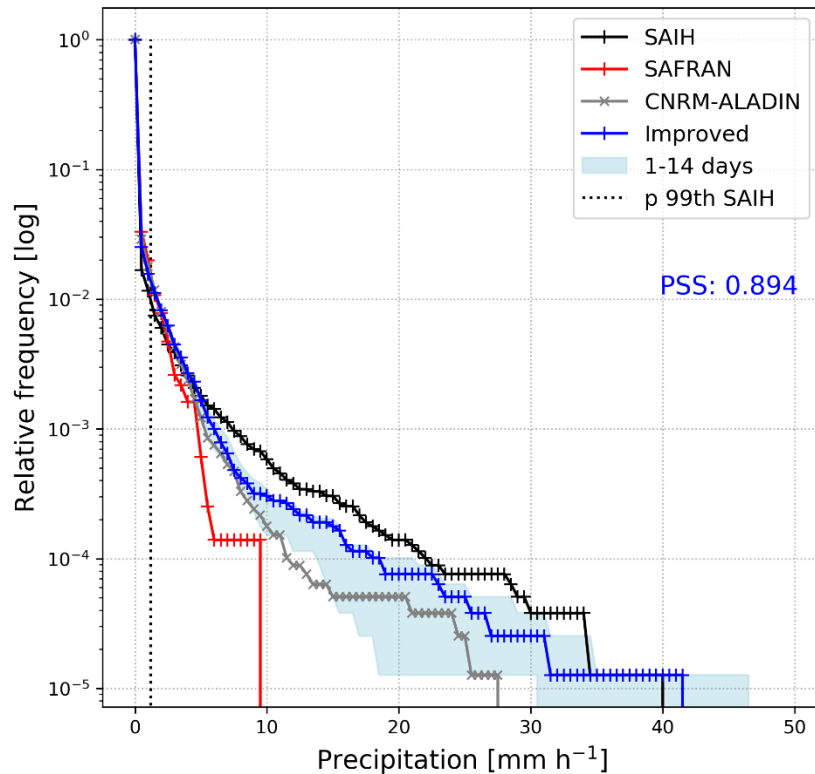


Figure 5-4 Relative frequencies of precipitation for observations (in black), SAFRAN (in red), CNRM-ALADIN (in gray), and correction (in blue) from different correction windows. Probabilities are computed for the period (2005 - 2014) hourly precipitation to the Ebro-Tortosa station. PSS number corresponds to Perkins Skill Score for corrected precipitation. The vertical dotted line represents the 99<sup>th</sup> percentile of the observation.

For low precipitation amounts (i.e.  $<5 \text{ mm h}^{-1}$ ) both products, SAFRAN and CNRM-ALADIN, match well with the observations, as depicted in Figure 5-4. In contrast, for higher rates, SAFRAN begins to differ markedly from the observations, which indicates that SAFRAN is not able to reproduce higher rainfall rates adequately. Both products underestimate the values, however, the distribution of the CNRM product remains similar to the observations. Focusing on the improved precipitation, blue boxes in Figure 5-2, have revealed significant improvements in the intensity rates, providing a more accurate representation of the precipitation patterns and distribution.

Table 5-2 shows the PSS calculated for precipitation amounts above three different percentile values (99<sup>th</sup>, 99.5<sup>th</sup>, and 99.99<sup>th</sup>). In this way, the accuracy of the correction method to reproduce the most extreme intensities was evaluated. It is evident that the PSS between SAFRAN and the observations for the 99.9<sup>th</sup> percentile experiences a sharp decline, indicating that SAFRAN is not able to accurately simulate the most extreme precipitation events. In some cases, there is a noticeable lack of similarity between the distributions, further demonstrating the limitations of SAFRAN in simulating these intense events.

The only station that has no reported events of intensity greater than  $10 \text{ mm h}^{-1}$ , after applying the correction, was station LAGRAN (Figure 5-5). Although the PSS of this station showed a notable improvement as registered in Table 5-1.

Table 5-1. PSS values for different time-step and each selected station.

ID	Station Name	Percentile 99 <sup>th</sup> (mm)	PSS (SAFRAN)	PSS (CNRM)	PSS (Correction with a window of $w$ days)							
					1	2	3	4	5	6	7	14
9027	EBRO TORTOSA	1.2	0.73	0.85	0.83	0.86	0.88	0.86	0.87	<b>0.91</b>	0.89	0.87
9102	NOGUERA	1.8	0.68	0.74	0.79	0.81	0.79	0.82	0.82	0.79	<b>0.82</b>	0.82
PC04	ZARAGOZA	1.0	0.73	0.87	0.77	0.81	0.81	0.83	0.84	0.83	0.83	<b>0.87</b>
9074	ZADORRA	1.6	0.59	0.84	0.83	0.84	0.86	0.89	0.87	0.88	0.89	<b>0.90</b>
9095	VERO	1.2	0.60	0.75	0.71	0.75	0.76	0.78	0.76	0.79	0.80	<b>0.81</b>
9256	SEGRE	1.4	0.72	0.89	0.80	0.84	0.83	0.85	0.88	0.86	<b>0.89</b>	0.88
9259	SALAZAR	3.0	0.75	0.77	0.86	<b>0.90</b>	0.90	0.88	0.88	0.87	0.84	0.87
9271	ARAGON	3.2	0.75	0.72	0.81	0.79	0.81	0.82	0.83	0.83	<b>0.85</b>	0.79
9282	ARAGÓN - MARTES	1.8	0.80	0.90	0.87	0.89	0.89	0.90	0.91	0.90	<b>0.92</b>	0.90
P008	LAGRAN	1.4	0.71	0.85	0.81	0.85	0.87	0.88	<b>0.92</b>	0.89	0.89	0.88
P016	ANSO	3.0	0.76	0.75	<b>0.87</b>	0.86	0.86	0.86	0.87	0.87	0.85	0.84
<b>Mean value</b>			0.71	0.81	0.81	0.84	0.84	0.85	0.86	0.85	<b>0.86</b>	0.86

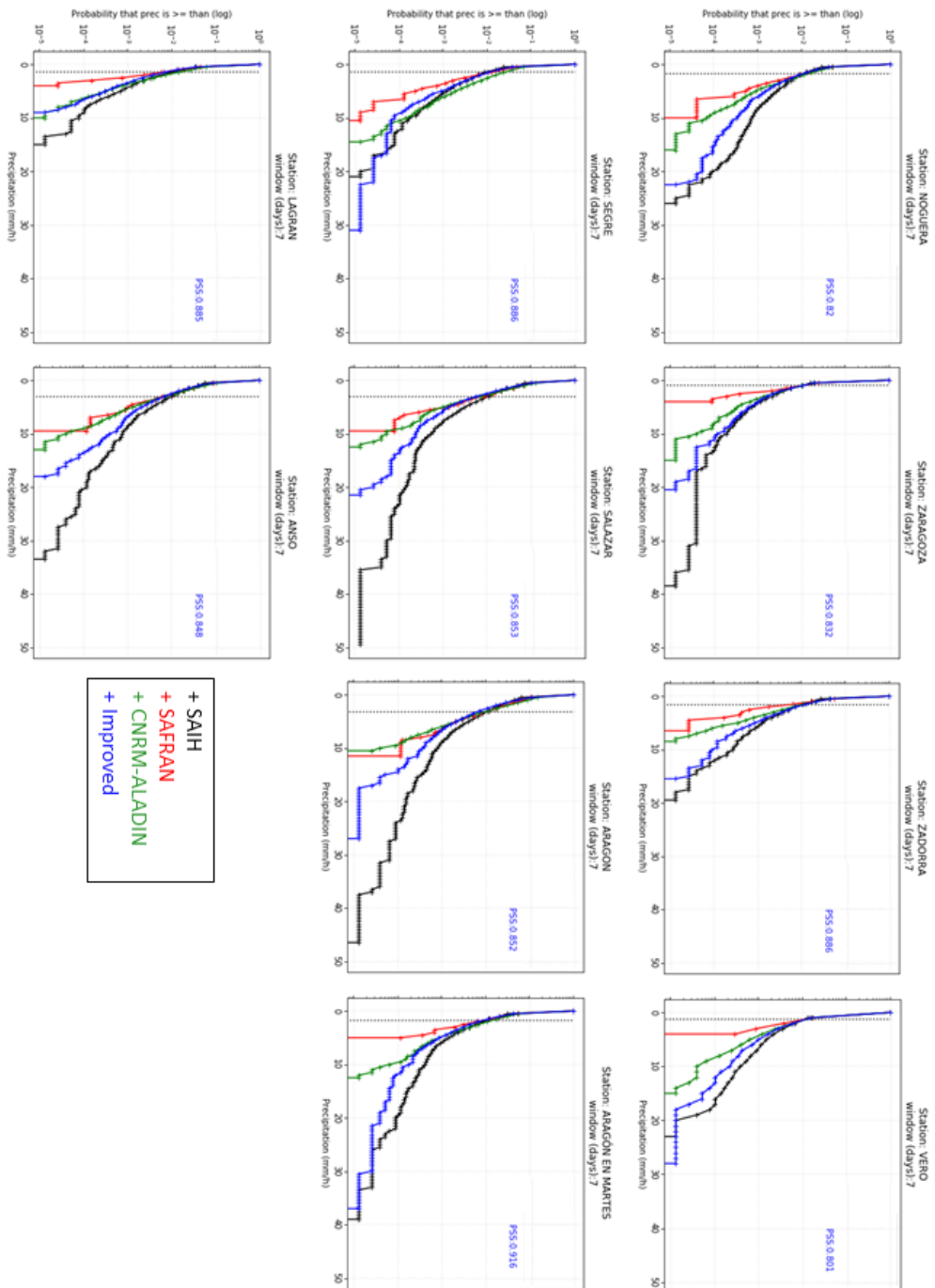


Figure 5-5 Same as Figure 5-4 but only for the 7 days correction for each station.

Table 5-2. PSS obtained for precipitation amounts above different percentiles for each station. Corresponding percentile values were calculated from the observed data (SAIH) for the whole period. The PSS value of the improved precipitation is indicated in bold in the third column for each percentile.

ID	Station Name	99th percentile			99.5th percentile			99.9th percentile					
		value	PSS (SAFRAN)	PSS (CNRM)	PSS	value	PSS (SAFRAN)	PSS (CNRM)	PSS	value	PSS (SAFRAN)	PSS (CNRM)	PSS
9027	<b>TORTOSA</b>	1.2	0.73	0.85	0.89	2.2	0.61	0.80	0.80	7.4	0.11	0.62	0.69
9102	NOGUERA	1.8	0.68	0.74	0.82	3.2	0.57	0.67	0.81	8.2	0.05	0.48	0.75
PC04	ZARAGOZA	1.0	0.73	0.87	0.83	1.6	0.60	0.80	0.76	4.2	0.29	0.77	0.81
9074	ZADORRA	1.6	0.59	0.84	0.89	2.5	0.78	0.80	0.88	5.6	0.27	0.65	0.76
9095	VERO	1.2	0.60	0.75	0.80	2.4	0.68	0.84	0.84	6.2	-	0.65	0.69
9256	SEGRE	1.4	0.72	0.89	0.89	2.4	0.76	0.88	0.86	5.4	0.42	0.77	0.82
9259	SALAZAR	3.0	0.75	0.77	0.84	4.2	0.66	0.78	0.85	7.7	0.15	0.63	0.70
9271	ARAGON	3.2	0.75	0.72	0.85	4.6	0.77	0.78	0.86	8.8	0.03	0.38	0.63
9282	AGON EN MAR	1.8	0.80	0.90	0.92	2.6	0.76	0.82	0.87	5.7	-	0.70	0.70
P008	LAGRAN	1.4	0.71	0.85	0.89	2.0	0.59	0.83	0.89	4.2	-	0.79	0.84
P016	ANSO	3.0	0.76	0.75	0.85	4.2	0.69	0.79	0.84	8.6	0.19	0.54	0.61

## 5.4.2. Impact on the water balance components

### 5.4.2.1. Impact on intense events

To investigate the hydrological response on the main variables (drainage, runoff, and evapotranspiration), SURFEX was implemented using the default SAFRAN and the improved precipitation datasets as inputs. Since SURFEX, when used in a configuration such as that in the current study, can be computationally-intensive, the model was run for the last three years (2011 to 2014) with output stored at an hourly time step.

For each station location, the  $n$  number of highly intense precipitation events and their respective variables simulated by SURFEX were extracted from the gridded precipitation data. Subsequently, the mean event was computed, centered at  $\pm 12$  hours. [Figure 5-6](#) shows the mean event for the Ebro-Tortosa station.

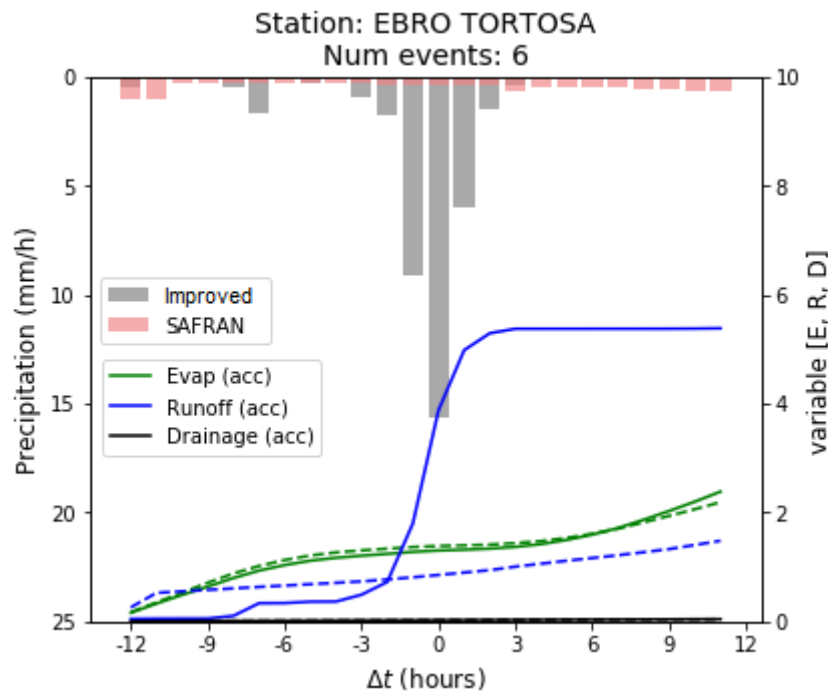


Figure 5-6 Composite of the 6 highest hourly events in the Ebro-Tortosa station. Mean precipitation is plotted in gray bars (the improved precipitation) and red bars (SAFRAN's precipitation). Solid lines represent the mean variables (accumulated) from the new simulation. The dashed lines represent the variables of the default simulation. In blue, the runoff; in green, the evaporation and in black the drainage.

[Figure 5-6](#) shows the cumulative volumes of the three main components of the water balance at the grid scale for the Tortosa station. A noticeable impact was found on the runoff, as expected, as higher precipitation intensities were introduced. However, no changes were observed in the drainage. In terms of evapotranspiration (ET), the response is less clear, however, follows a similar behavior. Similar patterns of hydrological response were found in the stations located in the dominated Mediterranean weather. In contrast stations 9256-SEGRE and 9102-NOGUERA show responses in both variables (runoff and ET) as shown in [Figure 5-7](#), these stations are located in mountainous areas of the basin. In general, the amount of runoff produced varies greatly across the stations analyzed. However, a common trend observed in all stations is that greater precipitation intensity leads to a corresponding increase in runoff.

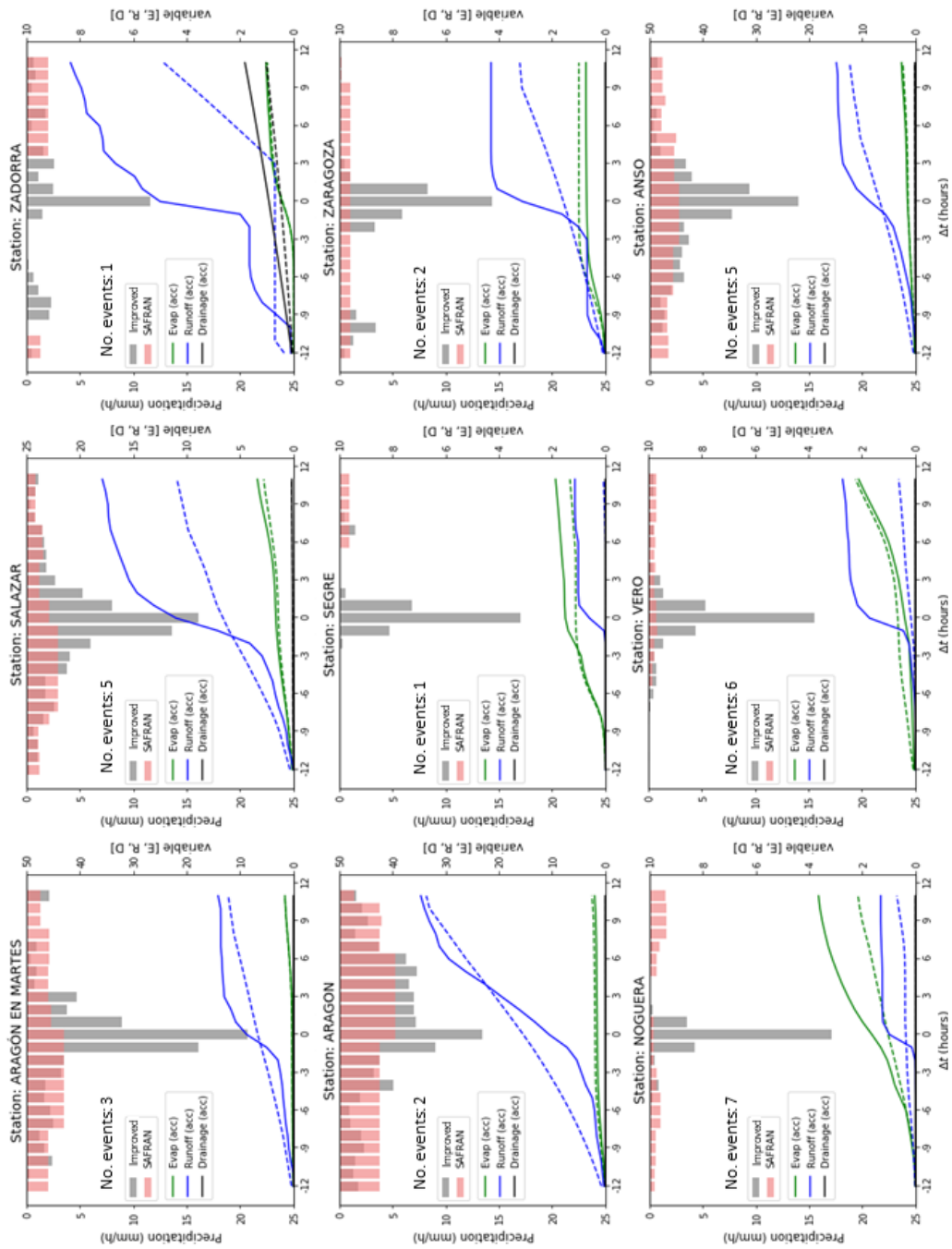


Figure 5-7 Same as Figure 5-6 but for each selected station.



### 5.4.2.2. Long-term water budget

To understand the impact on the water balance the long-term budget was evaluated (runoff, drainage, and ET) on the same grid points where the meteorological stations are located. It is important to mention that the total amount of water provided by SAFRAN was unchanged, it was only temporally redistributed using a more realistic precipitation distribution. The SURFEX hourly simulation for the last three years was used and computed the relative frequencies of the different water balance variables were. Figure 5-8 shows the change in the simulated variables using SURFEX driven by the new precipitation dataset for the Ebro-Tortosa station. Note that in particular low rates for runoff ( $<1 \text{ mm h}^{-1}$ ) nicely follow similar patterns in both simulations (SAFRAN and improved, blue dashed line and blue solid line, respectively). For higher rates, the runoff clearly shows an impact, increasing the extreme values to 3 times higher than the default simulation. In contrast, drainage and evapotranspiration have no noticeable changes. The same plot for each station can be found in Figure 5-9.

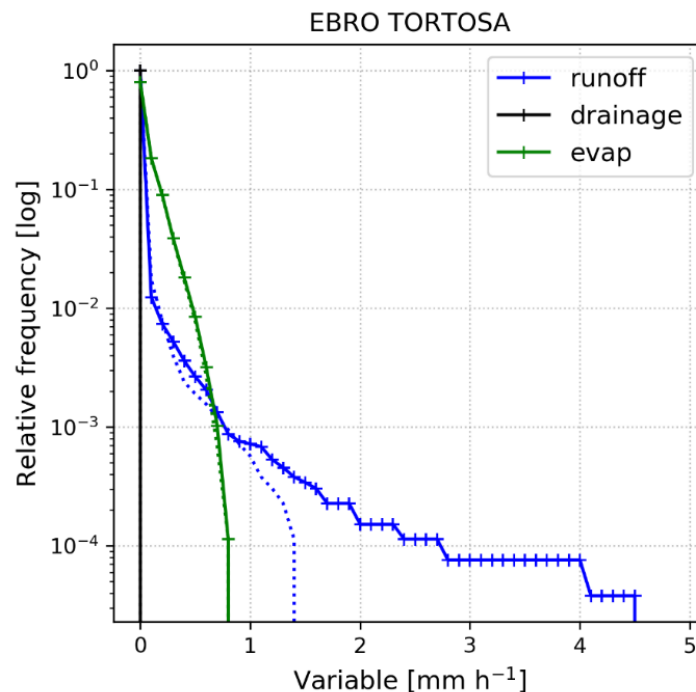


Figure 5-8 Relative frequencies of water balance variables (runoff, drainage, evapotranspiration) for the Ebro-Tortosa station. Solid lines represent the simulation driven by corrected precipitation; dashed lines correspond to the default simulation (SAFRAN). Frequencies are computed with the hourly simulation for the last 3 years (2011-2014)

The water budget was evaluated at the grid point level (Figure 5-8 and Figure 5-9), the pixel that corresponds with the location of each station. Similar patterns were found in each station, only for the station Salazar the drainage reported significant changes (Figure 5-9). The stations located in higher elevations (e.g. Salazar, Aragón, Anso) show major changes in the hydrological response, especially runoff that report extreme values on average two times higher than the produced by the simulation driven by SAFRAN; evapotranspiration also shows slight changes and drainage do not report significant changes. The rest of stations reported similar patterns in each variable.

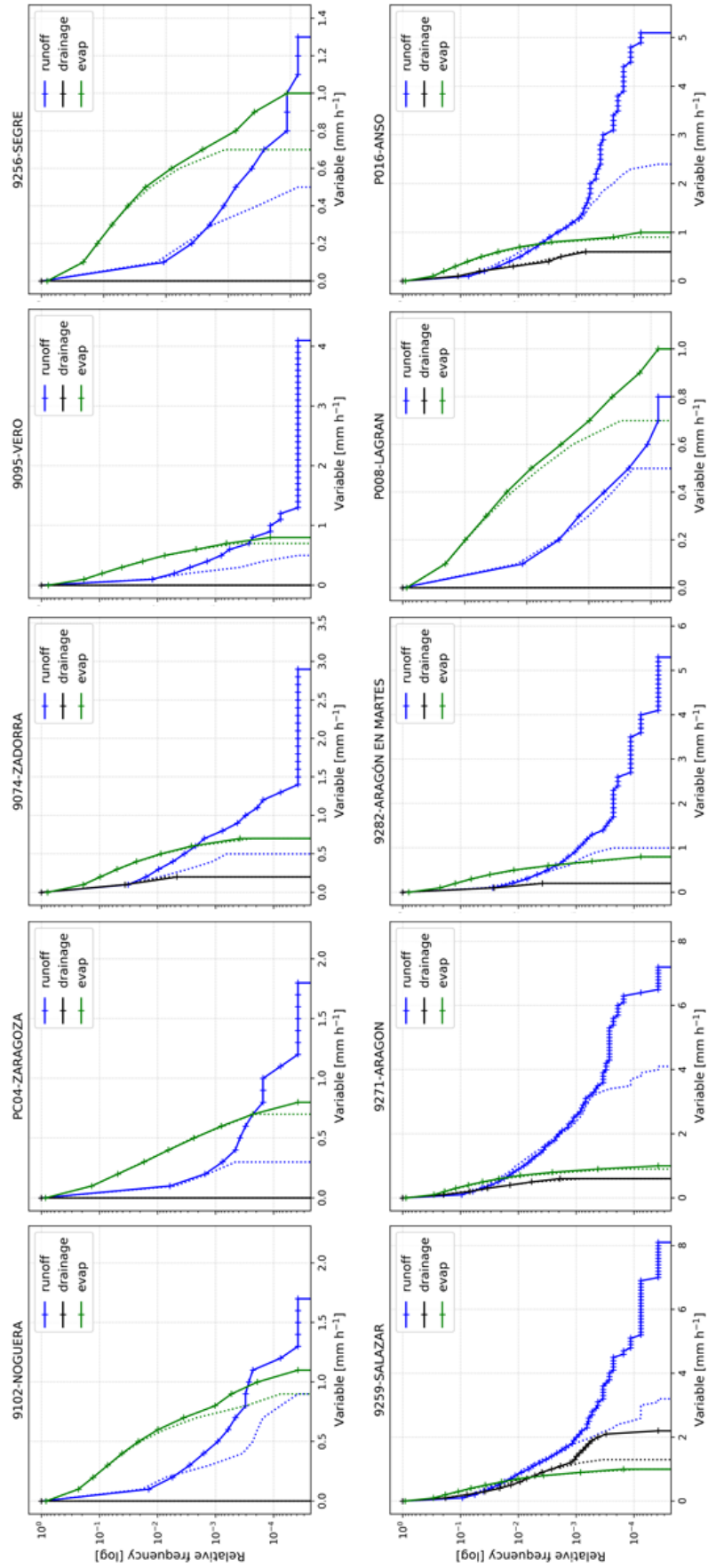


Figure 5-9 Same as figure 5-7 for each station.

In [Figure 5-10](#) the statistics of the variables simulated by the default precipitation data (SAFRAN, light colors) and by the improved precipitation (darker colors) are shown for three different (extreme) percentiles to the 11 stations. The simulation driven by the improved precipitation reported higher extreme values, especially in the percentile 99.9<sup>th</sup> of runoff (darker blue boxes in [Figure 5-10 a](#)) as expected. Evapotranspiration shows similar changes, whereas drainage exhibited much smaller changes (green and grey boxes, respectively in [Figure 5-10 b](#)).

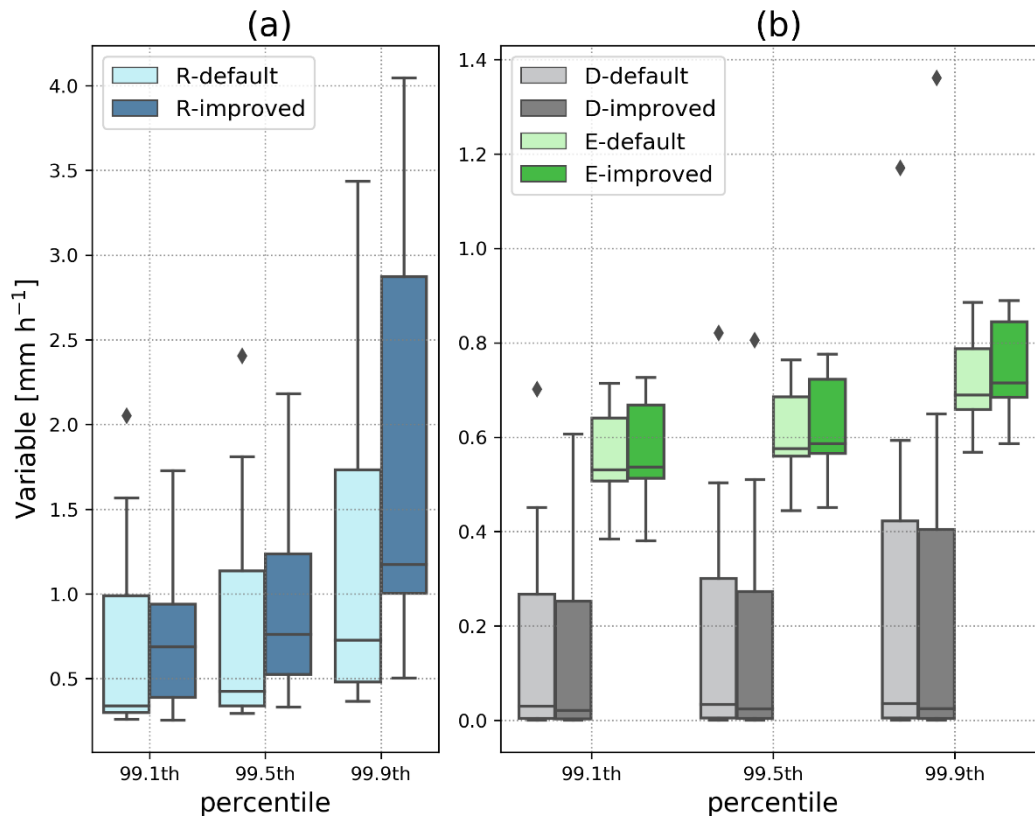


Figure 5-10. Comparison of different hourly percentiles (R=runoff, D=drainage, and E=evaporation) for simulation driven by SAFRAN (default, light colors) and by improved precipitation forcing (improved, darker colors). The horizontal line in each box represents the median, and the box represents the interquartile range. The whiskers extend a maximum of 1.5 times the interquartile range.

After evaluating the water budget at the grid point level (station), each variable of the water budget simulated by SURFEX was spatially aggregated to evaluate the water budget at the catchment scale using the yearly mean of each variable. The percentage of the water budget that represents each variable is presented in [Table 5-3](#).

Table 5-3 Water budget per year over the Ebro basin.

year	Default			Corrected			Total (mm)
	Drainage	Runoff	Evap	Drainage	Runoff	Evap	
2011	7.0%	10.8%	82.3%	6.6%	9.8%	83.7%	492.56
2012	15.4%	17.0%	67.6%	14.8%	16.2%	69.0%	865.68
2013	11.9%	14.1%	74.0%	11.4%	13.2%	75.4%	680.81

The results reveal only small changes in the water budget at the catchment scale. The main differences are related to ET, which increases by 1.5% on average, whereas runoff and drainage decrease by 1% and 0.5% on average, respectively. It indicates that the impact of the improved precipitation dataset is more noticeable at finer scales, whereas the changes become less evident as the scale increases, both temporal and spatial.

## 5.5. Discussion

The accuracy and reliability of hydrologic simulations are influenced by multiple factors, including not only the uncertainty of the input data but also the characteristics of the simulation model and the specific hydrologic variables being studied.

Precipitation is the main source of water for surface runoff, thus changes in precipitation can directly influence the amount and timing of surface runoff. Overall, the sensitivity of the surface runoff to differences in precipitation highlights the importance of accurately representing precipitation in hydrologic models. [Herrera et al. \(2016\)](#) found that the spatial distribution of precipitation is influenced by the complex orography and that the density of observation stations plays a crucial role in accurately representing precipitation patterns in gridded products. Thus, gridded precipitation products, such as SAFRAN, may not be representative in mountainous regions due to sparse weather station coverage, and the spatial heterogeneity of precipitation events that are not often captured by the gauge network ([Durand et al., 1993](#); [Prein & Gobiet, 2017](#)). It highlights the potential use of RCMs to improve the precipitation patterns in mountain regions, where observations are sparse.

The focus of this study was on the improvement of the hourly precipitation distribution in the Ebro basin, with the timing issue ([Figure 5-3](#)) not being addressed, which can be considered another limitation of our research. The enhancement of precipitation event timing would enable a more accurate simulation of the effects of rainfall on the overall water balance, which is of crucial importance for real-time water management. Nevertheless, improving the timing of precipitation (when an event occurs) is a more challenging task than improving its temporal distribution (disaggregating rainfall to neighboring time steps within some window). Future research could explore the effects of both the distribution and timing of precipitation on the hydrologic response of the basin.

In this study, the precipitation distribution was modified, while the remaining forcing variables were left unadjusted. It is essential to recognize that changes in precipitation have consequential effects on other atmospheric forcing. For instance, an increase in precipitation leads to an augmented presence of clouds, which can subsequently affect evapotranspiration processes. Consequently, this alteration in the energy balance may also lead to modifications in runoff or drainage patterns. Additionally, it is important to note that rainfall can also influence air temperature dynamics. Therefore, future research should consider these interrelated processes to ensure the preservation of variable homogeneity and to achieve a comprehensive understanding of the system dynamics.

Our results confirm that precipitation has a significant impact on the amount of runoff generated in a particular area, as expected. Increased precipitation can lead to increased surface runoff, and this relationship is incorporated into the corresponding runoff generation models. In mountainous areas, which tend to receive higher amounts of precipitation compared to the rest of the basin,

high-intensity precipitation events have a significant impact on runoff generation due to topography, soil characteristics, and permeability. Factors such as slope, soil depth, and land cover can also influence the reaction of runoff to high-intensity precipitation events in these areas. In contrast, the Mediterranean part of the basin experiences semi-arid and arid conditions, which often result in dry and compacted soil. Consequently, when high-intensity rainfall events occur, the water cannot easily infiltrate the soil and instead runs off quickly over the surface, resulting in a direct response to intense precipitation events. Additionally, the timing and duration of the intense precipitation event can also impact runoff, with longer-duration events generally leading to more infiltration and less runoff. These findings highlight the challenges of capturing the details of runoff generation processes in hydrological models due to the terrain's complexity and precipitation patterns' variability.

The responses of evapotranspiration (ET) and drainage to modified rainfall exhibit a reduced sensitivity compared to surface runoff. Particularly, these variables show slight changes only in areas that predominate wet conditions (the northern part of the Ebro basin). In these areas, soil retains more water, thus intense precipitation events can have a more significant impact on both evapotranspiration and drainage: intense precipitation events can increase the amount of water availability and can lead to raised evapotranspiration, resulting in a reduction of water available for drainage. In contrast, in semi-arid regions with a Mediterranean climate, the soil is generally drier and does not retain as much water, meaning that intense precipitation events may not have a significant impact on evapotranspiration and drainage, or at least impacts may be less pronounced.

As previously mentioned, our results suggest that precipitation has a stronger influence on surface runoff, which is in line with our initial expectations. Higher precipitation intensity can result in more surface runoff, i.e. the same precipitation amount over 1 hour has a much greater impact on surface runoff than if it were distributed over 3 or more hours. Furthermore, this is also associated with the representation of the fast runoff process in the model, which is an important factor in understanding the impacts of precipitation distribution on surface runoff. Hence, it is essential to carefully consider these factors when modeling surface runoff, particularly in regions that frequently experience intense precipitation events, such as arid or semiarid regions. In these areas, the infiltration mechanism tends to dominate the overland flow production, thus the Horton runoff approach is often more appropriate to describe these processes; within SURFEX, this approach can be activated to evaluate the impact on hydrological response. Although, the different runoff generation approaches in SURFEX were not evaluated. Therefore, further research could investigate and compare these different approaches. Finally, our study highlights the importance of using more detailed precipitation data to advance our understanding of hydrological processes and improve hydrological models at finer scales, particularly in areas with high spatial and temporal variability in precipitation.

The SURFEX model within the SASER suite has been used for simulating the water balance and streamflow, which is effective on average values (section 6.3.3.1). These findings suggest that the SURFEX model exhibits limited sensitivity in simulating hydrological variables in response to the use of finer precipitation inputs. This can be attributed to the catchment size, larger catchments have a lower sensitivity to forcing data due to the damping effect (Raimonet et al., 2017). This suggests that the choice of forcing data may not have a significant impact on the model performance in larger watersheds. Further investigations are needed to better understand the damping effect associated with catchment size on model sensitivity. Also, might be attributed to the nature of the model formulation itself, particularly in the runoff generation processes, which may not be capturing the complex details of precipitation information at higher temporal

resolution. This could result in the loss of information during the simulation of the hydrological response across the entire basin, leading to only minor variations in the results. This highlights the need for further investigation and consideration of alternative model formulations, or finer hydrological models, that are better suited to capture the complexities of precipitation and its impact on the hydrological response.

## 5.6. Conclusions

In this chapter, a novel linear correction method was introduced to enhance the accuracy of precipitation intensities by leveraging results from a regional climate model (RCM). Our proposed approach involves utilizing the precipitation distribution of the ERA-Interim driven CNRM-ALADIN RCM simulation to improve the hourly distribution of the SAFRAN meteorological forcing data. The resulting gridded precipitation dataset spans from 1979 to 2014 and has a high spatial resolution of 2.5 km and a time step of one hour. To evaluate the effectiveness of this improved precipitation dataset on the hydrological response, the SURFEX-LSM model was employed.

The results of our comparison between the SAFRAN meteorological forcing data, the improved precipitation data, and the observed precipitation data at the hourly time scale indicate that SAFRAN consistently underestimates precipitation intensities. However, the improved precipitation data, which was obtained through the correction of the RCM precipitation distribution, provides a better representation of the precipitation patterns in the Ebro basin, especially in the Mediterranean-dominated areas. Although the improved precipitation data still shows some underestimation of precipitation rates, it is a significant improvement over the original SAFRAN data and provides a more accurate representation of the actual precipitation patterns in the study area. One important limitation of our approach is that the timing of the precipitation events is not necessarily accurate. However, the weekly precipitation amount of the original SAFRAN dataset was preserved.

Our results show that the correction method has a clear impact on the simulated runoff at the grid point scale, which is consistent with our expectations. However, the changes in drainage and evapotranspiration are not straightforward to interpret, as they depend on multiple factors, such as the climate regime, as the response to drainage is higher in wet climates. During the analysis of the water balance at the watershed scale, it was observed that the overall balance, as represented by the sum of runoff, drainage, and evaporation, was found to be relatively minor in terms of its impact, with an average change of only 2%.

Finally, the new precipitation dataset presents a potential use in water resources particularly in improving the simulation of extreme weather events at finer temporal scales, such as floods and river discharge events. The accuracy of the dataset's magnitude is particularly critical in this context. However, its application would depend on the used model and the main purpose. Furthermore, the new dataset provides valuable insights into the impact of intense precipitation events on hydrological simulations by LSMs at sub-daily temporal scales. Therefore, it allows a more accurate and detailed understanding of the mechanisms that drive runoff generation during extreme weather events, which is essential for water resources.



---

## 6.Improvements in the SASER modeling chain

### 6.1. Introduction

Improving land surface models (LSM) is challenging. These challenges stem from the inherent complexities of the Earth's land surface and the multitude of processes that unfold within it. Consequently, the enhancement of LSM parameters that control hydrological response becomes essential for accurately representing land-atmosphere interactions, hydrological processes, and the feedback mechanisms that shape the Earth's system.

Several opportunities for improvement in the representation of hydrologic processes in land models can be identified across three distinct categories (Clark et al., 2015). The first category revolves around the direct enhancement of the model's representation of individual hydrologic processes, with critical factors such as soil moisture and groundwater dynamics being targeted for improvement. This category emphasizes the need to enhance data sets on geophysical attributes, including bedrock depth and permeability (Tesfa et al., 2009; Fan et al., 2015). Additionally, data sets on the physical characteristics of rivers are also identified as vital (Getirana et al., 2013; Gleason & Smith, 2014), providing a strong basis for these areas of improvement.

The second category involves the development of novel approaches that effectively capture the spatial heterogeneity and hydrologic connectivity present in real-world systems. For instance, several studies have shown that soil moisture can exert profound impacts on regional meteorology (Avisar & Pielke, 1989; F. Chen & Avisar, 1994; H. Y. Huang & Margulis, 2009), indicating that improved representation of soil moisture heterogeneity, and associated vegetation, can significantly enhance simulations of land-atmosphere interactions (Maxwell & Kollet, 2008). Addressing subgrid-scale heterogeneity can be achieved through explicit representation, utilizing parametrizations based on statistical-dynamical models (e.g. TOPMODEL (Beven & Kirkby, 1979) approach), or employing other approaches (Clark et al. (2015); Clark, Nijssen, et al. (2015) discuss them in detail).

The third category focuses on improving the representation of anthropogenic influences on the water cycle within land surface models. This aspect, beyond the scope of this chapter, is extensively covered in Chapter 7.

Therefore, the challenge of addressing uncertainties associated with model parametrization looms large. The simplifications and assumptions made during the parametrization process can propagate and impact the accuracy of model outputs. Understanding the sources of uncertainties and their propagation through the modeling system is crucial in addressing these challenges. Thus, developing strategies for quantifying and reducing uncertainties in LSM parametrization is crucial for improving model simulations.

---



The main objective of this chapter is to enhance the streamflow simulation in the hydrometeorological model SASER (SAFRAN – SURFEX – EauDyssée – RAPID) through different approaches. To achieve this goal, the first part of the chapter is focused on improving both high and low flows through calibration of the *runoff b* parameter and by improving soil information. For this purpose, a sensitivity analysis of the *runoff b* parameter was performed and then an attempt was made to calibrate this parameter using an index that compiles information on physical variables. Furthermore, the improvement in streamflow simulation was evaluated by enhancing the forcing of the soil database utilized by the SURFEX model.

In the second part, the low-flow simulation was enhanced, through the implementation of a well-known method: a conceptual reservoir (conceptual approach), which improves the representation of the slow component of the streamflow. To this end, and to determine the values of the new empirical parameters introduced by the reservoir, two methods were compared: (i) a catchment-by-catchment calibration approach (local calibration), which can only be used in near-natural basins where observational data are available, and (ii) a regionalization approach, which links the values of the parameters to physiographic and climate variables. This second approach allows determining the parameter values of the conceptual reservoir in human-influenced basins where observed low flows represent the water management effects of dams (which are not simulated) instead of the natural processes (which are expected to be simulated).

## 6.2. Early attempts aimed at improving inner model parametrization

This section will provide a concise overview of the key results regarding the early attempts at improving internal parameters that control hydrological response in the SURFEX model. These attempts were aimed to refine the representation of key model parameters to enhance the streamflow simulations. More detailed results are presented in [Appendix A](#).

### 6.2.1. Calibration of the *runoff b* parameter

The parameterization of the saturated fraction has a significant impact on runoff dynamics and is thus crucial for the determination of saturation-excess runoff. Variations in this parameter can have profound effects on the surface infiltration processes, subsequently influencing the generation of saturation-excess runoff and, in turn, base flow ([Boone et al., 2004](#); [Clark & Gedney, 2008](#); [Clark et al., 2008](#)). Considering this, an attempt was made to calibrate the *runoff b* parameter, within the SURFEX-LSM model, which is responsible for controlling runoff generation.

A sensitivity analysis was conducted to calibrate the parameter *runoff b*, which is critical in controlling runoff generation within the SURFEX model. The objective was to assess the sensitivity of model outputs to variations in the value of the *runoff b* parameter and identify the optimal value that best represents the observed hydrological processes. Multiple simulations were performed by systematically varying this parameter over a reasonable range. The simulated streamflow was compared against observed data to evaluate the model performance of each simulation. Therefore, KGE was calculated, as depicted in [Figure 6-1](#).

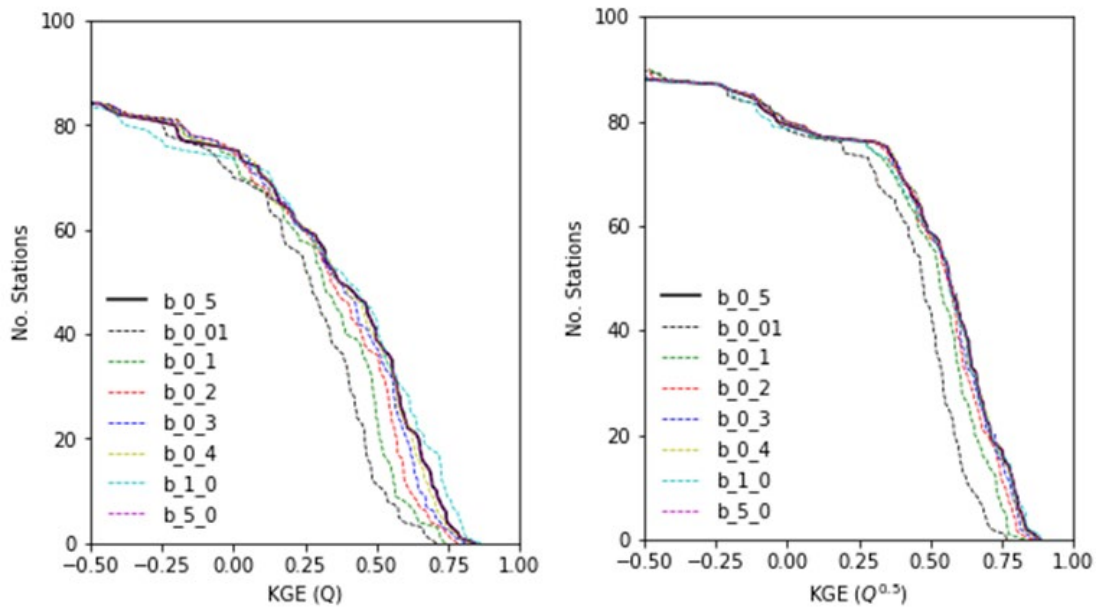


Figure 6-1 Accumulated distribution of the KGE from the different simulations varying the *runoff b* parameter. The left panel shows the KGE calculated on discharges and the right panel shows the KGE calculated on root-square transformed discharges.

The sensitivity analysis revealed that the *runoff b* parameter significantly influenced the simulated hydrological response, with variations in its value leading to noticeable changes in the model outputs (left panel in Figure 6-1). An optimal value for the *runoff b* parameter was determined that yielded the highest values of the KGE metric between simulated and observed streamflow.

The simulations revealed noticeable changes in the calculation of streamflow, indicating that the *runoff b* parameter associated with runoff has a discernible influence on the simulated results. However, despite these modifications, the performance of the simulated streamflow, as evaluated by the KGE metric, did not exhibit significant improvements. Consequently, it can be inferred that the default value of the parameter ( $b=0.5$ ) adequately represents the runoff generation within the study area. These findings provide valuable insights into the modeling of streamflow and reaffirm the suitability of the chosen parameter in accurately capturing the hydrological processes of the study region.

A first attempt to consider the spatial variability of the *runoff b* parameter within the study area, an exploration was undertaken to establish a relationship between the *b* parameter and the *Indice de Développement et Persistance des Reseaux*, IDPR in French, (Mardhel et al., 2021). A brief description of this index can be found in Appendix A.1.3. This is a hydrological index used to assess the development and persistence of river networks. It quantifies the connectivity and continuity of flow paths within a river network, reflecting the overall efficiency of water flow and runoff generation processes.

To achieve this, natural stations from the PIRAGUA project database were selected and analyzed. The objective was to investigate whether the variability of the *runoff b* parameter within the study area could be linked to the IDPR values. Visual analysis was conducted by comparing the best values of the *b* parameter obtained for each catchment with the IDPR map, as depicted in Figure A 1-7. However, despite examining the patterns, no clear relationship between this parameter and the IDPR emerged from visual inspection.

To further explore the potential relationship between the  $b$  parameter and the IDPR, a scatterplot was constructed, plotting the median IDPR values against the best *runoff b* parameter values for each of the selected natural basins (Figure A 1-6). However, similar to the visual comparison, no distinct pattern or correlation between the two variables was observed in this analysis. The scatterplot showed a scattered distribution of data points, indicating the absence of a clear relationship between the *runoff b* parameter and the IDPR index, suggesting that the *runoff b* parameter may not be directly linked by the IDPR index in the study area. Finally, it is worth noting that the absence of a clear pattern between them highlights the complexity and inherent uncertainties in calibrating this parameter and also in the IDPR formulation.

In a final attempt to account for the variability in the runoff  $b$  parameter values, a simulation using SURFEX-Eaudyssée-Rapid was conducted. This simulation aimed to incorporate non-uniform runoff  $b$  values across the entire study area. To achieve this, the IDPR values were categorized into three percentiles, and each percentile was assigned an initial approximation of the runoff  $b$  value (Figure A 1-8 in Appendix A.1.3 for details). The results of this simulation, referred to as the Runoff-B Model, were then compared with the default simulation, and the findings are presented in Figure 6-2. It is noteworthy that during the initial stages of this research, efforts were made to expand the database, eventually leading to the creation of the comprehensive database described in Section 3.2.2.1. Consequently, within the context of this specific stage of the research, the initial database from the PIRAGUA project, wherein the number of stations categorized as "natural" was comparatively smaller, was utilized (as visually demonstrated in Figure 6-2 and Figure A 1-9).

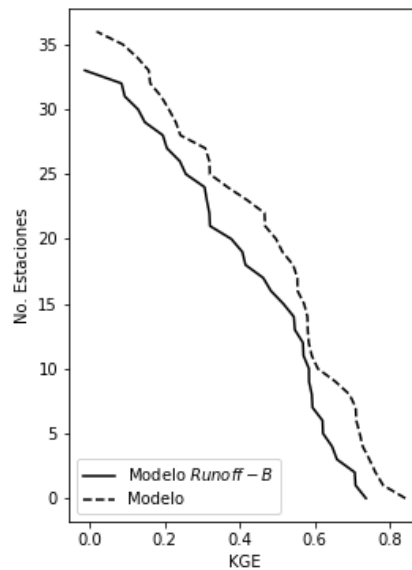


Figure 6-2 Accumulated distribution of KGE scores. The dashed line represents the default simulation and the solid line represents the IDPR terciles simulation.

The comparison of this new simulation (Modelo Runoff-B in Figure 6-2) with the default simulation revealed that there was no improvement in the KGE values; in fact, the KGE values decreased. This suggests that the incorporation of non-uniform runoff  $b$  parameter values based on IDPR percentiles did not lead to an enhancement in the model performance. It is important to acknowledge that conducting further simulations with additional percentile categories and assigning different runoff  $b$  parameter values may provide more insights. However, it should be noted that this approach becomes impractical due to the computational constraints of the SURFEX model.

### 6.2.2. Attempts to improve the soil information database

In recent years, the accurate representation of soil depth in land surface models has become increasingly recognized as a crucial factor in accurately simulating hydrological processes (Lovat et al., 2019). However, in the case of the SURFEX model, concerns arise regarding the realism of the soil depth values derived solely from the vegetation cover in the ECOCLIMAP II dataset (Faroux et al., 2013), particularly in diverse geographical regions like mountain areas. In this context, the inaccuracies associated with the representation of the soil database used by SURFEX are investigated, and the assessment of improvements in soil information through the incorporation of the ESDAC database (Panagos et al., 2012) in conjunction with Plant Rooting Depth (Zr) map (Guswa, 2008), for hydrological modeling is performed (see Appendix A.2). Thus, the impacts on hydrological simulations in SURFEX are evaluated by exploring this alternative soil data source.

At this stage of the research, a simulation was conducted incorporating data from the ESDAC database on the representation of soil information in the SURFEX model. In this simulation, only the soil information file was modified (Figure A 2-1), while the default values of the remaining parameters, including the *runoffb* parameter, were retained. The results of this simulation did not demonstrate significant improvements in the KGE values when compared to the default simulation (PIR1), as depicted in Figure 6-3. The right panel in Figure 6-3 indicates a substantial decrease in the number of stations with KGE values exceeding 0.5, accompanied by an increase in the number of stations with KGE values below -0.25.

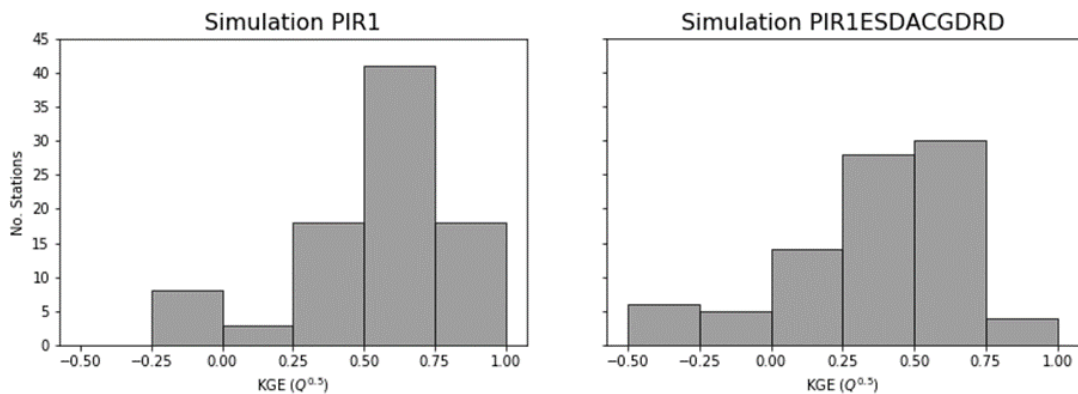


Figure 6-3 Histograms of the KGE values on the selected station. The left panel shows the default simulation (PIR1) and the right panel shows the simulation using improved soil information (PIR1ESDACGDRD)

In conclusion, the incorporation of the ESDAC and Zr databases into the existing database utilized by the SURFEX model did not yield enhancements in the hydrological simulation. This outcome can be attributed to the inherent uncertainty associated with the construction of the ESDAC database and that Zr is estimated using a carbon cost-benefit model, which may introduce biases and uncertainty in the representation of soil information.

Despite considerable efforts have been invested, enhancing the representation of hydrologic processes in the SURFEX model has proven challenging. Nevertheless, it has been established that the current configuration of the model is sufficiently accurate for the study region. Consequently, the default configuration will be retained, and emphasis will shift to enhancing the overall model formulation to improve the simulation of low flows.

### 6.3. Improvement of low flows simulation<sup>2</sup>

Droughts and low flows are characteristics of the natural water cycle (Van Loon, 2015). The former are usually defined by a water deficit in relation to a long-term average value and depending on which variable presents a deficit, drought is categorized into different types (Mishra & Singh, 2010): meteorological drought, related to a precipitation deficit; agricultural drought, due to a soil moisture deficit; and hydrological drought, which is related to a low streamflow condition. Each of them is characterized by different indices (Keyantash & Dracup, 2002; Mishra & Singh, 2010). Specifically, hydrological drought can be defined by the Standardized Flow Index, SFI, (Vidal et al., 2010); however, must not to be confused with low flow conditions, which are usual during the dry season every year (Smakhtin, 2001). Therefore, hydrological drought is a more general phenomenon, which is characterized by more factors than just low flows (Van Loon, 2015). Droughts have severe impacts on water availability to sustain the ecosystem and societal requirements (Sheffield et al., 2012; Stahl et al., 2016). To study drought impacts, and to improve water resource management, it is necessary to improve our knowledge of low flows. However, modeling low flows through hydrological models is still a challenge (Smakhtin, 2001; Staudinger et al., 2011).

Land-surface models (LSMs) have proven very useful for studying the hydrological cycle, including droughts (Lehner et al., 2006; Vidal et al., 2010; Prudhomme et al., 2011; Van Loon et al., 2012; Mo & Lettenmaier, 2014; Xia et al., 2014; Gaona et al., 2022) and seasonal low flows (Gudmundsson, Tallaksen, et al., 2012; Quintana-Seguí et al., 2020). Being mostly physically-based models, they help understand the underlying physical processes. However, the hydrological response in these models can be potentially improved, especially the representation of the slow component of the streamflow, which in many cases, is constrained by a limited description or even the absence of groundwater modeling (Stahl et al., 2011; Gudmundsson, Tallaksen, et al., 2012), among other processes, such as lateral subsurface flows.

Low-flow periods have not been well represented in large-scale models mainly due to a too fast response between precipitation and runoff (Van Loon et al., 2012; Barella-Ortiz & Quintana-Seguí, 2019; Quintana-Seguí et al., 2020). This represents a disadvantage in areas where streamflow is dominated by slower processes, such as groundwater discharge (i.e., from aquifers), mostly during the dry season (Van Loon et al., 2012). These limitations are even more important in mountainous areas, where groundwater is poorly known (Somers & McKenzie, 2020). Therefore, it is necessary to improve the simulation of processes that influence the flow's slow component and sustain the summer flows. This improvement can be done through (i) physical (groundwater models, improved lateral flows, etc.), or by (ii) conceptual approaches.

The improvement through physical models is a complex task due to the complexity and the high uncertainties involved, also demands good knowledge of the geological structures (Habets et al., 2008; Vergnes et al., 2012). For example, Sutanudjaja et al. (2011) and Tian et al. (2012) coupled groundwater models to offline LSM models, which do not allow feedback between groundwater

---

<sup>2</sup> Based on: **Cenobio-Cruz, O.**, Quintana-Seguí, P., Barella-Ortiz, A., Zabaleta, A., Garrote, L., Clavera-Gispert, R., Habets, F., & Beguería, S. (2023). Improvement of low flows simulation in the SASER hydrological modeling chain. *Journal of Hydrology X*, 18, 100147. <https://doi.org/10.1016/J.HYDROA.2022.100147>

storage and soil moisture. On the contrary, [York et al. \(2002\)](#); [Maxwell & Miller, \(2004\)](#); [Vergnes et al. \(2012, 2020\)](#) used coupling schemes where this kind of feedback was considered. Another physically-based approach, instead of coupling two models, is by modification of the model itself to consider the groundwater effects, such as the work done by [Miguez-Macho et al. \(2007\)](#). In this case, a two-way exchange between groundwater and rivers is allowed, together with the exchange between the vadose and the saturated zones.

Conceptual approaches use simple mathematical equations to describe hydrologic processes ([Z. Liu et al., 2019](#)), it should be stressed that implementing these is not as complex as the options described in the previous paragraph. Conceptual models depend on parameters to be calibrated, which do not correspond to a physical meaning or quantity. Several studies have tested this approach. For example, [Artinyan et al. \(2008\)](#) and [Getirana et al. \(2014\)](#) added two additional reservoirs to SURFEX LSM to evaluate the water budget. [Lafaysse et al. \(2011\)](#) added a reservoir to represent the effect of aquifers in mountain areas, that was extended in the plain over hard rock aquifer ([Le Moigne et al., 2020](#)) within the SIM (SAFRAN - ISBA - MODCOU) model. [Gascoin et al. \(2009\)](#) implemented an additional storage reservoir to consider the deep groundwater flow in France. [Huang et al. \(2019\)](#) added an additional layer to the DBH (Distributed Biosphere Hydrological) model to connect the soil layers with a groundwater reservoir. [Guimberteau et al. \(2014\)](#) compared a conceptual soil hydrology scheme against a physical approach using the ORCHIDEE (ORganising Carbon and Hydrology In Dynamic EcosystEm) model over the Amazonian basin and reported improvements in the simulated water budget with small differences between them.

### 6.3.1. Study area and data

The natural watersheds analyzed in this study are situated within the study area detailed in section [3.1.1](#). Similarly, the data employed for the analysis are outlined in section [3.2.2](#) and [3.2.3](#).

### 6.3.2. Methodology

This section presents a detailed description of the methods implemented to improve low flow simulation. [Figure 6-4](#) shows the schematic flowchart with the steps of the two methodologies used that are described below.

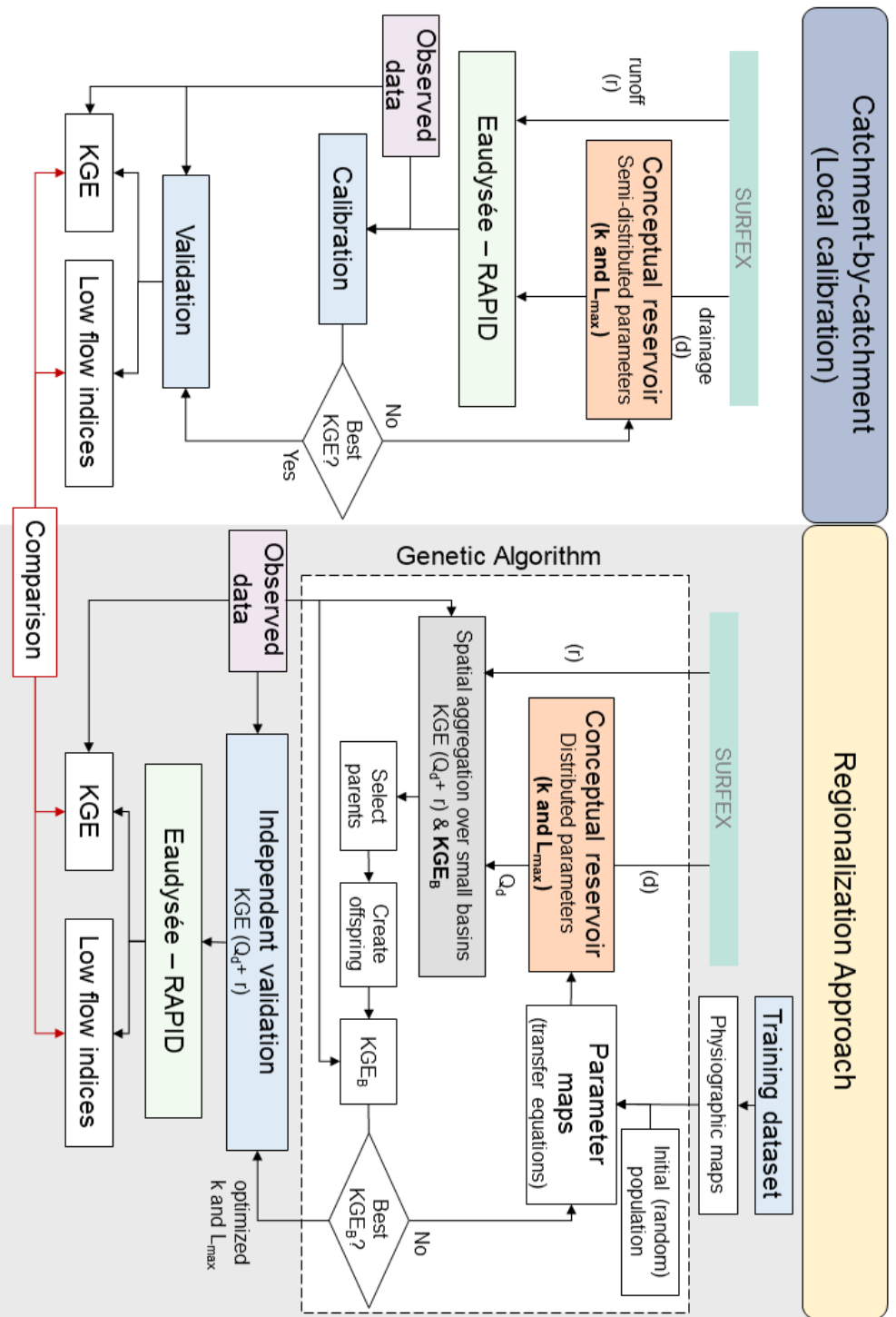


Figure 6-4 General framework used in this analysis. The left panel show steps used during the local calibration and the right panel detailed the steps of the regionalization approach.

### 6.3.2.1. Conceptual reservoir

The implementation of a conceptual reservoir is based on the formulation from rainfall-runoff models, like ARNO (Todini, 1996) or TOPMODEL (Beven & Kirkby, 1979). Particularly focus lies in the incorporation of a conceptual reservoir to enhance the streamflow simulations produced by the SASER model. Large-scale models exhibit quick responsiveness to rainfall events, a characteristic that often introduces challenges in accurately representing low-flow conditions (Van Loon et al., 2012; Quintana-Seguí et al., 2020). Consequently, there arises a need for a buffering mechanism to emulate the role of subsurface storage. It is within this context that the introduction of the conceptual reservoir emerges as a viable solution to address this limitation.

Notably, this implementation is confined to the drainage component, which predominantly characterizes the slow component of the streamflow. The hypothesis is that the integration of the conceptual reservoir into the modeling framework will effectively mitigate the limitations associated with low-flow representation in SASER. In doing so, it promises to facilitate a more comprehensive and precise simulation of the intricate hydrological processes at play. The major difference is that the reservoir here presented is implemented as an external module in the LSM model, as a postprocessing of the drainage, to account for a better representation of the slow component of simulated streamflow.

The introduction of a conceptual reservoir at grid point level was done, to improve the slow component of the streamflow. The partitioning between surface runoff and drainage done by SURFEX LSM was not modified. The reservoir's purpose is to modulate the drainage simulated by SURFEX (to sustain it during the dry period), before being fed to the river routing component Eaudysée-RAPID as shown in Figure 6-5. Moreover, surface runoff is not modified, to avoid an excessive role of empirical parameters on the hydrological response of the model.

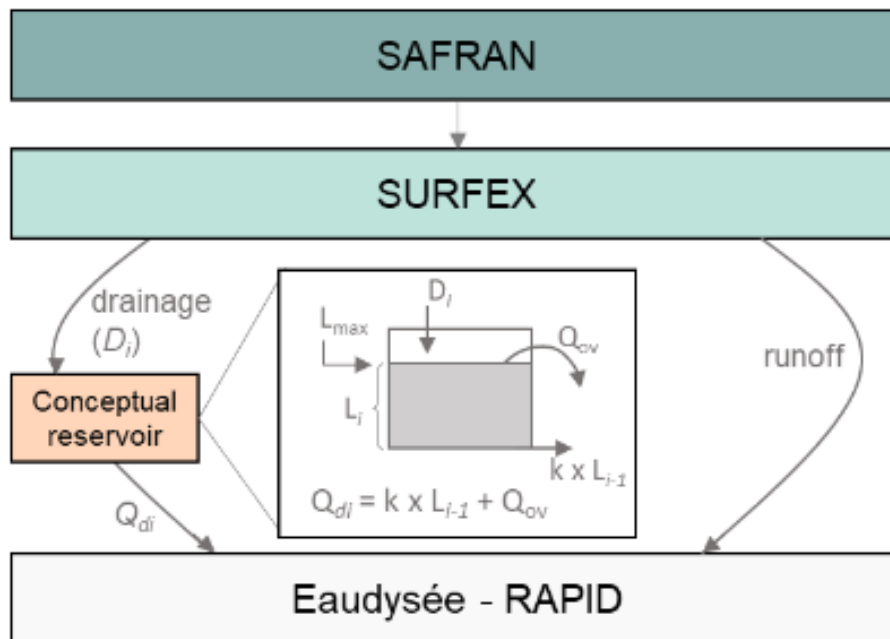


Figure 6-5 Diagram of the conceptual reservoir implementation, in the SASER modeling chain.



The input to the reservoir is the drainage generated by SURFEX. The reservoir has two outflows. The first mimics a baseflow and is the main contributing term sustaining flow during the dry period. The second occurs when the reservoir exceeds the maximum threshold, so there is no time lag when drainage is simulated during the wet season (when the reservoir is full). The total reservoir outflow is calculated following equations (6.1) to (6.3).

$$L_i = \tau(D_i + (1/\tau - k) \times L_{i-1} - Q_{ov}) \quad (6.1)$$

$$Q_{di} = k \times L_{i-1} + Q_{ov} \quad (6.2)$$

$$\text{and } Q_{ov} = \max(0, L_{i-1} - L_{\max})/\tau \quad (6.3)$$

Where  $D_i$  [mm day<sup>-1</sup>] is the drainage;  $L_i$  [mm], is the water content of the reservoir;  $k$  [day<sup>-1</sup>] and  $L_{\max}$  [mm] are empirical parameters, which correspond to the depletion coefficient and the size of the reservoir, respectively.  $Q_{di}$  [mm day<sup>-1</sup>] is the total reservoir outflow,  $Q_{ov}$  [mm day<sup>-1</sup>] is the reservoir outflow and  $\tau$  is a constant with a value of 1 day. The sub-indices  $i$  and  $(i-1)$  represent the current time step and the previous step, respectively. Finally,  $Q_{di}$  is added to SURFEX's runoff and sent to Eaudysée-RAPID to compute daily streamflow.

In different steps (calibration, validation, and regionalization), performance evaluation of the simulations is required. Thus, the Kling-Gupta Efficiency, KGE, was chosen (a detailed description of this performance metric is found in section 4.2.5.2).

### 6.3.2.2. Calibration procedure for reservoir parameters

The size of the reservoir ( $L_{\max}$ ) and the depletion coefficient ( $k$ ) have to be calibrated. For calibration and validation, a classical split-sample procedure was used. Therefore, the entire record into two halves was split. The calibration period spans from 01/09/1979 to 31/08/1997 and the validation period from 01/09/1997 to 31/08/2014. Both parameters were calibrated at the sub-catchment scale on a catchment-by-catchment basis against locally observed streamflow data, which involves that all the grid points belonging to the sub-catchment had the same values of the parameters. Hereafter, this step is referred to as local calibration.

The grid resolution and the distribution of hydrological stations allowed us to use a nested approach to calibrate the parameters where streamflow data were available. Thus, the parameters were calibrated first on the upstream sub-catchments and then progressively towards the outlet.

The valid range for both parameters was set using similar criteria defined by Artinyan et al. (2008). The accumulated streamflow of the dry period from July to September should be close to the average reservoir level ( $L_{\max}$  parameter). For each sub-catchment, the total runoff volume for the dry period of the driest year of the calibration period ( $Q_{\text{dry}}$ , in mm), and  $L_{\max}$  was estimated as  $12Q_{\text{dry}} \geq L_{\max} \geq Q_{\text{dry}}$ , was obtained. According to Artinyan et al. (2008), twelve times the volume of the driest months seems a reasonable upper bound for this parameter. The limits of the depletion coefficient ( $k$ ) were calculated considering the length of the dry period; thus, the reservoir has drainage releases during the length of the dry period.

A parameter space, for simulation purposes, where the range between the extreme values of each parameter was discretized into 12 values was generated. A total of 144 simulations were carried

out and the performance of each simulation was evaluated for each sub-catchment using the KGE ( $Q^{1/2}$ ) (see section 4.2.5.2). The best simulation for each sub-catchment was chosen, and the parameter set associated with each of them was saved.

### 6.3.2.3. Regionalization approach

When observational data are not available, or they do not have good quality, or they include processes that are not simulated, such as human processes (dams and irrigation), local calibration is unfeasible. To overcome this limitation, the regionalization approach presented by Beck et al. (2020) was used, which allows setting the values of the reservoir parameters all over the domain, going beyond the near-natural basins used in the calibration procedure.

The regionalization approach uses a genetic algorithm to optimize the coefficients of the transfer equations. These equations link the reservoir parameters (predictands) to the physiographic variables (predictors). The same near-natural basis that in the local calibration (all of them have an area smaller than 5,000 km<sup>2</sup>) was used.

For the regionalization approach, eight physiographic variables as predictors were selected:

- Three of them were related to climate: ARI, aridity index; MAP, mean annual precipitation; and PET, potential evaporation. Nijssen et al. (2001), Troch et al. (2013), Singh et al. (2014), Beck et al. (2016) demonstrated that these variables exert an important influence on the flow response in regionalization studies at a global scale. The MAP predictor was transformed to a square root to better fit a normal distribution.
- The NDVI, Normalized Difference Vegetation Index; and SNW, the fraction of snow with respect to the total precipitation, are predictors related to land cover. The NDVI was added because the vegetation influences the evaporation, infiltration, and hydrological function of the soil, which may also affect the slow component (low flows) and runoff-rainfall conversion processes (Zhang et al., 2001; Donohue et al., 2007; Peel, 2009). The snow affects the land cover and has an important role in streamflow generation in mountain regions, and also in the slow component of the flow.
- Finally, SL, the slope; SND, soil sand content; and CLY, soil clay content, are variables related to the topography and the soil. The slope predictor was included due to the good general correlation between surface slope and soil depth (Tesfa et al., 2009), and the soil texture has a strong influence on all soil-related processes, including subsurface runoff (Price, 2011).

Most of these variables were obtained from the ECOCLIMAP II database. Although these descriptors are not directly associated with groundwater, they help determine a landscape that can be prone or not to groundwater.

For the optimization, the reservoir scheme was run at daily time step and at the same SURFEX spatial resolution, for the whole period (1979-2014). The SURFEX runoff and reservoir output were spatially aggregated and compared with observed runoff. This comparison is possible due to the size of the catchments that allows us to discard channel routing effects (Gericke & Smithers, 2014). The methodology is shown in Figure 6-4 (right panel), and a detailed description is presented below.

Since the reservoir is implemented as an external module to post-process the SURFEX drainage before the routing step, there is no need to run SURFEX within the genetic algorithm (see [Figure 6-5](#)). This is a key benefit, as SURFEX is a computationally-expensive model. Furthermore, given the size of the catchments, there is no need to run the routing scheme (Eaudyssée-RAPID) at each iteration ([Figure 6-6](#)). A very high number of simulations can be undertaken, as the very simple reservoir model, consisting of a few lines of Python code, is the only component that is run.

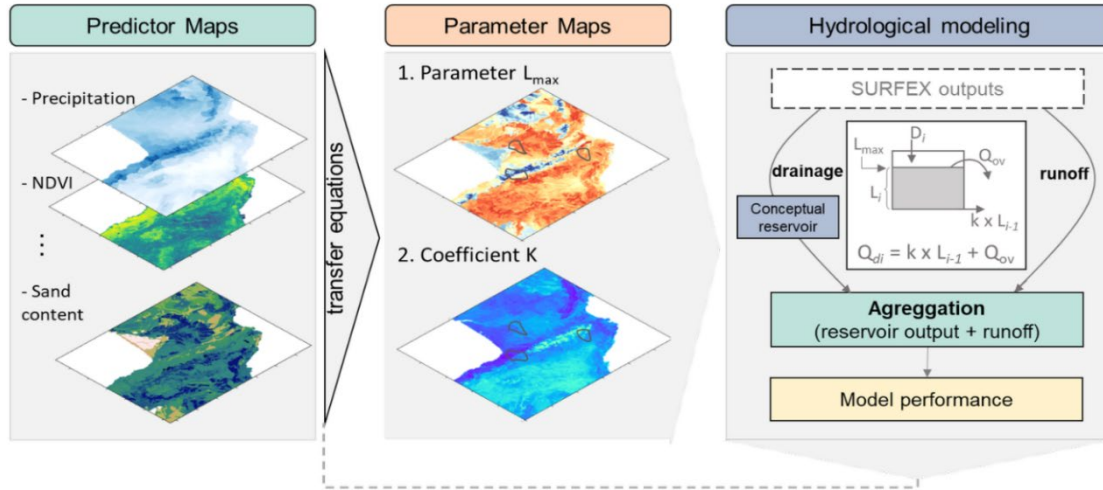


Figure 6-6 Scheme of the main steps of the regionalization approach. For each time that the algorithm is run, the steps (parameter maps and hydrological modeling) are repeated in each iteration for the optimization process.

The transfer equations that link the predictors with the predictands are expressed as follows:

$$MP_i = w_{i1}ARI + w_{i2}MAP + w_{i3}PET + w_{i4}NDVI + w_{i5}SNW + w_{i6}SL + w_{i7}SND + w_{i8}CLY + w_{i9} \quad (6.4)$$

where  $MP_i$  are the model parameters ( $k$  and  $L_{max}$ ) and  $w_i$  are the coefficients that will be optimized. The eight predictors chosen are (see the previous section):

- ARI, aridity index (P/PET);
- MAP, mean annual precipitation (root square transformed);
- PET, mean annual potential evaporation;
- NDVI, Mean Normalized Difference Vegetation Index;
- SNW, the fraction of snow with respect to the total precipitation;
- SL, topographic slope;
- SND, soil sand content; and
- CLY, soil clay content.

First, each predictor was interpolated to the same grid as the model uses (2.5 km of resolution). Next, as [Beck et al. \(2020\)](#) did, predictor values were clipped using the 99<sup>th</sup> and 1<sup>st</sup> percentiles of the area covered by the sub-catchments. Finally, to make the predictors comparable to each other, they were standardized by subtracting the mean and dividing the results by the standard deviation of the area covered by the sub-catchments.

The coefficients of the transfer equations ( $9 \times 2 = 18 w_i$ ) were optimized using our own implementation of the  $(\mu+\lambda)$  genetic algorithm (Slowik & Kwasnicka, 2020). The  $(\mu+\lambda)$  algorithm indicates that selected parents and children together comprise the new population (offspring) for the next iteration. The algorithm starts with a random population ( $\lambda$ ) of 32 members, all of them are evaluated using the performance score ( $KGE_B$ ), and the best three members are selected and saved for the next iteration ( $\mu$ , size of the parents in the population). Subsequently, through the mutation operator, the offspring is created ( $\lambda/\mu$  children are randomly created from each selected parent) following a normal distribution, within the search space. A maximum number of 100 iterations was set.

Figure 6-6 represents the main steps in the optimization process. First, predictor maps are obtained depending on the area covered by the catchments used. Second, the parameter maps are calculated using transfer equations, to subsequently apply the reservoir scheme. This scheme is run using as input the daily drainage simulated by SURFEX. The reservoir output (modulated drainage) and the SURFEX runoff are spatially aggregated (all cells that comprise each catchment) and compared to observed streamflow of each catchment using the KGE score.

To avoid overfitting, and to have an indicator of uncertainty in the parameter sets, cross-validation was used. For this, the catchment set was subdivided into training (87%) and validation (13%) subsets. This selection was performed randomly, the catchments used for validation were used only once in each iteration, performing different experiments until all of them were used in the validation.

In total, 8 experiments were run. Each experiment consists of a training subset (27 catchments) and 4 randomly selected catchments for independent validation. In this sense, the validation subset in each experiment is different, because each catchment was used only once.

#### 6.3.2.4. Low flow indices

Different low flow indices can be estimated (Gustard et al., 1992; Smakhtin, 2001), but our attention was directed toward two common ones. First, the ratio ( $Q_{90}/Q_{50}$ ), where  $Q_{50}$  is the median and the  $Q_{90}$  is the low value that is observed  $1/10^{\text{th}}$  of the time, at daily time step. This index is interpreted as the proportion of streamflow originating from groundwater stores, excluding the effects of the catchment area (Smakhtin, 2001). Second, the annual minimum monthly flow with a return period of 5 years, QMNA(5), which is widely used in France for water management issues and provides information about low flow severity. To compute the QMNA(5), the 5-year return period was calculated for each sub-catchment fitting it to a log-normal distribution for low flows (Catalogne, 2012), based on a series with at least 30 years of record.

Low flow indices for the summer period (July to September) for each station were derived and computed both using the observations and the simulations. Then, to evaluate and compare the performance of the simulations the relative bias was calculated.

### 6.3.3. Results

To evaluate the performance of the SASER model (default simulation) the  $KGE(Q^{1/2})$  was utilized and the 104 stations defined as natural or near-natural, which are indicated by circles with black borders in Figure 6-7, were used.

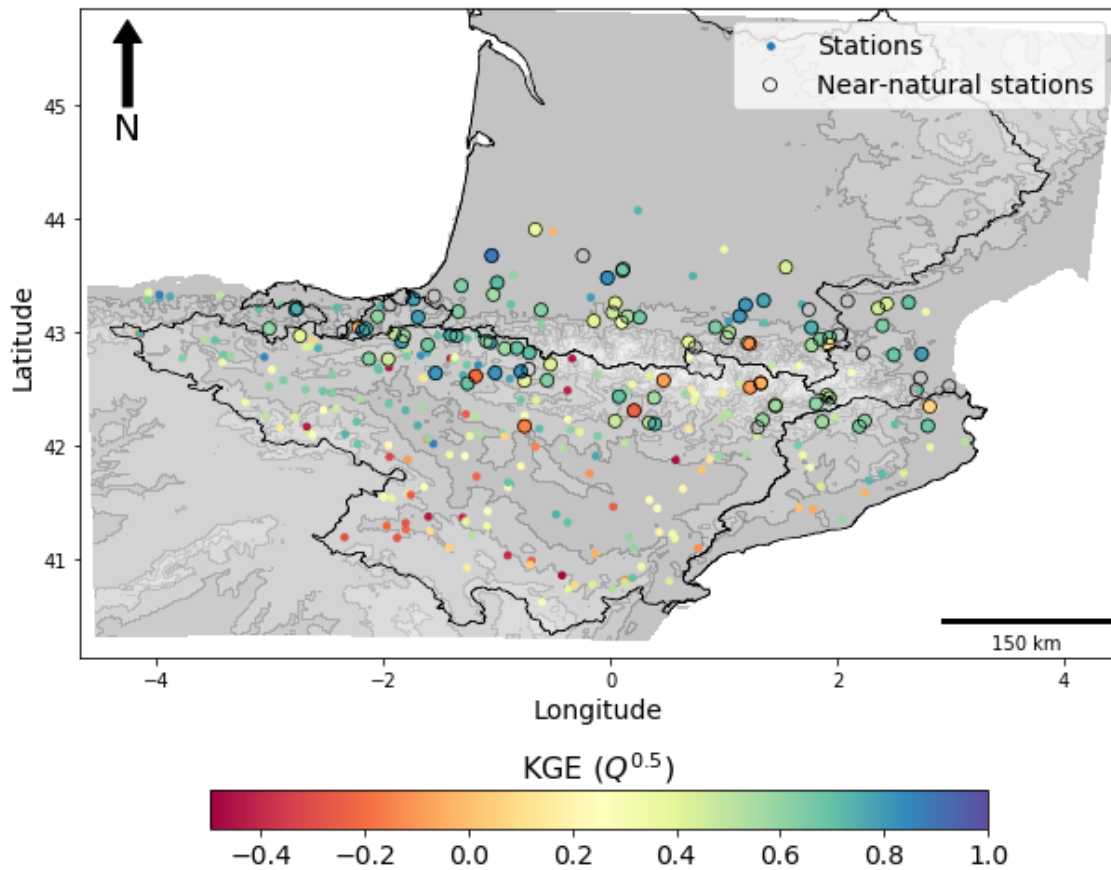


Figure 6-7  $KGE(Q^{1/2})$  scores between observed data and the default simulation, for the whole period (1979-2014). Larger circles with a black border indicate stations defined as natural or near-natural. The other stations are considered as influenced.

Figure 6-7 shows the calculated  $KGE$  scores for the entire period (1979-2014). Stations with the highest  $KGE$  values are located mainly in the Pyrenean region, where direct human influence is low. However, most of the stations in the Ebro River basin (a highly influenced basin) showed lower  $KGE$  values, especially in areas downstream of the reservoirs. This was expected since the model must perform poorly over human-influenced areas, as it only simulates natural processes.

In Figure 6-8, the observed (OBS, in beige) and simulated (Default, in red) statistics of the streamflow for the different percentiles (near-natural basins) and the 53 catchments where the reservoir was calibrated are compared. The SASER model (Default) simulates reasonably well high and median daily streamflow, represented by the 90th to 99th percentiles, and 50th to 75th percentiles respectively. However, low flows (25th percentile and below) are underestimated, as depicted in the red boxes in Figure 6-8. For example, the median relative bias between observed discharge and default simulation for the 25th percentile is -66%, whereas for the 95th percentile is 12%. This shows that low flows are poorly simulated by the default SASER model.

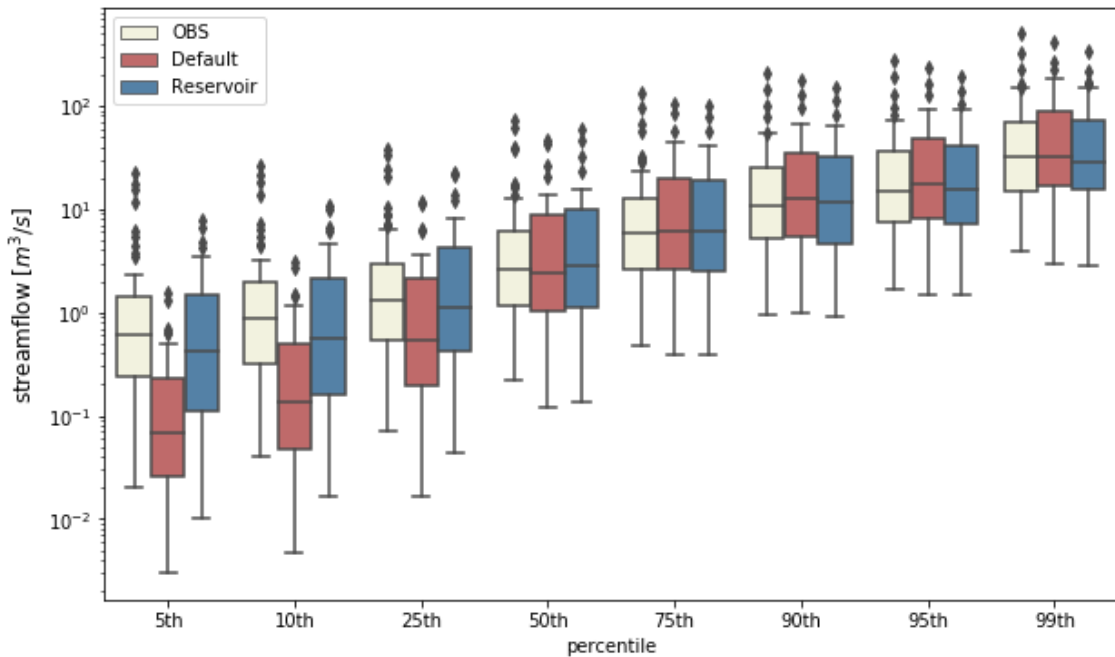


Figure 6-8 Comparison of different daily runoff percentiles for observed data (OBS) and simulated streamflow (default simulation in red and simulation with reservoir scheme in blue). The horizontal line in each box represents the median, the box represents the interquartile range. The whiskers extend a maximum of 1.5 times the interquartile range.

### 6.3.3.1. Evaluation of the model including the reservoir with calibrated parameters

Figure 6-9 shows the result of the calibration of the two model parameters  $L_{max}$  and  $k$  in the near-natural basins. They were calibrated empirically by running the reservoir scheme. The values of the  $L_{max}$  parameter ranged from a minimum of 4 mm to a maximum of 600 mm, with an average value of 108 mm, while the values of parameter  $k$  ranged from 0.01 to 0.04, with a median value of 0.018. At the end of the calibration process, the following results were observed: most Ebro catchments have the same value of parameter  $k$ , 0.02; whereas the parameter  $L_{max}$  varies over a wider range of values. These parameter values are explained by basin characteristics, such as soil type, topography, etc. For example, higher  $L_{max}$  values correspond to sub-catchments with high permeability (e.g., south of France); detailed information is presented in the discussion section.

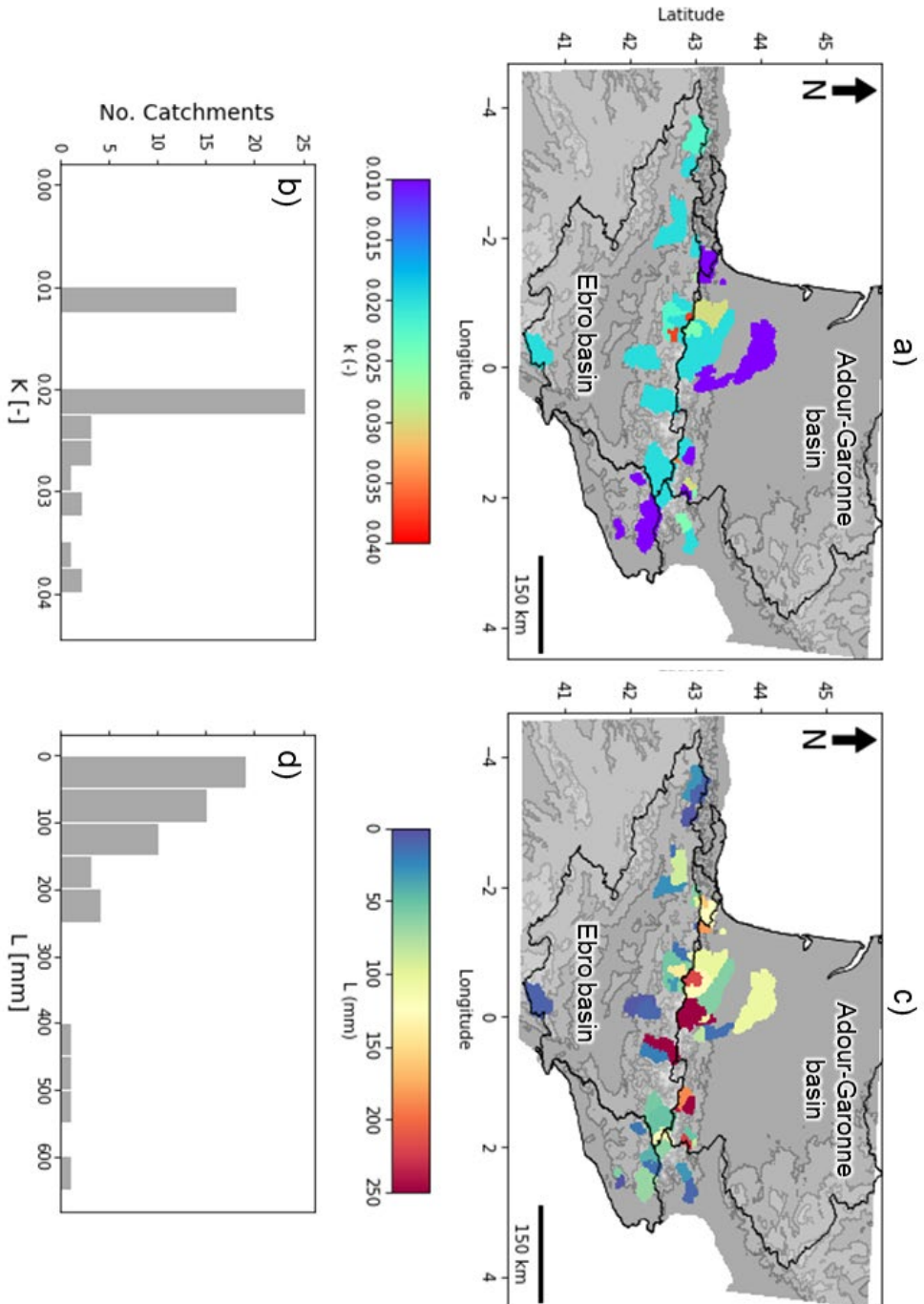


Figure 6-9 Distribution of the 53 catchments used in the local calibration (catchment by catchment). Panels (a) and (c) show each catchment's calibrated values of the  $k$  [-] and  $L_{\max}$  [mm] parameters, respectively. Lower panels, (b) and (d), show the histograms of each parameter.

Figure 6-10 summarizes the resulting KGE scores and shows that adding a calibrated conceptual reservoir improves them over all catchments. On the one hand, panel (a) shows that for the calibration period, the median KGE value of the default simulation was 0.63, and using the reservoir scheme it was 0.72, which represents a clear improvement with respect to the default simulation. For the validation period, panel (b), the default simulation has a score of 0.60 and the calibrated one of 0.71, which is a similar improvement to that from the calibration period. Panel (c) compares the difference between the scores of the calibrated model with the reservoir obtained during the calibration and validation periods. The two lines are very close, which is an indicator of robustness, the model performs similarly inside and outside the calibration period.

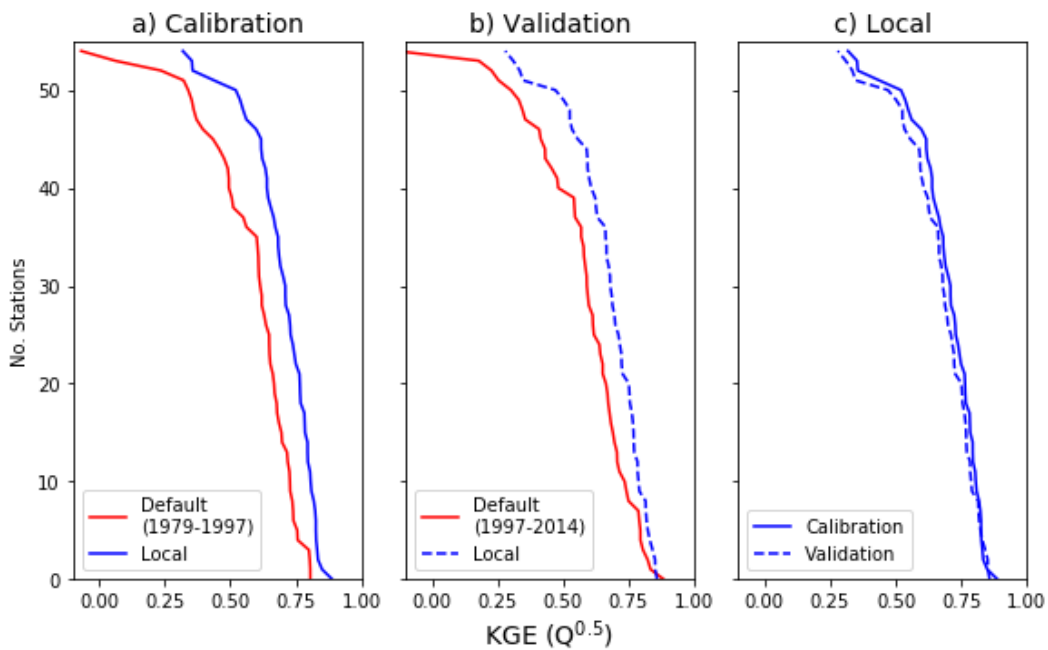


Figure 6-10 Accumulated distribution of KGE scores: a) for the calibration period (1979-1997), b) for the validation period (1997-2014), and c) the comparison between KGE obtained in both periods for local calibration.

The resulting time series (Figure 6-11) shows graphically that the calibrated reservoir produces time series closer to the observations. The KGE values were higher for the simulation using the reservoir scheme, for both periods. Panels (a) and (b) of Figure 6-11 show the time series of the daily streamflow at two stations (only two years of the calibration period are depicted in order to make the plots easy to read) and panels (c) and (d) show the same stations for the validation period. The improved model is able to sustain the summer flows much better than the default model, without affecting the median and high flows.



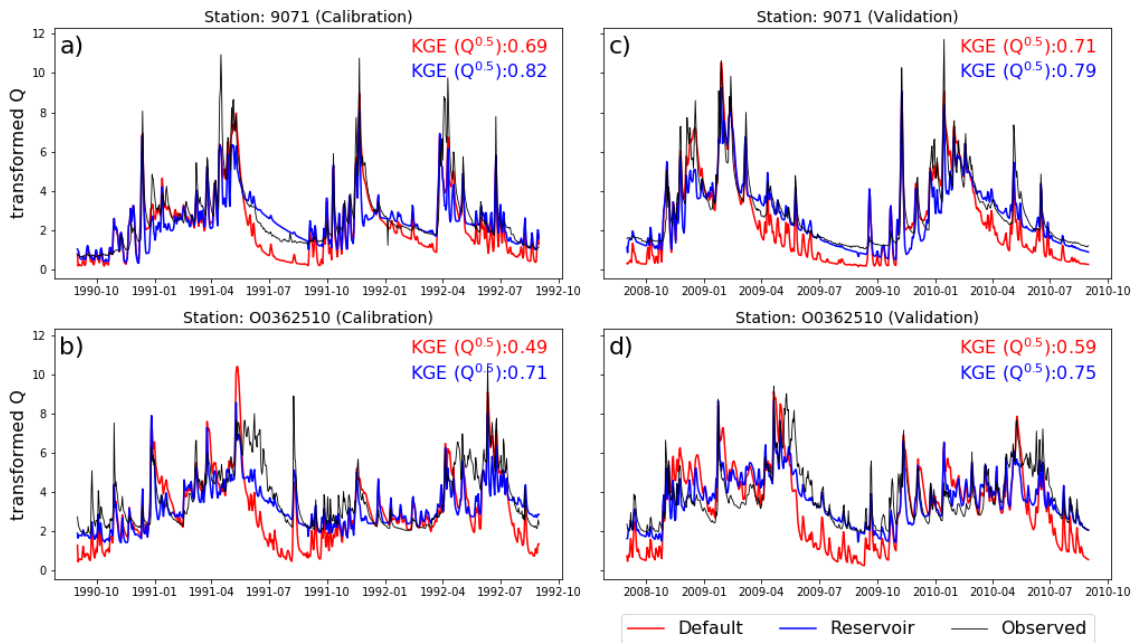


Figure 6-11 Daily time series comparison of two stations, for two hydrological years of the calibration (a and b) and validation (c and d) periods, respectively. Observed streamflow (black line), simulated streamflow without reservoir scheme (red line), and simulated streamflow adding a conceptual reservoir (blue line).  $KGE(Q^{1/2})$  is calculated over each complete period (1979-1997 to calibration and 1997-2014 to validation, respectively).

The blue boxes in [Figure 6-8](#), clearly show that the lower percentiles of the simulation with the calibrated reservoir are improved compared to the default simulation. For the three percentiles related to low flows (the 5<sup>th</sup>, 10<sup>th</sup>, and 25<sup>th</sup>), the values of median relative bias for default simulation were -90%, -84%, and -66% respectively. Whereas the values obtained from the simulation with the reservoir scheme were -37%, -33%, and -17% for the same percentiles. Even though the values remain slightly underestimated, it represents an improvement in low flow simulation.

### 6.3.3.2. Evaluation of the regionalization approach

As an example, [Figure 6-12](#) shows the evolution of the KGE and the  $KGE_B$  for one of the experiments. It is recalled that the KGE and  $KGE_B$  are related through equation 4.4. Each point represents the model performance after each iteration of the genetic algorithm while it searches for the best solution. For this experiment, during the first iterations, the KGE rapidly increases, and after iteration 30 the slope of the curve changes drastically to be almost flat, which indicates that the algorithm is close to a maximum (in this case, the median KGE is slightly higher than 0.53) as the new mutations do not improve the result and are not selected. Similar behavior was founded in all the experiments.

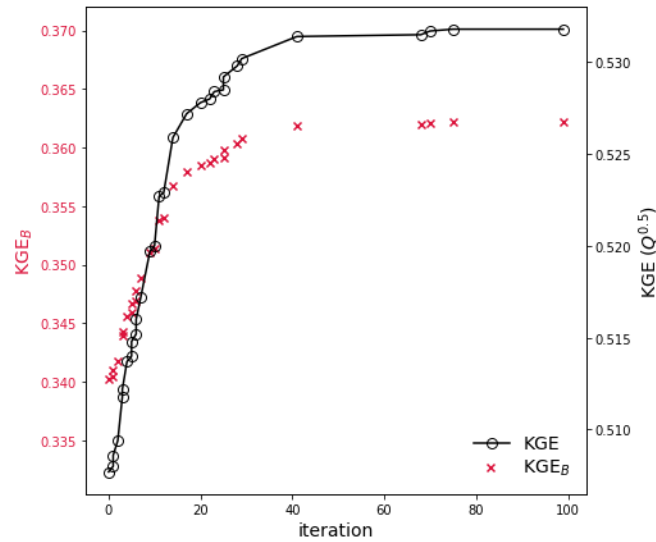


Figure 6-12 Evolution of performance metric (median  $KGE(Q^{1/2})$  and  $KGE_B$ ) in each iteration for one experiment

Figure 6-13 shows the boxplots of the resulting KGE for the independent catchments of each experiment and compares it with the KGE obtained from the default and local calibration experiments. The median daily KGE value of the default simulation was 0.41 and the median daily KGE value of the local calibration was 0.53, while for the regionalization it was 0.52, its value is close to the obtained by the local calibration. Furthermore, improvements in 79% of the validation catchments were obtained. This confirms the robustness of the regionalization approach to improve low flows in the catchments that were not used in the training dataset, also the KGE scores are as good as using the local calibration.

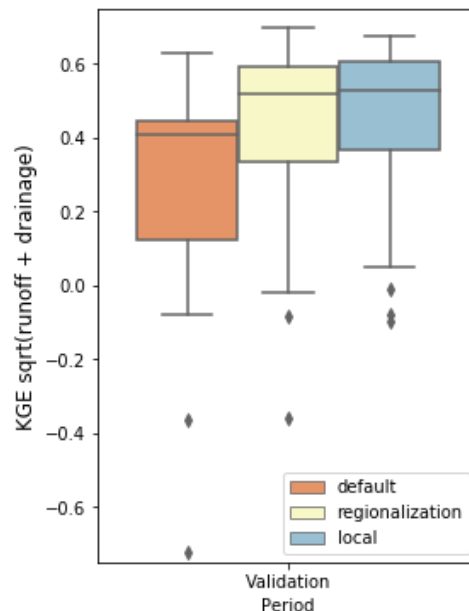


Figure 6-13 Boxplot of KGE scores for the validation period using the local calibration (adding conceptual reservoir), the regionalization (cross-validation), and default simulation (without conceptual reservoir).

Figure 6-14 shows the distribution of the KGE values for the different experiments. Starting from the left the graph shows (i) the default simulation (brown), (ii) the local calibration (dark blue), which represents a clear improvement, (iii) the eight different regionalization experiments (light green), and (iv) three additional experiments (light brown). The eight regionalization experiments show median KGE values very close to each other, around 0.51. In Figure 6-14, the 75<sup>th</sup> percentile (top edge of each box) of all experiments shows a similar value (close to 0.6), while the minimum values (lower whiskers) show greater variability, suggesting that catchments for which the KGE score was poor are more sensitive.

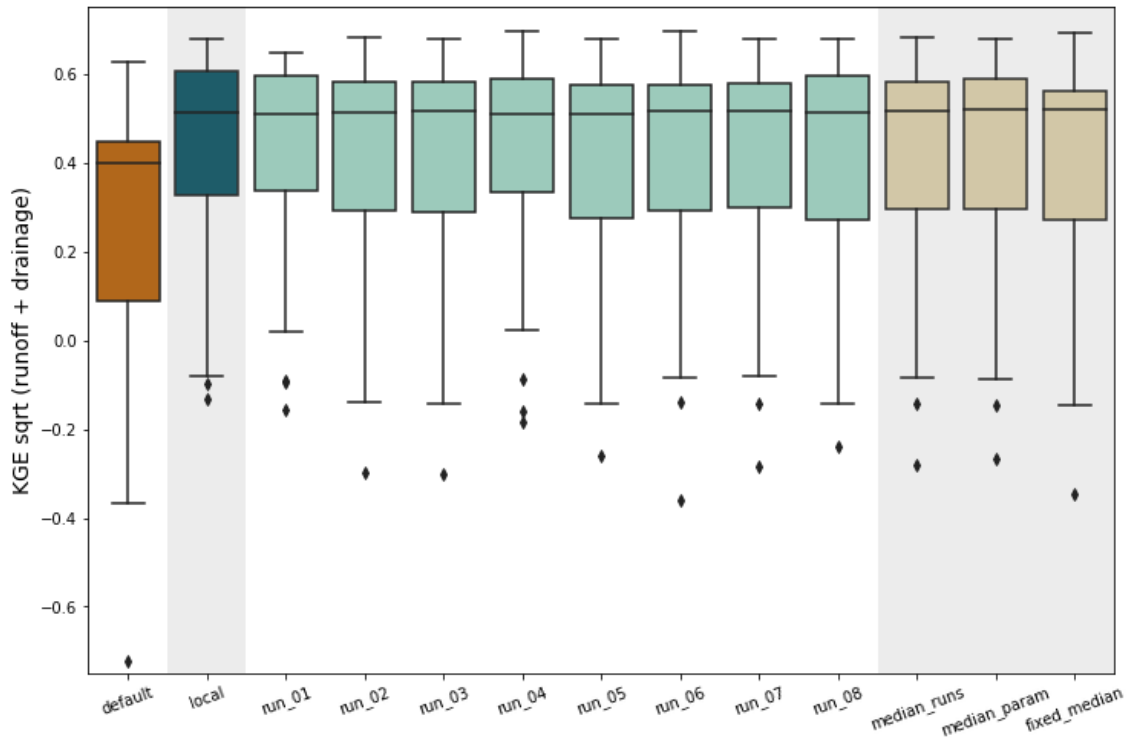


Figure 6-14 Box plot of KGE for streamflow of the local calibration, using the genetic algorithm (run 01 to 08), the median of simulated streamflow (median runs), the median of eight parameter maps (median params), and simulation using fixed parameter values over the full domain. Streamflow validation period from 1997 to 2014.

The three additional experiments (the last three boxes in Figure 6-14) were performed to see how the eight experiments can be combined to obtain a final result. In the first additional experiment, the median time series of the eight previous experiments was calculated. In the second, the reservoir scheme was run using the median value of the  $k$  and  $L_{max}$  parameter maps (median value of the parameters for each grid point) and streamflow was calculated. In the last experiment, the median value of each parameter (57 mm and 0.016 for  $L_{max}$  and  $k$ , respectively) was calculated, and the reservoir scheme was run with these homogeneous values over the entire domain. Surprisingly, these three extra experiments showed similar median values of KGE compared to the previous experiments, however, the last experiment (fixed median values) showed a slightly larger spread among KGE values. In any case, in the local calibration or regionalization approach, KGE values are not below -0.41, the benchmark defined previously.

An example of one year of observed and simulated (by aggregating runoff and drainage) daily streamflow for one catchment is given in [Figure 6-15](#). In this plot, the median flow of the eight regionalization experiments was computed (dark blue line) and also plotted, in light blue, the confidence interval of the simulations.

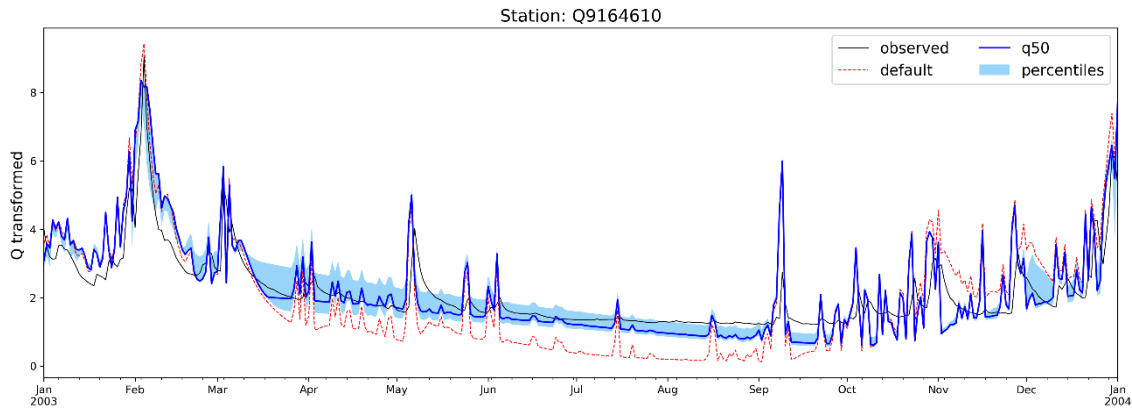


Figure 6-15 Comparison of the observed (black line), simulated by SASER without adding the reservoir (red dashed line), and the median values of the eight simulations (blue line) of daily streamflow for a catchment; shaded area represents the percentile 90th and 5<sup>th</sup> of the eight simulations. Y-axis is the discharge root square.

### 6.3.3.3. Computing natural streamflow with the improved model

Once the maps of the two parameters of the reservoir model were obtained using the median value of the parameter maps of the eight experiments ([Figure 6-18](#)), the final streamflow was calculated using the river routing scheme.

[Figure 6-16 a](#) presents the streamflow simulation performance obtained using the median values of the eight regionalization experiments for the entire record (1979-2014) over the complete database. Of the total stations, 47% showed higher KGE values than 0.5 (5% more compared to the default simulation). [Figure 6-16 b](#) shows the improvement, in terms of  $\Delta KGE$ , due to regionalization for the whole period.

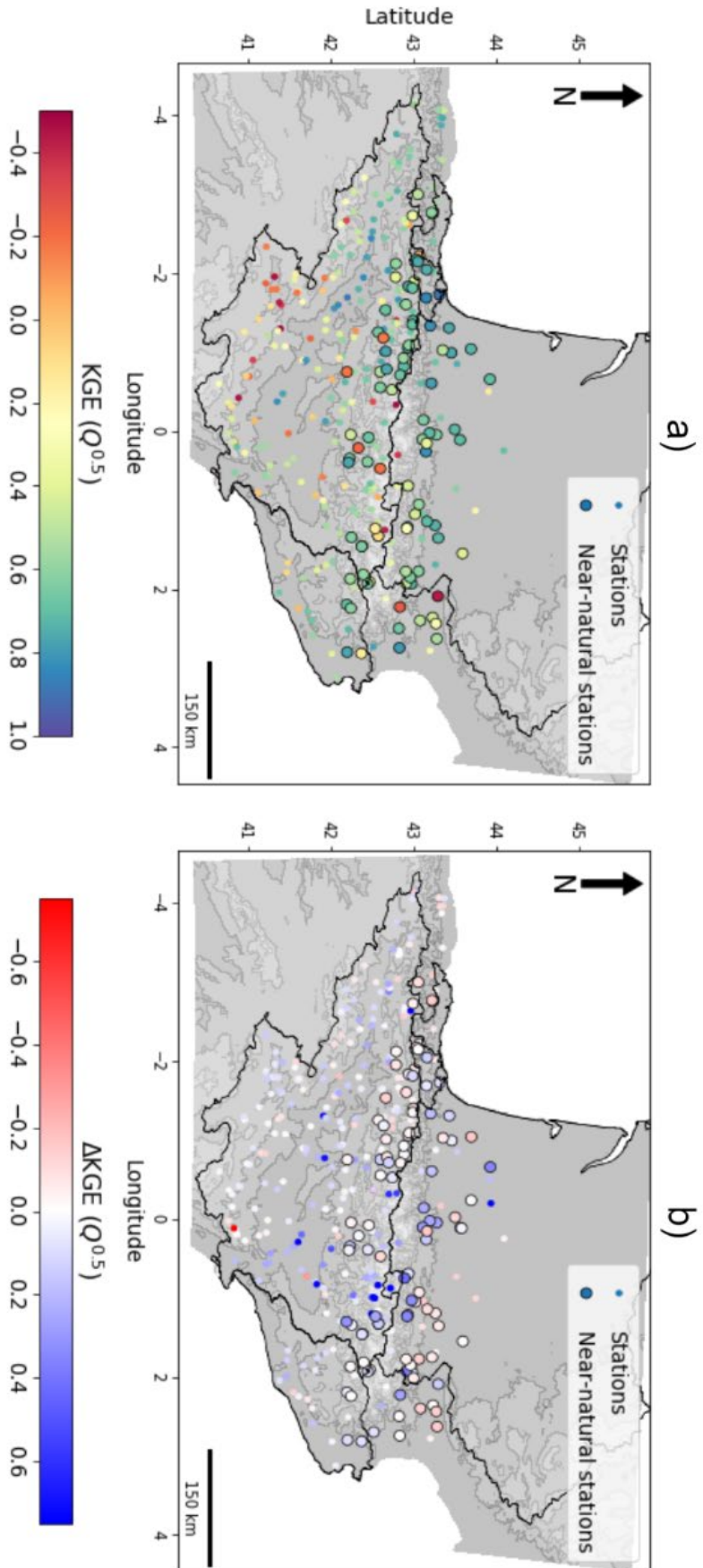


Figure 6-16 a) KGE scores obtained to calculate the streamflow with the routing scheme using the regionalization approach against the observed streamflow. (b) Improvement in KGE after regionalization (difference between Figure 6 4 and Figure 6 13(a)).

For comparison purposes, the KGE values were calculated over the same periods that were used for the local calibration (1979-1997) and validation (1997-2014). For the first period (calibration) the regionalization approach obtains a median KGE of 0.69 and for the second one (validation) it was 0.67, which is very close. **Figure 6-17** summarizes the performance of the local calibration and regionalization approach over the calibration (solid lines) and validation (dashed lines) periods on the near-natural basins. Both approaches showed an improvement compared to the default simulation (without the reservoir). The best KGE values are provided by the local calibration, as anticipated, even though the regionalization approach showed very close values to local calibration.

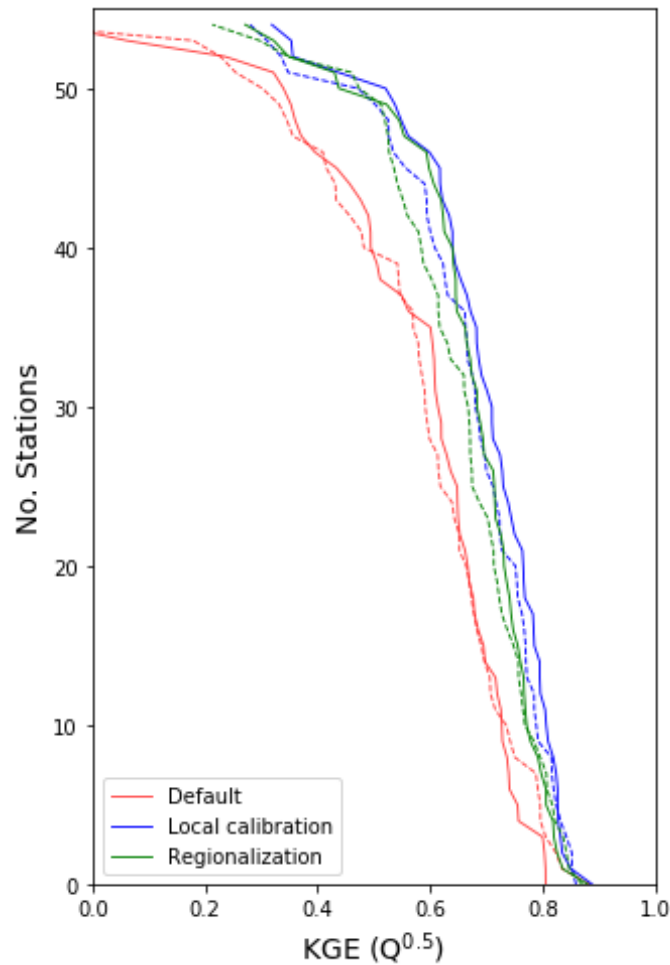


Figure 6-17 Same as **Figure 6-10**, comparing KGE from local calibration (blue) and KGE by the regionalization (green) against to default simulation (red) for calibration (solid line) and validation (dashed line) period.

The advantage of the regionalization approach is that it allows us to estimate the values of the parameters anywhere in the area of study, enabling the calculation of improved natural flows on influenced basins, where local calibration would be impossible.

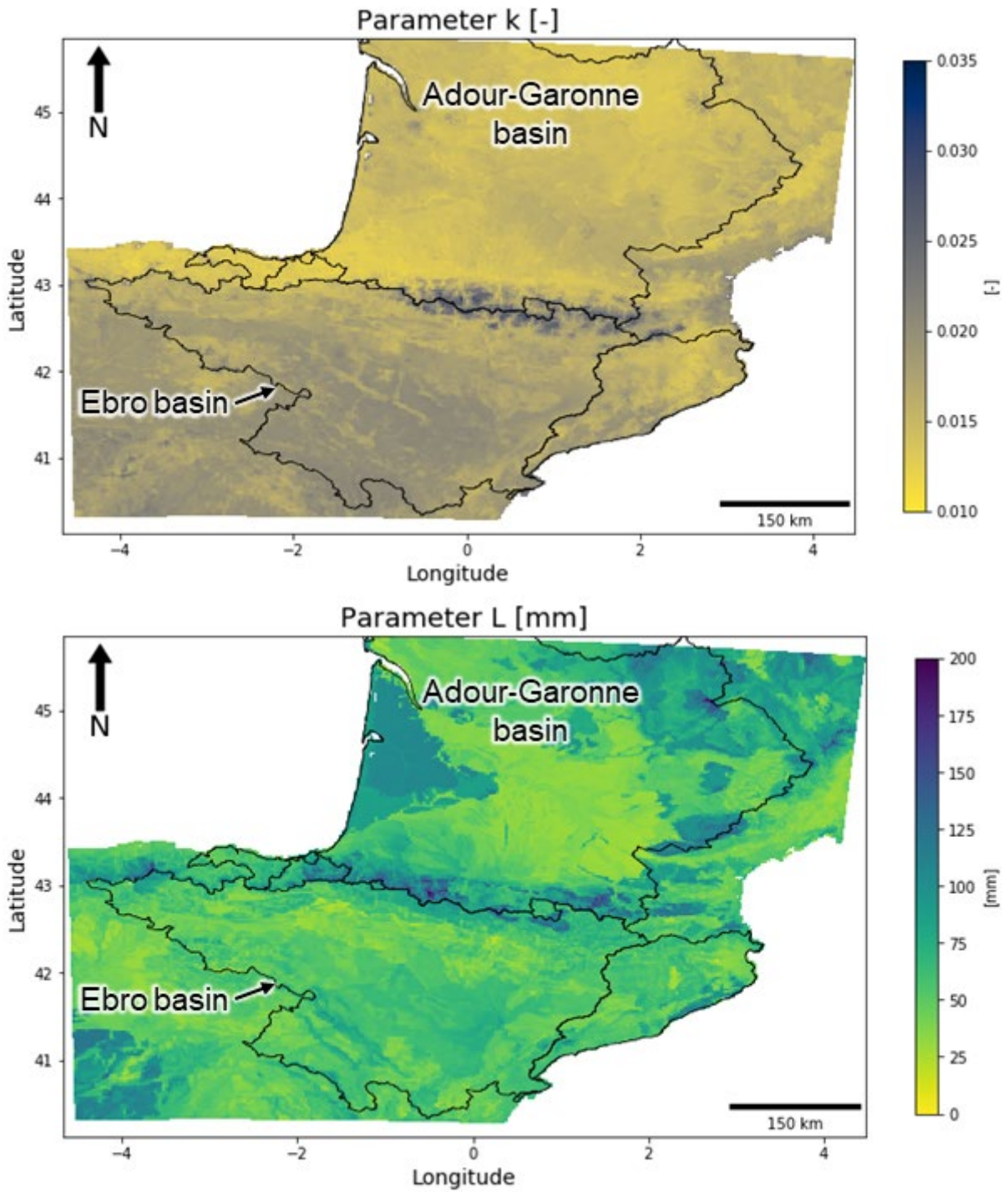


Figure 6-18 Median of the eight maps of the two parameters ( $k$  and  $L_{max}$ ) of the reservoir obtained applying the regionalization approach. The map set was obtained by cross-validation.

### 6.3.3.4. Evaluation of low-flows indices

In [Figure 6-19](#), the improvements in the low flow indices are depicted. For the  $Q_{90}/Q_{50}$  ratio (left panel of [Figure 6-19](#)), the default simulation (without reservoir) showed a median relative bias of -80% with respect to observations, whereas the median relative bias of the simulation adding a reservoir was of -32%. In both cases, this index is underestimated, but there is a significant gain due to the reservoir implementation. On the other hand, the QMNA (5) (right panel of [Figure 6-19](#)) also showed an improvement in median relative bias, from -64% of the default simulations to -20% of the simulation adding a reservoir.

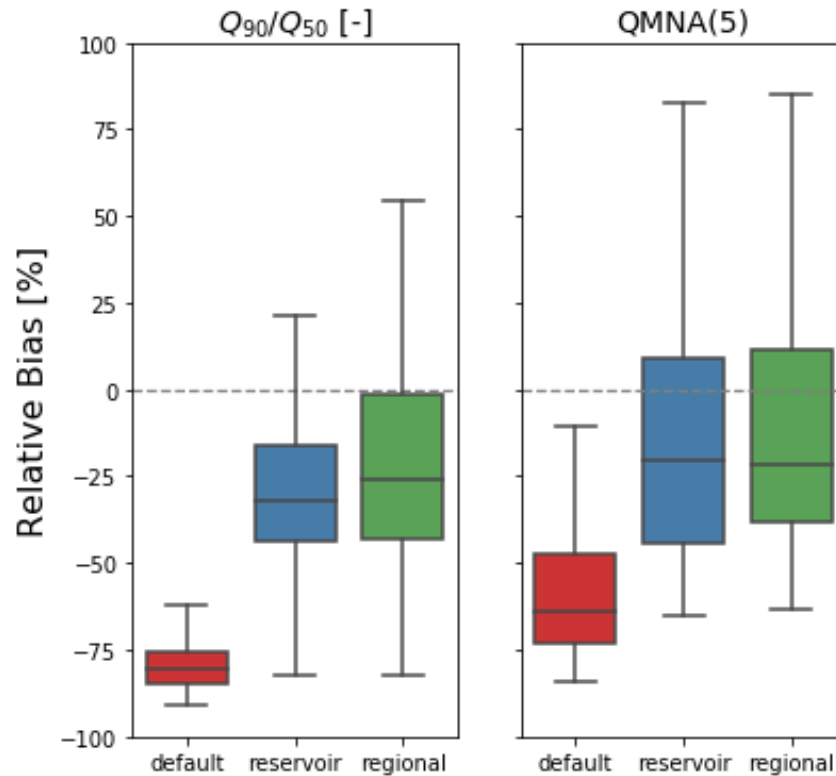


Figure 6-19 Comparison of relative bias [%] for low flow indices for the default simulation and for the two approaches. The left panel shows the ratio  $Q_{90}/Q_{50}$  and the right panel the QMNA(5). The line in each box represents the median and the box the interquartile range. The whiskers extend a maximum of 1.5 times the interquartile range.

In the case of the regionalization approach (green boxes in [Figure 6-19](#)), low flow indices reported values of median relative bias of -26% and -22% for the  $Q_{90}/Q_{50}$  ratio and QMNA(5), respectively. These values are practically same to the local calibration; only the 75<sup>th</sup> percentile (top edge of the box) for the  $Q_{90}/Q_{50}$  shows a larger difference. In any case, although low flow indices still remain underestimated, the inclusion and calibration of a reservoir (using either approach) noticeably improve the simulated values of the low flow indices and the regionalization approach behaves very well, compared to the local calibration one.



### 6.3.3.5. Comparison with a reference model

As the observations are affected by water management, the results are compared with an independent model. In this case, the SIMPA model, which is used by water managers in the Ebro river basin, is utilized for the comparison.

The time series simulated by default and the improved models were extracted at the outlet of the Ebro River basin, located in Tortosa. The mean annual cycle of streamflow was computed at a monthly step for the period 1980 to 2006. The computed mean annual cycle was then plotted (Figure 6-20) along with the observations (in black) and the SIMPA model (in green).

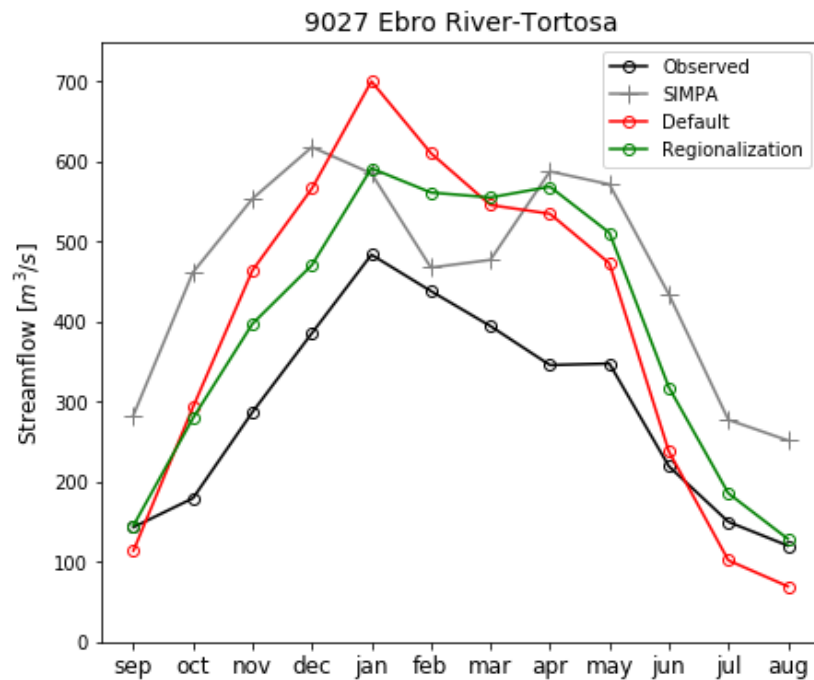


Figure 6-20 Mean monthly streamflow time series at Tortosa station (main Ebro River) from observations and different models.

The default simulation, in red, presents the lowest flows during the summer (from July to September), as expected, whereas the peak flow occurs in January. In general, the hydrograph of the default simulation has a shape similar to that of the observations, but with a positive bias. A positive bias is expected, as in the real basin there is more evapotranspiration, due to irrigation, than in the naturalized one. In contrast, the SIMPA model (gray line) shows two peaks, one in December and the other in April, and the minimum streamflow corresponds to the summer months, but with values twice higher than the observations. The flows obtained with the improved model, setting the parameters with the regionalization approach (green line), show a clear increase of low flows, but they are still very low compared to SIMPA. It is notable that the improved model reduces the January peak but increases the streamflow of the following months (February and March). The new hydrograph presents a double peak, which aligns with our expectations and is also observed in SIMPA. It is notable how the reservoir modifies the streamflow of the winter months. While this effect may not have been clearly visible in the daily hydrographs presented in Figure 6-15, it becomes apparent in the monthly mean annual cycle at the outlet. Nevertheless, is difficult to determine which model is closer to reality, because the observations represent the real basin, not the naturalized one, as the models do.

## 6.4. Discussion

### 6.4.1. Attempt to improve inner parametrization

The *runoff b* parameter plays a critical role in governing runoff generation and is highly responsive to changes in hydrological conditions. Therefore, it is essential to emphasize that the optimal value found in this analysis ( $b=0.5$ , the default value) should not be interpreted as universally applicable to the entire study area and all hydrological applications. Different regions or environmental conditions may require different values for this parameter, necessitating more comprehensive calibration processes and extensive sensitivity analysis.

However, it is important to acknowledge the challenges associated with conducting a more sophisticated calibration scheme for this parameter, such as employing Monte Carlo simulations or genetic algorithms. The significant computational and time requirements to perform a single simulation using the SURFEX model can limit the feasibility of such approaches.

Despite these limitations, it is crucial to recognize the significance of pursuing more refined calibration techniques in future research. Exploring advanced methods, such as machine learning algorithms, may offer potential solutions to expedite the calibration process and mitigate computational challenges. These techniques can help automate parameter estimation, optimize parameter sets, and improve the overall accuracy of the model. For instance, these approaches might help link the IDPR with the *runoff b* parameter.

Concerning soil information, ECOCLIMAP II determines the soil depth using vegetation cover, this assumption is based on that vegetation cover is a good indicator of soil depth, as plants are known to develop root systems that extend to different depths depending on the soil type and other soil characteristics. Thus, in each pixel of the ECOCLIMAP II dataset, the vegetation cover is assigned a specific rooting depth according to the root system development of typical plant species for that particular vegetation type. The rooting depth is defined as the maximum depth of the soil profile to which plant roots can penetrate and access soil water and nutrients.

The above represents some disadvantages, for example: within the same pixel vegetation cover class have the same rooting depth, which may not always be the case, in reality, the rooting depth of plants within a vegetation class can vary depending on factors such as local soil conditions (geology) and water availability. Consequently, this approach only considers the effect of vegetation cover on soil depth, neglecting other factors that can also play an important role in soil depth, such as topography and geology, which can be not realistic, especially in areas with shallow soils, like mountain areas.

To estimate the soil depth, the ESDAC database uses a combination of different methods and resources that include pedotransfer functions, remote sensing data, and modeling approaches. While ESDAC provides a valuable resource for estimating soil depth, has some limitations. Modeling approaches and functions may not accurately capture the complex soil properties that influence soil depth, and their accuracy may vary depending on the soil type and location

It is noteworthy that soil depth provided by ESDAC is a modeled estimation based on various sources and environmental factors, so there may be inaccuracies and uncertainties associated with this estimation, whereby simulations carried out using this information are subject to uncertainties from both the model itself and soil data. This may explain the fact that the performance metric of the simulation does not improve.

### 6.4.2. Improvement on low flows representation

A conceptual approach, based on rainfall-runoff models, to improve the streamflow simulated by SASER (adding a reservoir at the grid-scale resolution) was used. This is intended to provide a better representation of the slow component in the hydrological response, which is not well simulated by SURFEX. Results show that the additional reservoir, which is simple and easy to calibrate, has a very positive impact on the streamflow simulation. However, the calibration of the reservoir parameters is only possible in gauged natural basins, which are not numerous in the area of study.

The implementation of the conceptual reservoir has as its main objective to sustain the flows without having a significant impact on the daily high and medium flows (surface runoff). For this reason, the reservoir scheme is implemented as a postprocessing of just the drainage, which is the slow component. This redistribution of the water volume does not affect the shape of the hydrograph during peak events. During the summer months, there is a significant improvement in the low flow simulation, as shown in [Figure 6-20](#). This fact supports the effectiveness of the reservoir to improve the streamflow simulation. At the same time, at the monthly time step, it is evident that the annual cycle has undergone significant changes, redistributing water from winter to summer and obtaining a more realistic double-peaked hydrograph at the outlet of the Ebro basin.

A regionalization approach was established to find the values of the parameters for all the grid points of the area of study, not only those located in near-natural basins. This approach uses physiographic and climate-related predictors, although these variables are not immediately associated with groundwater, they exert an indirect influence on the runoff response. Therefore, those predictors are acting as proxies for defining the predictands. Moreover, several previous regionalization studies have emphasized the use of those predictors ([Nijssen et al., 2001](#); [Singh et al., 2014](#); [Beck et al., 2016, 2020](#)).

The performance of the model with regionalized parameters is almost as good as that of the catchment-by-catchment (local calibration) approach as reported KGE values. In the local calibration approach the values of the parameters are lumped, which probably would not work well in larger basins. Thus, the regionalization approach would probably be more advantaged if tested in larger basins. Additionally, having lumped values of the parameters per basin does not play well with a model that is mostly physical and which tries to be as spatially distributed as possible.

The regionalization approach allows us to apply the reservoir everywhere in the study domain, even in heavily human-influenced areas where a local calibration approach is not feasible. Due to the lack of validation data, our simulation with a reference one (SIMP) has been compared. The results from such an experiment are less easily interpretable. Still, at least it makes it evident that the differences are lower now, even if they remain very large when compare with the reference model.

The maps of the reservoir parameters produced by the regionalization approach are presented in [Figure 6-18](#). The full domain is covered by these maps at a 2.5 km resolution, and they vary according to climate and physiographic information that was used as predictors. It is difficult to explain the spatial patterns due to the complex and strong connection between the different variables (e.g. climate, vegetation, and soil properties) involved ([Troch et al., 2013](#)).

Despite that, spatial patterns related to known hydrological processes can be identified at least in one of the parameter maps (L, reservoir size). Patterns in this parameter, associated with soil moisture content, can be explained by the land cover, precipitation, and soil granulometric distribution. For example, in the region of the south-west of France where large sand deposits exist (Landes), the runoff response is quick, and infiltration has high rates, thus a buffer is required to play the role of groundwater storage and sustain the flows during the dry season, and hence the values of the reservoir size are expected to be larger than in clay predominated regions. On the other hand, the patterns in the map of the k parameter are not easily interpreted. Both, soil properties and topography influence the distribution of water storage, and isolating the influence of each other is problematic (Price, 2011).

Different regionalization experiments were carried out, to account for the equifinality problem (multiple optimal solutions providing reasonably similar or equal model performance values), which is one of the most important sources of uncertainty in hydrological modeling (Beven & Freer, 2001). Furthermore, in each experiment cross-validation process was used, which allows us to estimate the generalizability of the parameters and provides an indication of uncertainty. Previous experiments done (not shown here) indicated that the parameters used to initialize the genetic algorithm have a strong influence over the search direction and efficiency score.

As shown in Figure 6-15 (light blue bands), the time series of simulated daily streamflow provide, in general, a wide range of streamflow uncertainty bands derived from the parameter sets, especially at the end of the wet season and gradually decreasing during the dry season (July to August). Otherwise, the uncertainty bands during the winter months were of much lesser extent, except in some months (November and December), this could be explained by the fact that the reservoir configuration focuses only on low flows, however, an extensive parameter uncertainty assessment is beyond the scope of this study.

In addition to KGE scores, and to understand how well the additional reservoir simulates low flows, which is the main objective of the study, the  $Q_{90}/Q_{50}$  and the QMNA (5) indices were evaluated. The negative relative bias in both indices of default simulation suggests a fast precipitation-to-runoff reaction of the SASER model; hence, the low flows are underestimated during the dry periods. Results of our different simulations (local calibration or regionalization approach) adding the reservoir showed a considerable improvement in both indices, although they are still slightly underestimated, suggesting the suitability of the conceptual reservoir to improve the simulation of the slow component of the streamflow, even though other aspects of the model still need to be improved.

A key result of this work is that the introduction of a conceptual reservoir in the SASER model is found to be useful, even in cases where it is not feasible to easily calibrate the parameters in each catchment. This is possible as long as the values of the parameters are reasonable. This was demonstrated by different simulations (eight experiments and the three extra experiments using lumped parameters) carried out. Even though determining the most appropriate parameter map is challenging, it is noteworthy that all of the parameter maps yield reasonable results and are significantly better than the simulation without the reservoir (default).

## 6.5. Conclusions

The calibration of internal model parameters in SURFEX models is a complex task that requires careful attention and rigorous analysis. The process of calibrating the *runoff b* parameter and improving the soil database information in the SURFEX model proved to be a complex and demanding endeavor, both in terms of calibration efforts and computational requirements. Despite these challenges, our findings led to the conclusion that the default value ( $b = 0.5$ ) of the *runoff b* parameter adequately captures the dynamics of runoff generation within the model. This implies that the default setting offers a reliable representation of the hydrological processes under consideration. The potential relationship between the hydrological model parameter, specifically the *runoff b* parameter, and the Indice de Développement et Persistance des Réseaux (IDPR) was explored, however, no significant correlation between the IDPR and the *runoff b* parameter was found.

Simulations conducted using the improved soil information from the ESDAC database did not demonstrate significant impacts on the hydrological response, in terms of KGE. In fact, they even increased the uncertainty associated with the variables considered, such as the root zone. These findings suggest that the incorporation of the ESDAC database for soil information did not yield improvements in the modeling of hydrological response.

Despite the extensive efforts made, the improvement of the internal parametrization of the SURFEX model to enhance the simulation of hydrological processes was not achieved. Consequently, the decision was made to maintain the default parametrization.

In the second part of the chapter, to improve the simulation of low streamflow in the hydrometeorological model SASER by using a simple conceptual reservoir scheme to post-process the drainage and thus improve the slow component of the streamflow, the results can be summarized as follow.

The default SASER model presents a strong negative bias of low flow indices. The addition of a reservoir scheme to modulate the drainage had a positive result in terms of KGE values, when the parameters were set using a local calibration method, both for the calibration and validation periods. The addition of a conceptual reservoir proved to be a simple and efficient option, with a limited number of parameters, which improves the low flows simulated by SURFEX without deteriorating high flows, as shown in the improvement of the low flow indices studied (QMNA(5) and  $Q_{90}/Q_{50}$ ).

A regionalization approach, based on a genetic algorithm, was introduced to determine the values of the parameters all over the domain, including basins heavily influenced by water management, where a standard local calibration of these parameters is not possible. Results of the regionalization approach showed a clear general improvement of simulated streamflow ( $\Delta KGE=0.11$ ) with an improvement for 79% of the validation catchments. Those results were almost as good as those using local calibration. Both, KGE scores and the two low flow indices indicate improvements, especially for the low flow indices, although a small negative bias of the low flow indices remains.

The regionalization approach based on a genetic algorithm was possible due to the simplicity of the conceptual model and its implementation as an external module of SURFEX. Applying this

approach to calibrate other empirical parameters within the SURFEX model itself would be desirable, but impractical due to computational constraints.

A relationship between the parameters of the conceptual reservoir with climate and physiographic variables was established through the genetic algorithm, which allows us to take into account the within-catchment variability all over the study area. Although this approach is not physically based, it allows linking the two new parameters with physical variables, which is a good compromise for a model that tries to be distributed and as physical as possible.

In conclusion, the addition of a conceptual reservoir to postprocess the SASER simulated drainage led to considerable improvement in low flow simulation. The regionalization approach allows us to apply the reservoir all over the domain including the human influenced basins, not just natural ones.



---

# 7. Water management and drought

## 7.1. Introduction

The Earth's landscape has been profoundly influenced by humans through natural resource exploitation (Postel et al., 1996; Marsh, 2003). These human-induced impacts on the natural environment have now reached a significant magnitude, marking a new geological epoch known as the Anthropocene (Montanari et al., 2013; Savenije et al., 2014; Lewis & Maslin, 2015). The large-scale flow and storage of water are significantly influenced by human factors, for example, one evident manifestation of these impacts is the reduction in river flows and the alteration of hydrological regimes attributed to the construction of large dams (Nilsson et al., 2005). These observable changes highlight the expanding human footprint on freshwater resources and ecosystem services, raising concerns about the rapid rate of alteration occurring across the Earth (Sanderson et al., 2002; Vörösmarty et al., 2010; Carpenter et al., 2011; Gleeson et al., 2012). Moreover, the effects of human activities on freshwater systems are overwhelming, with substantial alterations observed across diverse spatiotemporal scales (Postel et al., 1996; Vitousek et al., 1997; Nilsson et al., 2005; Rockström et al., 2009).

The exploitation of freshwater resources has yielded remarkable socio-economic benefits; however, these advantages have been also accompanied by negative environmental consequences (M. Palmer et al., 2004). The spatial and temporal variability in water availability and usage has led to water scarcity in numerous regions worldwide (Postel, 2000; Hanasaki et al., 2013). To address the uneven distribution and ensure water availability across different locations and times, humans have significantly modified the natural patterns of freshwater flows and storage (Vörösmarty et al., 2000; Lehner et al., 2011). Thus, three major land-water management practices have emerged as key drivers of water cycle dynamics on a global scale: agricultural irrigation, flow regulation, and groundwater use (Pokhrel et al., 2016)

Over the past century, a considerable number of dams have been built in major river systems (Nilsson et al., 2005; Lehner et al., 2011), serving purposes such as guaranteeing water supply, controlling floods, and generating hydropower (Liu et al., 2015), which has resulted in the fragmentation of large river systems worldwide, causing a wide range of impacts (Dynesius & Nilsson, 1994; Graf, 1999; Nilsson et al., 2005). Simultaneously, irrigation plays a vital role in global water consumption (~70% of the world's freshwater), food production, and the terrestrial water balance. While irrigation has been practiced since the advent of agriculture, a rapid expansion of irrigated areas occurred during the last century (Pervez & Brown, 2010; Siebert et al., 2015), therefore intensifying the impacts on freshwater systems and climate (Hanasaki et al., 2013; Leng et al., 2015). Moreover, the growing global temperatures are projected to further strain Earth's water resources in some areas of the world, leading to increased water demands, particularly for agriculture (Wada et al., 2013; Dirmeyer et al., 2014; Haddeland et al., 2014; Schewe et al., 2014). Consequently, the integration of reservoirs, their operational dynamics, and irrigation practices into hydrological modeling is increasingly vital for developing effective

---



adaptation strategies, with a specific focus on the agricultural sector (Iglesias et al., 2012; Iglesias & Garrote, 2015). Therefore, continued research and development in the field of incorporating human influences in hydrological modeling will contribute to a comprehensive understanding of water management and improve the characterization of interactions and feedback between natural and human systems, thus will remain imperative in future studies (Pokhrel et al., 2016). As interdisciplinary approaches to addressing the challenges of adapting water systems, especially under uncertain and changing conditions (Garrote, 2017).

Land-surface models (LSMs) have been widely recognized as a powerful tool for understanding and simulating the hydrological cycle, focusing on droughts (Lehner et al., 2006; Vidal et al., 2010; Prudhomme et al., 2011; Van Loon et al., 2012; Barella-Ortiz & Quintana-Seguí, 2019; Gaona et al., 2022). They allow a deeper understanding of the physical processes involved in droughts and how they interact with other components of the hydrological cycle, providing valuable insights for understanding the dynamics of droughts and can assist in the management of droughts by providing information on water availability and potential drought hotspots.

In recent years, significant advancements have been made in LSMs, especially through improvements in vegetation, soil moisture, and groundwater schemes (Fisher & Koven, 2020; Blyth et al., 2021). And therefore, to ensure consistent analysis of human-induced changes in water resources at large scales, numerous large hydrological models that account for these interactions have been developed since the late 1990s (Sood & Smakhtin, 2015). Recently hydrological models now incorporate dynamic feedback mechanisms that account for the interplay between hydrology and human water management. This is achieved through the integration of various components such as irrigation-soil moisture dynamics, reservoir-streamflow interaction, and water allocation-return flow dynamics (Döll et al., 2012; Wada et al., 2014; Pokhrel et al., 2015). However, despite these advancements, the representation of human factors in current-generation LSMs remains somewhat limited and often oversimplified, thereby may not fully capture the complexity inherent in their interactions with natural processes (Pokhrel et al., 2016; Wada et al., 2017).

The hydrological system encompasses not only natural processes but also the crucial role of human behavior, and thus humans are not be considered as external drivers or boundary conditions (Montanari et al., 2013; Sivapalan, 2015; Troy et al., 2015; Van Loon et al., 2016). The field of socio-hydrology has emerged as a discipline aimed at unraveling the intricate dynamics that connect humans and water within a coupled hydrological-social system (Sivapalan et al., 2012, 2014; Gober & Wheeler, 2015). The development of socio-hydrology has brought a shift in perspective that allows for an assessment of the co-evolution of human activities and hydrology, driven by feedback mechanisms operating over extended temporal scales, an aspect not comprehensively previously addressed (Wada et al., 2017).

However, socio-hydrology must transcend individual case studies and undertake efforts to establish generalized yet locally relevant frameworks that capture changes in the dynamics of the human-water system on a larger scale (McMillan et al., 2016). While many recent studies incorporate human water management, significant uncertainties persist in model simulations (Döll et al., 2016). Nonetheless, it is worth noting that recent research reports indicate that integrating human influences into regional hydrology models improves their performance in simulating river discharge or groundwater storage (Wanders & Wada, 2015; Wada et al., 2016), thereby enhancing the realism of large-scale hydrological models and fostering more accurate predictions of the co-evolution of the coupled human-water system.

This chapter aims to integrate a reservoir regulation scheme into the SASER hydrological modeling framework to enhance the accuracy of simulating highly regulated basins, such as the Ebro basin. The improved modeling approach leads to a better comprehension of the historical conditions of water resource systems. To achieve this, two objectives are raised: (i) a simplified reservoir operation scheme that can be incorporated into the SURFEX-LSM model is proposed, which is applicable at any scale, particularly at large scales. The model utilizes a simple yet effective parameterization approach that demands minimal data availability. And (ii) quantifying the impact of human activities, especially reservoir operation and irrigation, on drought propagation.

## 7.2. Case study and data

The irrigated area, Canal de Aragón y Cataluña (CAyC) located in the northeastern part of the Ebro basin was used to implement the reservoir operation module in this chapter. It has been studied intensively in several researches (Milano et al., 2013; Linés et al., 2017, 2018).

For a description of the study area see section 3.1.3.

Data used in this chapter are presented in section 3.2.4.

## 7.3. Methodology

The following section provides a detailed account of the methodology adopted to incorporate an independent reservoir operation module into the SASER model. Figure 7-1 depicts a schematic flowchart that highlights the main steps involved, which are described in detail below.

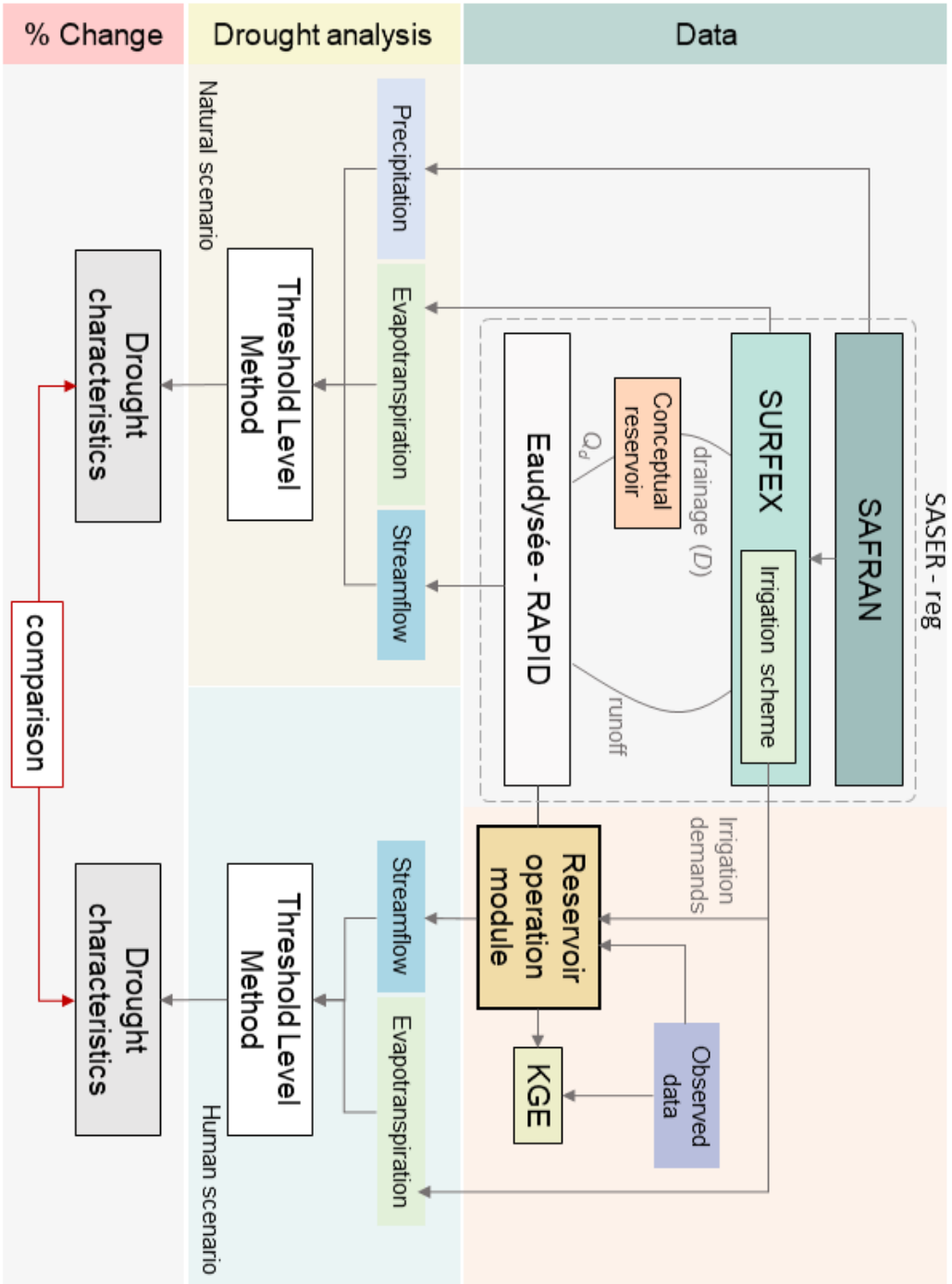


Figure 7-1 Scheme used to implement the reservoir simulation to SASER modeling chain.

### 7.3.1. Reservoir operation scheme<sup>3</sup>

A simplified reservoir operation scheme was implemented to simulate human water management in the framework of the SASER suite, as depicted in Figure 7-1. This scheme is based on the Water Availability and Adaptation Policy Analysis (WAAPA) model (Sordo-Ward et al., 2019, 2020) which is briefly described in the next subsection.

The scheme implemented in this research has been developed in Python code and retains several considerations of the WAAPA model. The main difference is that the simulations performed by our scheme only consider each reservoir individually at a time. It is noteworthy that the scheme employed in this study is not an integral component of the SASER chain. Instead, the scheme was utilized as an external module in this application, as depicted in Figure 7-1.

#### 7.3.1.1. Description of the WAAPA model

The WAAPA model (Garrote et al., 2015; Sordo-Ward et al., 2019, 2020) is a GIS-based model that performs simulations of reservoir operation, enabling the computation of the supply of water to demands from an individual reservoir or a system of reservoirs, Figure 7-2. The platform takes into account ecological flows and evaporation losses in its calculations. The fundamental elements of WAAPA comprise reservoirs, inflows, and demands that are interconnected with nodes of the river network.

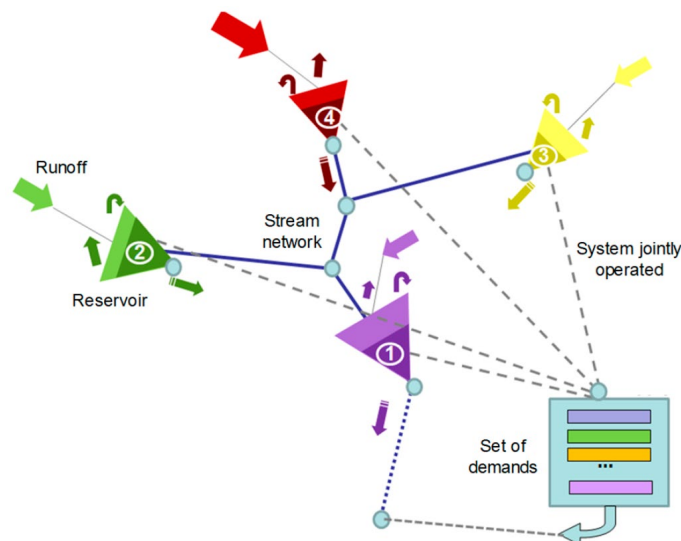


Figure 7-2 Operation scheme of the high-resolution Water Availability and Adaptation Policy Assessment (WAAPA) model (Sordo-Ward et al., 2019).

Initially, the model releases water from reservoirs located in the lower regions of the basin to meet the demands. Should these reservoirs reach their full capacity and continue to receive additional

<sup>3</sup> Based on: **Cenobio-Cruz, O., Quintana-Seguí, P., & Garrote, L. (2023).** Drought Propagation under Combined Influences of Reservoir Regulation and Irrigation over a Mediterranean Catchment. *Environmental Sciences Proceedings 2023*, Vol. 25, Page 8, 25(1), 8. <https://doi.org/10.3390/ECWS-7-14239>

inflows, uncontrolled spillage occurs, resulting in water being discharged from the system. Conversely, if upstream reservoirs are at full capacity and experience further inflows, the surplus water is collected by downstream reservoirs. However, this management criterion is a simplification, as real-world systems take into account more conditions and constraints. The model approach aims to maximize water availability while minimizing excess storage. The WAAPA model, in each timestep, computes the following operations:

1. The environmental flow requirements are satisfied in each reservoir by considering the available inflow. Environmental flows are subsequently transmitted to downstream reservoirs and incorporated into their respective inflows.
2. Computing evaporation in each reservoir, and thus the evaporation losses and adjusting the storage accordingly,
3. Calculation of the excess storage (storage exceeding the maximum capacity) in each reservoir, which is the increment in storage resulting from the remaining inflow.
4. The model meets demands in a prioritized manner by utilizing the excess storage first, followed by available storage, starting from the reservoirs with higher priority.
5. The model computes uncontrolled spills, if excess storage persists in any reservoir, to any surplus water.

As a result, the model generates a set of time series data encompassing monthly volumes supplied to each demand, monthly storage values, spills, environmental flows, and evaporation losses in every reservoir.

### **7.3.1.2. Model input data**

The model requires several key data inputs to simulate the reservoir systems obtained from the CHE. These essential data include the monthly series of inflows, maximum storage capacity, and the threshold values used for reservoir zoning. This scheme divides the reservoir storage into 3 zones (prealert, alert, and emergency), which correspond to the short-term scarcity threshold levels established by the CHE. Similarly, the monthly series of irrigation demands are crucial for comprehensive modeling.

Furthermore, to calculate the monthly rate of evaporation losses within the reservoir, the utilization of stored volume-area curves becomes imperative. The detailed procedure for this calculation is provided in Appendix **B.1**.

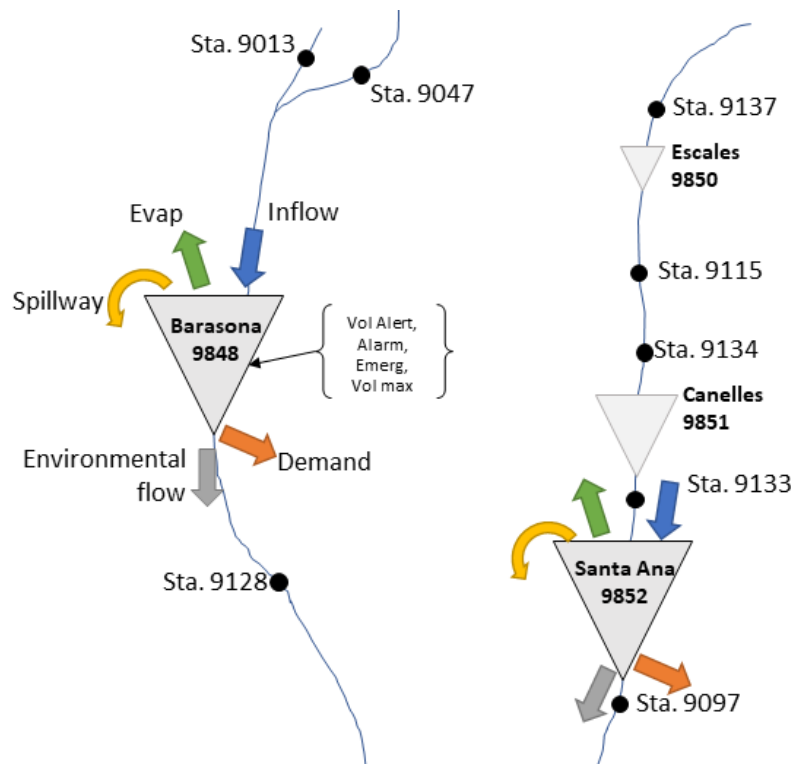


Figure 7-3 Schematic representation of the reservoir model as implemented in the area of study. Dams are represented by triangles; inflows and outflows are represented by arrows. Light triangles represent dams not considered in the simulation.

### 7.3.1.3. Model configuration

The CHE established shortfall thresholds for each reservoir, which are thoroughly described in section 3.2.4 of the study. These thresholds play a critical role in determining the zoning of the reservoir within the model. The zoning concept entails classifying the reservoir based on its storage levels, allowing water management strategies to be implemented. When the reservoir's storage level falls within its designated zone, an allocation coefficient is applied, influencing the water allocation decisions. By incorporating these thresholds and allocation coefficients, the model captures the dynamic nature of the reservoirs, enabling more realistic water allocation simulations.

To determine the proportion of available resources that effectively reach the crops, an allocation factor is applied to the accumulated inflow in the reservoir. This factor takes into consideration various factors, such as water supply to other uses. In this research, by defining the allocation factor, the model only considers the amount of water available for irrigation purposes.

As the precise allocation factor for each area is unknown, it is necessary to test the sensitivity of the model. This is achieved by running the model with different allocation factors, assuming perfect knowledge of the expected water availability. By conducting these sensitivity tests, the modeler assesses the impact of different allocation factors on irrigation outcomes. An allocation factor of 1 represents a theoretical scenario where all incoming water into the reservoir is directly accessible for irrigation purposes.

An allocation factor of 1.0 was selected for the Barasona reservoir due to its low storage capacity and therefore its regulation capacity is also low. Conversely, for the Santa Ana reservoir, an allocation factor of 0.55 was established since it was found as a benchmark (Linés et al., 2018).

#### 7.3.1.4. Evaluation criteria

To assess the performance of the reservoir module in emulating the outflow and storage for the selected reservoirs, the Kling-Gupta Efficiency (KGE) metric, as outlined in section 4.2.5.2 was employed. The KGE was computed to evaluate the agreement between the simulated volume storage and releases generated by the reservoir operation scheme, and their corresponding observed variables. This metric provides a comprehensive evaluation of the model's ability to reproduce the dynamics of the reservoir operation.

#### 7.3.2. Irrigation water demands

The CAyC is supplied mainly by the Barasona and Santa Ana reservoirs, as mentioned in section 3.1.3, to determine the corresponding irrigation demands, the monthly distribution provided by the CHE was utilized. The upstream zone comprises 55% of the total area within the CAyC region and exhibits an annual water demand of 436 Hm<sup>3</sup>. In contrast, the downstream zone, which is supplied by the Santa Ana reservoir, accounts for the remaining 45% of the CAyC area (equivalent to 357 Hm<sup>3</sup>) and includes the irrigation districts of Piñana (with a demand of 215 Hm<sup>3</sup>) and Algerri-Balaguer (with a demand of 48 Hm<sup>3</sup>). Both monthly distribution values are depicted in Table 7-1.

Table 7-1 Monthly distribution of irrigation demands for each irrigated area (Hm<sup>3</sup>)

Irrigated Zone	Oct	Nov	Dec	Jan	Feb	Mar	Apr	May	Jun	Jul	Ago	Sep
Barasona (Upstream)	21.37	21.37	21.37	21.37	21.37	21.37	12.65	54.51	86.35	81.12	46.66	25.73
Santa Ana (Downstream)	15.51	0	6.20	9.30	0	12.41	37.22	86.84	99.24	136.46	136.46	80.64

The San Salvador reservoir, with a capacity of 137 Hm<sup>3</sup>, holds a distinctive position as it is not situated along any river course. Instead, it receives water from the Barasona reservoir through the Zaidin channel. The primary function of the San Salvador reservoir is to store water during the winter months, which subsequently provides vital support to the Barasona reservoir during the summer months.

To ensure an accurate representation of the system dynamics, the monthly distribution of demand has been meticulously adjusted to implicitly account for the presence of the San Salvador reservoir. This adjustment takes into consideration the winter filling period, during which the reservoir experiences a steady inflow from October to March (first row in Table 7-1). By incorporating this constant value, the model effectively captures the interplay between the San Salvador reservoir and the broader water management scheme within the analyzed system.

Moreover, in this research, the irrigation scheme implemented within the SURFEX model (see section 3.3.2.1) was also utilized to estimate the irrigation demands corresponding to the areas supplied by each reservoir. This estimation takes into account the variability of weather conditions and thus every year, the calculated demands are different.

The model performs a detailed calculation of the crop water requirements. The model generates irrigation water based on soil moisture thresholds during the period of the irrigation campaign, representing the amount of irrigation water needed at each grid point within the defined irrigation zone, [Figure 7-4](#). This level of spatial resolution allows for a more accurate representation of the spatial variability in water demands across the study area. The default configuration of the irrigation scheme was adopted for this simulation, taking into account various parameters that influence the irrigation process. Specifically, sprinkler irrigation was considered, irrigation duration was set to 8 hours, and a maximum water amount of 30 mm per irrigation event was specified. Additionally, the irrigation events were scheduled on a weekly basis. At the time of writing this manuscript, new simulations have been performed with more realistic parameters of irrigation (closer to the actual irrigation patterns). Unfortunately, these simulations could not be included in the analysis due to time constraints.

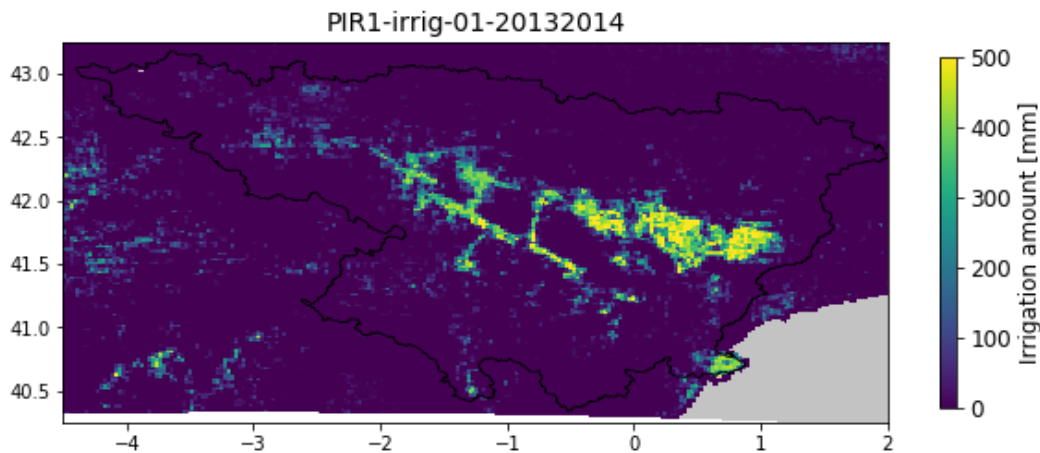


Figure 7-4 Total irrigation amount simulated by SURFEX for the hydrological year 2013-2014.

The previous figure shows all irrigated points within the Ebro basin. Hence, the total water amount for irrigation is calculated as the sum of the grid points corresponding to each irrigated zone at the end of each month every year for the whole period.

### 7.3.3. Drought analysis

To characterize a drought event and thus understand the processes involved, some features such as timing, duration, and intensity are necessary. Hence, given the complex nature of droughts, onset and recovery, and the different types of drought (mentioned in [section 2.1.1](#)), several indices have been developed to characterize a drought event ([Mishra & Singh, 2010](#); [Dai, 2011](#); [Zargar et al., 2011](#)). Most of them are based on probability distributions or statistical methods, which transform the original data series into standardized data. Besides, there are other approaches to characterize drought while maintaining the original series utilizing a defined threshold.

The standardized indices used for drought assessment have limitations when it comes to evaluating anthropogenic drought, as early mentioned in [section 2.1.1](#). The primarily rely on meteorological variables, that by themselves, may not fully account for the influence of human activities on water availability. The omission of human factors can limit the accuracy of drought assessment focused on anthropogenic impacts (see [Appendix B.3](#)). To address these limitations,



it is important to incorporate additional data sources and modeling approaches that explicitly consider the human influences on the water cycle.

In this study, droughts are identified and analyzed through the widely-used threshold level method (Dracup et al., 1980b; Fleig et al., 2006; Tallaksen et al., 2009; Vidal et al., 2010; Van Loon, 2013), that detailed described following.

### 7.3.3.1. Threshold level method

The threshold level method is based on the run theory (Yevjevich, 1967; Guerrero-Salazar & Yevjevich, 1975). The threshold level method is a widely used approach for characterizing droughts in hydrology, particularly in temperate regions where runoff values are typically larger than zero. The method involves defining a threshold value for a hydrological variable, such as streamflow, but it can be applied to any other, below which a drought is considered to occur. The duration and severity of the drought are then calculated based on the number of consecutive time periods that the variable remains below the threshold level (Figure 7-5).

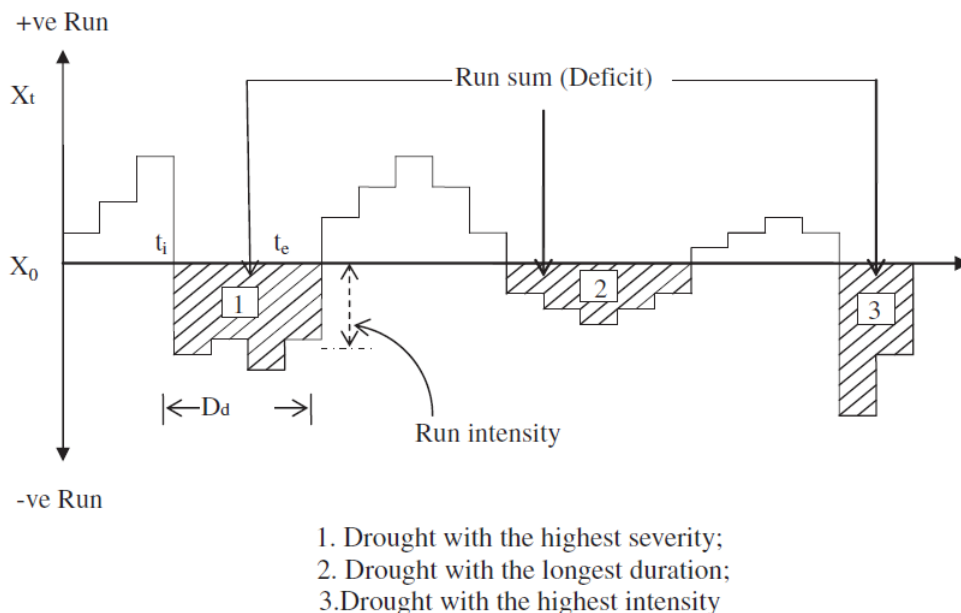


Figure 7-5 Scheme of drought characteristics using the run theory, from (Mishra & Singh, 2010).

One of the main advantages of the threshold level method over standardized indices, such as the Standardized Precipitation Index (SPI) or the Palmer Drought Severity Index (PDSI), is that it does not require prior knowledge of probability distributions, although nonparametric indices are available. Instead, the drought characteristics such as frequency, duration, and severity are directly determined from the original time series. Hence, the threshold level method allows for calculating the so-called deficit volume, which represents the total amount of water shortage that occurs during a drought event, a crucial drought characteristic in water resources management. Additionally, physical meaning is straightforward to interpret, which is valuable in a water management context.

Furthermore, several approaches have been developed to estimate the return period of droughts, defined according to the run method. These approaches include statistical procedures, such as the

method proposed by Fernández & Salas (1999), which is based on the extreme value theory, and the method proposed by Shiau & Shen, (2001), which uses a frequency analysis approach. Additionally, Bonaccorso et al. (2003) proposed a procedure to estimate the return period of droughts based on the probability distribution of drought duration. Cancelliere & Salas (2004) proposed a method to estimate drought risk using a Monte Carlo simulation approach. These procedures have proven to be effective in quantifying the risk associated with drought events and can provide valuable information for decision-making in drought-prone regions. In this context, the run method has emerged as an ideal candidate for performing drought risk analysis, as it identifies drought events based on hydrological data and provides a straightforward way to estimate their return period.

However, despite its usefulness, this method has some limitations, for example, the calculation of the threshold level method does not consider a standard classification of drought, which can result in significant differences between climate types and hinder global comparison. Therefore, standardization is often required for global drought studies (Wanders et al., 2010). Moreover, in extremely arid regions with ephemeral rivers, the threshold level method (as well as other drought analysis methods) faces an additional challenge. In these areas, long periods of almost no precipitation and natural zero flow can lead to a threshold level of zero, making it difficult to identify and characterize drought events (Scanlon et al., 2006). Finally, the threshold level method is limited by the need for accurate and reliable data on hydrological variables, and the choice of an appropriate threshold level can be subjective and dependent on expert judgment. In our case study, these limitations do not apply, because the comparison of different regions is not involved, the rivers under study are not intermittent, and adequate thresholds based on stakeholder experience can be defined.

The determination of the threshold level is a fundamental aspect of the threshold level method for drought analysis. Various approaches to defining the threshold level have been proposed, including historical averages and statistical methods. The fixed threshold level approach, which uses a constant threshold level to identify drought, represents the simplest form of this method. However, variations in climate and land use can affect the hydrological regime, leading to temporal changes in the threshold level. To address this, alternative versions of the threshold level method have been developed. These include the seasonal and monthly-varying threshold level approach, which uses different threshold levels for each season or month, based on historical data or statistical methods. These approaches aim to improve the accuracy of drought identification by accounting for temporal variations in the hydrological regime as depicted in Figure 7-6.

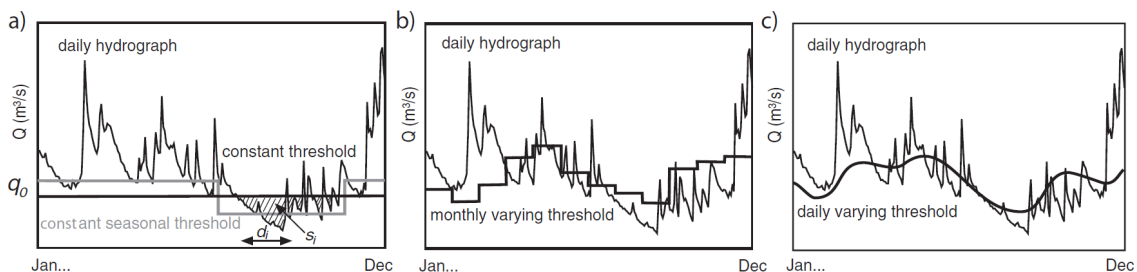


Figure 7-6 Illustration of the threshold level method, with a) constant and seasonally constant threshold, b) monthly-varying threshold, and c) daily-varying threshold (Stahl, 2001).

### 7.3.3.2. Calculation procedure

The threshold level method defines a drought event when a specific hydrological variable of interest, falls below a predetermined threshold value ( $q$ ). The onset of a drought event occurs when the variable ( $x$ ) drops below the threshold level ( $t=1$ ), and the event continues until the threshold is exceeded once again (recovery;  $t=T$ ). Each drought event ( $i$ ) can be identified by its duration ( $\Delta$ ) and a severity measure. Thus, the duration of a drought event is obtained through the following equations:

$$\delta(t) = \begin{cases} 1, & x(t) < q(t) \\ 0, & x(t) \geq q(t) \end{cases} \quad (7-1)$$

In this equation, the binary variable  $\delta(t)$  represents whether a drought situation is occurring at time  $t$ , while  $x(t)$  represents the value of the hydrometeorological variable at time  $t$ . It is important to note that time  $t$  is measured in discrete time steps.

$$\Delta_i = \sum_{t=1}^T \delta(t) \cdot \Delta t \quad (7-2)$$

The duration of a drought event ( $i$ ) is denoted by  $\Delta$ , and  $\Delta t$  is the time step (one month in this case).

The deficit volume ( $D$ ), is obtained by adding up the differences between the actual flux and the threshold level during the drought period. The procedure can be expressed using the equations 7-3 and 7-4.

$$d(t) = \begin{cases} q(t) - x(t), & x(t) < q(t) \\ 0, & x(t) \geq q(t) \end{cases} \quad (7-3)$$

The volume deficit ( $D$ ) of drought event  $i$  (in mm), is obtained as following:

$$D_i = \sum_{t=1}^T d(t) \cdot \Delta t \quad (7-4)$$

Using a threshold-level method related to the drought-impacted sectors is crucial to effectively manage water resources during drought events. Each sector, such as irrigation, drinking water, and ecology requires specific threshold levels that reflect their needs (Hisdal et al., 2004; Fleig et al., 2006; Sheffield & Wood, 2012). The threshold level can be either fixed or variable, depending on the scale and purpose of the analysis [Figure 7-6](#). A variable threshold level, which accounts for seasonal variations, is commonly used in global drought studies (Stahl, 2001; Vidal et al., 2010; Hannaford et al., 2011; Prudhomme et al., 2011; Parry et al., 2012). In this study, a variable threshold level was employed to better capture the seasonal variations in drought events. This approach provides a more accurate representation of the severity and duration of drought events, which can aid in the development of effective drought management strategies.

Depending on the research question and the specific context of the study different threshold levels can be used (Mishra & Singh, 2010), which can be derived from the flow duration curves (FDC). By selecting a different percentile in the calculation of the threshold level, the drought characteristics can be altered. For instance, a 95<sup>th</sup> percentile threshold identifies fewer events with lower deficit volumes and maximum deviations but shorter durations, while a 70<sup>th</sup> percentile threshold identifies the opposite. Nonetheless, the relationship between the drought characteristics of different hydrometeorological variables or catchments is unlikely to be impacted. This has been demonstrated in several studies, including (KO & Tarhule, 1994; TATE & FREEMAN, 2000). Therefore, the selection of the percentile should be based on the specific needs of the study and the characteristics of the catchment in question. For example, in regions with scarce water resources, it may be appropriate to use a lower percentile threshold to identify drought events with larger deficit volumes and longer durations. In contrast, in areas with abundant water resources, a higher percentile threshold may be used to identify more extreme drought events with shorter durations. The choice of threshold level should also consider the availability and quality of the data, as well as the objectives and scope of the study.

For the study presented here, and to take into account seasonality a variable threshold based on the 80<sup>th</sup> percentile (Q80) from the monthly FDC was used to identify drought events as depicted in Figure 7-7. This threshold was chosen because it represents the discharge level that is exceeded 80% of the time and is a commonly used threshold in drought studies (Hisdal et al., 2001; Tallaksen & Van Lanen, 2004; Fleig et al., 2006; Tallaksen et al., 2009; Van Loon, 2013).

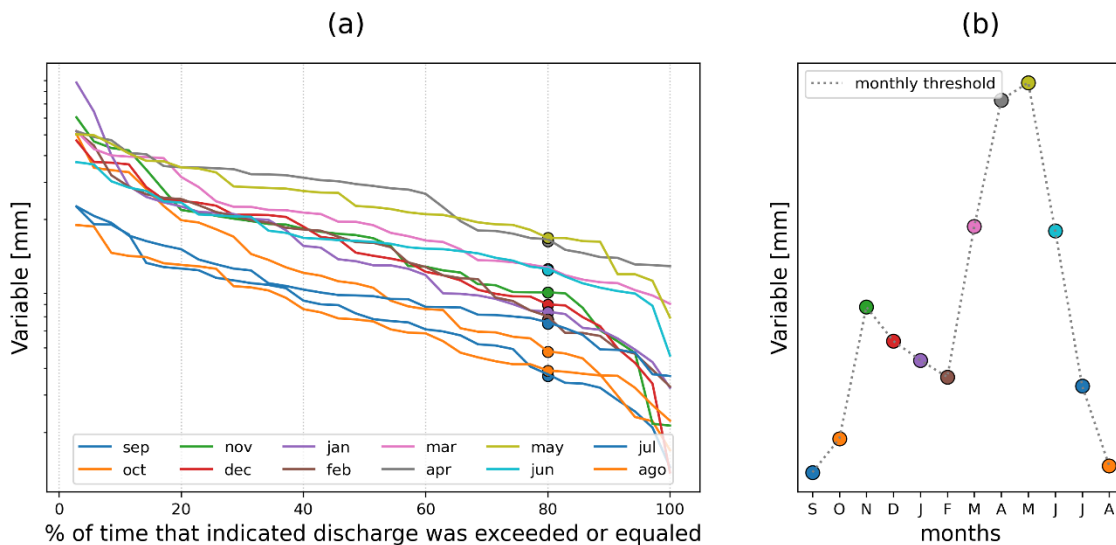


Figure 7-7 Panel (a) shows the FDC for each month and (b) the variable threshold level scheme based on the 80<sup>th</sup> percentile from the FDC.

### 7.3.3.3. Drought characteristics

Drought metrics can be obtained from drought event analysis, the comparison between flow and threshold levels, such as frequency, duration, and deficit volume. It is noteworthy that the use of different drought metrics provides an overall understanding of the characteristics of drought in each region. To ensure that all drought events analyzed have a duration longer than the time step of the threshold, drought events with a duration of only 1 month are not included in the analysis process.

The first drought metric is drought frequency (occurrence of drought events, which is calculated as the total number of drought events identified in the period). The second drought metric analyzed is the duration of drought events. The average duration of all events and the duration of the maximum event were used.

The third drought metric is drought severity (the strength of a drought), it can be quantified through different approaches, such as standardized indices, e.g. SPI (Mckee et al., 1993), this index quantifies drought severity by expressing it in terms of the number of standard deviations from the mean. Notable examples of their application can be found in studies by (Mishra et al. (2009), Vicente-Serrano et al. (2010), and Joetzjer et al. (2013). While standardized indices provide valuable insights, it is important to note that for many impacts, a more comprehensive understanding of drought severity, physical measures are required (Wong et al., 2013). These physical measures offer a deeper exploration of the severity's tangible effects and provide an extended perspective on the implications of drought across various sectors.

In this analysis, the deficit volume of drought events was used as a severity drought metric, which is defined as the cumulative difference between the flow and the threshold over the drought event. Same as for drought duration, the total deficit over the entire period, the average deficit of all events, and the deficit of the maximum event were used.

#### 7.3.3.4. Quantifying the human influence

The drought characteristics for each type were obtained through the drought analysis and then the human influence on drought (difference between human-influenced and naturalized scenarios) was quantified through the following equation:

$$\text{change (\%)} = \left( \frac{\text{human} - \text{reference}}{\text{reference}} \right) * 100 \quad (7-5)$$

The reported percentages indicate the variation in human-influenced conditions compared to the naturalized state. These values reflect the extent of change or deviation from the baseline conditions that occur because of human activities or interventions.

## 7.4. Application of the methodology to the CAyC

In this section, the application of the adopted framework, described in section 7.3 and illustrated in Figure 7-1 in the CAyC is presented.

### 7.4.1. Irrigations demands from SURFEX-LSM

The initial step involved comparing the irrigation demands derived from the SURFEX irrigation scheme with the data obtained from the CHE, as depicted in Figure 7-8. Examining the results for the Barasona reservoir, it is evident that the model-estimated demand closely aligns with the reference data. Conversely, for the Santa Ana reservoir, a notable disparity emerges, with the estimated demand significantly lower than the data provided by the CHE.

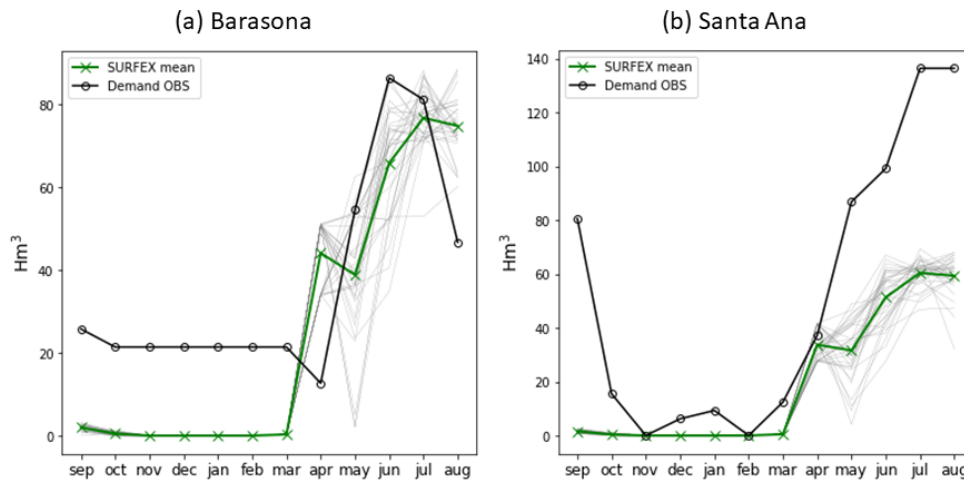


Figure 7-8 Irrigation demands estimated by SURFEX for both areas supplied by (a) Barasona and (b) Santa Ana. Gray lines represent each year and the green line represents the mean. The black solid line represents the irrigated demand derived from the CHE data.

For the Barasona reservoir, the simulation results indicate that the monthly values of irrigation demand closely align with the reference data. The main variations are observed during the months of October to March, which coincide with the adjustments made to implicitly account for the influence of the San Salvador reservoir. However, the simulation results for the Santa Ana reservoir exhibit greater disparities compared to the observed demands, particularly during the months of May to August. In this period, the estimated values are approximately half of the observed values, indicating a significant deviation in the simulation results.

It is important to highlight the advantage of utilizing the model-estimated demand, which exhibits interannual variability. Unlike fixed values every year, this dynamic approach captures the year-to-year fluctuations in demand, enabling a more realistic representation of the system. While the model-estimated demand demonstrates favorable agreement for the Barasona reservoir, further investigations and refinement are required to align the estimated demand with the data from the CHE for the Santa Ana reservoir, and also these simulations require refinements in order to make them closer to the actual practices of irrigators.

#### 7.4.2. Performance of the reservoir operation scheme

The results presented in this study focus on the simulation of reservoirs individually, with a specific emphasis on the demand for irrigation as the primary anthropogenic activity. To accomplish this, data obtained from the CHE and SURFEX simulations utilizing the newly implemented irrigation scheme (Druel et al., 2022) were employed. The latter allows for estimating realistic amounts of irrigation water and, consequently, the associated evapotranspiration (ET). As a result, four different scenarios encompassing different combinations of irrigation demand and inflow data were defined:

- S1. Observed data; inflow provided by SAIH and demands obtained from CHE data.
- S2. Inflow data from SAIH and irrigation demands extracted from SURFEX
- S3. Inflow obtained from (bias-corrected) SASER-reg, and irrigation demand obtained from CHE.
- S4. Simulated data: inflow from (bias-corrected) SASER-reg and irrigation extracted from SURFEX

These scenarios are then compared with the naturalized scenario, without human influence, this simulation is performed by the SASER model.

The ability of the new module that simulates human-water management (reservoir operation) is evaluated through the performance metric KGE. Figure 7-9 shows performance metric results in terms of KGE for simulated storage and releases compared to the non-reservoir assumption (without human influence). The results show a good agreement, especially for the Barasona reservoir that reported in general higher KGE values for the different scenarios, panel (a) in Figure 7-9. KGE values using the outflows reported values around 0.75. These results demonstrate the efficacy of the proposed reservoir operation strategy in meeting the water demands within the respective systems.

In contrast, the Santa Ana reservoir exhibits lower KGE values for the simulated storage. Even in the best-case scenario (S1), the KGE values do not exceed 0.25, panel (b) in Figure 7-9. On the other hand, the KGE values for releases show slightly higher values, ranging above 0.4 in all cases. However, these values are significantly lower when compared to the Barasona reservoir. This discrepancy suggests that the model performance for simulating storage and releases in the Santa Ana reservoir is relatively weaker than that of the Barasona reservoir.

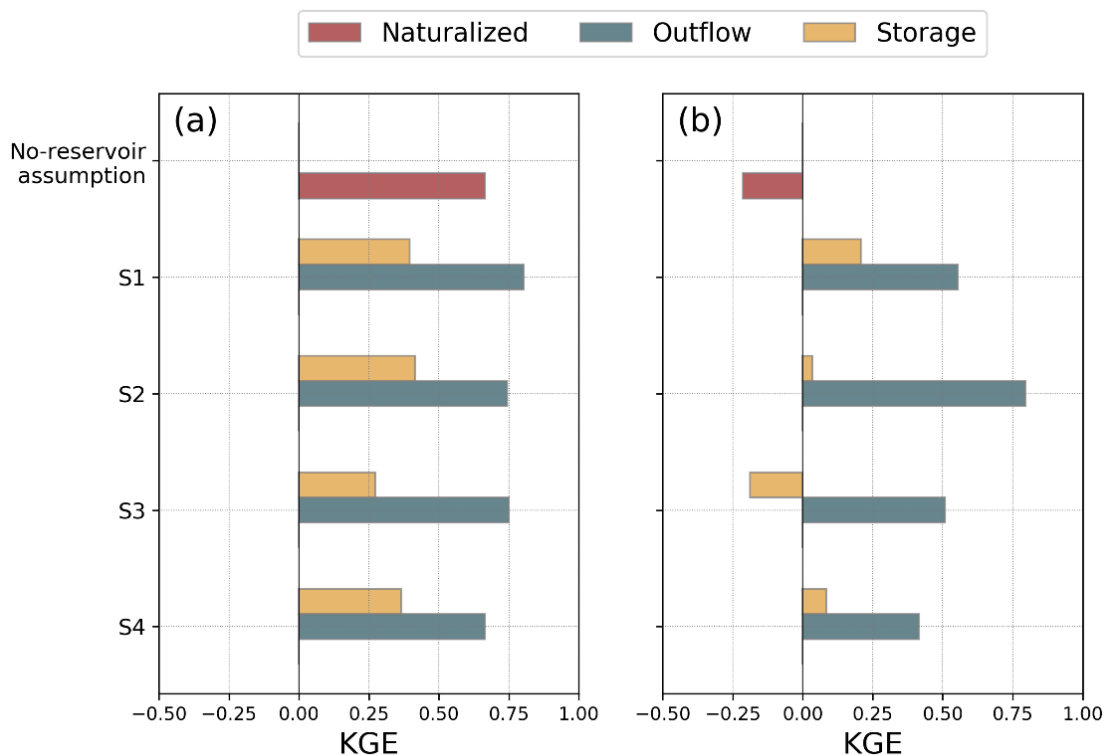


Figure 7-9 Performance evaluation results of the reservoir operation scheme. KGE metric for the naturalized scenario and the human-influenced scenarios (S1 to S4). Panel (a) for Barasona and (b) for Santa Ana reservoir.

The naturalized scenario (no reservoir assumption), red bars in Figure 7-9, for the Barasona reservoir depicted a KGE value of 0.66, whereas for the Santa Ana reservoir resulted in a negative KGE value (-0.2), which indicates the significant influence of the reservoir regulation in the hydrological regime, and thus it also indicates that the Santa Ana case is more difficult, as the results depend more on the model than in the Barasona case. In general, for the Barasona reservoir,

KGE values (outflow, blueish bars in [Figure 7-9 a](#)) reported similar positive values, which demonstrate a lower influence on reservoir regulation in the hydrograph shape. As anticipated, a notable degradation in performance was observed in the S3 scenario, primarily attributable to the uncertainty associated with the simulated inflow by SASER and the higher irrigation demands provided by CHE, in contrast to the estimations provided by SURFEX. The inclusion of these factors introduced significant challenges in accurately capturing the dynamics of the system.

In contrast, the S1 scenario served to represent the module's capability to reproduce the current behavior of each dam as indicated the upper right square in [Figure 7-1](#). To achieve this, observed data for both streamflow and irrigation demands were utilized as inputs for the module. The simulated results were then compared against the observed data for volume and reservoir outflow, providing a comprehensive assessment of the model's performance. This scenario (S1) demonstrated that the model's outputs aligned closely with the real-world behavior of the dam, enabling a more reliable evaluation of its effectiveness in capturing the system dynamics as depicted in [Figure 7-10](#) and [Figure 7-11](#), respectively.

The results of the reservoir operation module shown here, indicate a satisfactory performance to simulate storage and outflows, with KGE values of 0.4 and 0.82, respectively ([Figure 7-10](#)). The simulated volume storage in the Barasona reservoir follows the same dynamics, except for the events from 1995 to 1997, which correspond to other factors and not to irrigation demands.

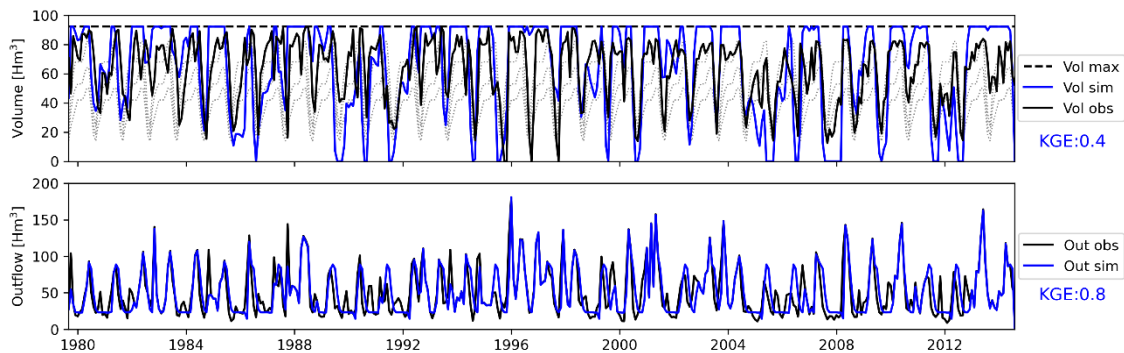


Figure 7-10 Simulated storage and releases (blue solid lines) for the S1 (observed data as input) scenario for the Barasona reservoir.

It is worth noting that although the reservoir's maximum capacity is 236 Hm<sup>3</sup>, it is rarely reached after 1996. Therefore, a maximum volume consistent with observations (200 Hm<sup>3</sup>) is considered for the simulation. Results for the Santa Ana reservoir show KGE values lower, especially for simulated storage (0.2), whereas for releases the value is acceptable (0.56), as indicated in [Figure 7-11](#).

Overall, the simulation results indicate a satisfactory match between the observed and modeled dynamics of the reservoir, particularly after 1996 (gray area indicated in upper panel in [Figure 7-11](#)). The stored volume demonstrates a similar pattern to the observations, suggesting that the model reasonably captures the reservoir's behavior. Furthermore, the model performs favorably in simulating the outflow values, closely approximating the observed data.



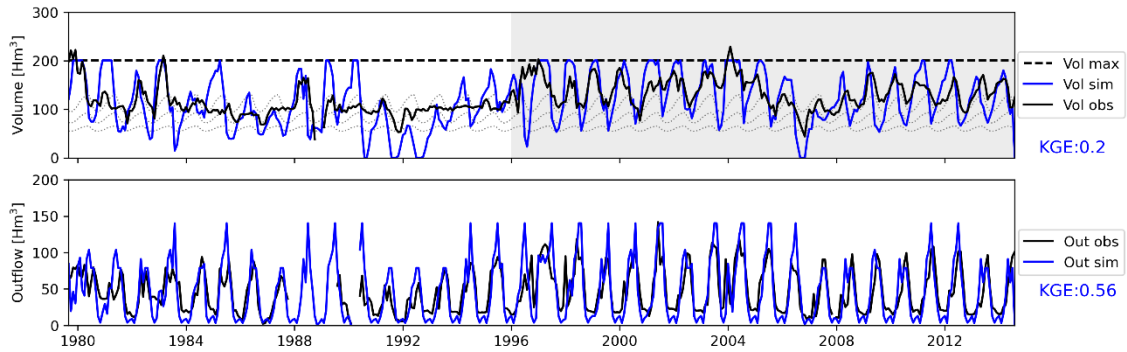


Figure 7-11 Same as Figure 7-10 but for Santa Ana reservoir.

Appendix B.2 contains supplementary figures presenting additional reservoir results that complement the findings presented in the main body of this study. These additional figures provide a more comprehensive visualization of the reservoir results, including variations in storage levels, outflow rates, and deficits.

The KGE results demonstrate that the reservoir operation module is capable to simulate the storage and outflows reasonably well. It is worth highlighting that for the S1 and S2 scenarios, the same irrigation demand was assumed every year, which does not accurately reflect realistic conditions. Nevertheless, this approach has yielded reasonably good results, especially S1 which only uses observed data and can be viewed as a calibration scenario.

### 7.4.3. Identifying drought events and analysis

#### 7.4.3.1. Barasona case study

The results presented in Figure 7-12 provide valuable insights into the impact of human activities on the streamflow and evapotranspiration (ET) dynamics in the Barasona case study. The left column of the figure represents the natural condition, non-reservoir assumption, and non-irrigation considerations, while the right column represents the human scenario.

In the natural condition (right column in Figure 7-12), the streamflow exhibits temporal variability, characterized by fluctuating levels that correspond to the wet and dry seasons. The data reveals distinct high peaks during the wet season and low peaks during the dry season, capturing the natural hydrological processes. These variations in streamflow reflect the natural dynamic of the river in the absence of human interventions. Additionally, the evapotranspiration values in the natural condition display a consistent pattern, indicating the influence of natural processes on the water cycle.

However, in the human scenario, the presence of the reservoir and the implementation of irrigation practices have noticeable effects. The upper right panel in Figure 7-12 illustrates the simulated flow downstream of the reservoir using the reservoir model. Here, a significant decrease in flow is observed compared to the natural condition. This reduction is a consequence of water diversion for irrigation purposes, resulting in a decreased volume of water flowing downstream.

Furthermore, **Figure 7-12** (lower right panel) shows the ET associated with irrigation, simulated using the SURFEX irrigation module. The ET levels show a marked increase in response to the introduction of irrigation, as water is redirected from the river to meet the demands of irrigated areas. This increase in ET further exacerbates the decrease in downstream flow since the water is intended for irrigation purposes.

The identification of drought events is an important aspect of this study. The reddish areas in **Figure 7-12** indicate deficit events, which are considered drought events according to the variable threshold method. The threshold used for identifying drought events was derived from the naturalized data series, obtained through simulations without using the irrigation scheme and the SASER model. This threshold was then applied to both the natural condition and the human scenario, providing a comprehensive assessment of drought occurrence.

In the natural condition, it is evident that the system responds to drought events by propagating hydrological drought events to evapotranspiration (ET), leading to negative anomalies in this variable. The drought periods in both variables are similar. This consistent pattern demonstrates the clear propagation of drought within the system.

In contrast, the findings in the human scenario reveal a notable discrepancy. The reservoir's presence downstream induces hydrological drought events, which deviate from the natural condition, but, in exchange, ET deficits are greatly reduced. This is the point of water management, agronomical droughts (ET) are reduced, in exchange for an increase of hydrological droughts.

However, a comment on the ET plot must be made. The model's irrigation water is created, it is not extracted from the dams (there is not a bidirectional coupling); thus, allows for indefinite irrigation. Consequently, extreme droughts that cause a reduction in water allocations might be not correctly represented. Furthermore, it has been determined that the irrigation parameters utilized in this simulation are not realistic enough. Nonetheless, the point is the same, dams contribute to an increase in hydrological drought when compared with natural thresholds, but they also allow to avoid most ET deficits, as they enable irrigation. Hence, it is of great interest to analyze these variables in conjunction. It is worth mentioning that the improvement of our analysis would undoubtedly be facilitated by the implementation of a fully coupled model and we hope in the future this will be possible.

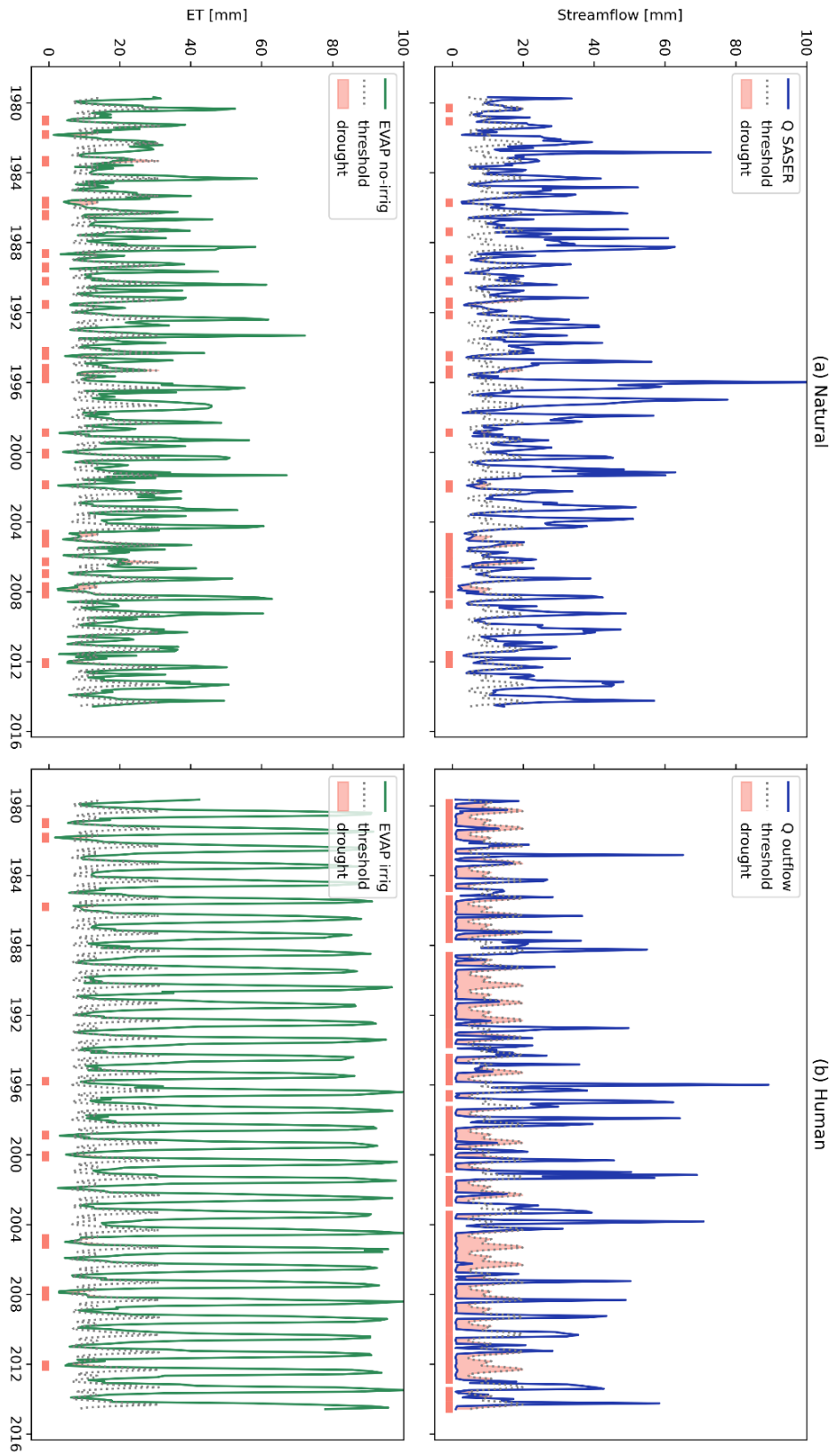


Figure 7-12 Time series comparison for Barasona reservoir.

Figure 7-13 presents the monthly deficits for the variables used in this study, precipitation, streamflow, and evapotranspiration (ET), under both natural (upper panels) and human (lower panels) scenarios. The analysis reveals the occurrence of a meteorological drought event, characterized by prolonged precipitation deficits, in the year 1991. This drought event is observed to propagate to both streamflow and ET, indicating a strong propagation effect within the hydrological system. Furthermore, it is noteworthy that the period from 2004 onwards exhibits an increased frequency of hydrological drought events. Notably, drought events in 2004, 2006, and 2007-2008, which are widely documented in the literature, are clearly identified using the proposed approach, underscoring its effectiveness in accurately capturing and identifying drought events.

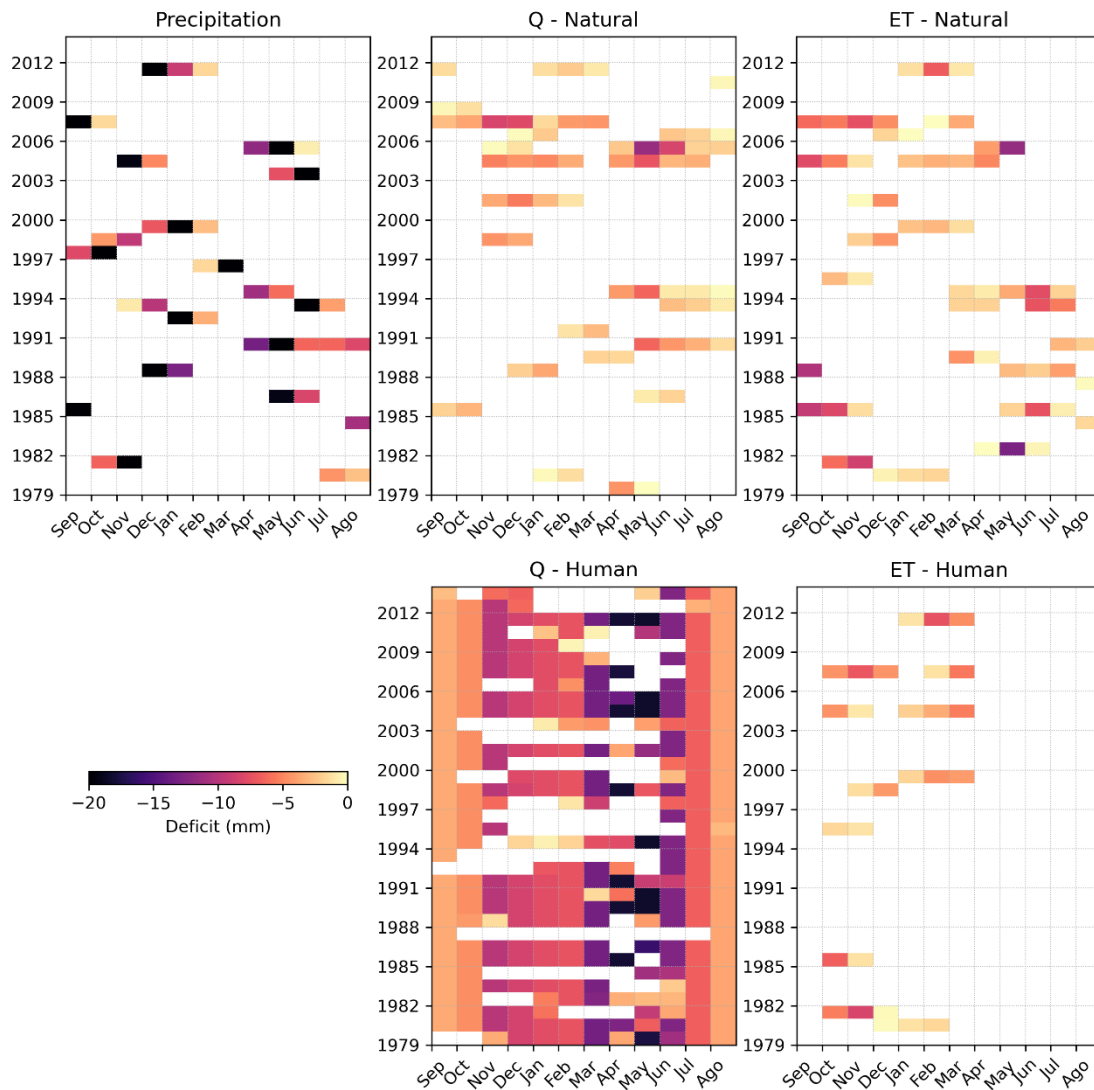


Figure 7-13. Monthly deficits for precipitation, streamflow, and ET for the Barasona case study. The upper panels represent the natural situation and the lower panels represent the human situation.

The Figure 7-13 also shows, in the “Q-Human” panel, that currently the river, compared to the natural behavior, is almost permanently in deficit, especially in winter, when the dams are being filled, except those years when the dam is already at capacity and thus outflow is closer to inflow. Of course, this allows to reduce ET deficits (“ET-Human” panel). It is also important to note that the ET-Human (lower right panel), during the months that the model irrigates (from April to

August) no deficit events are recorded, which is the main objective of the reservoir. Here, all the caveats mentioned before on the lack of a link between irrigation and dams apply.

In [Figure 7-14](#), the deficit events for scenario S4 are graphically presented, showcasing the simulation results obtained by utilizing the flows simulated by SASER as input data, in conjunction with the irrigation demands simulated by SURFEX, which vary from year to year. The comparison reveals a notable shift in the deficit patterns. It is worth highlighting that a considerable number of months exhibit no deficits, particularly during the winter months when water availability is relatively abundant. However, as the irrigation season commences in April and May, a discernible surge in deficit values becomes evident. This surge is attributed to irrigation demand estimated by SURFEX being higher during April in comparison to reference demands.

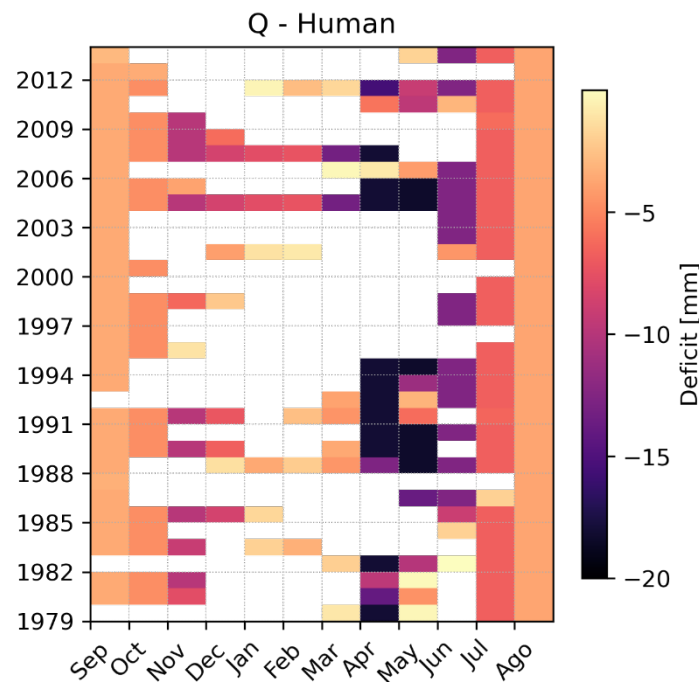


Figure 7-14 Deficits in downstream flow simulated by the reservoir scheme, for the S4 scenario.

### 7.4.3.2. Santa Ana case study

In the Santa Ana case study, the impacts of the reservoir are even more prominent, as demonstrated in [Figure 7-15](#). The left column of the figure represents the natural condition, non-reservoir assumption, and non-irrigation considerations, while the right column represents the human scenario. Similar to the Barasona case, the reservoir's influence on downstream flow is evident, albeit significantly greater in magnitude. Throughout the analyzed period, streamflow consistently falls below the established threshold, highlighting the substantial alteration caused by the reservoir (right upper panel in [Figure 7-15](#)).

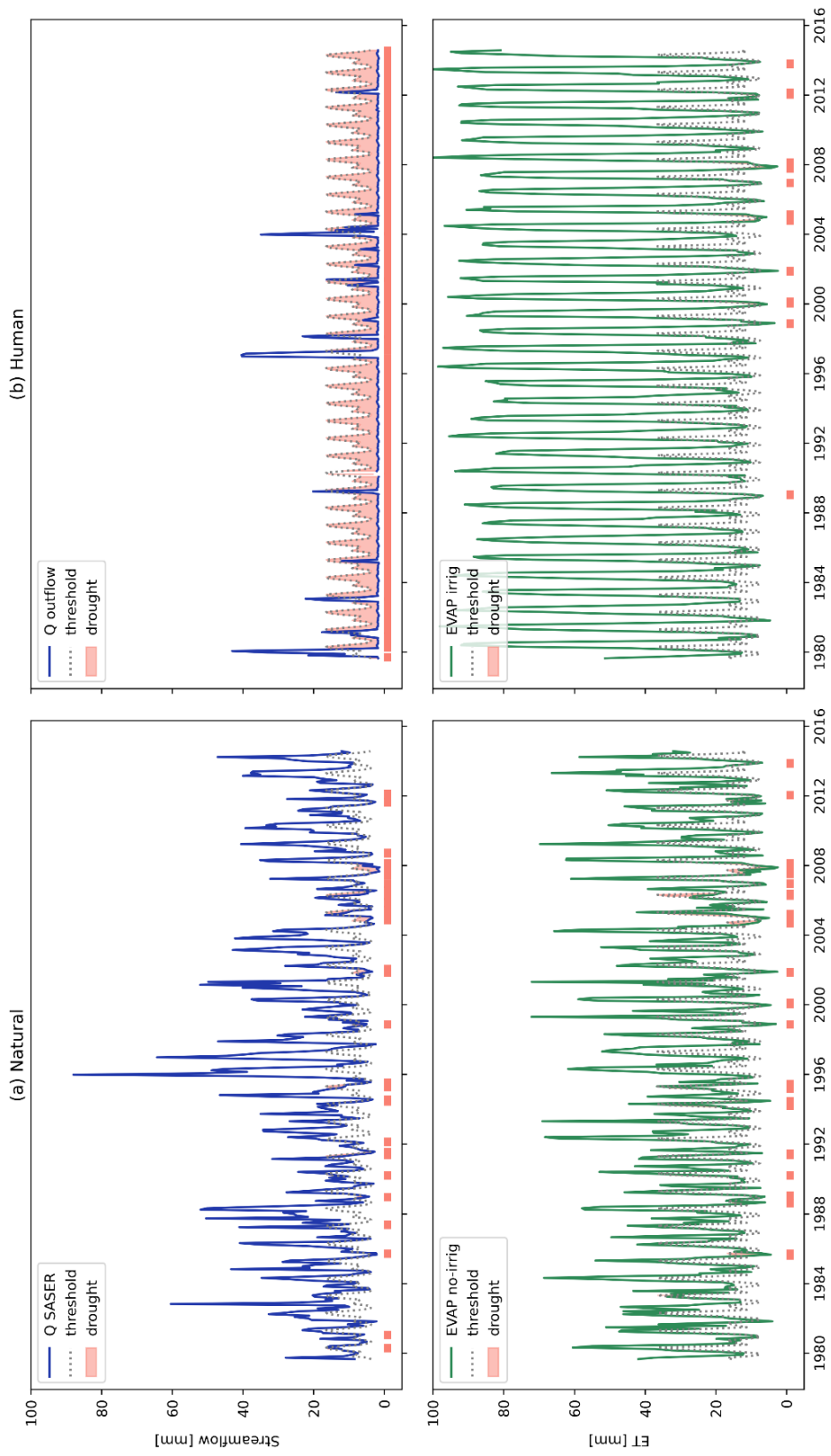


Figure 7-15 Time series comparison for Santa Ana reservoir.

Similar to the Barasona case study, the lower right panel of [Figure 7-15](#) shows the simulated evapotranspiration (ET) associated with irrigation using the SURFEX irrigation module, and demonstrates similar behavior, in both cases the ET increase two times approximately under irrigation scenario (as previously mentioned before, this simulation is not realistic enough, but it makes the qualitative point of showing the dramatic increase of ET allowed by irrigation).

In the absence of human interventions, the natural condition exhibits a clear response of the system to drought events (left panels in [Figure 7-15](#)). This is evident in the propagation of hydrological drought events to evapotranspiration (ET), resulting in negative anomalies in this variable. Thus, drought propagation shows a consistent pattern within the system, as in Barasona, and hydrological drought is related to agronomical drought.

In [Figure 7-16](#), the monthly deficits for the Santa Ana case study are displayed, depicting both natural (upper panels) and human (lower panels) scenarios. Similar to the Barasona case study, it is revealed through the analysis that meteorological drought events occur, which subsequently propagate to impact both streamflow and ET, indicating a strong propagation effect within the hydrological system.

As observed in the Santa Ana case study, a discernible trend of increasing hydrological drought events becomes apparent from the year 2004 onwards. Among these events, the drought episode spanning 2007-2008 stands out as the longest-lasting, persisting for an extensive duration of 10 months (“Q-natural” panel in [Figure 7-16](#)). This particular event has also been documented in the scientific literature, validating the effectiveness of the proposed scheme in identifying and capturing severe drought occurrences in this area.

Furthermore, it is worth highlighting the discrepancy between the deficit events in the ET-natural and Q-Natural. The deficit events recorded in the ET-natural exhibit more pronounced negative values compared to those observed in the Q-Natural (upper panels in [Figure 7-16](#)). This disparity indicates that agronomic drought events, associated with ET, manifest with greater severity in this study case. This insight provides valuable information regarding the vulnerability of the agricultural sector to drought impacts for this study area.

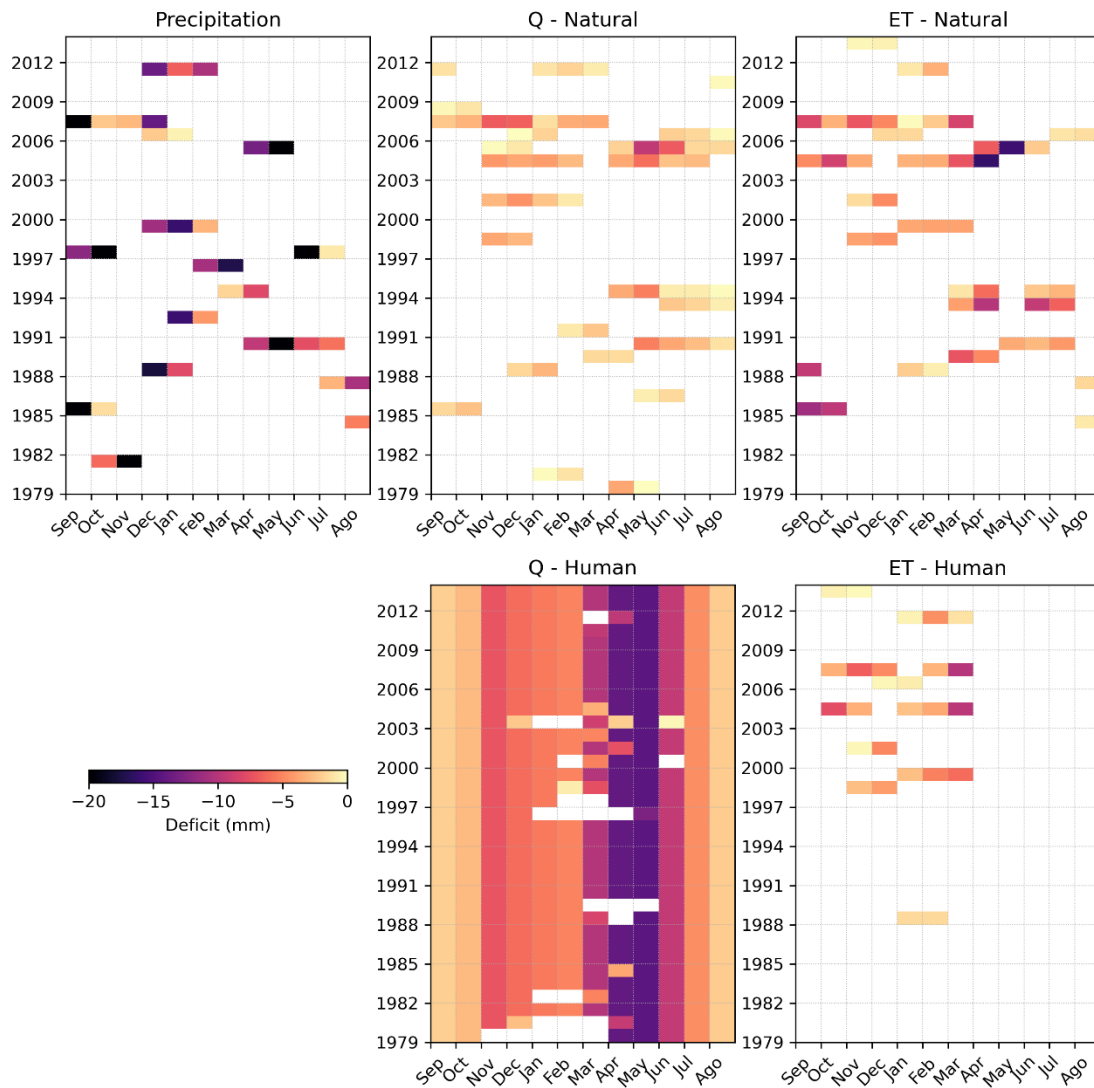


Figure 7-16. Monthly deficits for precipitation, streamflow, and ET for the Santa Ana case study. Upper panels represent the natural situation and lower panels represent the human situation.

Figure 7-16 presents valuable insights into the behavior of the river in the "Q-Human" panel, indicating a sustained and practically continuous deficit in the current state compared to its natural behavior. This persistent hydrological drought can be primarily attributed to the implementation of environmental flows downstream in the reservoir scheme employed, which are set at significantly low levels throughout the period. As a consequence, the deficits in river flow are further intensified, exacerbating the drought effects. Conversely, the "ET-Human" panel illustrates a reduction in ET deficits.

Notably, in the "ET-Human" panel (lower right in Figure 7-16), it is crucial to highlight that during the months when the model initiates irrigation operations (from April to August), no deficit events are observed. This outcome aligns with the primary objective of the reservoir, which aims to ensure sufficient water supply for irrigation purposes. However, it is important to acknowledge that the aforementioned conclusions should be interpreted with caution, as the existing limitations regarding the lack of direct linkage between irrigation and dam operations persist.



Figure 7-17 presents the deficit events resulting from the simulation (S4), where the flows simulated by SASER and the irrigation demands simulated by SURFEX (with variable demands in each year) are used as input data. The visualization of the deficits clearly illustrates the changes that occur throughout the simulation period in comparison with the same panel in Figure 7-16.

Notably, a considerable number of months exhibit no deficits, especially during the winter months, indicating a more favorable water balance during that period. However, as the irrigation season commences in April and May, the values of deficits experience a significant surge. This observation highlights the increased water demand during the irrigation period (values are similar to those reported by the reference data, Figure 7-8 panel b), leading to higher deficits and potential water stress in the system.

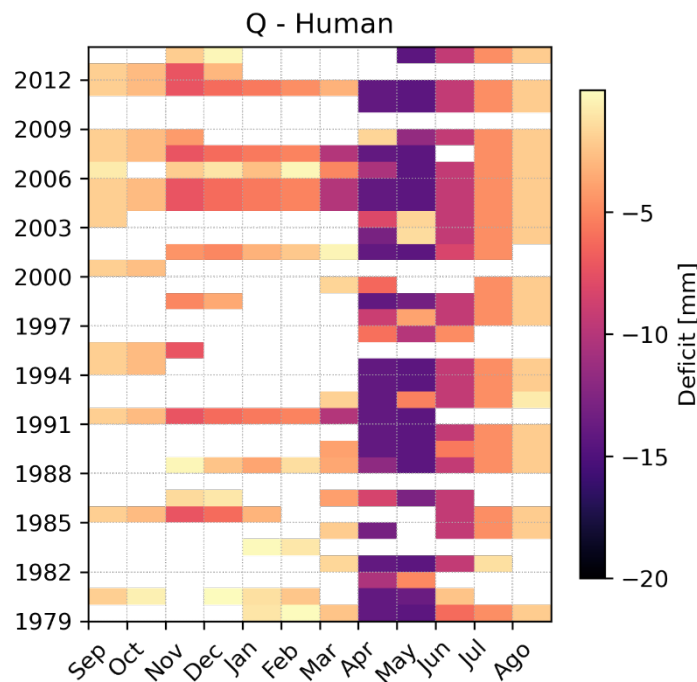


Figure 7-17 Deficits in downstream flow simulated by the reservoir scheme, for the S4 scenario.

#### 7.4.4. Human influence on drought events

The analysis of the time series data clearly demonstrates the significant role played by the reservoirs in regulating the downstream flow of both basins. A visual comparison of the time series, as depicted in Figure 7-12 and Figure 7-15, both reveal distinct patterns and variations between the naturalized and human scenarios. Notably, the impact of drought events is more severe in the human scenario compared to the naturalized conditions, as depicted in Figure 7-13 and Figure 7-16, respectively.

In the human scenario, the presence of reservoirs enables the storage and controlled release downstream. The reservoirs act as buffers, maintaining a more stable water supply during dry periods and supporting various water-dependent sectors, mainly agriculture. The regulated flow from the reservoirs helps to alleviate the impacts of droughts on the agricultural sector, reducing the severity and duration of drought events associated with evapotranspiration, but with a cost on the river itself.

**Table 7-2** reveals a clear and consistent trend of worsening hydrological drought characteristics as a result of anthropogenic influences. For both case studies, drought characteristics are negative, indicating an aggravation of hydrological drought conditions. The findings demonstrate the substantial impact that human activities have on the hydrological system. It is evident that human-induced modifications to the environment and water resources management practices contribute to an exacerbation of hydrological drought.

On the other hand, it is important to note that the impact of human activities on drought is not uniform across all aspects. While hydrological droughts show a worsening trend, the findings also indicate that agronomic droughts, specifically those associated with evapotranspiration (ET), have been ameliorated due to irrigation practices, specifically the frequency of drought events as reported in **Table 7-2**.

Table 7-2 Drought metrics results from naturalized and human-influenced data, respectively.

case study	Natural					Human				
	Freq	mean duration (months)	mean deficit (mm)	max duration (months)	max intensity (mm)	Freq	mean duration (months)	mean deficit (mm)	max duration (months)	max intensity (mm)
<b>Barasona</b>										
<b>Q</b>	20	3.4	9.7	10	37.7	26	12.3	89.0	49	385
<b>ET</b>	20	3.3	11.4	8	28.3	9	3.3	10.7	6	23
<b>Santa Ana</b>										
<b>Q</b>	20	3.4	8.0	10	31.2	9	44.2	294.7	126	852
<b>ET</b>	16	3.4	15.3	9	47.3	9	3.1	10.3	6	28

The total duration of drought events was examined in both natural and human-induced scenarios for the Barasona and Santa Ana case studies. In the natural conditions, the occurrence of drought was relatively consistent between the two case studies. Barasona experienced 67 months of hydrological drought out of a total of 420 months, while agronomic drought was recorded for 65 months. Similarly, Santa Ana recorded 67 months of hydrological drought and 55 months of agronomic drought.

However, when considering the human simulation, a notable shift in the total number of drought months was observed. In both the Barasona and Santa Ana case studies, there was a substantial increase in the duration of hydrological drought, with 321 months and 398 months, respectively. This signifies a significant impact of human activities, such as reservoir regulation and water diversion, on exacerbating hydrological drought conditions. In contrast, the total number of months in agronomic drought decreased to 30 months for Barasona and 28 months for Santa Ana.

**Figure 7-18** presents the boxplots depicting the duration and deficit of drought events for the natural and human-influenced scenarios in both case studies. The analysis of the boxplots reveals distinct patterns in the characteristics of drought for evapotranspiration (ET) and streamflow (Q).

Regarding ET, a noticeable decrease is observed in both the duration and deficit of drought events (green boxes in **Figure 7-18**). This implies that human influences (irrigation practices) have effectively mitigated the severity and duration of agronomic drought (darker green boxes in **Figure 7-18**). The boxplots indicate a shift towards lower values, indicating a (slightly) positive impact on reducing the duration and deficit of drought events associated with ET.

In contrast, for streamflow, the boxplots show a different trend (blue boxes in Figure 7-18). The upper values, represented by the top of the darker blue boxes in Figure 7-18, are significantly higher in both the duration and deficit of drought events due to human activities. This confirms that human influences altered hydrological regimes and thus, contributed to an exacerbation of hydrological droughts, leading to longer durations and greater deficits in streamflow.

Overall, the boxplots provide a visual representation of the contrasting effects of human activities on different aspects of drought. While the changes in ET indicate an improvement in drought characteristics (slightly significant), the boxplots for streamflow highlight the markable adverse impacts of human interventions.

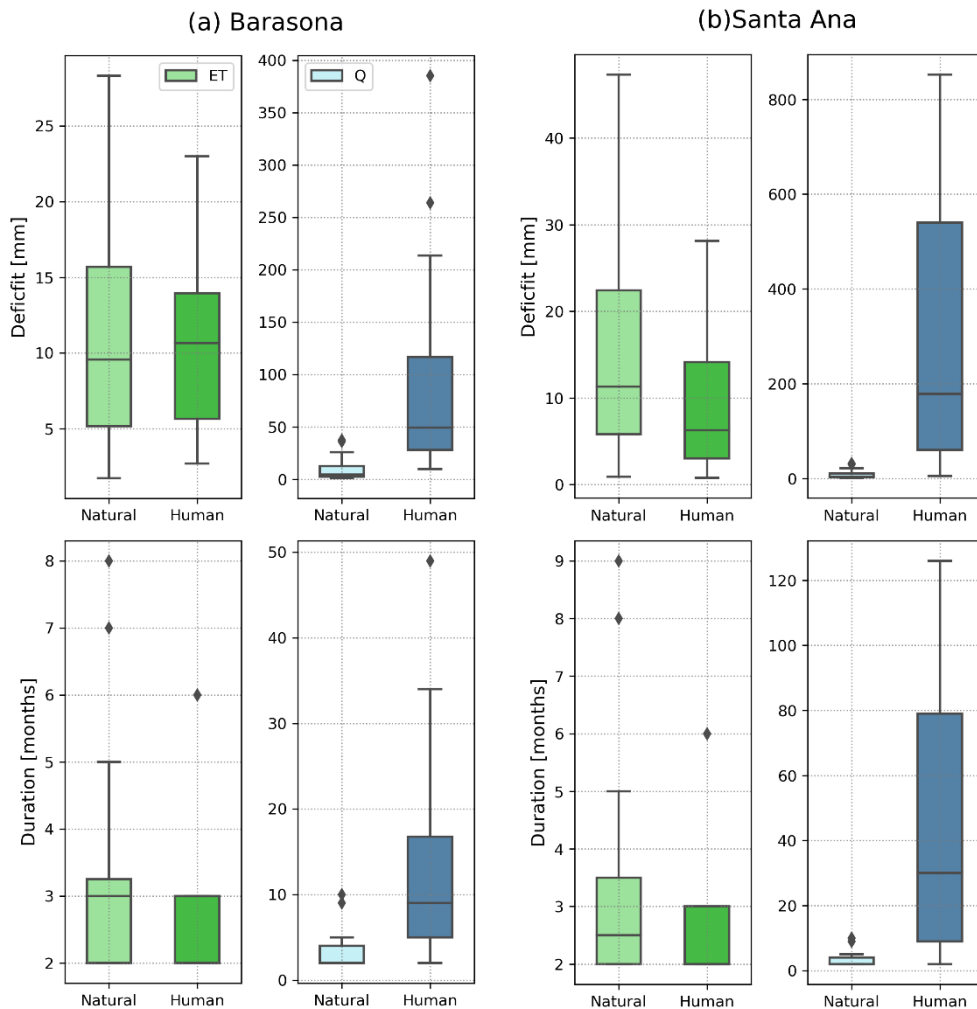


Figure 7-18. Drought boxplot results for natural and human influenced droughts in the (a) Barasona and (b) Santa Ana case studies. The y-axis shows different scales. The horizontal line in each box represents the median, the box represents the interquartile range. The whiskers extend a maximum of 1.5 times the interquartile range.

The influence of human activities on drought characteristics is evident, with a clear and consistent negative trend observed (drought events are aggravated), especially for hydrological drought, while the opposite is true for drought associated with ET, however, it is less notable in comparison with the streamflow.

In human-influenced scenarios, hydrological drought characteristics are notably aggravated, as reported in [Table 7-3](#), with drought durations extending up to 268% and 1220% longer compared to the naturalized scenario, for Barasona and Santa Ana, respectively. Furthermore, the maximum intensity of hydrological droughts increases by up to 922% and 2627%, respectively. It highlights the amplified severity of drought events in the presence of anthropogenic factors.

Table 7-3 Percentage change results from naturalized to human-induced data

	Freq	mean duration	mean deficit	max duration	max intensity
<b>Barasona</b>					
<b>Q</b>	+30%	+268%	+819%	+390%	+922%
<b>ET</b>	-55%	+2%	-6%	-25%	-19%
<b>Santa Ana</b>					
<b>Q</b>	-55%	+1220%	+3572%	+1160%	+2627%
<b>ET</b>	-44%	-10%	-33%	-33%	-41%

In contrast, the agronomical drought (ET) situation has been ameliorated under human influenced scenario ([Table 7-3](#)). All metrics used to measure the severity and duration of agronomic drought consistently demonstrate a decreasing trend, indicating a positive impact on irrigation practices. The mean duration of agronomic droughts has been alleviated in most cases, with only a slight increase of 2% observed in the Barasona case study. Moreover, the frequency of agronomic drought events has shown substantial reductions in both the Barasona and Santa Ana case studies. The frequency has decreased by 55% and 44%, respectively, indicating a significant reduction in the occurrence of drought periods.

## 7.5. Discussion

The development of a comprehensive water management simulation that integrates the reservoir module with SASER results represents a significant advancement in optimizing water resources. While this study focused on simulating the reservoir operations considering only the demand for irrigation as the primary anthropogenic activity, there is a broader potential to expand the model's capabilities. Furthermore, the integration of human-water management into the SASER model would facilitate the assessment of different management scenarios and strategies, allowing for the exploration of trade-offs between various water uses, such as irrigation. This comprehensive approach would enable decision-makers to evaluate the impacts of different policies and interventions on water availability, environmental and socio-economic development.

It is noteworthy that in the context of a cascade of reservoirs (e.g., Santa Ana reservoir), the scheme presented here may implicitly incorporate, to a certain extent, the effects of upstream regulation from the cascade's preceding reservoirs. This is achieved by utilizing the regulated inflow as input for downstream reservoirs, thereby reflecting the regulatory actions taken by the upstream reservoirs. In practice, cascade reservoirs follow interconnected operation rules, especially during the flood season, and exhibit a high level of interdependency. However, the presented scheme does not precisely capture such complex interlinked operations, as it assumes that each reservoir operates independently. Depending on the modeling objective, an alternative may be to aggregate these reservoirs into a single hypothetical reservoir to enhance downstream simulations ([Ehsani et al., 2016](#)). In any case, accurately modeling these systems necessitates

detailed operational considerations, which are challenging to achieve in large-scale hydrological models.

Simulating the Santa Ana reservoir poses unique challenges due to its specific characteristics. Upstream of the reservoir, two reservoirs are primarily utilized for hydroelectric power generation, adding to the system's complexity. The upper panel in [Figure 7-11](#) reveals an interesting observation from the years 1984 to 1995, that suggests observed volume follows distinct management rules, maintaining a nearly constant storage level. Replicating such a situation proves difficult for the model. These findings highlight the model's robustness in replicating the storage and release dynamics, particularly to the Santa Ana reservoir.

Another potential source of uncertainty in reservoir operations is attributed to temporal changes in demand resulting from increasing needs for irrigation, power generation, water supply, and other purposes. Moreover, the intended purpose of a reservoir can also undergo modifications, such as enlarging the reservoir, or the addition of a hydropower station to an initially designated irrigation dam. The scheme, as developed and implemented here, implicitly incorporates these changes through the utilization of storage and release time series.

The results of this research highlight the complexity and challenges involved in accurately simulating reservoir operations, particularly when considering the intricate dynamics of multiple reservoirs and subjectivity in the irrigation demands. Future research efforts should focus on improving not only the reservoir operation schemes but also the model's representation of agricultural practices, local conditions, and other factors that influence water management. By enhancing the model's capabilities, these kinds of models can help policymakers and water managers to make more informed decisions regarding water allocation and resource management.

By incorporating environmental flow considerations into the reservoir management strategy presented here, it acknowledges the interconnectedness between the reservoir operation and the downstream ecosystem dynamics. Hence, becomes a critical factor in shaping the downstream conditions. Environmental flows are the water allocations within a river system that aim to maintain the ecological integrity and functions of the aquatic ecosystem. At the same time, ensuring an adequate water supply for agricultural activities is crucial for sustaining food production and supporting rural livelihoods. Thus, achieving harmonious balanced environmental flows requires a thorough understanding of the hydrological, ecological, and socio-economic dynamics of the region, which represents a complex challenge in water resource management and in the case of the model presented here, resulted in significant results discrepancies when it environmental flows change into the simulation.

Balancing the ecological and agricultural aspects to establish environmental flows requires a nuanced approach that considers the specific characteristics of each river system and the associated ecosystems. Collaborative approaches that involve water managers, ecologists, agricultural experts, and local communities are vital for defining environmental flow regimes. Moreover, incorporating tools like remote sensing, data analytics, and hydrological modeling can enhance the understanding of water availability and thus environmental flow definition.

Human activities exacerbate drought conditions, leading to a decrease in water availability and prolonged drought periods compared to the natural state. Additionally, the presence of reservoirs has been found to contribute to the aggravation of streamflow drought downstream ([Firoz et al., 2018](#); [Tijdeman et al., 2018](#); [Van Loon et al., 2022](#)). However, it is important to consider a comprehensive evaluation of the various variables involved in the hydrological cycle, rather than

solely focusing on the negative impacts attributed to dams. It should be noted that reservoirs also have positive effects on certain aspects, such as downstream evapotranspiration (ET) and agriculture productivity. Therefore, to gain a comprehensive understanding of the overall impact of reservoirs on drought, it is necessary to conduct an integrated assessment that takes into account the diverse factors influencing the hydrological cycle, rather than solely emphasizing the negative consequences produced by reservoirs.

However, it is important to acknowledge that developing such a complete water management simulation is a challenging assignment that requires further research and data integration. Data availability, model calibration, and uncertainty quantification are challenges that need to be addressed to ensure the reliability and accuracy of the simulation results. Moreover, collaborative efforts involving stakeholders, researchers, and policymakers are crucial in advancing toward a comprehensive water management framework that optimizes water resources in the region.

An important aspect of our future work lies in the integration of the reservoir management module presented in this study into the SASER modeling chain. The integration of the reservoir management module holds significant potential for enhancing the representation of fluxes in the hydrometeorological chain of SASER within a coupled human system. By incorporating this module, our objective is to achieve a more comprehensive and integrated approach to water resources management. This integration will enable us to simulate and optimize reservoir operations more accurately and realistically.

Moreover, the incorporation of a fully coupled model that enables bidirectional coupling between the irrigation scheme and dam operation would greatly enhance and advance the analysis presented in this study. Such a model would provide a more holistic approach to investigating the intricate interactions between irrigation practices, reservoir operations, and their impact on the hydrological system. This would enable a more accurate representation of the complex feedback mechanisms between human water-land activities and the hydrological cycle. Furthermore, the bidirectional coupling would provide a more realistic assessment of the dynamic changes in water availability and demand under varying climatic and operational conditions. Thus, the development of a fully coupled model represents a promising avenue for future research in this field.

## **7.6. Conclusions**

A framework has been developed to assess the impact of human activities on agricultural and hydrological droughts in a Mediterranean catchment by incorporating evapotranspiration processes associated with irrigation. This framework represents an important step forward in understanding the complex interactions between human activities and drought dynamics in this region. Thus, a reservoir operation scheme as an external module, which allows for a flexible approach (rapid iteration process), was implemented in this research. The reservoir model showed good performance, considering the model's simplifications.

In general, the findings of this research demonstrate favorable agreement for the Barasona case study in terms of both the model-estimated irrigation demand and reservoir operation scheme. However, further investigations and refinement are required for the Santa Ana case study in both models.

The utilization of the estimated demand by SURFEX offers a notable advantage due to its capacity to capture interannual variability. By accommodating year-to-year fluctuations in demand instead of relying on fixed values, this dynamic approach provides a more realistic representation of the system. It also enhances the temporal variations in water demand, enabling more accurate assessments.

The evaluation of the new module, simulating human-water management in different scenarios, was conducted using the performance metric KGE. The results indicate a good agreement, particularly for the Barasona reservoir, which consistently reported higher KGE values across the various scenarios. The KGE values for outflows averaged around 0.75, while Santa Ana exhibited lower values. Overall, these results demonstrate the capability of the reservoir operation module to simulate storage and outflows reasonably well in both case studies.

The threshold level method proved to be an effective approach for accurately capturing and identifying drought events in a human-natural system, allowing to compare the natural and the human scenarios. Under natural conditions, the system responded to meteorological drought events by propagating to hydrological and agronomical droughts, revealing strong propagation effects within the hydrological system. Conversely, in a human-influenced scenario, the presence of the downstream reservoir induced streamflow deficits, exacerbating the hydrological drought situation. However, this was accompanied by reduced evapotranspiration deficits.

Human influences, compared to naturalized conditions, led to longer hydrological drought characteristics in both case studies, with mean deficits reaching values up to +819%. Additionally, the time of the year of higher hydrological drought events shifted in response to human influences. In contrast, the human-influenced scenario alleviated agronomical drought situations, with a decrease in the frequency of events by -55% and -44% for Barasona and Santa Ana, respectively. However, the remaining agronomical drought characteristics exhibited fewer notable effects compared to hydrological drought.

The impact of irrigation on drought conditions, both hydrological and agronomical, was evident in both basins. These findings highlight the importance of considering human influences and irrigation practices in drought assessment and management strategies.

---

## 8. Conclusions and further work

In this last chapter, the conclusions of the research will be presented. It begins with a concise summary of the scientific framework, followed by the main conclusions derived from this research, providing a comprehensive overview of the findings. Finally, an overview of the implications will be provided, along with recommendations and potential areas for future research.

The main objective of this thesis has been to improve the performance of the SASER hydrological framework and to enhance the comprehension of drought, including the underlying processes, within the context of Spain. This was achieved by employing physics-based modeling with a particular focus on the influence of anthropogenic activities. This aim was achieved by the following steps:

- The enhancement of the representation of temporal precipitation patterns in the SAFRAN forcing dataset, used by the SURFEX model within the SASER framework, and thereby striving for a more realistic simulation of hydrological processes (Chapter 5).
  - The improvement of the hydrologic response, particularly the simulation of low flows, in the SASER hydrometeorological model (Chapter 6).
  - The simulation of reservoirs, as a first step for a future inclusion within the SASER modeling chain, evaluates the impact of water management practices on (anthropic) drought dynamics (Chapter 7).
-



## 8.1. Scientific framework synthesis

The modeling of the hydrological cycle in several domains over Spain and southern France has been carried out in this research by utilizing the SASER hydrometeorological model, which integrates the SURFEX Land Surface Model. The LSM models are being widely used in the hydrology field. Hence, in Chapter 2 a comprehensive overview of the existing knowledge and research and current challenges regarding the use of LSM to represent the hydrological processes and their application to drought studies are presented.

Chapter 3 provides an in-depth description of the study area, encompassing various domains situated between Spain and France, with a focus on the Pyrenean region. Furthermore, Chapter 4 outlines the methodology employed in this research, elucidating the approach taken to investigate the research objectives.

In Chapter 5, the objective was to enhance the hydrological impact of SAFRAN hourly precipitation distribution on SURFEX LSM simulations. A correction method was employed to adjust the SAFRAN distribution using a more realistic distribution derived from a regional climate model simulation forced by ERA-Interim (CNRM-ALADIN). Evaluation of the correction method was conducted across different time windows to identify the optimal performance and determine the most effective correction time windows.

Chapter 6 outlines the efforts undertaken to improve hydrologic modeling in the SASER model. The initial focus was on enhancing the simulation of the hydrological response of both low and high flow simultaneously (section 6.2). This involved calibrating the internal parameter controlling runoff generation and exploring the possibility of a distributed calibration based on physical variables. Additionally, efforts were made to enhance the physiographic information utilized in the model.

In the subsequent phase, section 6.3 presents an improvement of the SASER modeling chain through the introduction of a conceptual reservoir to improve the representation of the slow component (drainage) in the hydrological response. The conceptual reservoir introduced two new empirical parameters. The parameter values were determined on a catchment-by-catchment basis through calibration against daily observed data. Furthermore, a regionalization approach was employed, linking physiographic information to reservoir parameters using linear equations optimized with a genetic algorithm. The regionalization approach proved valuable for determining the new empirical reservoir parameters in basins where traditional calibration methods were not feasible, such as ungauged or human-influenced basins.

Finally, in Chapter 7, the focus shifted to a heavily irrigated area located in the Ebro river basin, northeast of the Iberian Peninsula, specifically the Canal of Aragon and Catalonia (CAyC) district supplied by a reservoir system. In this case study, a simple water management model was implemented, based on the WAAPA model, to simulate reservoir operations under a human-influenced scenario. This simulation was compared against naturalized variables obtained from the default SASER simulation, allowing an examination of the contribution of human activities, including irrigation and reservoir regulation, to the water budget and propagation of drought.

## 8.2. Conclusions

In this research, different approaches have been integrated with the aim of improving the representation of the hydrological processes underlying drought within an LSM model. Furthermore, a module has been developed to incorporate the human factor into the hydrological simulation chain of the current SASER model. The main results are summarized in the following paragraphs.

The novel linear correction method improves the accuracy of precipitation intensities by leveraging regional climate model (RCM) data. The improved precipitation dataset, derived from the SAFRAN meteorological forcing data, provides a better representation of precipitation statistics in the Ebro basin, especially in Mediterranean-dominated areas, compared to the original SAFRAN data. As the number and the resolution and quality of RCM simulations with hourly outputs increase, these kinds of approaches can be used to compensate for the limitations of observations-based interpolation methods such as SAFRAN. Similar approaches can be used to improve other aspects of observational forcing datasets, for example, the improvement of precipitation over the highest relief, where observations are scarce and not very representative.

The effectiveness of the precipitation correction method was demonstrated through the implementation of a weekly time step. Significant improvements in precipitation statistics were achieved by leveraging data from the regional climate model CNRM-ALADIN, allowing for the adjustment of the hourly precipitation distribution of SAFRAN and the attainment of more reliable and representative results. The use of a weekly window to apply the corrections allowed for better capture of the temporal variability and patterns in precipitation, leading to a more realistic depiction of precipitation events (in statistical terms). The impact of simulation forced by the improved precipitation on simulated runoff, at the grid point scale, was evident and aligned with our expectations. However, interpreting the changes in drainage and evapotranspiration was more complex due to various factors, including climate regime and the higher response to drainage in wet climates. At the watershed scale, the overall water balance, represented by the sum of runoff, drainage, and evaporation, was only minimally affected.

The new precipitation dataset provides valuable insights into the impact of intense precipitation events on hydrological simulations, enabling a more detailed understanding of the mechanisms driving runoff generation during extreme weather events, which is vital for effective water resources management.

Achieving an accurate calibration of the runoff parameter and improving the soil database information in the SURFEX model proved to be a challenging task, demanding both meticulous calibration procedures and extensive computational resources. Despite the limitations imposed by these complexities, our findings indicate that, in our area of study, the default value of the *runoff b* parameter satisfactorily captures the mechanisms governing runoff generation within the model. This implies that the default setting offers a reliable representation of the hydrological processes under consideration.

The default SASER model exhibited a significant negative bias in low flow indices. However, the introduction of a reservoir scheme to regulate drainage and thus, improve the slow component of streamflow, demonstrated positive outcomes in terms of KGE values. The inclusion of the conceptual reservoir proved to be a straightforward and efficient approach, requiring only a

limited number of parameters. It effectively improved the simulation of low flows in SURFEX without compromising high flows.

The regionalization approach was made feasible by the simplicity of the conceptual model and its implementation as an external module of SURFEX. It allows the establishment of a relationship between the parameters of the conceptual reservoir and climate and physiographic variables through the genetic algorithm. This enabled the consideration of within-catchment variability throughout the study area. Although the reservoir approach lacks a physical basis, it successfully links the two new parameters with physical variables, striking a favorable compromise for a model striving to be both distributed and physically representative. Additionally, the regionalization approach allowed for the application of the reservoir across the entire domain, encompassing both natural and human-influenced basins, thereby enhancing its utility beyond natural systems.

An approach that accurately captures drought dynamics has been achieved by incorporating a reservoir simulation scheme and utilizing the SURFEX irrigation scheme. This provides valuable insights into the impact of human activities on agricultural and hydrological droughts in a Mediterranean catchment.

The implementation of a reservoir operation scheme as an external module in the SASER modeling chain has shown good streamflow performance in a human-natural system, for both study cases, despite its simplifications. Nevertheless, the Barasona case study demonstrated better agreement in both the model-estimated irrigation demand and reservoir operation scheme, highlighting the potential application of this scheme. However, further investigations and refinements are needed for the Santa Ana case study.

The utilization of SURFEX's irrigation scheme has proved advantageous due to its ability to capture interannual variability in water demand. Therefore, the framework proposed in this research provides a more realistic representation of the system, enhancing accuracy in assessments. The evaluation of the new module showed good agreement against reference data, particularly for the Barasona case study, indicating its capability to simulate storage and outflows effectively.

Under natural conditions, meteorological drought events propagated to hydrological and agronomical droughts, demonstrating strong propagation effects in both case studies. In a human-influenced scenario, the presence of a downstream reservoir exacerbated hydrological drought by inducing streamflow deficits, although it reduced evapotranspiration deficits, and hence, alleviated the agronomical drought.

Human influences resulted in longer hydrological drought characteristics in the case studies presented here, with significant shifts in the time of the year of higher hydrological drought events. Conversely, agronomical drought situations were alleviated to some extent in the human-influenced scenario. The impact of irrigation on both hydrological and agronomical droughts was evident in the basins, emphasizing the importance of considering human influences and irrigation practices in drought assessment and management strategies. Finally, it is noteworthy these findings contribute to a better understanding of the complex interactions between human activities, water resources, and drought dynamics.

---

### 8.3. Implications and recommendations

This research mainly aimed to develop modeling tools that integrate a more accurate representation of natural processes and incorporate human water management practices for the comprehensive study of drought. Consequently, the main scientific implication of this research is to foster a holistic understanding of drought in coupled natural-human systems.

The enhancement of hydrological process representation in Land Surface Models (LSMs), as demonstrated in this study, yields valuable insights into the intricate interactions among various variables within a human-influenced hydrological cycle. This improvement holds particular importance for the Iberian Peninsula, and specifically the Ebro basin, which is known for its susceptibility to drought.

An important outcome of this research is the necessity to balance the trade-off between complexity and parsimony in LSMs to be useful tools for simulating a wide range of land surface processes and future scenarios. On the one hand, the models must be complex enough to represent the heterogeneity and complexity of the real world, including interactions between land, atmosphere, and hydrology in coupled natural-human systems, as well as the inherent feedback and uncertainties associated with these processes. On the other hand, the models must be parsimonious enough to be computationally efficient, flexible, and applicable across various spatial and temporal scales and scenarios.

This trade-off creates several limitations in LSMs that need to be acknowledged and addressed. One limitation is that LSMs may oversimplify some processes or neglect important feedback, leading to biases and inaccuracies in model simulations. Another limitation is that LSMs may require extensive calibration and parameterization, which can introduce uncertainties and limit their transferability to other regions or scenarios. Additionally, the trade-off between complexity and parsimony may limit the ability of LSMs to represent new or emerging processes, land use changes, or extreme events that fall outside the range of conditions for which the model was designed.

While acknowledging that the methodology proposed in section 6.3 to enhance the simulation of low flows in LSMs lacks a physical basis, it successfully links the two new parameters with physical variables, striking a favorable compromise for a model striving to be both distributed and physically representative.

Furthermore, it is crucial to identify and prioritize the critical processes and drivers of change that necessitate representation or inclusion in the LSMs. This includes obtaining improved and higher-quality forcing data, as discussed in Chapter 5, which serves as another fundamental component for achieving a more accurate hydrological response in these models. Nevertheless, caution should be exercised when utilizing these forcings, particularly in areas characterized by high precipitation variability, both in terms of spatial distribution and temporal patterns, such as mountainous regions. Thus, detailed validation processes should be conducted, and uncertainties associated with the forcing data should be carefully considered.

Given the complex nature of LSMs and their broad implications for understanding and managing drought, interdisciplinary collaboration is crucial. Therefore, to address the practical challenges associated with water management and decision-making, active engagement with stakeholders is paramount. This includes involving experts from fields such as ecology, meteorology, and remote

sensing, along with water managers, policymakers, and other decision-makers throughout the research process. By incorporating their insights, needs, and perspectives, the resulting LSMs can be more relevant and useful for real-world applications.

The outcomes of this research extend beyond the scope of drought analysis. While Chapter 7 did not explicitly target water management, the outcomes hold substantial relevance for water managers, contributing to valuable insights. Therefore, the framework proposed in this study offers water managers a robust tool for formulating and evaluating water and drought management policies, particularly in the context of agricultural use.

Although the focus of this approach was primarily on assessing the impact of reservoir construction and irrigation on drought dynamics, its application can be extended to other human activities, such as land use change or groundwater extraction, provided that reliable data and an appropriate model capable of simulating the associated human influence are available. By employing this approach, a comprehensive understanding of the effects of diverse human activities on hydrological systems can be obtained, assisting in decision-making processes and enabling the implementation of effective drought management strategies.

Finally, it is worth noting that while indices serve as a convenient approach to assess drought, caution must be exercised when evaluating the influence of human activities, also known as anthropogenic drought. Given the complexity of drought phenomena, relying solely on indices may not capture the full range of causal mechanisms, particularly within natural-human systems. Hence, it is highly recommended to complement the use of indices with robust modeling tools to obtain a more comprehensive understanding. The foremost recommendation is to integrate modeling tools alongside drought indices, as this combination enables a more nuanced analysis of drought dynamics, especially within the context of natural-human interactions.

By employing modeling tools, a deeper understanding of the various causal mechanisms behind drought can be attained, facilitating more informed decision-making processes. Moreover, modeling tools provide the flexibility to account for the intricate complexities inherent in natural-human systems, enhancing the accuracy and reliability of drought assessments. Alternatively, the variable threshold method (discussed in section 7.4) offers a viable alternative to traditional indices. This approach proves particularly valuable for water resources management and planning fields.

## **8.4. Perspectives and further research**

Although the methodologies gathered and utilized in this research have varying applications, their collective aim remains shared: to enhance the modeling of land surface hydrological processes. To make further progress in refining these models, it is imperative to explore different perspectives regarding the respective processes involved.

Moving forward, there are several avenues for further progress in the use of LSMs for drought studies. First and foremost, there is a need to enhance the representation of key hydrological processes within these models. This includes improving the representation of soil moisture dynamics, vegetation dynamics, and groundwater interactions, to name a few. By refining the process-level understanding and incorporating more accurate representations of these processes,

LSMs can provide more reliable and robust simulations of hydrological response and thus drought onset, severity, and duration.

Advancements in computing power and data availability open up new possibilities for the use of artificial intelligence (AI) and machine learning (ML) techniques in drought studies. Machine learning algorithms can assist in pattern recognition, feature extraction, and data assimilation, enabling LSMs to learn from historical observations and improve their predictive capabilities. Leveraging big data sources, such as global climate and hydrological databases, can further enhance our understanding of drought patterns and their underlying drivers. Therefore, an interesting area is the application of AI and ML to calibrate some internal parameters to improve the representation of hydrological processes in physically-based models, such as SURFEX-LSM.

Furthermore, incorporating the influence of human activities on drought dynamics represents a crucial frontier in LSM research. Anthropogenic factors, such as irrigation practices, water management policies, and land use changes, can significantly alter the hydrological cycle and exacerbate or mitigate drought impacts. Furthermore, integrating human-induced modifications into LSMs can provide a more comprehensive understanding of drought processes and facilitate better-informed decision-making in water resources management and drought mitigation strategies. Hence, future research efforts could focus on the development of a bidirectionally coupled model to simulate human activities, specifically reservoir management, and irrigation. And therefore, developing a fully coupled model that integrates the improvement of hydrological response and the land-water management in the SASER model is a potential interest area.

In the context of future research, the possibility of conducting a comprehensive comparative analysis of various modeling strategies in the field of land surface modeling and water management is being considered. This analysis aims to highlight the strengths, weaknesses, and nuances of the various approaches utilized.

In addition, immense potential lies in the application of this fully coupled model for the creation of effective strategies in water resources management. Valuable insights might be gained through the utilization of this framework, facilitating the optimization of water allocation, ensuring the sustainability of water usage, and addressing the challenges posed by water scarcity and the ever-changing climate conditions. By employing the fully coupled model, various management scenarios can be explored by water resource managers, allowing for the evaluation of their impacts on water availability. Through the consideration of the dynamic feedback between human actions and hydrological responses, decision-makers can devise robust strategies that effectively balance competing demands, minimize conflicts, and foster water security.

Finally, advancing the integration of remote sensing data and satellite observations into LSMs holds immense potential for improving drought monitoring and especially drought forecasting. Remote sensing provides valuable information on key variables such as soil moisture, vegetation, and evapotranspiration, which are critical for assessing drought conditions, particularly in semiarid environments where these variables play an essential role in the development of drought. The accuracy and spatial resolution of drought monitoring systems can be improved by assimilating these observations into LSMs, enabling more timely and precise assessments of drought conditions at various scales. Therefore, an intriguing area to explore is the application of the research outcomes in drought forecasting, including future scenarios.



---

# Appendix A. Attempts to improve internal model parameters of the SASER model

## A.1. Runoff generation scheme

### A.1.1. Background

The SASER suite incorporates the Land Surface Model, SURFEX, which plays a crucial role in estimating the catchment's water balance. Within the SURFEX model, the simulation of surface runoff is carried out using the saturation excess mechanism, commonly known as the Dune mechanism. According to this mechanism, runoff occurs only when precipitation exceeds the soil's saturation capacity. However, this poses a challenge at the scale considered in the SASER suite, as the variability of runoff production is smaller than the typical size of the grid cell (2.5 x 2.5 km).

Consequently, when the ISBA model is run at these lower resolutions, the soil seldom reaches saturation, leading to minimal or no runoff production. To address this limitation, Habets et al. (1999) introduced the Variable Infiltration Capacity (VIC) scheme, as described by DÜMENIL & TODINI (1992) and Wood et al. (1992). The VIC scheme takes into account the subgrid variability by considering the fraction of the grid cell that is saturated. This fraction depends on various soil parameters, the soil water content of the root zone ( $w_2$ ), and a new parameter denoted as "b", which represents the shape of the heterogeneity distribution of effective soil moisture capacity (see Figure A 1-1).

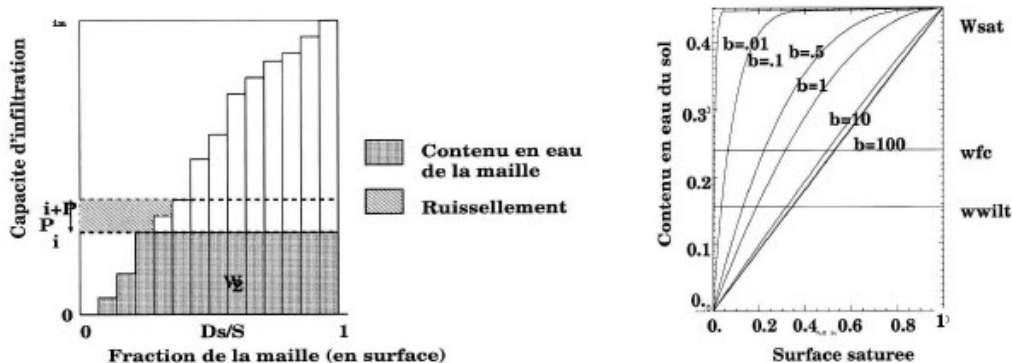


Figure A 1-1 Scheme of the variable infiltration model at sub-grid runoff. The right panel shows the variation of the saturated proportion of the grid cell to different values of the parameter  $b$ .

In this empirical approach, determining the optimal value for the shape parameter ( $b$ ) poses a significant challenge since it cannot be obtained in advance or through direct measurement. This parameter selection is a crucial aspect that requires careful consideration and calibration to ensure an accurate representation of the sub-grid variability. Therefore, in the VIC scheme, finding an

---



appropriate value for the shape parameter is a key task, as it directly impacts the simulation outcomes

This parameter,  $b$ , is a dimensionless value that represents the proportion of precipitation that flows over the surface of the catchment as runoff, rather than infiltrating into the soil (Figure A 1-1). The value of the coefficient of runoff is determined by several factors, including the type of vegetation cover, the soil type, and the topography of the catchment. For example, catchments with dense vegetation cover and permeable soils tend to have lower coefficients of runoff, while catchments with sparse vegetation and impermeable soils tend to have higher coefficients of runoff. The topography of the catchments is another important factor that affects the parameter  $b$ . Catchments with steep slopes tend to have higher coefficients of runoff, as the steep slopes increase the rate of runoff and reduce the amount of time that the precipitation is in contact with the soil, allowing it to infiltrate. In contrast, catchments with gentle slopes tend to have lower coefficients of runoff, as the precipitation has more time to infiltrate into the soil.

### A.1.2. Calibration of the parameter $b$

To calibrate the parameter governing runoff generation (referred to as runoff  $b$ ), a series of simulations were conducted. The objective was to investigate the impact of different values of this parameter on the model's performance in representing the runoff processes.

However, it is worth noting that the SURFEX model used in this study imposes certain computational constraints due to its high computational cost. The extensive computations required by the model demand significant computational resources and execution time. Given these limitations, a total of eight simulations were performed to cover a range of parameter values. These values were carefully selected based on a previous study by Quintana Seguí et al. (2009) that explored similar ranges of parameter values. The chosen parameter values for the simulations were  $b = (0.01, 0.1, 0.2, 0.3, 0.4, 0.5, 1.0, \text{ and } 5.0)$ . Figure A 1-2 illustrates the histogram displaying KGE values obtained from the 8 simulations conducted.

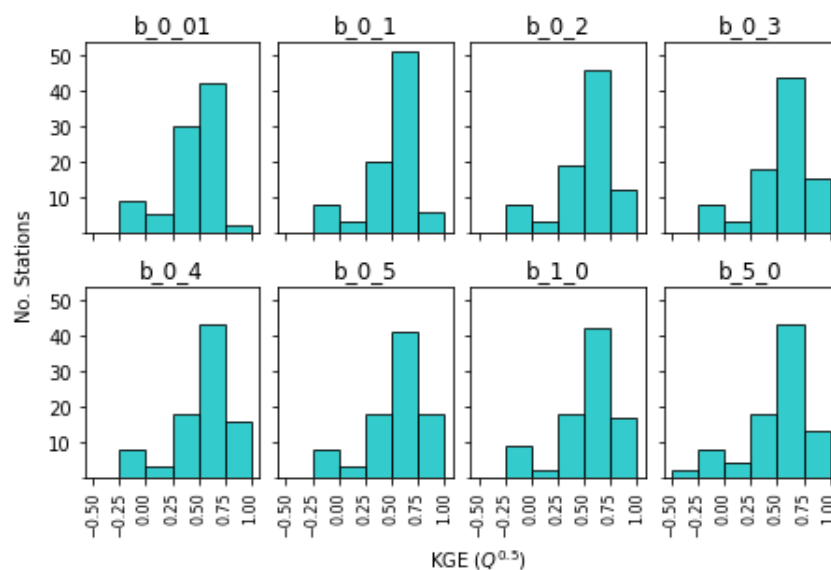


Figure A 1-2 Histograms of the KGE calculated on root-squared transformed discharge for the different simulations

Although a more extensive range of parameter values would have been desirable, the selected range was deemed representative of the plausible values for the specific study area and research objectives. These values aimed to capture a spectrum of runoff characteristics. Despite the limited number of simulations, this approach provided valuable insights into the relationship between the parameter controlling runoff generation and the model's ability to accurately represent runoff processes.

On the other hand, to further investigate the relationship between Indice de Développement et Persistance des Réseaux (IDPR, [Mardhel et al. \(2021\)](#)) and the runoff parameter ( $b$ ), a thorough analysis was conducted by classifying the selected stations based on the specific value of the runoff parameter that resulted in the highest KGE value. This classification, represented in [Figure A 1-3](#), provides valuable insights into the distribution of stations across different runoff parameter ranges.

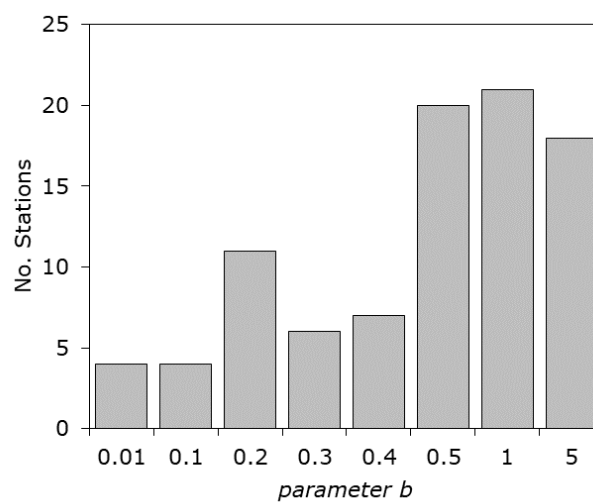


Figure A 1-3 Histogram of the selected stations with KGE values above -0.5, to each B value

The findings imply that the default value results in several stations that showcase higher agreement between observed and simulated daily streamflow, as indicated by their relatively higher KGE values. This suggests that selecting a value within the range of 0.5 to 1 for the runoff parameter can yield more accurate and reliable simulations of daily streamflow.

After evaluating various parameter values for the runoff parameter ( $b$ ), it was found that the default value provided the best-fit metrics. Subsequently, the monthly flows of the Ebro-Tortosa station were compared with the SIMPA reference model. Once again, it was observed that a value of  $b=0.5$  resulted in the highest Kling-Gupta Efficiency (KGE) values and exhibited a strong correlation with the reference model, [Figure A 1-4](#).

These findings further reinforce the appropriateness of the default value of the runoff parameter for the study area. The consistent performance of the default value in terms of KGE and correlation with the SIMPA model supports its suitability for accurately representing the monthly flow dynamics at the Ebro-Tortosa station.

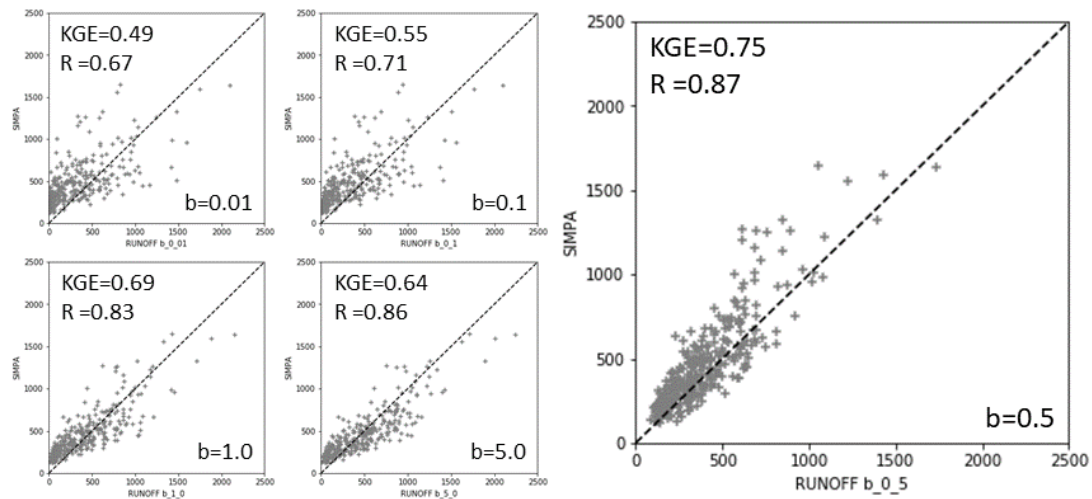


Figure A 1-4 Comparison between the SIMPA (reference) model and the SASER model for the Ebro-Tortosa station.

By demonstrating the compatibility of the default parameter value with an established reference model, this analysis affirms the reliability and robustness of the default setting within the context of the study area. This provides confidence in the application of the default value of the runoff parameter in future modeling studies and reinforces its adequacy for representing the hydrological behavior of the study area.

### A.1.3. Finding a relationship between runoff $b$ and IDPR

The Indice de Développement et Persistance des Reseaux (IDPR, [Mardhel et al. \(2021\)](#)) is a metric used in hydrology and water resources management, particularly in the context of studying and analyzing river networks. It is a measure that assesses the development and persistence of river networks over time. The IDPR is typically calculated based on various characteristics of the river network, such as the length of the main channel, the total length of tributaries, and the number of loops or bifurcations in the network.

The IDPR is often used to evaluate the connectivity and overall functioning of river systems. It provides insights into the network's complexity, stability, and ability to maintain water flow and transport processes. High IDPR values indicate a well-developed and persistent river network with interconnected channels, while low values suggest a less developed or fragmented network ([Figure A 1-5](#)). Overall, the IDPR serves as a useful tool for understanding the structural properties of river networks and their implications for hydrological processes.

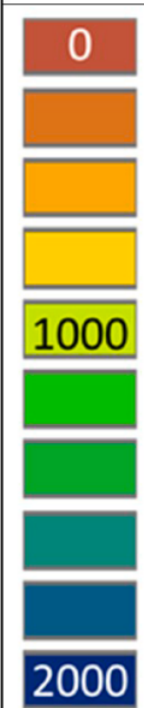
IDPR		Interpretation	
 0	< 1000	Primarily Infiltration rather than surface runoff	There is non-conformity between the availability of drainage axes linked to thalwegs and observed hydrologic axes. Runoff on natural terrain joins a drainage axis defined by thalweg analysis without showing a concrete expression of a natural hydrologic axis. Development of a thalweg network of higher density than the expression of the natural drainage network.
	= 1000	Infiltration and surface runoff of equal importance	There is conformity between the availability of drainage axes linked to thalweg and in-place flows.
1000	> 1000	Primarily surface runoff as compared to infiltration toward the subsurface.	Runoff on natural terrain rapidly joins a natural hydrologic axis without its presence being directly justified by a thalweg.
	> 2000	Primarily comparable to a wet environment.	Transitory or permanent water stagnation, which leads to two different interpretations. If the water-bearing layer is near the natural ground surface (watercourses and humid zones), the land is saturated and water will not infiltrate. If the waterbearing layer is deep, the flowing nature may demonstrate impermeability of natural terrain. We offer the hypothesis that IDPR values higher than 2000 are primarily applicable to wet environments (possibility of flooding by the hydraulic barrier effect).
2000			

Figure A 1-5 IDPR table's guide (Mardhel et al., 2021).

The scatter plot presented in [Figure A 1-6](#) depicts the relationship between the median value of the Network Development and Persistence Index (IDPR) for each watershed and the corresponding value of the runoff parameter ( $b$ ). Despite careful examination, no significant correlation or discernible pattern was observed between these variables.

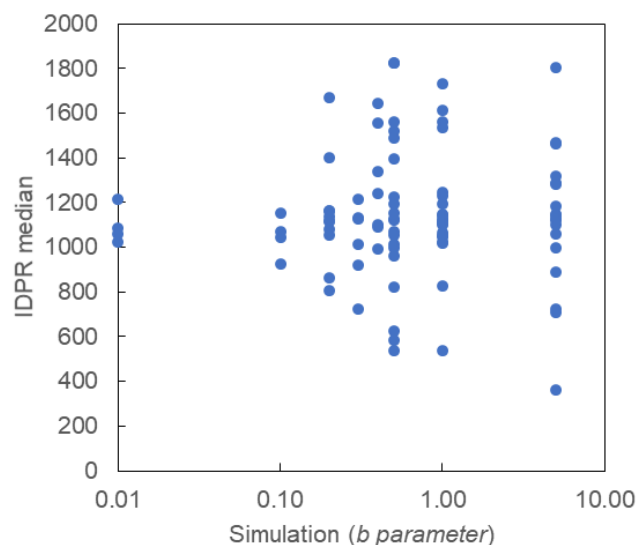


Figure A 1-6 Relationship between the median IPDR value and the *runoff b* parameter. Each data point represents a catchment selected as near-natural or natural.

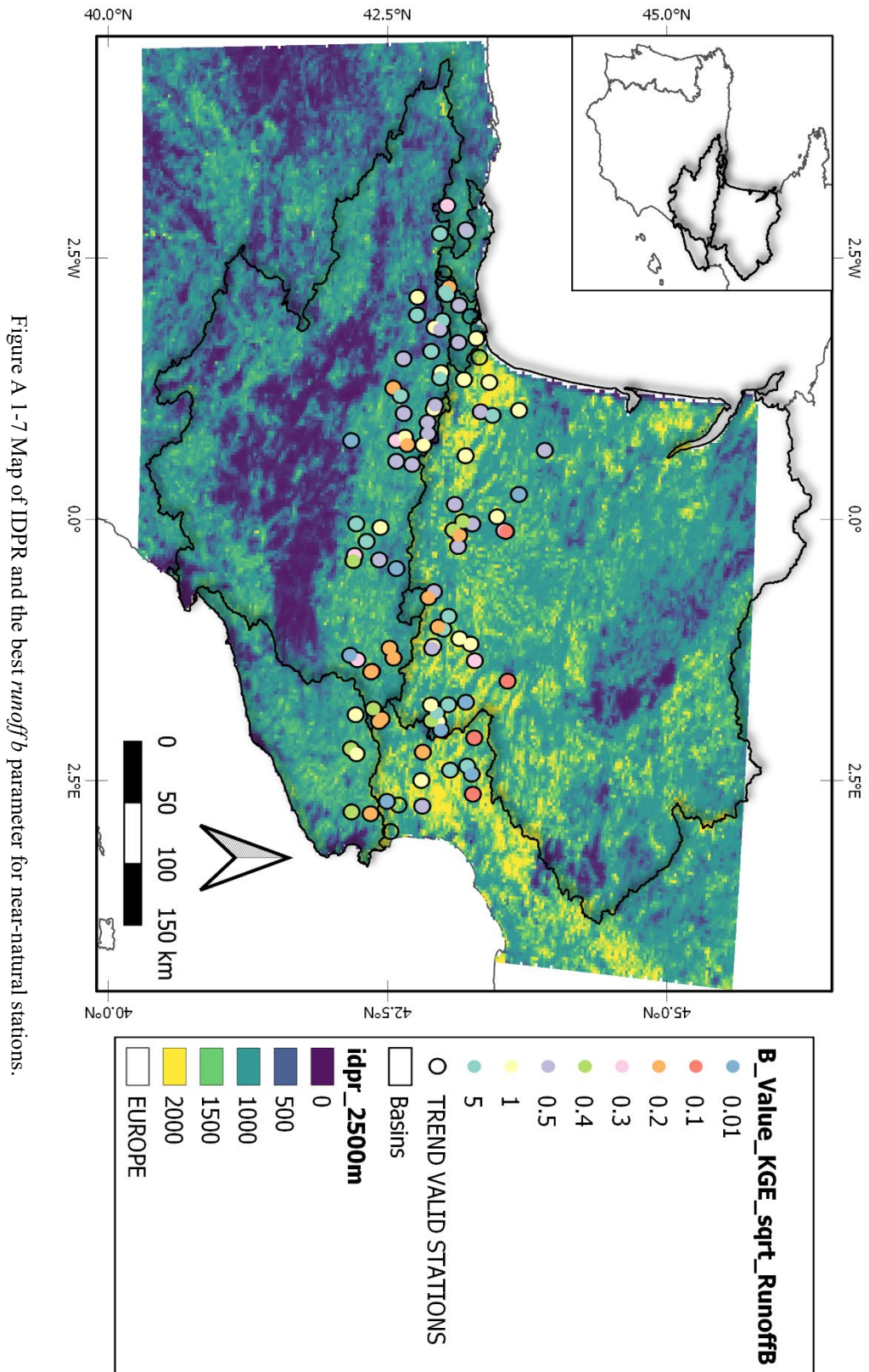


Figure A 1-7 Map of IDPR and the best runoff parameter for near-natural stations.

To analyze the impact of variability in the runoff parameter ( $b$ ) on the simulation, the original IDPR map (panel (a) in [Figure A 1-8](#)) was divided into three distinct categories based on percentile values. The categorization process employed the following thresholds:

- IDPR values below the 33.3<sup>rd</sup> percentile were assigned a fixed value of  $b=1.0$ .
- IDPR values ranging between the 33.3<sup>rd</sup> and 66.6<sup>th</sup> percentiles were assigned a fixed value of  $b=0.5$ .
- IDPR values falling between the 66.6<sup>th</sup> percentile and the 100<sup>th</sup> percentile were assigned a fixed value of  $b=0.1$ .

The resulting categorization is depicted in panel (b) of [Figure A 1-8](#), providing a representation of how the IDPR values align with the assigned runoff parameter values.

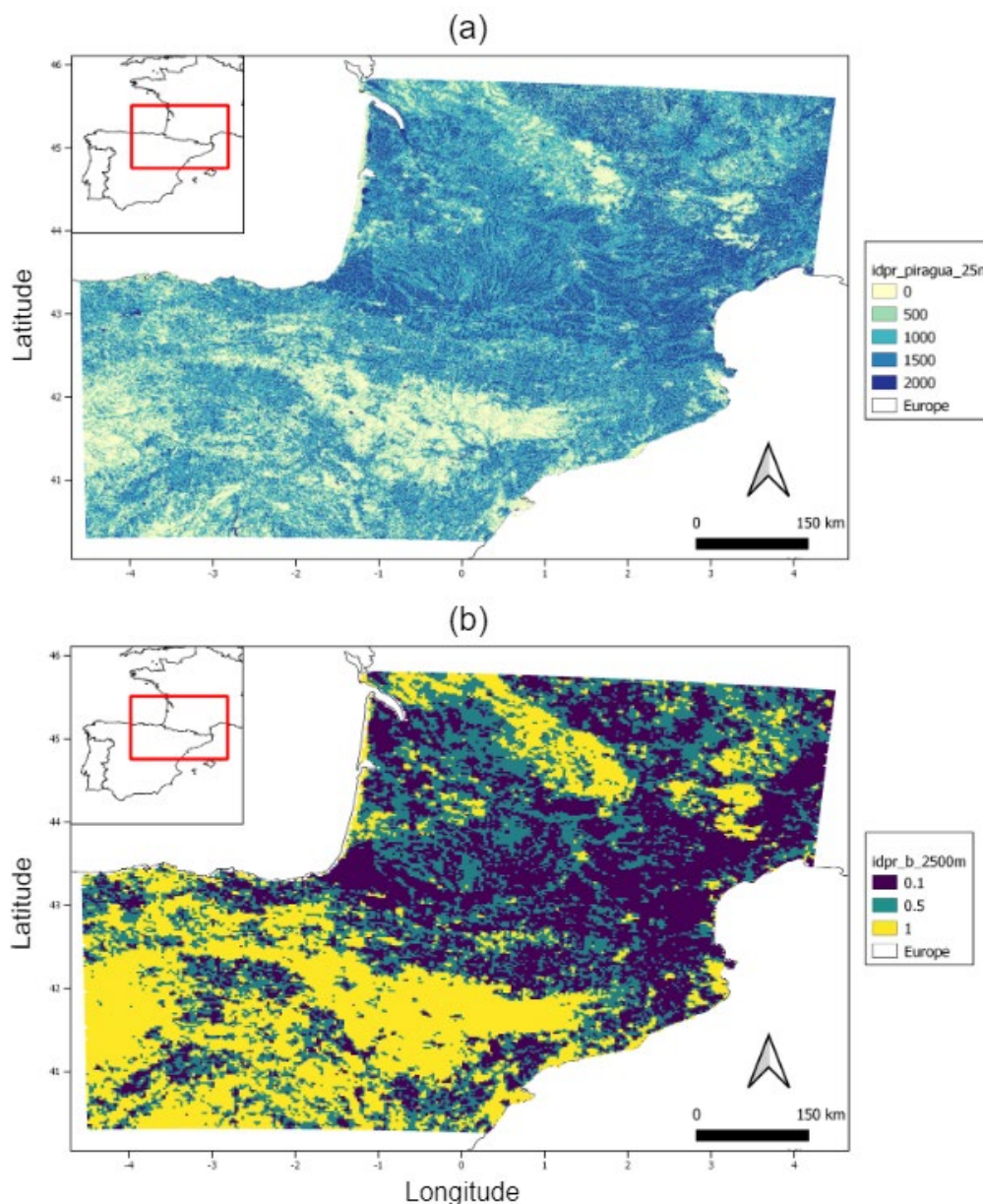


Figure A 1-8 (a) IDPR at 25 m (original) spatial resolution over the whole domain, and (b) classification of IDPR terciles used for simulation

Furthermore, **Figure A 1-9** presents a map illustrating the initial stations considered in this investigation, which are derived from the PIRAGUA project's initial database.

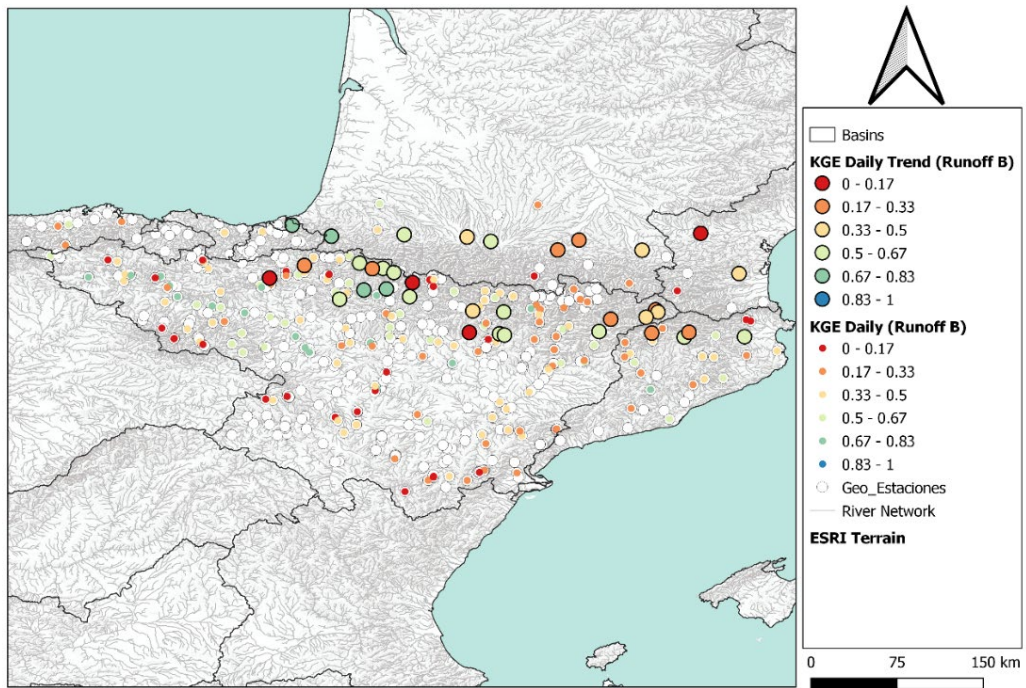


Figure A 1-9 Selected station (natural and near-natural), in black circles, in the initial database of the PIRAGUA project

## A.2. Improvement of Soil Information

### A.2.1. Background

The European Soil Data Centre (ESDAC) is a European Union (EU) project that was launched in 2009. Its goal is to provide access to a range of soil data and information, in order to help policymakers, researchers, and other stakeholders make informed decisions related to soil management and conservation. The data available through the ESDAC covers a wide range of topics, including soil properties, soil erosion, soil organic carbon, soil biodiversity, and soil contamination. The ESDAC is managed by the European Commission's Joint Research Centre (JRC), and it is part of the EU's broader effort to promote sustainable land management practices and improve the state of the environment

The ESDAC database, despite its utility, is not without limitations that warrant careful consideration. One such limitation is the variability in the availability and completeness of soil data across different regions. While some areas may benefit from comprehensive data coverage, others may suffer from limited or incomplete information (Panagos et al., 2012). This variability can significantly impact the accuracy and reliability of soil-related analyses and modeling efforts. Additionally, it is important to acknowledge that the ESDAC database relies on various modeling approaches and assumptions to estimate soil properties beyond the scope of available direct measurements. These models, while valuable, are not exempt from limitations and uncertainties that can introduce biases into the derived soil information. Therefore, when utilizing the ESDAC database, it is crucial to exercise caution and account for these limitations.

The estimation of plant rooting depth ( $Z_r$ ) is based on a carbon cost-benefit model developed by Guswa (2008), which offers valuable insights into the relationship between root depth, soil moisture availability, and carbon uptake. This model operates on the premise that deeper roots enable plants to access a larger reservoir of soil moisture, allowing them to withstand extended dry periods and optimize carbon assimilation. The carbon cost-benefit model takes into account the carbon investment required for root construction and maintenance. It posits that there exists an optimal rooting depth where the additional carbon benefit gained from accessing more soil moisture is balanced against the carbon cost of sustaining those additional roots.

The model developed by Guswa (2008) provides an estimation of the effective rooting depth across various geographical locations. This parameterization considers the inherent spatial variability of rooting depth within different biomes, emphasizing the limitations of using simplistic look-up tables to define rooting depth in contemporary land surface and hydrological models (Yang et al., 2016). By incorporating the carbon cost-benefit framework, a more realistic and ecologically sound representation of plant rooting depth can be achieved, enabling improved modeling of land-atmosphere interactions and hydrological processes.



### A.2.2. Search for an improved soil depth database

A new soil information map was generated for the PIR1ESDACGDRD simulation, incorporating two key variables sourced from the ESDAC<sup>4</sup> database and the plant rooting depth (Zr) map (Guswa, 2008). The description of the ESDAC's variables is provided below:

- ROO: The depth class of an obstacle to roots within the Soil Taxonomical Unit (STU).
- DR: The depth to rock.

The ROO variable provides information on the depth at which an obstacle restricts the growth of plant roots within a specific soil unit. This variable is important because it helps to assess the availability of rooting space for plants and the potential limitations that certain obstacles may pose to root development. Consequently, the root distribution within the soil profile can significantly impact water uptake by plants and influence hydrological processes. Whereas, the DR variable is important for various applications that involve understanding soil characteristics and processes, as well as for hydrological and geological studies. It helps to identify the presence and depth of the bedrock or hard rock layer, which can have significant implications for soil properties, water movement, and plant growth.

It is crucial to emphasize that the ROO variable represents the "depth available to roots," which should not be confused with the real root depth. Consequently, when comparing and interpreting these values, it is essential to consider them for accurate analysis.

The creation of the resulting map involved merging the hydro\_depth\_eu and Zr maps. Given the primary focus of the ESDAC map on geological characteristics rather than biological factors, the decision was made to prioritize the rooting depth information from the Zr map. However, when the rooting depth indicated by the Zr map exceeded the values provided in the ESDAC map, the depth values from the ESDAC map were used instead. As a result, the representation of root depth closely corresponds to the information sourced from the Zr map, except in cases where the soil exhibits unusually shallow characteristics ( [Figure A 2-1](#)).

---

<sup>4</sup> (<https://esdac.jrc.ec.europa.eu/content/european-soil-database-v2-raster-library-1kmx1km>)

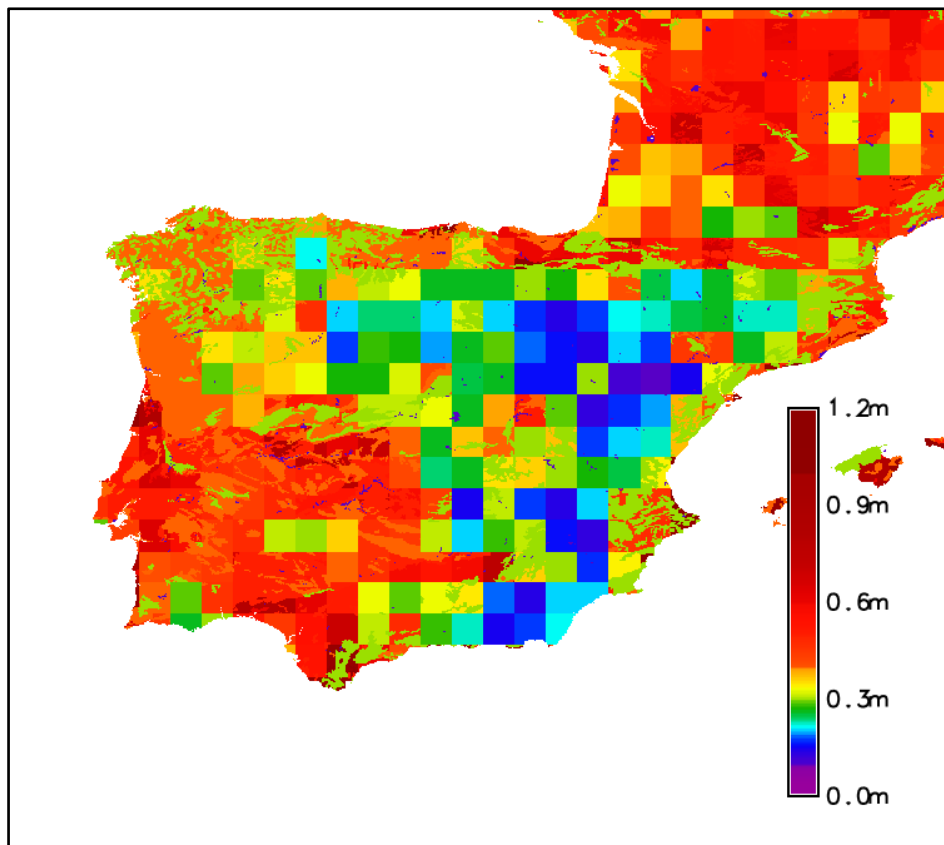


Figure A 2-1 Improved soil depth map used in PIR1ESDACGDRD simulation

One limitation that arises when incorporating the ESDAC's variables in the SURFEX model is the lack of direct compatibility between the two datasets. ESDAC's variables cannot be directly utilized within the SURFEX model as they do not correspond exactly to the variables required by SURFEX, as previously mentioned. Furthermore, ESDAC's variables do not consider the vegetation component. This mismatch between the variables and the absence of vegetation considerations can result in uncertainties and inaccuracies in simulating hydrological processes.

Finally, the streamflow was obtained, and the impact of the modified soil information was evaluated by launching the last part of the modeling chain (Eaudyssée-Rapid) using the results of the SURFEX simulation.

**Figure A 2-2** displays the simulated flow series obtained from the PIR1ESDAC simulation, integrating the ESDAC data and Zr map. For clarity, two stations and a limited number of years are depicted in this figure. It is noteworthy that the new simulation (represented by the blue line) exhibits a noticeable increase in peak flows, accompanied by a slight alteration (decrease) in mean and low flows. However, the critical observation to highlight is that the KGE metric does not indicate any improvement.

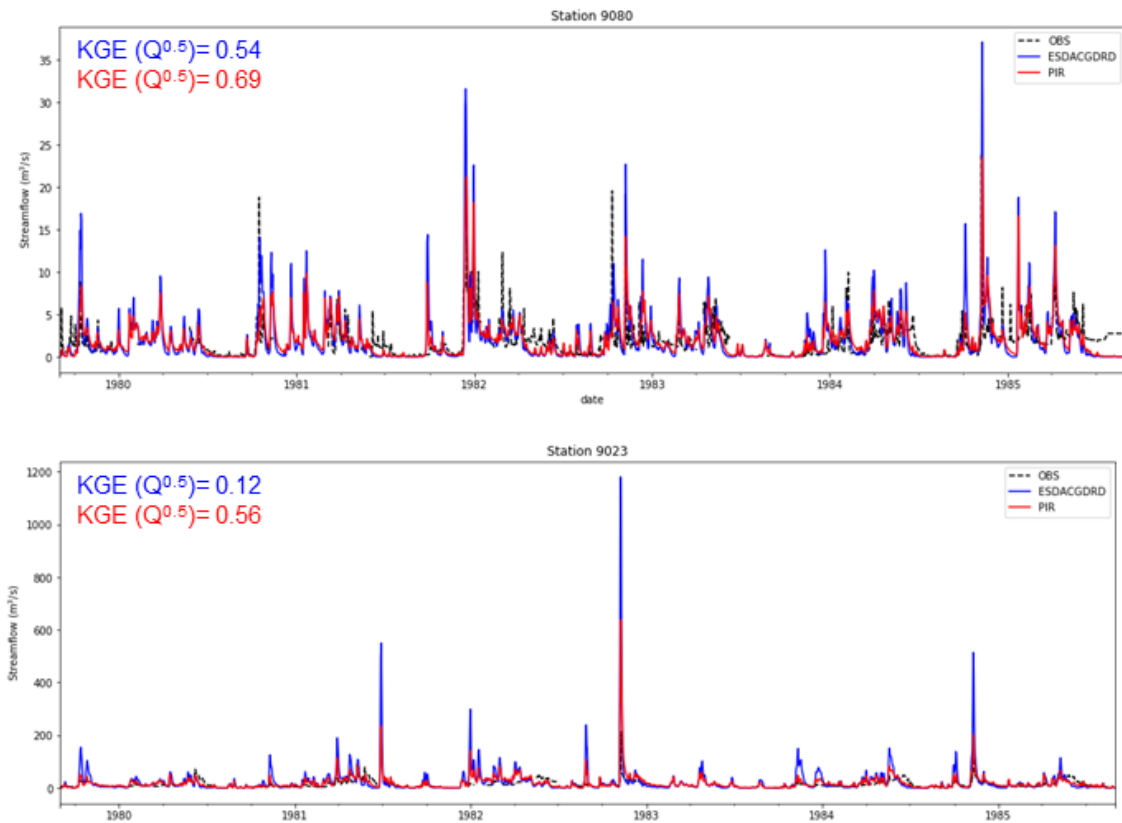


Figure A 2-2 Daily time series comparison for two stations, for five hydrological years (to make the plots easy to read). Observed streamflow (dashed black line), simulated streamflow using ESDAC soil database (blue line), and simulated streamflow using default configuration (red line). The  $KGE(Q^{1/2})$  is calculated over the complete period (1979-2014)

The visualization in [Figure A 2-2](#) provides a comprehensive overview of the simulated flow dynamics resulting from the PIR/ESDAC simulation, offering valuable insights into the impact of incorporating the ESDAC data and Zr into the hydrological simulation. Nevertheless, despite these observed alterations in the flow characteristics, the KGE metric, which serves as an indicator of model performance, does not demonstrate any enhancement. This suggests that the simulation, despite capturing changes in flow patterns, fails to accurately reproduce the observed flow dynamics.

The collaboration with the National Institute of Meteorology and Hydrology (Bulgaria) played a pivotal role in conducting this research stage. I would like to express my sincere gratitude to Dr. Eram Artinyan for his invaluable contribution to preparing the soil information maps utilized in these simulations. And I would also like to extend my appreciation to Dr. Aaron Boone from the Centre National de Recherches Météorologiques (France) for his generous assistance and detailed explanations regarding the configuration of the ISBA scheme.

## Appendix B. Results of the reservoir scheme using different inputs

### B.1. Estimation volume – area curves

The accurate estimation of reservoir volume is of paramount importance for effective water resource management and planning. However, direct volume measurements can be challenging, costly, or impractical in certain scenarios. In such cases, the volume-area curve offers a practical solution by establishing a mathematical relationship between the reservoir's surface area and its corresponding volume.

Firstly, volume measurements, which their corresponding dates, were obtained from historical records provided by the SAIH platform. Subsequently, with these meticulously chosen dates were utilized to conduct an extensive search for SENTINEL images to estimate the area. It is important to look for images ideally with minimal cloud cover and high quality. In this analysis, the Sentinel-2 product was used (<https://www.sentinel-hub.com/explore/data/>). Then, the sentinel satellite images were used to calculate the Normalized Difference Water Index (NDWI, McFEETERS, 1996) as depicted in Figure B 1-1.

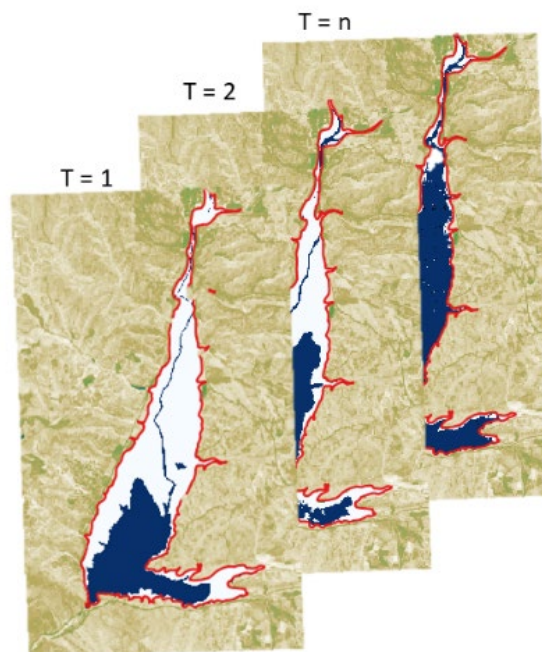


Figure B 1-1 Example of the determination of reservoir area for different time steps

The NDWI is a widely used index for water body detection and monitoring. The NDWI formula involves subtracting the green band reflectance from the near-infrared (NIR) band reflectance and dividing it by their sum. This index yields a normalized index that enhances the discrimination of water bodies. Later, to calculate the area of the reservoir, a geographic information system (QGIS software) was utilized.

With the reservoir area on the x-axis and the corresponding observed volume on the y-axis, a scatter plot was created. Each data point represents a specific instance of the reservoir's area and the associated volume (Figure B 1-2). The best-fitting curve that represents the relationship between the reservoir area and volume was determined through linear interpolation. This step was developed with Python code packages.

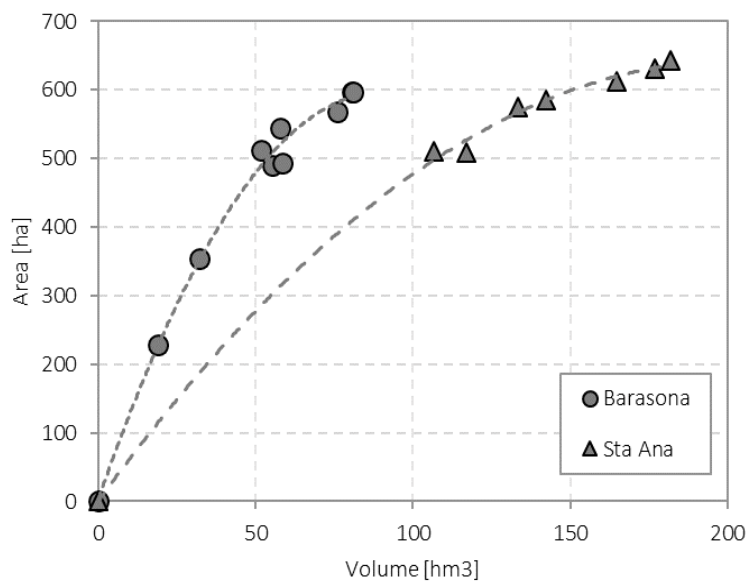


Figure B 1-2 Area-Volume curves determined for Barasona and Santa Ana.

Figure B 1-2 represents the obtained volume-area curves for both reservoirs considered in this analysis. Based on the interpretation of the volume-area curve, it is evident that both the Barasona and Santa Ana reservoirs exhibit comparable surface area values. However, a notable distinction arises when examining their regulation capacities, as reflected in the storage volume measurements. The volume values associated with the Barasona reservoir are consistently lower than those of the Santa Ana reservoir. This discrepancy implies that the Barasona Reservoir possesses a relatively lower storage capacity in comparison to its counterpart, the Santa Ana Reservoir.

Finally, it is important to highlight that the volume-area curve is specific to each reservoir and can change over time due to various factors such as sedimentation, changes in storage capacity, or alterations in the reservoir's shape. Regular updates and validation of the curve are essential to maintain accurate volume estimations.

## B.2. Reservoir simulation plots

In this Appendix, complementary plots of the reservoir operation results are presented. Plots for each case study and scenarios (S1 to S4) are depicted. Result plots for the Barasona case study.

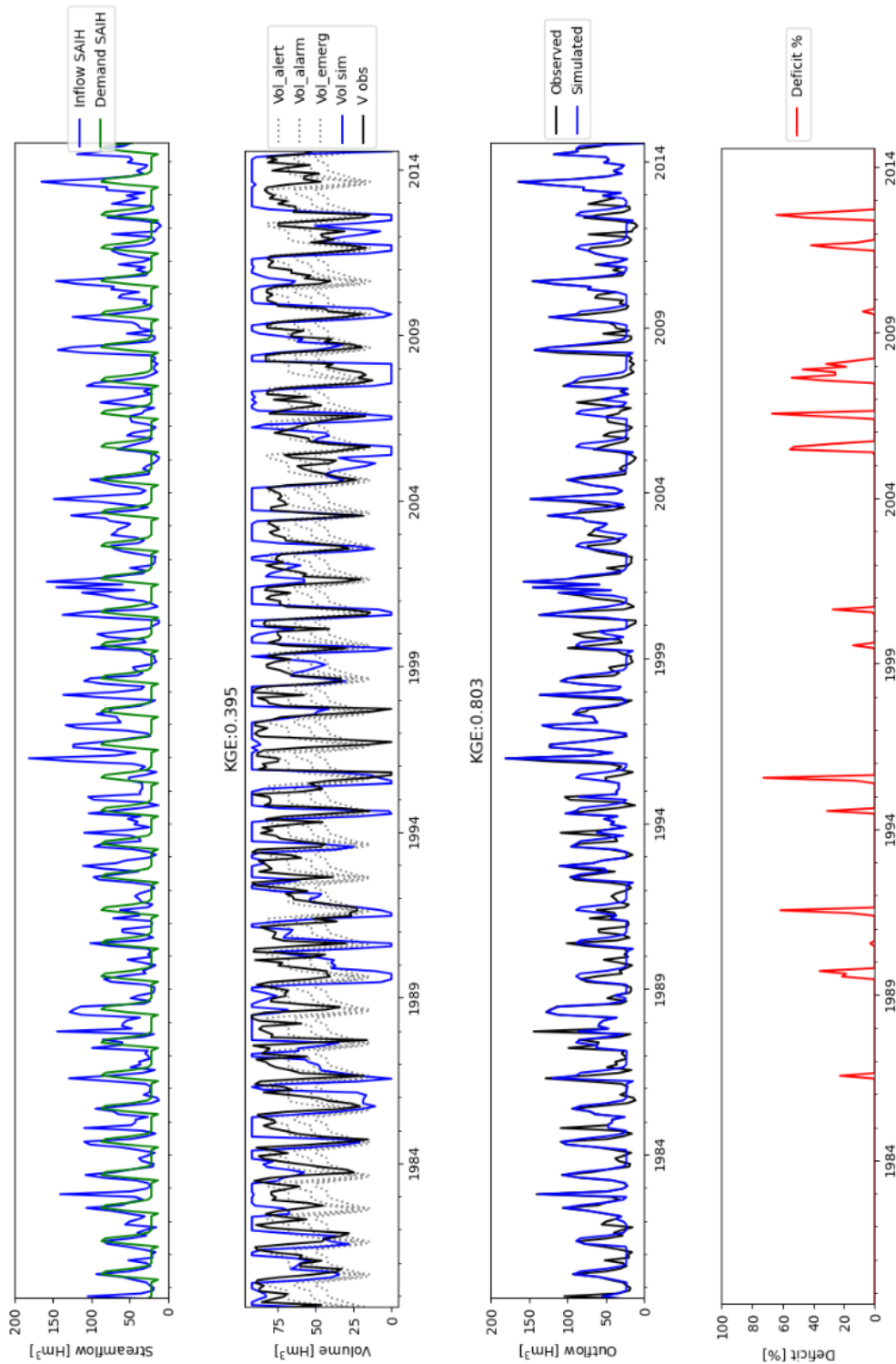


Figure B 2-1 Reservoir simulation results to Barasona case study for S1 scenario. The upper panel shows the input data used in this simulation. Middle panels show the storage and releases (Hm<sup>3</sup>), respectively. The lower panel depicts the percentage of deficit.

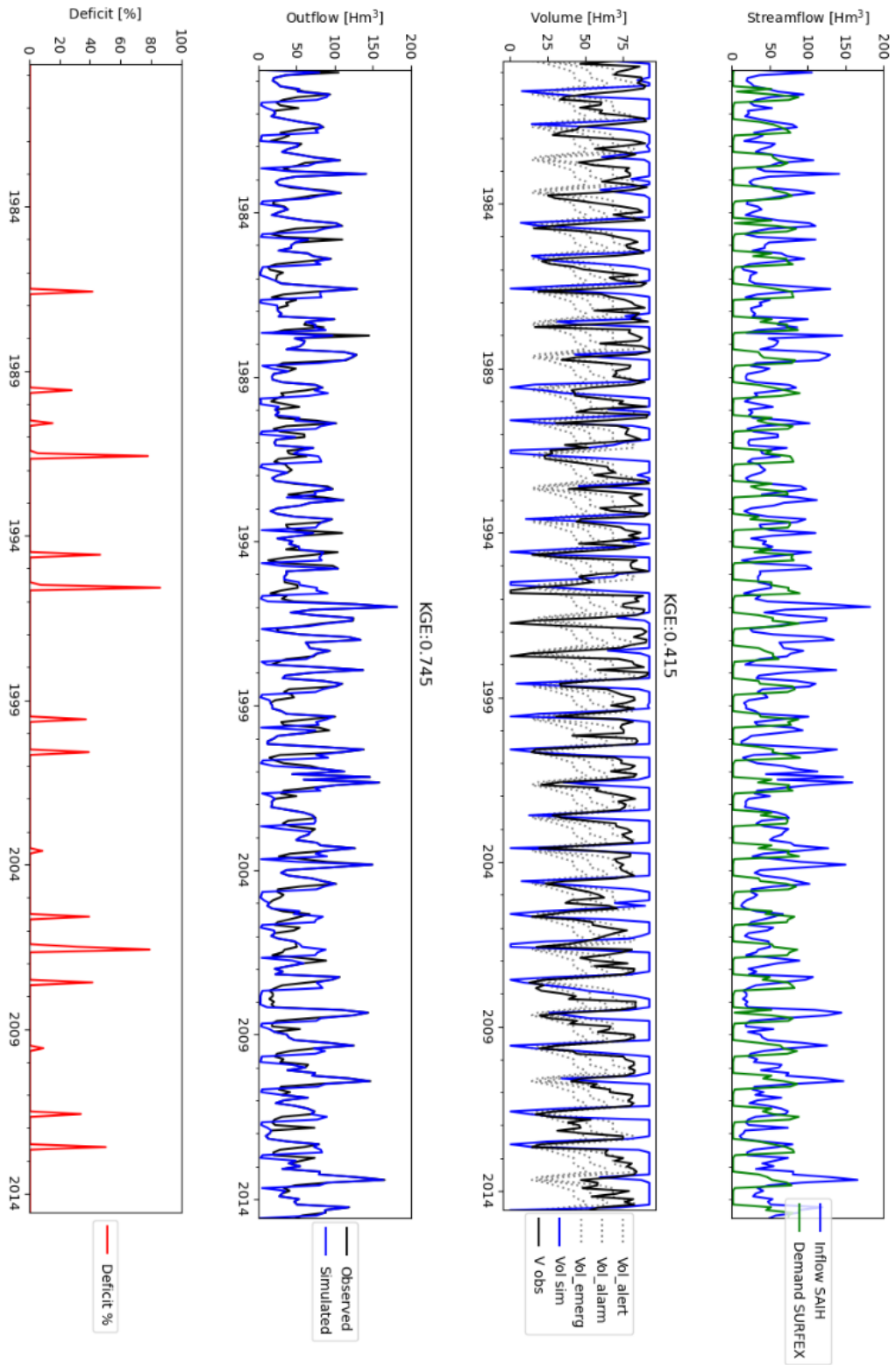


Figure B 2-2 Same as Figure B 2-1 but for the S2 scenario.

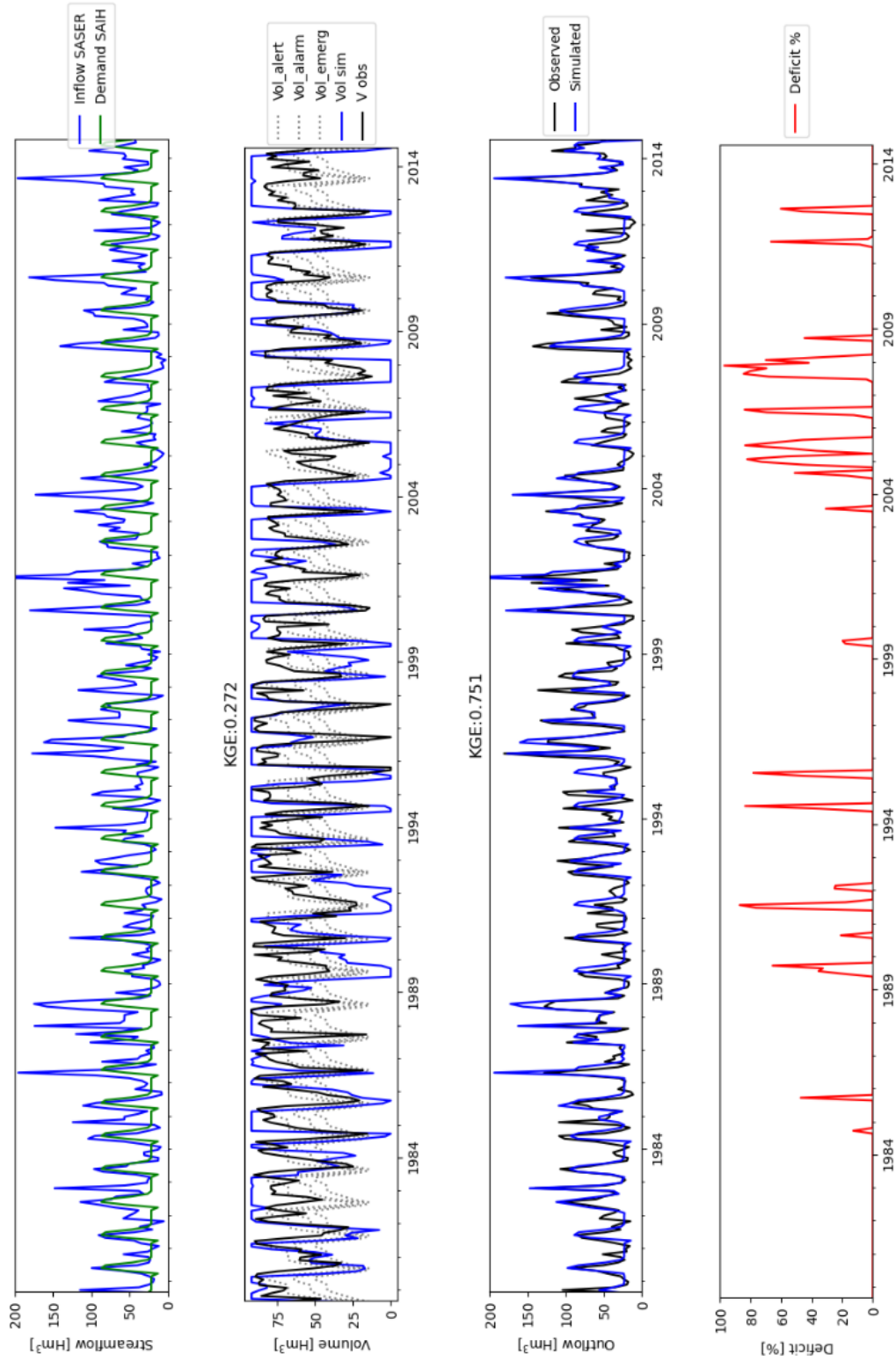


Figure B 2-3 Same as Figure B 2-1 but for the S3 scenario.



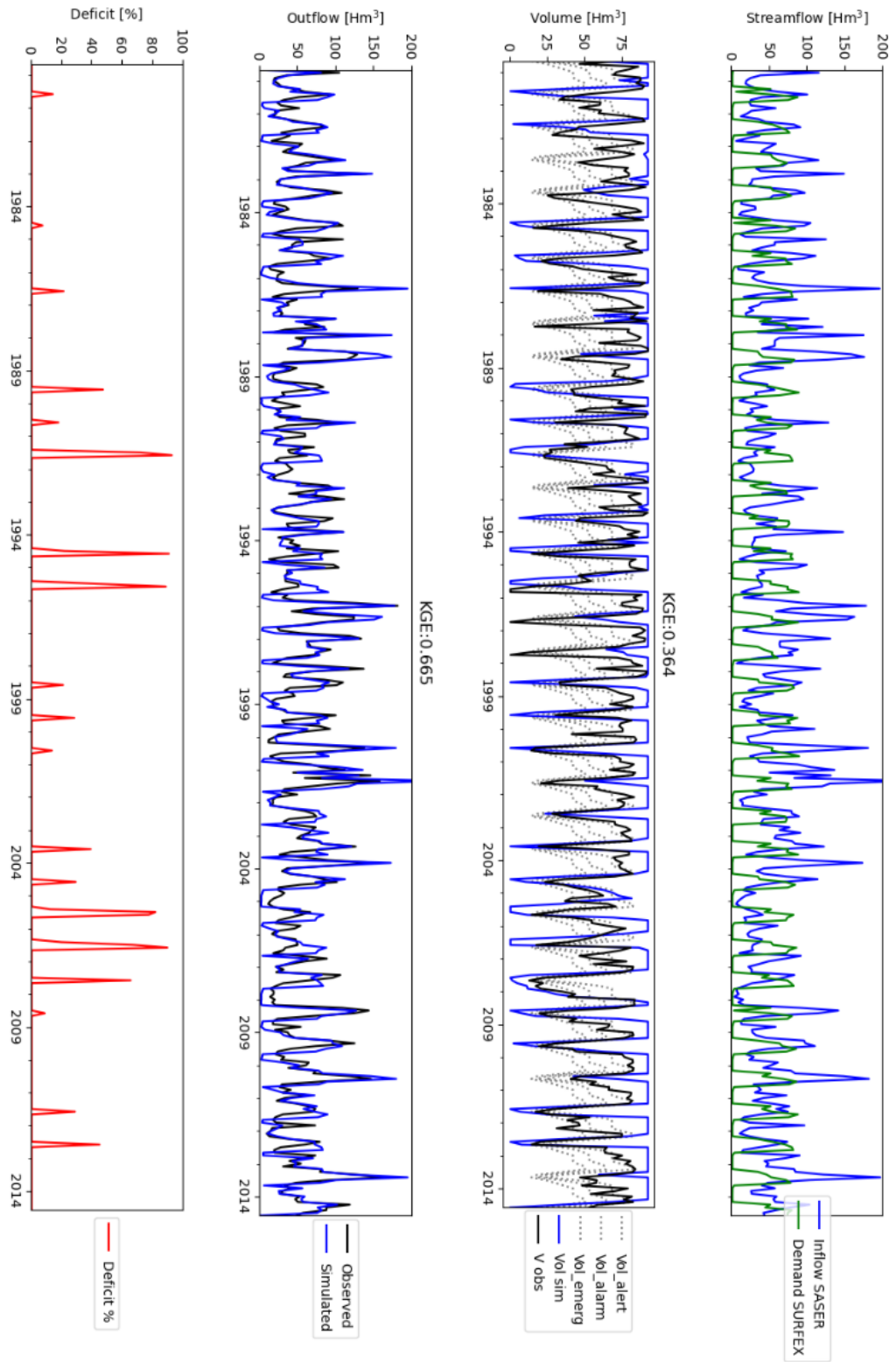


Figure B 2-4 Same as Figure B 2-1 but for the S4 scenario.

Result plots for the Santa Ana case study.

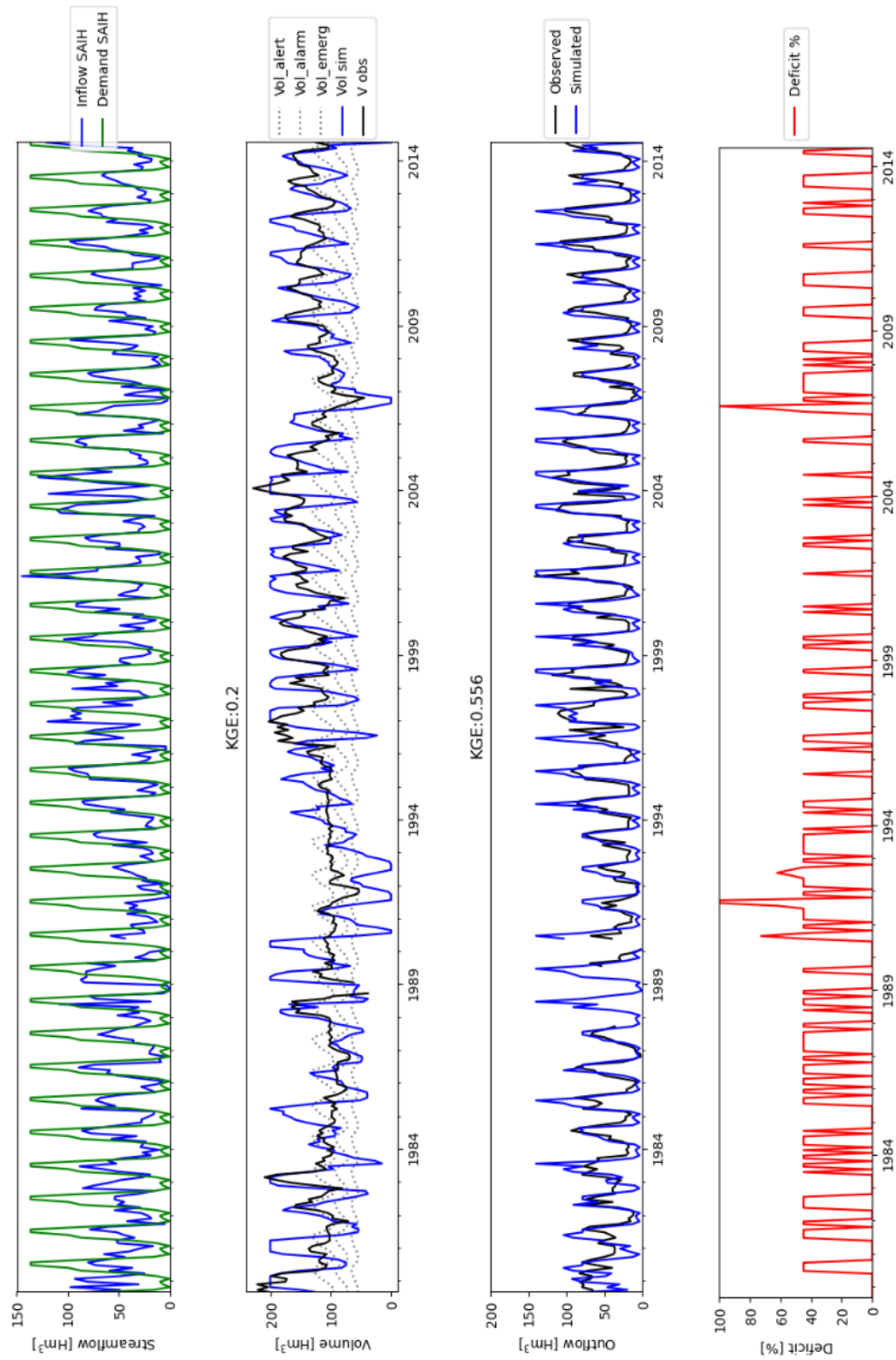


Figure B 2-5 Reservoir simulation results to Santa Ana case study for S1 scenario. The upper panel shows the input data used in this simulation. Middle panels show the storage and releases (Hm<sup>3</sup>), respectively. The lower panel depicts the percentage of deficit.

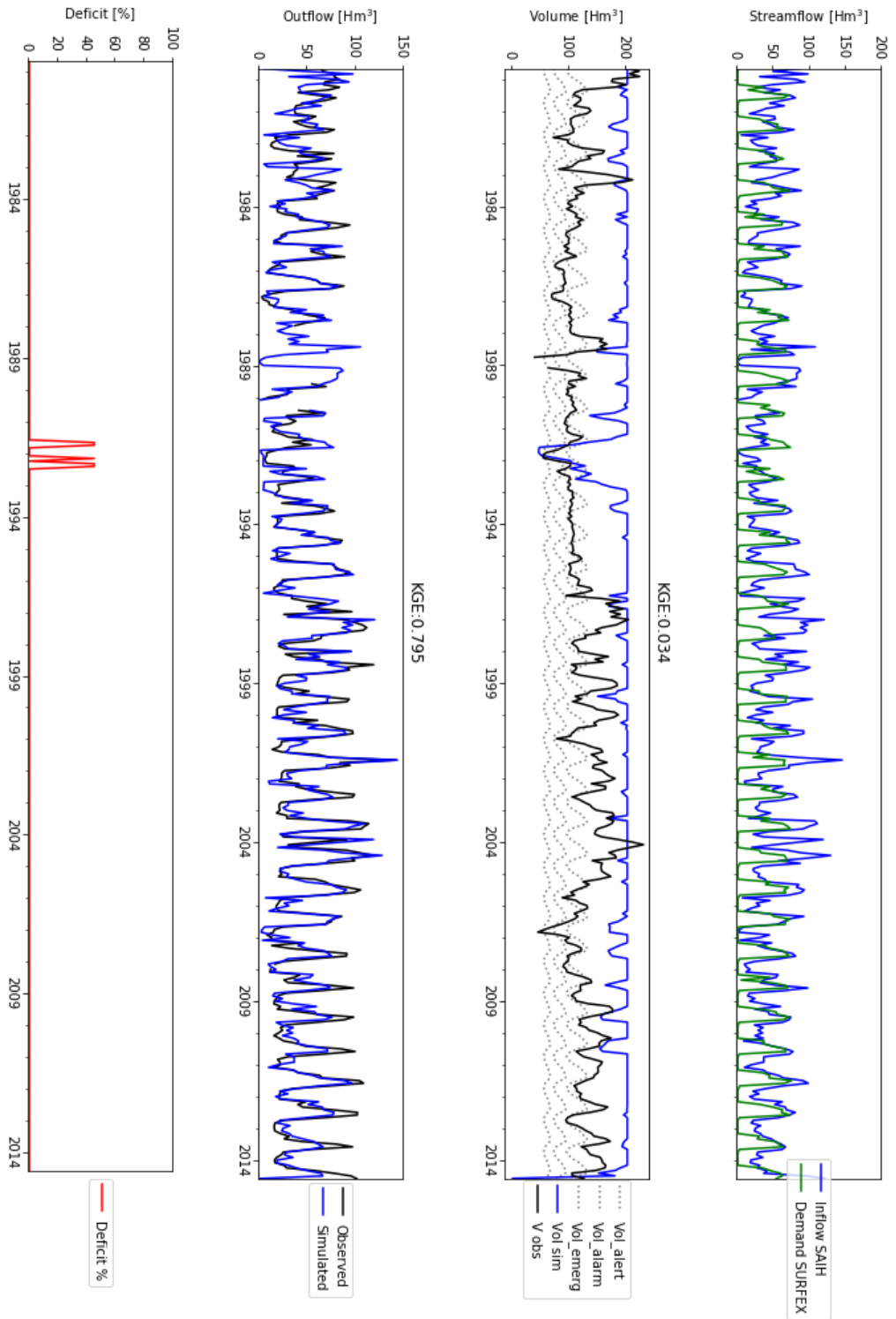


Figure B 2-6 Same as Figure B 2-5 but for the S2 scenario.

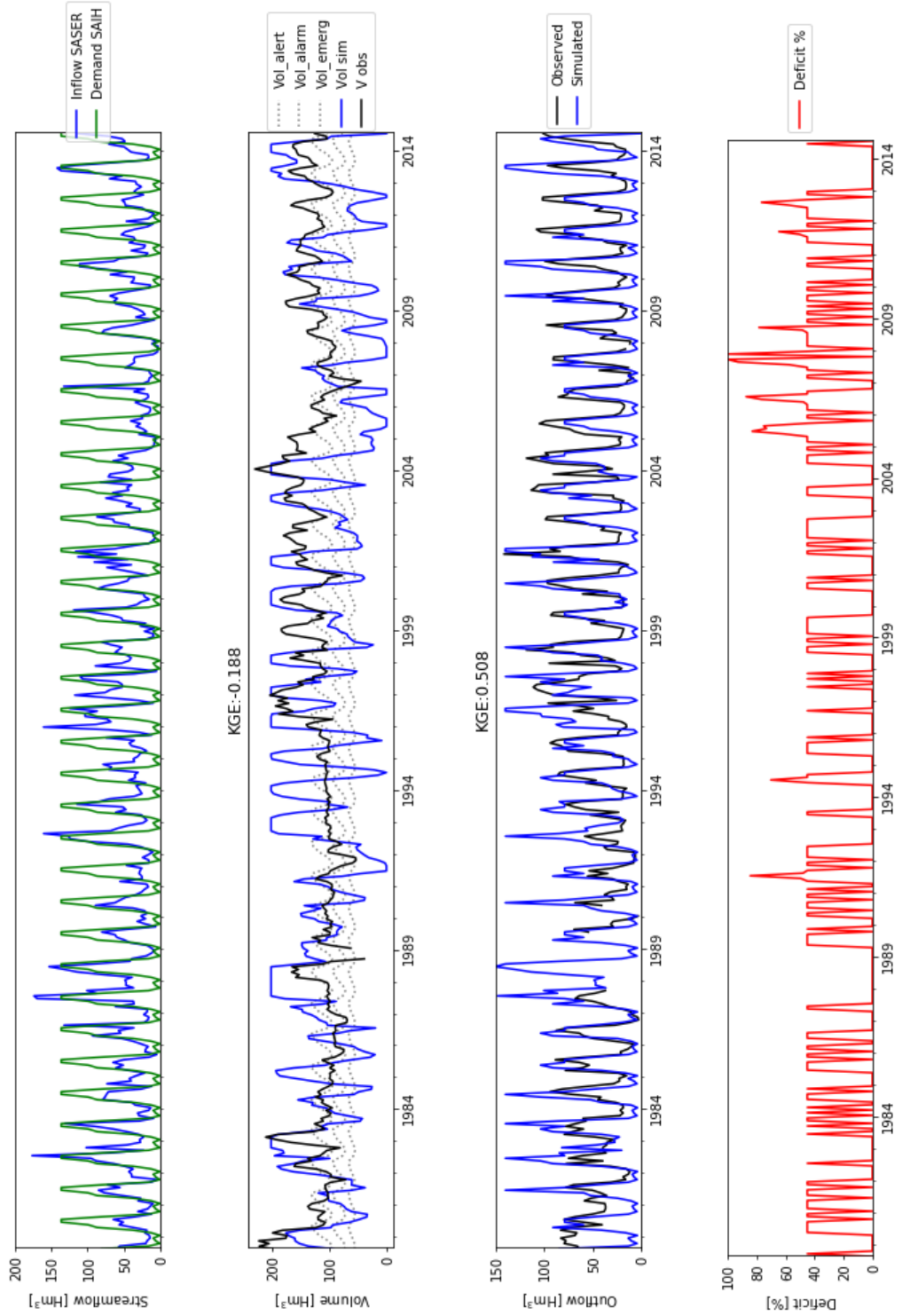


Figure B 2-7 Same as Figure B 2-5 but for the S3 scenario.

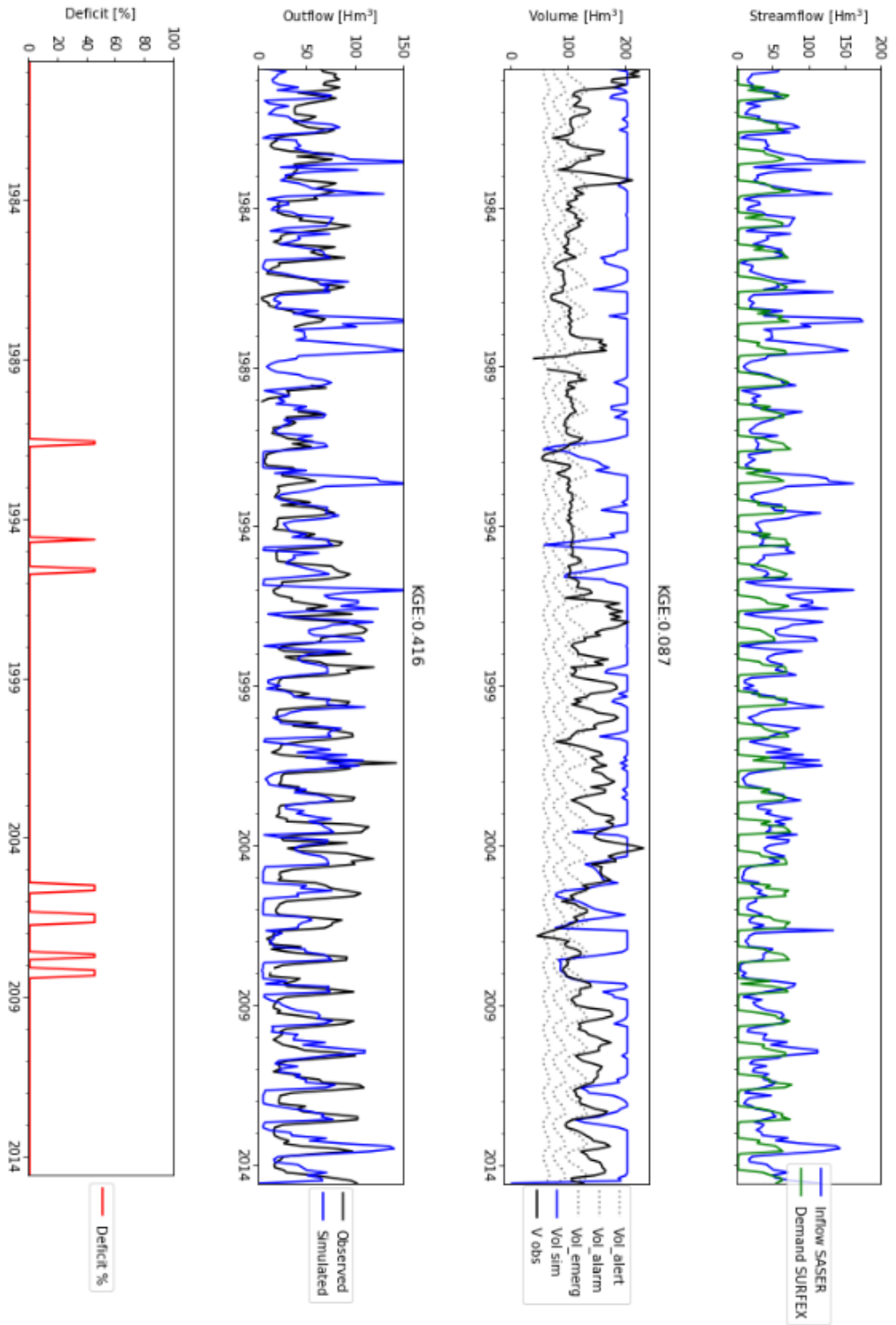


Figure B-2-8 Same as Figure B-2-5 but for the S4 scenario.

---

### B.3. Drought analysis using standardized indices

One important limitation in evaluating anthropogenic drought using distribution-based approaches is the reliance on historical data in which human influences are not fully captured or easily separate from natural drivers on the water cycle. These approaches typically assume that the observed data, such as precipitation or streamflow, represent natural conditions unaffected by human interventions.

However, in many regions, human activities such as water abstraction, reservoir operations, and land-use changes can significantly alter the hydrological system, leading to shifts in the distribution of these variables. Consequently, using distribution-based methods without accounting for these human influences may not accurately capture the occurrence and severity of anthropogenic drought. Additionally, changes in water management practices, such as the implementation of irrigation schemes or water conservation measures, can further modify the distribution of meteorological and hydrological variables.

To estimate the impact of human influence on drought using standardized indices, a calculation procedure similar to the Standardized Precipitation Index (SPI, [McKee et al., 1993](#)) was employed, but with adaptations for monthly data. Parametric indices were utilized for the analysis, necessitating the identification of the best-fitting distribution function for the naturalized data series obtained through the SASER modeling chain. The monthly series of streamflow, and evapotranspiration (ET) were considered, as depicted by the blue and green bars in [Figure B 3-1](#).

Different distribution functions, such as log-normal, log-Pearson, GVE, gamma, etc., were tested, thus a Python code script was developed to determine the appropriate distribution function. Once the distribution function was determined, their respective parameters were derived from the observed data, which accounts for human influence. Subsequently, the standardization process, following the same procedure as the SPI, was applied, and the results of the standardized index are presented in [Figure B 3-1](#).

[Figure B 3-1](#) clearly demonstrates the significant alterations in the distribution of hydrological variables due to human influence. The presence of the reservoir leads to a remarkable reduction in flow from May to September, resulting in a distinct distribution pattern. Conversely, ET exhibits a substantial increase in values during the same months due to irrigation, causing them to fall outside the distribution range.

These changes in the distributions have a profound impact on the results shown in [Figure B 3-1](#). The Standardized Index (SRI) for flow displays highly negative values, making the interpretation impractical. In contrast, the standardized index for ET takes positive values that exceed the distribution, posing the opposite challenge. As a result, it becomes challenging to directly estimate the impact of human activities on drought using statistical indices within this framework.

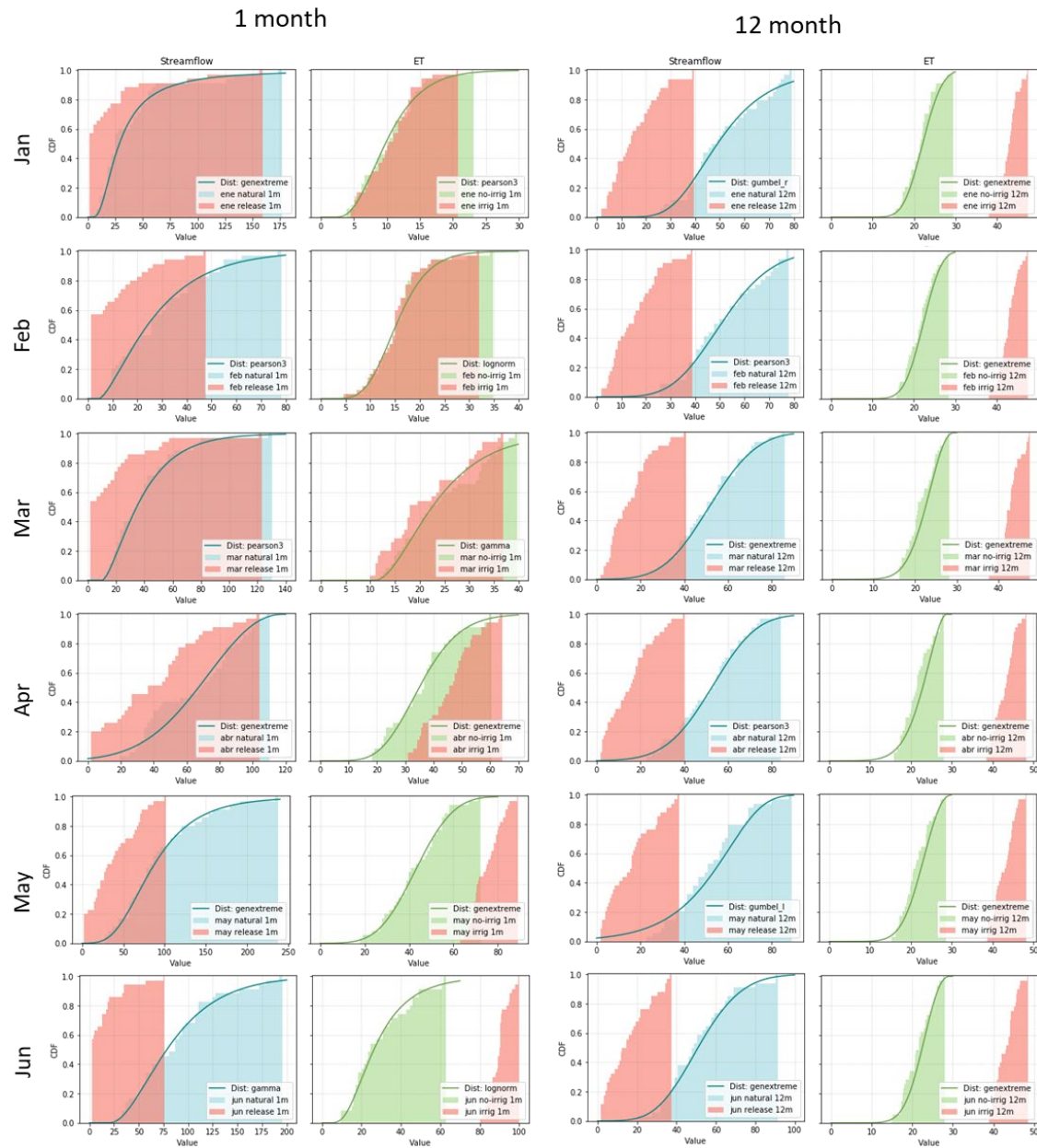


Figure B 3-1 Example of some monthly fitted distribution for both variables (streamflow and ET) at different time scales. Blue and green bars represent the natural distribution of streamflow and ET, respectively. Red bars show the shift in these variables due to human influences.

In conclusion, the utilization of standardized indices to evaluate the impact of human activities on drought encounters several limitations in this study. While these indices offer a valuable tool for assessing drought based on meteorological variables, their application becomes challenging when analyzing anthropogenic influences. Therefore, it becomes crucial to incorporate knowledge of human-induced alterations in the water cycle, along with appropriate modeling approaches that account for the impacts of human activities on drought dynamics.

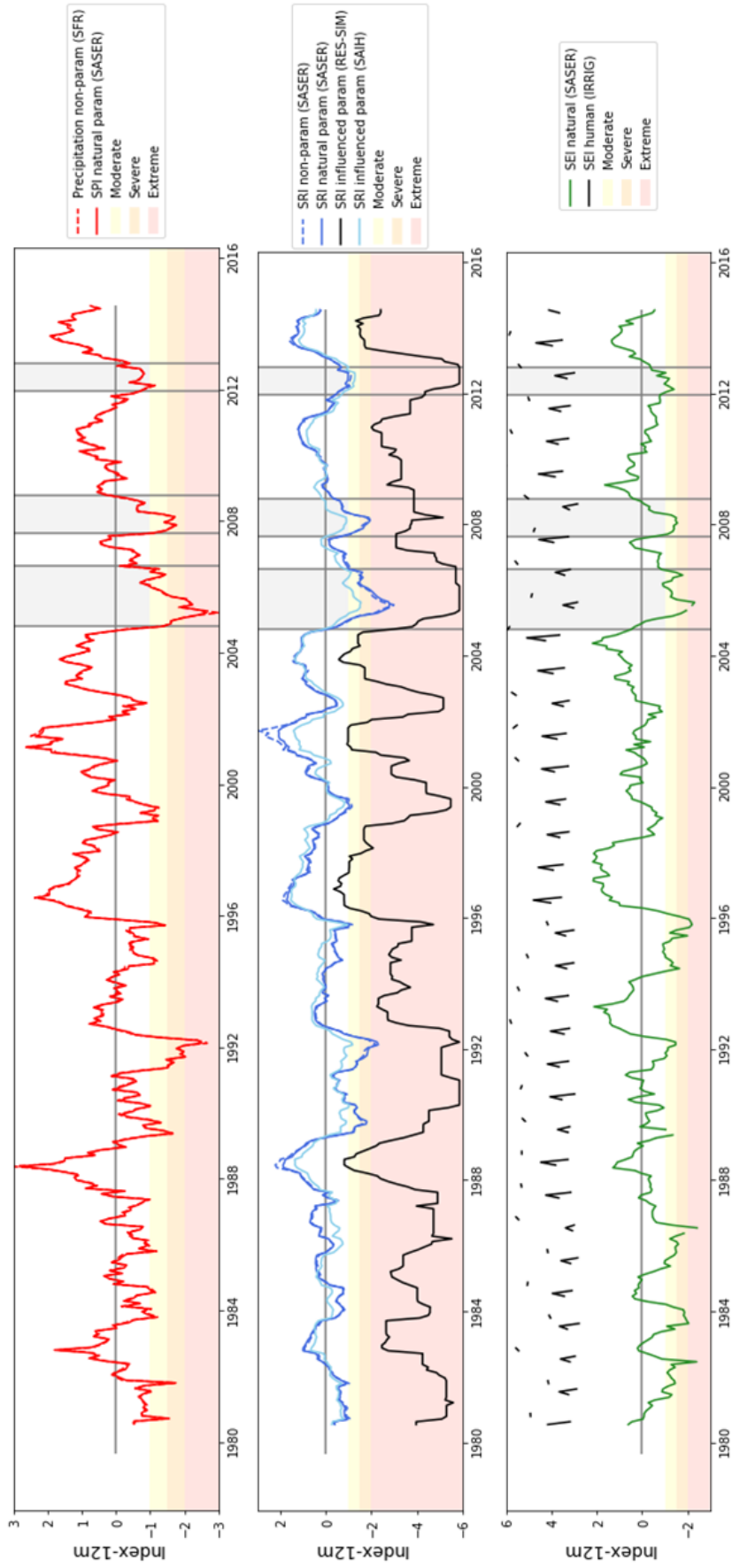


Figure B 3-2 Standardized drought indices (a) SPI-12 (precipitation), (b) SRI-12 (streamflow), and (c) SEI-12 (evapotranspiration) for the Barasona case study. Blue and Green lines represent the natural situation. Black lines in each respective panel represent the standardized index considering the human influences based on natural data distribution.





---

## References

- Acreman, M. C. (2001). *Hydro-ecology: Linking Hydrology and Aquatic Ecology: Proceedings of an International Workshop (HW2) Held During the IUGG 99, the XXII General Assembly of the International Union of Geodesy and Geophysics (IUGG) Held at Birmingham, UK, in July 1999...* (Issue 266). International Assn of Hydrological Sciences.
- Adegoke, J. O., Pielke, R. A., Eastman, J., Mahmood, R., & Hubbard, K. G. (2003). Impact of irrigation on midsummer surface fluxes and temperature under dry synoptic conditions: A regional atmospheric model study of the U.S. high plains. *Monthly Weather Review*, *131*(3), 556–564. [https://doi.org/10.1175/1520-0493\(2003\)131<0556:IOIOMS>2.0.CO;2](https://doi.org/10.1175/1520-0493(2003)131<0556:IOIOMS>2.0.CO;2)
- Aghakouchak, A., Farahmand, A., Melton, F. S., Teixeira, J., Anderson, M. C., Wardlow, B. D., & Hain, C. R. (2015). Reviews of geophysics remote sensing of drought: Progress, challenges. *Reviews of Geophysics*, *53*, 1–29. <https://doi.org/10.1002/2014RG000456>. Received
- AghaKouchak, A., Mirchi, A., Madani, K., Di Baldassarre, G., Nazemi, A., Alborzi, A., Anjileli, H., Azarderakhsh, M., Chiang, F., Hassanzadeh, E., Huning, L. S., Mallakpour, I., Martinez, A., Mazdiyasn, O., Moftakhari, H., Norouzi, H., Sadegh, M., Sadeqi, D., Van Loon, A. F., & Wanders, N. (2021). Anthropogenic Drought: Definition, Challenges, and Opportunities. *Reviews of Geophysics*, *59*(2), 1–23. <https://doi.org/10.1029/2019RG000683>
- Albergel, C., Calvet, J. C., Gibelin, A. L., Lafont, S., Roujean, J. L., Berne, C., Traullé, O., & Fritz, N. (2010). Observed and modelled ecosystem respiration and gross primary production of a grassland in southwestern France. *Biogeosciences*, *7*(5), 1657–1668. <https://doi.org/10.5194/bg-7-1657-2010>
- Albergel, C., Munier, S., Jennifer Leroux, D., Dewaele, H., Fairbairn, D., Lavinia Barbu, A., Gelati, E., Dorigo, W., Faroux, S., Meurey, C., Le Moigne, P., Decharme, B., Mahfouf, J. F., & Calvet, J. C. (2017). Sequential assimilation of satellite-derived vegetation and soil moisture products using SURFEX-v8.0: LDAS-Monde assessment over the Euro-Mediterranean area. *Geoscientific Model Development*, *10*(10), 3889–3912. <https://doi.org/10.5194/gmd-10-3889-2017>
- Alcamo, J., Döll, P., Henrichs, T., Kaspar, F., Lehner, B., Rösch, T., & Siebert, S. (2003). Development and testing of the WaterGAP 2 global model of water use and availability. *Hydrological Sciences Journal*, *48*(3), 317–337. <https://doi.org/10.1623/hysj.48.3.317.45290>
- Alcamo, J. M., Vörösmarty, C. J., Naiman, R. J., Lettenmaier, D. P., & Pahl-Wostl, C. (2008). A grand challenge for freshwater research: Understanding the global water system. In *Environmental Research Letters* (Vol. 3, Issue 1, p. 010202). IOP Publishing. <https://doi.org/10.1088/1748-9326/3/1/010202>
- Ament, F., & Simmer, C. (2006). Improved representation of land-surface heterogeneity in a non-
-

- hydrostatic numerical weather prediction model. *Boundary-Layer Meteorology*, 121(1), 153–174. <https://doi.org/10.1007/s10546-006-9066-4>
- Andrade, C., & Belo-Pereira, M. (2015). Assessment of droughts in the Iberian Peninsula using the WASP-Index. *Atmospheric Science Letters*, 16(3), 208–218. <https://doi.org/10.1002/ASL2.542>
- Andreu, J., Ferrer-Polo, J., Pérez, M. A., & Solera, A. (2009). Decision support system for drought planning and management in the Jucar river basin, Spain. *18th World IMACS/MODSIM Congress, Cairns, Australia*, 1317.
- Apurv, T., Sivapalan, M., & Cai, X. (2017). Understanding the Role of Climate Characteristics in Drought Propagation. *Water Resources Research*, 53(11), 9304–9329. <https://doi.org/10.1002/2017WR021445>
- Artinyan, E., Habets, F., Noilhan, J., Ledoux, E., Dimitrov, D., Martin, E., & Le Moigne, P. (2008). Modelling the water budget and the riverflows of the Maritsa basin in Bulgaria. *Hydrology and Earth System Sciences*, 12(1), 21–37. <https://doi.org/10.5194/hess-12-21-2008>
- Avissar, R., & Pielke, R. A. (1989). A Parameterization of Heterogeneous Land Surfaces for Atmospheric Numerical Models and Its Impact on Regional Meteorology. *Monthly Weather Review*, 117(10), 2113–2136. [https://doi.org/https://doi.org/10.1175/1520-0493\(1989\)117<2113:APOHLS>2.0.CO;2](https://doi.org/10.1175/1520-0493(1989)117<2113:APOHLS>2.0.CO;2)
- Bai, Y., Chen, Z., Xie, J., & Li, C. (2016). Daily reservoir inflow forecasting using multiscale deep feature learning with hybrid models. *Journal of Hydrology*, 532, 193–206. <https://doi.org/10.1016/j.jhydrol.2015.11.011>
- Barella-Ortiz, A., & Quintana-Seguí, P. (2019). Evaluation of drought representation and propagation in regional climate model simulations across Spain. *Hydrology and Earth System Sciences*, 23(12), 5111–5131. <https://doi.org/10.5194/hess-23-5111-2019>
- Batalla, R. J., Gómez, C. M., & Kondolf, G. M. (2004). Reservoir-induced hydrological changes in the Ebro River basin (NE Spain). *Journal of Hydrology*, 290(1–2), 117–136. <https://doi.org/10.1016/j.jhydrol.2003.12.002>
- Bates, B. C., Kundzewicz, Z. W., Wu, S., & Palutikof, J. P. (2008). Climate Change and Water. Technical Paper of the Intergovernmental Panel on Climate Change,. *IPCC Secretariat*, 210.
- Beck, H. E., Pan, M., Lin, P., Seibert, J., van Dijk, A. I. J. M., & Wood, E. F. (2020). Global Fully Distributed Parameter Regionalization Based on Observed Streamflow From 4,229 Headwater Catchments. *Journal of Geophysical Research: Atmospheres*, 125(17). <https://doi.org/10.1029/2019JD031485>
- Beck, H. E., van Dijk, A. I. J. M., de Roo, A., Miralles, D. G., McVicar, T. R., Schellekens, J., & Bruijnzeel, L. A. (2016). Global-scale regionalization of hydrologic model parameters. *Water Resources Research*, 52(5), 3599–3622. <https://doi.org/10.1002/2015WR018247>
- Beck, H. E., Wood, E. F., Pan, M., Fisher, C. K., Miralles, D. G., van Dijk, A. I. J. M., McVicar, T. R., & Adler, R. F. (2019). MSWEP V2 Global 3-Hourly 0.1° Precipitation: Methodology and Quantitative Assessment. *Bulletin of the American Meteorological Society*, 100(3), 473–500. <https://doi.org/10.1175/BAMS-D-17-0138.1>

- Beguiría, S., López-Moreno, J. I., Lorente, A., Seeger, M., & García-Ruiz, J. M. (2003). Assessing the Effect of Climate Oscillations and Land-use Changes on Streamflow in the Central Spanish Pyrenees. *AMBIO: A Journal of the Human Environment*, 32(4), 283–286. <https://doi.org/10.1579/0044-7447-32.4.283>
- Belo-Pereira, M., Dutra, E., & Viterbo, P. (2011). Evaluation of global precipitation data sets over the Iberian Peninsula. *Journal of Geophysical Research Atmospheres*, 116(20), 20101. <https://doi.org/10.1029/2010JD015481>
- Best, M. J., Pryor, M., Clark, D. B., Rooney, G. G., Essery, R. . L. H., Ménard, C. B., Edwards, J. M., Hendry, M. A., Porson, A., Gedney, N., Mercado, L. M., Sitch, S., Blyth, E., Boucher, O., Cox, P. M., Grimmond, C. S. B., & Harding, R. J. (2011). The Joint UK Land Environment Simulator (JULES), model description – Part 1: Energy and water fluxes. *Geoscientific Model Development*, 4(3), 677–699. <https://doi.org/10.5194/gmd-4-677-2011>
- Beven, K., & Freer, J. (2001). Equifinality, data assimilation, and uncertainty estimation in mechanistic modelling of complex environmental systems using the GLUE methodology. *Journal of Hydrology*, 249(1–4), 11–29. [https://doi.org/10.1016/S0022-1694\(01\)00421-8](https://doi.org/10.1016/S0022-1694(01)00421-8)
- Beven, K. J., & Kirkby, M. J. (1979). A physically based, variable contributing area model of basin hydrology. *Hydrological Sciences Bulletin*, 24(1), 43–69. <https://doi.org/10.1080/02626667909491834>
- Biemans, H., Hutjes, R. W. A., Kabat, P., Strengers, B. J., Gerten, D., & Rost, S. (2009). Effects of precipitation uncertainty on discharge calculations for main river basins. *Journal of Hydrometeorology*, 10(4), 1011–1025. <https://doi.org/10.1175/2008JHM1067.1>
- Bierkens, M. F. P., Bell, V. A., Burek, P., Chaney, N., Condon, L. E., David, C. H., de Roo, A., Döll, P., Drost, N., Famiglietti, J. S., Flörke, M., Gochis, D. J., Houser, P., Hut, R., Keune, J., Kollet, S., Maxwell, R. M., Reager, J. T., Samaniego, L., ... Wood, E. F. (2015). Hyper-resolution global hydrological modelling: what is next? *Hydrological Processes*, 29(2), 310–320. <https://doi.org/10.1002/hyp.10391>
- Blauhut, V., Gudmundsson, L., & Stahl, K. (2015). Towards pan-European drought risk maps: quantifying the link between drought indices and reported drought impacts. *Environmental Research Letters*, 10(1), 014008. <https://doi.org/10.1088/1748-9326/10/1/014008>
- Bloomfield, J. P., & Marchant, B. P. (2013). Analysis of groundwater drought building on the standardised precipitation index approach. *Hydrology and Earth System Sciences*, 17(12), 4769–4787. <https://doi.org/10.5194/hess-17-4769-2013>
- Blyth, E. M., Arora, V. K., Clark, D. B., Dadson, S. J., De Kauwe, M. G., Lawrence, D. M., Melton, J. R., Pongratz, J., Turton, R. H., Yoshimura, K., & Yuan, H. (2021). Advances in Land Surface Modelling. In *Current Climate Change Reports* (Vol. 7, Issue 2, pp. 45–71). Springer. <https://doi.org/10.1007/s40641-021-00171-5>
- Boers, N., Bookhagen, B., Marwan, N., & Kurths, J. (2016). Spatiotemporal characteristics and synchronization of extreme rainfall in South America with focus on the Andes Mountain range. *Climate Dynamics*, 46(1–2), 601–617. <https://doi.org/10.1007/S00382-015-2601-6/FIGURES/10>
- Bonaccorso, B., Cancelliere, A., & Rossi, G. (2003). An analytical formulation of return period of drought severity. *Stochastic Environmental Research and Risk Assessment*, 17(3), 157–174. <https://doi.org/10.1007/s00477-003-0127-7>

- Bonan, G. B., Williams, M., Fisher, R. A., & Oleson, K. W. (2014). Modeling stomatal conductance in the earth system: Linking leaf water-use efficiency and water transport along the soil-plant-atmosphere continuum. *Geoscientific Model Development*, 7(5), 2193–2222. <https://doi.org/10.5194/gmd-7-2193-2014>
- Boone, A. A., Best, M., Cuxart, J., Polcher, J., Quintana-Segui, P., Bellvert, J., Brooke, J., Canut, G., & Price, J. (2019). Land Surface Interactions with the Atmosphere over the Iberian Semi-Arid Environment (LIAISE). *AGU Fall Meeting Abstracts*, 2019, GC53H-1227. <https://ui.adsabs.harvard.edu/abs/2019AGUFMGC53H1227B>
- Boone, A., Calvet, J.-C., Joe, J., & Noilhan, J. (1999). Inclusion of a Third Soil Layer in a Land Surface Scheme Using the Force–Restore Method. *Journal of Applied Meteorology and Climatology*, 38(11), 1611–1630. [https://doi.org/10.1175/1520-0450\(1999\)038](https://doi.org/10.1175/1520-0450(1999)038)
- Boone, A., & Etchevers, P. (2001). An Intercomparison of Three Snow Schemes of Varying Complexity Coupled to the Same Land Surface Model: Local-Scale Evaluation at an Alpine Site. *Journal of Hydrometeorology*, 2(4), 374–394. [https://doi.org/https://doi.org/10.1175/1525-7541\(2001\)002<0374:AIOTSS>2.0.CO;2](https://doi.org/https://doi.org/10.1175/1525-7541(2001)002<0374:AIOTSS>2.0.CO;2)
- Boone, A., Habets, F., Noilhan, J., Clark, D., Dirmeyer, P., Fox, S., Gusev, Y., Haddeland, I., Koster, R., Lohmann, D., Mahanama, S., Mitchell, K., Nasonova, O., Niu, G.-Y., Pitman, A., Polcher, J., Shmakin, A. B., Tanaka, K., van den Hurk, B., ... Yang, Z.-L. (2004). The Rhône-Aggregation Land Surface Scheme Intercomparison Project: An Overview. *Journal of Climate*, 17(1), 187–208. [https://doi.org/https://doi.org/10.1175/1520-0442\(2004\)017<0187:TRLSSI>2.0.CO;2](https://doi.org/https://doi.org/10.1175/1520-0442(2004)017<0187:TRLSSI>2.0.CO;2)
- Boone, A., Masson, V., Meyers, T., & Noilhan, J. (2000). The Influence of the Inclusion of Soil Freezing on Simulations by a Soil–Vegetation–Atmosphere Transfer Scheme. *Journal of Applied Meteorology*, 39(9), 1544–1569. [https://doi.org/10.1175/1520-0450\(2000\)039<1544:TIOTIO>2.0.CO;2](https://doi.org/10.1175/1520-0450(2000)039<1544:TIOTIO>2.0.CO;2)
- Boone, A., Samuelsson, P., Gollvik, S., Napoly, A., Jarlan, L., Brun, E., & Decharme, B. (2017). The interactions between soil-biosphere-atmosphere land surface model with a multi-energy balance (ISBA-MEB) option in SURFEXv8-Part 1: Model description. *Geoscientific Model Development*, 10(2), 843–872. <https://doi.org/10.5194/gmd-10-843-2017>
- Boucher, O., Myhre, G., & Myhre, A. (2004). Direct human influence of irrigation on atmospheric water vapour and climate. *Climate Dynamics*, 22(6–7), 597–603. <https://doi.org/10.1007/s00382-004-0402-4>
- Boysen, L. R., Brovkin, V., Arora, V. K., Cadule, P., De Noblet-Ducoudré, N., Kato, E., Pongratz, J., & Gayler, V. (2014). Global and regional effects of land-use change on climate in 21st century simulations with interactive carbon cycle. *Earth System Dynamics*, 5(2), 309–319. <https://doi.org/10.5194/esd-5-309-2014>
- Bradford, R. B. (2000). Drought Events in Europe. In *Drought and Drought Mitigation in Europe* (pp. 7–20). [https://doi.org/10.1007/978-94-015-9472-1\\_2](https://doi.org/10.1007/978-94-015-9472-1_2)
- Bussi, G., Whitehead, P. G., Bowes, M. J., Read, D. S., Prudhomme, C., & Dadson, S. J. (2016). Impacts of climate change, land-use change and phosphorus reduction on phytoplankton in the River Thames (UK). *Science of the Total Environment*, 572, 1507–1519. <https://doi.org/10.1016/j.scitotenv.2016.02.109>
- Calvet, J. C., Gibelin, A. L., Roujean, J. L., Martin, E., Le Moigne, P., Douville, H., & Noilhan,

- J. (2008). Past and future scenarios of the effect of carbon dioxide on plant growth and transpiration for three vegetation types of southwestern France. *Atmospheric Chemistry and Physics*, 8(2), 397–405. <https://doi.org/10.5194/acp-8-397-2008>
- Calvet, J. C., Noilhan, J., Roujean, J. L., Bessemoulin, P., Cabelguenne, M., Olioso, A., & Wigneron, J. P. (1998). An interactive vegetation SVAT model tested against data from six contrasting sites. *Agricultural and Forest Meteorology*, 92(2), 73–95. [https://doi.org/10.1016/S0168-1923\(98\)00091-4](https://doi.org/10.1016/S0168-1923(98)00091-4)
- Calvet, J. C., Rivalland, V., Picon-Cochard, C., & Guehl, J. M. (2004). Modelling forest transpiration and CO<sub>2</sub> fluxes - Response to soil moisture stress. *Agricultural and Forest Meteorology*, 124(3–4), 143–156. <https://doi.org/10.1016/j.agrformet.2004.01.007>
- Calvin, K., & Bond-Lamberty, B. (2018). Integrated human-earth system modeling—state of the science and future directions. *Environmental Research Letters*, 13(6), 063006. <https://doi.org/10.1088/1748-9326/aac642>
- Cancelliere, A., & Salas, J. D. (2004). Drought length properties for periodic-stochastic hydrologic data. *Water Resources Research*, 40(2), 2503. <https://doi.org/10.1029/2002wr001750>
- Carpenter, S. R., Stanley, E. H., & Vander Zanden, M. J. (2011). State of the world's freshwater ecosystems: physical, chemical, and biological changes. *Annual Review of Environment and Resources*, 36, 75–99.
- Catalogne, C. (2012). *Amélioration des méthodes de prédétermination des débits de référence d'étiage en sites peu ou pas jaugés*. Irstea (Lyon), Université Joseph Fourier (Grenoble).
- CHE. (2007). *Plan Especial de Actuación en Situaciones de Alerta y Eventual Sequía en la Cuenca Hidrográfica del Ebro*.
- CHE. (2022). *Plan Hidrológico de la parte española de la Demarcación Hidrográfica del Ebro 2022-2027*.
- Chen, F., & Avissar, R. (1994). Impact of Land-Surface Moisture Variability on Local Shallow Convective Cumulus and Precipitation in Large-Scale Models. *Journal of Applied Meteorology and Climatology*, 33(12), 1382–1401. [https://doi.org/https://doi.org/10.1175/1520-0450\(1994\)033<1382:IOLSMV>2.0.CO;2](https://doi.org/https://doi.org/10.1175/1520-0450(1994)033<1382:IOLSMV>2.0.CO;2)
- Chen, J., Brissette, F. P., Chaumont, D., & Braun, M. (2013). Finding appropriate bias correction methods in downscaling precipitation for hydrologic impact studies over North America. *Water Resources Research*, 49(7), 4187–4205. <https://doi.org/10.1002/wrcr.20331>
- Christensen, J. H., Boberg, F., Christensen, O. B., & Lucas-Picher, P. (2008). On the need for bias correction of regional climate change projections of temperature and precipitation. *Geophysical Research Letters*, 35(20). <https://doi.org/10.1029/2008GL035694>
- Christian, J. I., Basara, J. B., Otkin, J. A., Hunt, E. D., Wakefield, R. A., Flanagan, P. X., & Xiao, X. (2019). A Methodology for Flash Drought Identification: Application of Flash Drought Frequency across the United States. *Journal of Hydrometeorology*, 20(5), 833–846. <https://doi.org/https://doi.org/10.1175/JHM-D-18-0198.1>
- Christian, J. I., Martin, E. R., Basara, J. B., Furtado, J. C., Otkin, J. A., Lowman, L. E. L., Hunt,

- E. D., Mishra, V., & Xiao, X. (2023). Global projections of flash drought show increased risk in a warming climate. *Communications Earth & Environment*, 4(1), 165.
- Clark, D. B., & Gedney, N. (2008). Representing the effects of subgrid variability of soil moisture on runoff generation in a Land surface model. *Journal of Geophysical Research Atmospheres*, 113(10), 10111. <https://doi.org/10.1029/2007JD008940>
- Clark, M. P., Fan, Y., Lawrence, D. M., Adam, J. C., Bolster, D., Gochis, D. J., Hooper, R. P., Kumar, M., Leung, L. R., Mackay, D. S., Maxwell, R. M., Shen, C., Swenson, S. C., & Zeng, X. (2015). Improving the representation of hydrologic processes in Earth System Models. *Water Resources Research*, 51(8), 5929–5956. <https://doi.org/10.1002/2015WR017096>
- Clark, M. P., Nijssen, B., Lundquist, J. D., Kavetski, D., Rupp, D. E., Woods, R. A., Freer, J. E., Gutmann, E. D., Wood, A. W., Brekke, L. D., Arnold, J. R., Gochis, D. J., & Rasmussen, R. M. (2015). A unified approach for process-based hydrologic modeling: 1. Modeling concept. *Water Resources Research*, 51(4), 2498–2514. <https://doi.org/10.1002/2015WR017198>
- Clark, M. P., Slater, A. G., Rupp, D. E., Woods, R. A., Vrugt, J. A., Gupta, H. V, Wagener, T., & Hay, L. E. (2008). Framework for Understanding Structural Errors (FUSE): A modular framework to diagnose differences between hydrological models. *Water Resources Research*, 44(12), 0–02. <https://doi.org/10.1029/2007wr006735>
- Clark, M. P., Vogel, R. M., Lamontagne, J. R., Mizukami, N., Knoben, W. J. M., Tang, G., Gharari, S., Freer, J. E., Whitfield, P. H., Shook, K. R., & Papalexiou, S. M. (2021). The Abuse of Popular Performance Metrics in Hydrologic Modeling. In *Water Resources Research* (Vol. 57, Issue 9, p. e2020WR029001). John Wiley & Sons, Ltd. <https://doi.org/10.1029/2020WR029001>
- Coll, J. R., Aguilar, E., & Ashcroft, L. (2017). Drought variability and change across the Iberian Peninsula. *Theoretical and Applied Climatology*, 130(3–4), 901–916. <https://doi.org/10.1007/s00704-016-1926-3>
- Cook, E. R., Seager, R., Cane, M. A., & Stahle, D. W. (2007). North American drought: Reconstructions, causes, and consequences. *Earth-Science Reviews*, 81(1–2), 93–134. <https://doi.org/10.1016/J.EARSCIREV.2006.12.002>
- Cornes, R. C., van der Schrier, G., van den Besselaar, E. J. M., & Jones, P. D. (2018). An Ensemble Version of the E-OBS Temperature and Precipitation Data Sets. *Journal of Geophysical Research: Atmospheres*, 123(17), 9391–9409. <https://doi.org/10.1029/2017JD028200>
- Cox, P. M., Betts, R. A., Jones, C. D., Spall, S. A., & Totterdell, I. J. (2000). Acceleration of global warming due to carbon-cycle feedbacks in a coupled climate model. *Nature*, 408(6809), 184–187. <https://doi.org/10.1038/35041539>
- Crow, W. T., Kumar, S. V., & Bolten, J. D. (2012). On the utility of land surface models for agricultural drought monitoring. *Hydrology and Earth System Sciences*, 16(9), 3451–3460. <https://doi.org/10.5194/hess-16-3451-2012>
- Dai, A. (2011). Drought under global warming: a review. *Wiley Interdisciplinary Reviews: Climate Change*, 2(1), 45–65. <https://doi.org/10.1002/WCC.81>

- 
- Dai, A., Trenberth, K. E., & Qian, T. (2004). A global dataset of Palmer Drought Severity Index for 1870-2002: Relationship with soil moisture and effects of surface warming. *Journal of Hydrometeorology*, 5(6), 1117–1130. <https://doi.org/10.1175/JHM-386.1>
- Daniel, M., Lemonsu, A., Déqué, M., Somot, S., Alias, A., & Masson, V. (2019). Benefits of explicit urban parameterization in regional climate modeling to study climate and city interactions. *Climate Dynamics*, 52(5–6), 2745–2764. <https://doi.org/10.1007/S00382-018-4289-X/TABLES/8>
- David, C. H., Maidment, D. R., Niu, G.-Y., Yang, Z.-L., Habets, F., & Eijkhout, V. (2011). River Network Routing on the NHDPlus Dataset. *Journal of Hydrometeorology*, 12(5), 913–934. <https://doi.org/10.1175/2011JHM1345.1>
- de Graaf, I. E. M., Gleeson, T., (Rens) van Beek, L. P. H., Sutanudjaja, E. H., & Bierkens, M. F. P. (2019). Environmental flow limits to global groundwater pumping. *Nature*, 574(7776), 90–94. <https://doi.org/10.1038/s41586-019-1594-4>
- de Graaf, I. E. M., Sutanudjaja, E. H., Van Beek, L. P. H., & Bierkens, M. F. P. (2015). A high-resolution global-scale groundwater model. *Hydrology and Earth System Sciences*, 19(2), 823–837. <https://doi.org/10.5194/hess-19-823-2015>
- de Rosnay, P., & Polcher, J. (1998). Modelling root water uptake in a complex land surface scheme coupled to a GCM. *Hydrology and Earth System Sciences*, 2(2/3), 239–255. <https://doi.org/10.5194/hess-2-239-1998>
- de Rosnay, P., Polcher, J., Laval, K., & Sabre, M. (2003). Integrated parameterization of irrigation in the land surface model ORCHIDEE. Validation over Indian Peninsula. *Geophysical Research Letters*, 30(19). <https://doi.org/10.1029/2003GL018024>
- De Troch, R., Hamdi, R., Van de Vyver, H., Geleyn, J. F., & Termonia, P. (2013). Multiscale performance of the ALARO-0 model for simulating extreme summer precipitation climatology in Belgium. *Journal of Climate*, 26(22), 8895–8915. <https://doi.org/10.1175/JCLI-D-12-00844.1>
- De Vrese, P., & Hagemann, S. (2016). Explicit representation of spatial subgrid-scale heterogeneity in an ESM. *Journal of Hydrometeorology*, 17(5), 1357–1371. <https://doi.org/10.1175/JHM-D-15-0080.1>
- Decharme, B., Boone, A., Delire, C., & Noilhan, J. (2011). Local evaluation of the Interaction between Soil Biosphere Atmosphere soil multilayer diffusion scheme using four pedotransfer functions. *Journal of Geophysical Research: Atmospheres*, 116(D20). <https://doi.org/10.1029/2011JD016002>
- Decharme, B., Brun, E., Boone, A., Delire, C., Le Moigne, P., & Morin, S. (2016). Impacts of snow and organic soils parameterization on northern Eurasian soil temperature profiles simulated by the ISBA land surface model. *Cryosphere*, 10(2), 853–877. <https://doi.org/10.5194/tc-10-853-2016>
- Decharme, B., Delire, C., Minvielle, M., Colin, J., Vergnes, J. P., Alias, A., Saint-Martin, D., Séférian, R., Sénési, S., & Voldoire, A. (2019). Recent Changes in the ISBA-CTRIP Land Surface System for Use in the CNRM-CM6 Climate Model and in Global Off-Line Hydrological Applications. *Journal of Advances in Modeling Earth Systems*, 11(5), 1207–1252. <https://doi.org/10.1029/2018MS001545>
-



- Dee, D. P., Uppala, S. M., Simmons, A. J., Berrisford, P., Poli, P., Kobayashi, S., Andrae, U., Balmaseda, M. A., Balsamo, G., Bauer, P., Bechtold, P., Beljaars, A. C. M., van de Berg, L., Bidlot, J., Bormann, N., Delsol, C., Dragani, R., Fuentes, M., Geer, A. J., ... Vitart, F. (2011). The ERA-Interim reanalysis: configuration and performance of the data assimilation system. *Quarterly Journal of the Royal Meteorological Society*, *137*(656), 553–597. <https://doi.org/10.1002/QJ.828>
- Di Baldassarre, G., Martinez, F., Kalantari, Z., & Viglione, A. (2017). Drought and flood in the Anthropocene: Feedback mechanisms in reservoir operation. *Earth System Dynamics*, *8*(1), 225–233. <https://doi.org/10.5194/esd-8-225-2017>
- Di Baldassarre, G., Viglione, A., Carr, G., Kuil, L., Salinas, J. L., & Blöschl, G. (2013). Socio-hydrology: Conceptualising human-flood interactions. *Hydrology and Earth System Sciences*, *17*(8), 3295–3303. <https://doi.org/10.5194/hess-17-3295-2013>
- Di Baldassarre, G., Viglione, A., Carr, G., Kuil, L., Yan, K., Brandimarte, L., & Blöschl, G. (2015). Debates - Perspectives on socio-hydrology: Capturing feedbacks between physical and social processes. In *Water Resources Research* (Vol. 51, Issue 6, pp. 4770–4781). John Wiley & Sons, Ltd. <https://doi.org/10.1002/2014WR016416>
- Dirmeyer, P. A., Fang, G., Wang, Z., Yadav, P., & Milton, A. (2014). Climate change and sectors of the surface water cycle in CMIP5 projections. *Hydrology and Earth System Sciences*, *18*(12), 5317–5329. <https://doi.org/10.5194/hess-18-5317-2014>
- Döll, P., Douville, H., Güntner, A., Müller Schmied, H., & Wada, Y. (2016). Modelling Freshwater Resources at the Global Scale: Challenges and Prospects. In *Surveys in Geophysics* (Vol. 37, Issue 2, pp. 195–221). Springer. <https://doi.org/10.1007/s10712-015-9343-1>
- Döll, P., & Fiedler, K. (2008). Global-scale modeling of groundwater recharge. *Hydrology and Earth System Sciences*, *12*(3), 863–885. <https://doi.org/10.5194/hess-12-863-2008>
- Döll, P., Fiedler, K., & Zhang, J. (2009). Global-scale analysis of river flow alterations due to water withdrawals and reservoirs. *Hydrology and Earth System Sciences*, *13*(12), 2413–2432. <https://doi.org/10.5194/hess-13-2413-2009>
- Döll, P., Hoffmann-Dobrev, H., Portmann, F. T., Siebert, S., Eicker, A., Rodell, M., Strassberg, G., & Scanlon, B. R. (2012). Impact of water withdrawals from groundwater and surface water on continental water storage variations. *Journal of Geodynamics*, *59–60*, 143–156. <https://doi.org/https://doi.org/10.1016/j.jog.2011.05.001>
- Döll, P., Müller Schmied, H., Schuh, C., Portmann, F. T., & Eicker, A. (2014). Global-scale assessment of groundwater depletion and related groundwater abstractions: Combining hydrological modeling with information from well observations and GRACE satellites. *Water Resources Research*, *50*(7), 5698–5720. <https://doi.org/10.1002/2014WR015595>
- Döll, P., & Siebert, S. (2002). Global modeling of irrigation water requirements. *Water Resources Research*, *38*(4), 8-1-8–10. <https://doi.org/10.1029/2001WR000355>
- Domínguez-Castro, F., Ribera, P., García-Herrera, R., Vaquero, J. M., Barriendos, M., Cuadrat, J. M., & Moreno, J. M. (2012). Assessing extreme droughts in Spain during 1750-1850 from rogation ceremonies. In *Climate of the Past* (Vol. 8, Issue 2, pp. 705–722). <https://doi.org/10.5194/cp-8-705-2012>

- Donohue, R. J., Roderick, M. L., & McVicar, T. R. (2007). On the importance of including vegetation dynamics in Budyko's hydrological model. *Hydrology and Earth System Sciences*, *11*(2), 983–995. <https://doi.org/10.5194/hess-11-983-2007>
- Dracup, J. A., Lee, K. S., & Paulson, E. G. (1980a). On the definition of droughts. *Water Resources Research*, *16*(2), 297–302. <https://doi.org/10.1029/WR016i002p00297>
- Dracup, J. A., Lee, K. S., & Paulson, E. G. (1980b). On the statistical characteristics of drought events. *Water Resources Research*, *16*(2), 289–296. <https://doi.org/10.1029/WR016i002p00289>
- Druel, A., Munier, S., Mucia, A., Albergel, C., & Calvet, J.-C. (2022). Implementation of a new crop phenology and irrigation scheme in the ISBA land surface model using SURFEX\_v8.1. *Geoscientific Model Development*, *15*(22), 8453–8471. <https://doi.org/10.5194/GMD-15-8453-2022>
- DÜMENIL, L., & TODINI, E. (1992). A rainfall–runoff scheme for use in the Hamburg climate model. In *Advances in Theoretical Hydrology* (pp. 129–157). Elsevier. <https://doi.org/10.1016/B978-0-444-89831-9.50016-8>
- Durand, Y., Brun, E., Merindol, L., Guyomarc'h, G., Lesaffre, B., & Martin, E. (1993). A meteorological estimation of relevant parameters for snow models. *Annals of Glaciology*, *18*, 65–71. <https://doi.org/10.3189/s0260305500011277>
- Dynesius, M., & Nilsson, C. (1994). Fragmentation and Flow Regulation of River Systems in the Northern Third of the World. *Science*, *266*(5186), 753–762. <https://doi.org/10.1126/science.266.5186.753>
- Ehsani, N., Fekete, B. M., Vörösmarty, C. J., & Tessler, Z. D. (2016). A neural network based general reservoir operation scheme. *Stochastic Environmental Research and Risk Assessment*, *30*(4), 1151–1166. <https://doi.org/10.1007/s00477-015-1147-9>
- Estrela, T., & Quintas, L. (1996). El sistema integrado de modelización precipitación-aportación SIMPA. *Ingeniería Civil, ISSN 0213-8468, N° 104, 1996, Págs. 43-52, 0(104)*, 43–52. <http://ingenieriacivil.cedex.es/index.php/ingenieria-civil/article/view/1153>
- Famiglietti, J. S., Cazenave, A., Eicker, A., Reager, J. T., Rodell, M., & Velicogna, I. (2015). Satellites provide the big picture. *Science*, *349*(6249), 684–685. <https://doi.org/10.1126/science.aac9238>
- Fan, Y., Clark, M., Lawrence, D. M., Swenson, S., Band, L. E., Brantley, S. L., Brooks, P. D., Dietrich, W. E., Flores, A., Grant, G., Kirchner, J. W., Mackay, D. S., McDonnell, J. J., Milly, P. C. D., Sullivan, P. L., Tague, C., Ajami, H., Chaney, N., Hartmann, A., ... Yamazaki, D. (2019). Hillslope Hydrology in Global Change Research and Earth System Modeling. *Water Resources Research*, *55*(2), 1737–1772. <https://doi.org/10.1029/2018WR023903>
- Fan, Y., Li, H., & Miguez-Macho, G. (2013). Global patterns of groundwater table depth. *Science*, *339*(6122), 940–943. <https://doi.org/10.1126/science.1229881>
- Fan, Y., Richard, S., Bristol, R. S., Peters, S. E., Ingebritsen, S. E., Moosdorf, N., Packman, A., Gleeson, T., Zaslavsky, I., Peckham, S., Murdoch, L., Fienen, M., Cardiff, M., Tarboton, D., Jones, N., Hooper, R., Arrigo, J., Gochis, D., Olson, J., & Wolock, D. (2015). DigitalCrust - a 4D data system of material properties for transforming research on crustal

- fluid flow. *Geofluids*, 15(1–2), 372–379. <https://doi.org/10.1111/gfl.12114>
- Fang, K., Shen, C., Kifer, D., & Yang, X. (2017). Prolongation of SMAP to Spatiotemporally Seamless Coverage of Continental U.S. Using a Deep Learning Neural Network. *Geophysical Research Letters*, 44(21), 11,030–11,039. <https://doi.org/10.1002/2017GL075619>
- Farahmand, A., & Aghakouchak, A. (2015). *A generalized framework for deriving nonparametric standardized drought indicators*. <https://doi.org/10.1016/j.advwatres.2014.11.012>
- Faroux, S., Kaptué Tchuenté, A. T., Roujean, J.-L., Masson, V., Martin, E., & Le Moigne, P. (2013). ECOCLIMAP-II/Europe: a twofold database of ecosystems and surface parameters at 1 km resolution based on satellite information for use in land surface, meteorological and climate models. *Geosci. Model Dev*, 6, 563–582. <https://doi.org/10.5194/gmd-6-563-2013>
- Fernández, B., & Salas, J. D. (1999). Return Period and Risk of Hydrologic Events. II: Applications. *Journal of Hydrologic Engineering*, 4(4), 308–316. [https://doi.org/10.1061/\(asce\)1084-0699\(1999\)4:4\(308\)](https://doi.org/10.1061/(asce)1084-0699(1999)4:4(308))
- Firoz, A. B. M., Nauditt, A., Fink, M., & Ribbe, L. (2018). Quantifying human impacts on hydrological drought using a combined modelling approach in a tropical river basin in central Vietnam. In *Hydrology and Earth System Sciences* (Vol. 22, Issue 1, pp. 547–565). Copernicus GmbH. <https://doi.org/10.5194/hess-22-547-2018>
- Fisher, R. A., & Koven, C. D. (2020). Perspectives on the Future of Land Surface Models and the Challenges of Representing Complex Terrestrial Systems. *Journal of Advances in Modeling Earth Systems*, 12(4), e2018MS001453. <https://doi.org/10.1029/2018MS001453>
- Fleig, A. K., Tallaksen, L. M., Hisdal, H., & Demuth, S. (2006). A global evaluation of streamflow drought characteristics. *Hydrology and Earth System Sciences*, 10(4), 535–552. <https://doi.org/10.5194/hess-10-535-2006>
- Fowler, H. J., Ekström, M., Blenkinsop, S., & Smith, A. P. (2007). Estimating change in extreme European precipitation using a multimodel ensemble. *Journal of Geophysical Research Atmospheres*, 112(18), 18104. <https://doi.org/10.1029/2007JD008619>
- Funk, C., Peterson, P., Landsfeld, M., Pedreros, D., Verdin, J., Shukla, S., Husak, G., Rowland, J., Harrison, L., Hoell, A., & Michaelsen, J. (2015). The climate hazards infrared precipitation with stations—a new environmental record for monitoring extremes. *Scientific Data* 2015 2:1, 2(1), 1–21. <https://doi.org/10.1038/sdata.2015.66>
- Gandin, L. S. (1966). Objective analysis of meteorological fields. Translated from the Russian. Jerusalem (Israel Program for Scientific Translations). *Quarterly Journal of the Royal Meteorological Society*, 92(393), 447–447. <https://doi.org/10.1002/qj.49709239320>
- Gaona, J., Quintana-Seguí, P., Escorihuela, M. J., Boone, A., & Llasat, M. C. (2022). Interactions between precipitation, evapotranspiration and soil-moisture-based indices to characterize drought with high-resolution remote sensing and land-surface model data. *Natural Hazards and Earth System Sciences*, 22(10), 3461–3485. <https://doi.org/10.5194/nhess-22-3461-2022>
- García-Herrera, R., Paredes, D., Trigo, R. M., Trigo, I. F., Hernández, E., Barriopedro, D., & Mendes, M. A. (2007). The outstanding 2004/05 drought in the Iberian Peninsula: Associated atmospheric circulation. *Journal of Hydrometeorology*, 8(3), 483–498.

---

<https://doi.org/10.1175/JHM578.1>

- García-Valdecasas Ojeda, M., Gámiz-Fortis, S. R., Castro-Díez, Y., & Esteban-Parra, M. J. (2017). Evaluation of WRF capability to detect dry and wet periods in Spain using drought indices. *Journal of Geophysical Research*, *122*(3), 1569–1594. <https://doi.org/10.1002/2016JD025683>
- Garcia, F., Folton, N., & Oudin, L. (2017). Which objective function to calibrate rainfall–runoff models for low-flow index simulations? *Hydrological Sciences Journal*, *62*(7), 1149–1166. <https://doi.org/10.1080/02626667.2017.1308511>
- Garcia Gonzalez, R., Verhoef, A., Luigi Vidale, P., & Braud, I. (2012). Incorporation of water vapor transfer in the JULES land surface model: Implications for key soil variables and land surface fluxes. *Water Resources Research*, *48*(5). <https://doi.org/10.1029/2011WR011811>
- Garrote, L. (2017). Managing Water Resources to Adapt to Climate Change: Facing Uncertainty and Scarcity in a Changing Context. *Water Resources Management*, *31*(10), 2951–2963. <https://doi.org/10.1007/s11269-017-1714-6>
- Garrote, L., Granados, A., & Iglesias, A. (2016). Strategies to reduce water stress in Euro-Mediterranean river basins. *Science of The Total Environment*, *543*, 997–1009. <https://doi.org/10.1016/j.scitotenv.2015.04.106>
- Garrote, L., Iglesias, A., Granados, A., Mediero, L., & Martin-Carrasco, F. (2015). Quantitative Assessment of Climate Change Vulnerability of Irrigation Demands in Mediterranean Europe. *Water Resources Management*, *29*(2), 325–338. <https://doi.org/10.1007/s11269-014-0736-6>
- Gascoin, S., Ducharne, A., Ribstein, P., Carli, M., & Habets, F. (2009). Adaptation of a catchment-based land surface model to the hydrogeological setting of the Somme River basin (France). *Journal of Hydrology*, *368*(1–4), 105–116. <https://doi.org/10.1016/j.jhydrol.2009.01.039>
- Gelati, E., Decharme, B., Calvet, J. C., Minvielle, M., Polcher, J., Fairbairn, D., & Weedon, G. P. (2018). Hydrological assessment of atmospheric forcing uncertainty in the Euro-Mediterranean area using a land surface model. *Hydrology and Earth System Sciences*, *22*(4), 2091–2115. <https://doi.org/10.5194/hess-22-2091-2018>
- Gentine, P., Pritchard, M., Rasp, S., Reinaudi, G., & Yacalis, G. (2018). Could Machine Learning Break the Convection Parameterization Deadlock? *Geophysical Research Letters*, *45*(11), 5742–5751. <https://doi.org/10.1029/2018GL078202>
- Gericke, O. J., & Smithers, J. C. (2014). Revue des méthodes d'évaluation du temps de réponse d'un bassin versant pour l'estimation du débit de pointe. *Hydrological Sciences Journal*, *59*(11), 1935–1971. <https://doi.org/10.1080/02626667.2013.866712>
- Getirana, A. C. V., Boone, A., & Peugeot, C. (2014). Evaluating LSM-based water budgets over a West African basin assisted with a river routing scheme. *Journal of Hydrometeorology*, *15*(6), 2331–2346. <https://doi.org/10.1175/JHM-D-14-0012.1>
- Getirana, A. C. V., Boone, A., Yamazaki, D., & Mognard, N. (2013). Automatic parameterization of a flow routing scheme driven by radar altimetry data : Evaluation in the Amazon basin. *Water Resources Research*, *49*(1), 614–629. <https://doi.org/10.1002/wrcr.20077>

- Gibelin, A. L., Calvet, J. C., Roujean, J. L., Jarlan, L., & Los, S. O. (2006). Ability of the land surface model ISBA-A-gs to simulate leaf area index at the global scale: Comparison with satellites products. *Journal of Geophysical Research Atmospheres*, *111*(18). <https://doi.org/10.1029/2005JD006691>
- Gioia, A., Iacobellis, V., Manfreda, S., & Fiorentino, M. (2008). Runoff thresholds in derived flood frequency distributions. *Hydrology and Earth System Sciences*, *12*(6), 1295–1307. <https://doi.org/10.5194/hess-12-1295-2008>
- Giorgi, F., Marinucci, M. R., & Visconti, G. (1990). Use of a limited-area model nested in a general circulation model for regional climate simulation over Europe. *Journal of Geophysical Research: Atmospheres*, *95*(D11), 18413–18431. <https://doi.org/10.1029/JD095ID11P18413>
- Gleason, C. J., & Smith, L. C. (2014). Toward global mapping of river discharge using satellite images and at-many-stations hydraulic geometry. *Proceedings of the National Academy of Sciences of the United States of America*, *111*(13), 4788–4791. <https://doi.org/10.1073/pnas.1317606111>
- Gleeson, T., Wada, Y., Bierkens, M. F. P., & Van Beek, L. P. H. (2012). Water balance of global aquifers revealed by groundwater footprint. *Nature*, *488*(7410), 197–200.
- Gober, P., & Wheeler, H. S. (2015). Debates - Perspectives on socio-hydrology: Modeling flood risk as a public policy problem. *Water Resources Research*, *51*(6), 4782–4788. <https://doi.org/10.1002/2015WR016945>
- González-Hidalgo, J. C., Vicente-Serrano, S. M., Peña-Angulo, D., Salinas, C., Tomas-Burguera, M., & Beguería, S. (2018). High-resolution spatio-temporal analyses of drought episodes in the western Mediterranean basin (Spanish mainland, Iberian Peninsula). *Acta Geophysica*, *66*(3), 381–392. <https://doi.org/10.1007/s11600-018-0138-x>
- Gouveia, C. M., Bastos, A., Trigo, R. M., & Dacamara, C. C. (2012). Drought impacts on vegetation in the pre- and post-fire events over Iberian Peninsula. *Natural Hazards and Earth System Science*, *12*(10), 3123–3137. <https://doi.org/10.5194/nhess-12-3123-2012>
- Graf, W. L. (1999). Dam nation: A geographic census of american dams and their large-scale hydrologic impacts. *Water Resources Research*, *35*(4), 1305–1311. <https://doi.org/10.1029/1999WR900016>
- Gu, L., Chen, J., Yin, J., C Sullivan, S., Wang, H. M., Guo, S., Zhang, L., & Kim, J. S. (2020). Projected increases in magnitude and socioeconomic exposure of global droughts in 1.5 and 2°C warmer climates. *Hydrology and Earth System Sciences*, *24*(1), 451–472. <https://doi.org/10.5194/hess-24-451-2020>
- Gudmundsson, L., Bremnes, J. B., Haugen, J. E., & Engen-Skaugen, T. (2012). Technical Note: Downscaling RCM precipitation to the station scale using statistical transformations – a comparison of methods. *Hydrology and Earth System Sciences*, *16*(9), 3383–3390. <https://doi.org/10.5194/hess-16-3383-2012>
- Gudmundsson, L., Tallaksen, L. M., Stahl, K., Clark, D. B., Dumont, E., Hagemann, S., Bertrand, N., Gerten, D., Heinke, J., Hanasaki, N., Voss, F., & Koirala, A. S. (2012). Comparing large-scale hydrological model simulations to observed runoff percentiles in Europe. *Journal of Hydrometeorology*, *13*(2), 604–620. <https://doi.org/10.1175/JHM-D-11-083.1>

- Guerrero-Salazar, P., & Jevjevich, V. (1975). Analysis of Drought Characteristics by The Theory of Runs. *Hydrology Papers* 80, 80, 53.
- Guimberteau, M., Drapeau, G., Ronchail, J., Sultan, B., Polcher, J., Martinez, J. M., Prigent, C., Guyot, J. L., Cochonneau, G., Espinoza, J. C., Filizola, N., Fraizy, P., Lavado, W., De Oliveira, E., Pombosa, R., Noriega, L., & Vauchel, P. (2012). Discharge simulation in the sub-basins of the Amazon using ORCHIDEE forced by new datasets. *Hydrology and Earth System Sciences*, 16(3), 911–935. <https://doi.org/10.5194/hess-16-911-2012>
- Guimberteau, M., Ducharme, A., Ciais, P., Boisier, J. P., Peng, S., De Weirtdt, M., & Verbeeck, H. (2014). Testing conceptual and physically based soil hydrology schemes against observations for the Amazon Basin. *Geoscientific Model Development*, 7(3), 1115–1136. <https://doi.org/10.5194/gmd-7-1115-2014>
- Guimberteau, M., Laval, K., Perrier, A., & Polcher, J. (2012). Global effect of irrigation and its impact on the onset of the Indian summer monsoon. *Climate Dynamics*, 39(6), 1329–1348. <https://doi.org/10.1007/s00382-011-1252-5>
- Guinaldo, T., Munier, S., Le Moigne, P., Boone, A., Decharme, B., Choulga, M., & Leroux, D. J. (2021). Parametrization of a lake water dynamics model MLake in the ISBA-CTRIP land surface system (SURFEX v8.1). *Geoscientific Model Development*, 14(3), 1309–1344. <https://doi.org/10.5194/gmd-14-1309-2021>
- Gupta, H. V., Kling, H., Yilmaz, K. K., Martinez, G. F., & Kling, H. (2009). Decomposition of the mean squared error and NSE performance criteria: Implications for improving hydrological modelling. *Journal of Hydrology*, 377, 80–91. <https://doi.org/10.1016/j.jhydrol.2009.08.003>
- Gustard, A., Bullock, A., & Dixon, J. M. (1992). *Low flow estimation in the United Kingdom*.
- Guswa, A. J. (2008). The influence of climate on root depth: A carbon cost-benefit analysis. *Water Resources Research*, 44(2). <https://doi.org/10.1029/2007WR006384>
- Habets, F., Boone, A., Champeaux, J. L., Etchevers, P., Franchistéguy, L., Leblois, E., Ledoux, E., Le Moigne, P., Martin, E., Morel, S., Noilhan, J., Seguí, P. Q., Rousset-Regimbeau, F., & Viennot, P. (2008). The SAFRAN-ISBA-MODCOU hydrometeorological model applied over France. *Journal of Geophysical Research Atmospheres*, 113(6). <https://doi.org/10.1029/2007JD008548>
- Habets, F., Boone, A., & Noilhan, J. (2003). Simulation of a Scandinavian basin using the diffusion transfer version of ISBA. *Global and Planetary Change*, 38(1–2), 137–149. [https://doi.org/10.1016/S0921-8181\(03\)00016-X](https://doi.org/10.1016/S0921-8181(03)00016-X)
- Habets, F., Noilhan, J., Golaz, C., Goutorbe, J. P., Lacarrère, P., Leblois, E., Ledoux, E., Martin, E., Ottlé, C., & Vidal-Madjar, D. (1999). The ISBA surface scheme in a macroscale hydrological model applied to the Hapex-Mobilhy area. Part I: Model and database. *Journal of Hydrology*, 217(1–2), 75–96. [https://doi.org/10.1016/S0022-1694\(99\)00019-0](https://doi.org/10.1016/S0022-1694(99)00019-0)
- Habib, E., Haile, A. T., Tian, Y., & Joyce, R. J. (2012). Evaluation of the High-Resolution CMORPH Satellite Rainfall Product Using Dense Rain Gauge Observations and Radar-Based Estimates. *Journal of Hydrometeorology*, 13(6), 1784–1798. <https://doi.org/10.1175/JHM-D-12-017.1>
- Haddeland, I., Heinke, J., Biemans, H., Eisner, S., Flörke, M., Hanasaki, N., Konzmann, M.,

- Ludwig, F., Masaki, Y., Schewe, J., Stacke, T., Tessler, Z. D., Wada, Y., & Wisser, D. (2014). Global water resources affected by human interventions and climate change. *Proceedings of the National Academy of Sciences of the United States of America*, *111*(9), 3251–3256. <https://doi.org/10.1073/pnas.1222475110>
- Haddeland, I., Skaugen, T., & Lettenmaier, D. P. (2006). Anthropogenic impacts on continental surface water fluxes. *Geophysical Research Letters*, *33*(8). <https://doi.org/10.1029/2006GL026047>
- Hanasaki, N., Fujimori, S., Yamamoto, T., Yoshikawa, S., Masaki, Y., Hijioka, Y., Kainuma, M., Kanamori, Y., Masui, T., & Takahashi, K. (2013). A global water scarcity assessment under Shared Socio-economic Pathways–Part 2: Water availability and scarcity. *Hydrology and Earth System Sciences*, *17*(7), 2393–2413.
- Hanasaki, N., Yoshikawa, S., Pokhrel, Y., & Kanae, S. (2018). A global hydrological simulation to specify the sources of water used by humans. *Hydrology and Earth System Sciences*, *22*(1), 789–817. <https://doi.org/10.5194/hess-22-789-2018>
- Hannaford, J., Lloyd-Hughes, B., Keef, C., Parry, S., & Prudhomme, C. (2011). Examining the large-scale spatial coherence of European drought using regional indicators of precipitation and streamflow deficit. *Hydrological Processes*, *25*(7), 1146–1162. <https://doi.org/https://doi.org/10.1002/hyp.7725>
- Hannah, D. M., Wood, P. J., & Sadler, J. P. (2004). Ecohydrology and hydroecology: a ‘new paradigm’? *Hydrological Processes*, *18*(17), 3439–3445.
- Hao, Z., AghaKouchak, A., Nakhjiri, N., & Farahmand, A. (2014). Global integrated drought monitoring and prediction system. *Scientific Data*, *1*, 140001. <https://doi.org/10.1038/sdata.2014.1>
- Hernandez-Mora, N., Garrido, A., Gil, M., & Rodríguez-Casado, R. (2013). *La sequía 2005-2008 en la cuenca del Ebro: Vulnerabilidad, impactos y medidas de gestión*. Tech. rep., Universidad Politécnica de Madrid – Centro de Estudios e Investigación para Gestión de Riesgos Agrarios y Medioambientales – CEIGRAM.
- Herrera, S., Fernández, J., & Gutiérrez, J. M. (2016). Update of the Spain02 gridded observational dataset for EURO-CORDEX evaluation: Assessing the effect of the interpolation methodology. *International Journal of Climatology*, *36*(2), 900–908. <https://doi.org/10.1002/joc.4391>
- Herrera, S., Fita, L., Fernández, J., & Gutiérrez, J. M. (2010). Evaluation of the mean and extreme precipitation regimes from the ENSEMBLES regional climate multimodel simulations over Spain. *Journal of Geophysical Research Atmospheres*, *115*(21), 21117. <https://doi.org/10.1029/2010JD013936>
- Hersbach, H., Bell, B., Berrisford, P., Hirahara, S., Horányi, A., Muñoz-Sabater, J., Nicolas, J., Peubey, C., Radu, R., Schepers, D., Simmons, A., Soci, C., Abdalla, S., Abellan, X., Balsamo, G., Bechtold, P., Biavati, G., Bidlot, J., Bonavita, M., ... Thépaut, J. N. (2020). The ERA5 global reanalysis. *Quarterly Journal of the Royal Meteorological Society*, *146*(730), 1999–2049. <https://doi.org/10.1002/qj.3803>
- Hisdal, H., Stahl, K., Tallaksen, L. M., & Demuth, S. (2001). Have streamflow droughts in Europe become more severe or frequent? *International Journal of Climatology*, *21*(3), 317–333. <https://doi.org/10.1002/joc.619>

- Hisdal, H., Tallaksen, L. M., Clausen, B., Peters, E., Gustard, A., & VanLauen, H. (2004). Hydrological drought characteristics. *Developments in Water Science*, 48(5), 139–198.
- Hoerling, M., Eischeid, J., Perlwitz, J., Quan, X., Zhang, T., & Pegion, P. (2012). On the increased frequency of Mediterranean drought. *J. Clim.*, 25(6), 2146–2161. <https://doi.org/10.1175/jcli-d-11-00296.1>
- Hofstra, N., Haylock, M., New, M., Jones, P., & Frei, C. (2008). Comparison of six methods for the interpolation of daily, European climate data. *Journal of Geophysical Research: Atmospheres*, 113(D21), 21110. <https://doi.org/10.1029/2008JD010100>
- Hogue, T. S., Bastidas, L., Gupta, H., Sorooshian, S., Mitchell, K., & Emmerich, W. (2005). Evaluation and transferability of the Noah land surface model in semiarid environments. *Journal of Hydrometeorology*, 6(1), 68–84. <https://doi.org/10.1175/JHM-402.1>
- Huang, H. Y., & Margulis, S. A. (2009). On the impact of surface heterogeneity on a realistic convective boundary layer. *Water Resources Research*, 45(4). <https://doi.org/10.1029/2008WR007175>
- Huang, Z., Tang, Q., Lo, M. H., Liu, X., Lu, H., Zhang, X., & Leng, G. (2019). The influence of groundwater representation on hydrological simulation and its assessment using satellite-based water storage variation. *Hydrological Processes*, 33(8), 1218–1230. <https://doi.org/10.1002/HYP.13393>
- Huffman, G. J., Bolvin, D. T., Braithwaite, D., Hsu, K., Joyce, R., Kidd, C., Nelkin, E. J., & Xie, P. (2014). *NASA Global Precipitation Measurement (GPM) Integrated Multi-Satellite Retrievals for GPM (IMERG)*. NASA/GSFC Algorithm Theoretical Basis Doc.
- Iglesias, A., & Garrote, L. (2015). Adaptation strategies for agricultural water management under climate change in Europe. *Agricultural Water Management*, 155, 113–124. <https://doi.org/https://doi.org/10.1016/j.agwat.2015.03.014>
- Iglesias, A., Garrote, L., Flores, F., & Moneo, M. (2007). Challenges to manage the risk of water scarcity and climate change in the Mediterranean. *Water Resources Management*, 21(5), 775–788. <https://doi.org/10.1007/s11269-006-9111-6>
- Iglesias, A., Quiroga, S., Moneo, M., & Garrote, L. (2012). From climate change impacts to the development of adaptation strategies: Challenges for agriculture in Europe. *Climatic Change*, 112(1), 143–168. <https://doi.org/10.1007/s10584-011-0344-x>
- Immerzeel, W. W., Lutz, A. F., Andrade, M., Bahl, A., Biemans, H., Bolch, T., Hyde, S., Brumby, S., Davies, B. J., Elmore, A. C., Emmer, A., Feng, M., Fernández, A., Haritashya, U., Kargel, J. S., Koppes, M., Kraaijenbrink, P. D. A., Kulkarni, A. V., Mayewski, P. A., ... Baillie, J. E. M. (2019). Importance and vulnerability of the world's water towers. *Nature* 2019 577:7790, 577(7790), 364–369. <https://doi.org/10.1038/s41586-019-1822-y>
- Isotta, F. A., Vogel, R., & Frei, C. (2014). Evaluation of European regional reanalyses and downscalings for precipitation in the Alpine region. *Meteorologische Zeitschrift*, 24(1), 15–37. <https://doi.org/10.1127/metz/2014/0584>
- Jacob, D., Petersen, J., Eggert, B., Alias, A., Christensen, O. B., Bouwer, L. M., Braun, A., Colette, A., Déqué, M., Georgievski, G., Georgopoulou, E., Gobiet, A., Menut, L., Nikulin, G., Haensler, A., Hempelmann, N., Jones, C., Keuler, K., Kovats, S., ... Yiou, P. (2014). EURO-CORDEX: New high-resolution climate change projections for European impact



- research. *Regional Environmental Change*, 14(2), 563–578. <https://doi.org/10.1007/S10113-013-0499-2/FIGURES/8>
- Joetzjer, E., Douville, H., Delire, C., Ciais, P., Decharme, B., & Tyteca, S. (2013). Hydrologic benchmarking of meteorological drought indices at interannual to climate change timescales: A case study over the Amazon and Mississippi river basins. *Hydrology and Earth System Sciences*, 17(12), 4885–4895. <https://doi.org/10.5194/hess-17-4885-2013>
- Joyce, R. J., Janowiak, J. E., Arkin, P. A., & Xie, P. (2004). CMORPH: A method that produces global precipitation estimates from passive microwave and infrared data at high spatial and temporal resolution. *Journal of Hydrometeorology*, 5(3), 487–503. [https://doi.org/10.1175/1525-7541\(2004\)005<0487:CAMTPG>2.0.CO;2](https://doi.org/10.1175/1525-7541(2004)005<0487:CAMTPG>2.0.CO;2)
- Keyantash, J., & Dracup, J. A. (2002). The quantification of drought: An evaluation of drought indices. *Bulletin of the American Meteorological Society*, 83(8), 1167–1180. <https://doi.org/10.-0477>
- Kidd, C., Becker, A., Huffman, G. J., Muller, C. L., Joe, P., Skofronick-Jackson, G., & Kirschaum, D. B. (2017). So, how much of the Earth's surface is covered by rain gauges? *Bulletin of the American Meteorological Society*, 98(1), 69–78. <https://doi.org/10.1175/BAMS-D-14-00283.1>
- Kidd, C., & Huffman, G. (2011). Global precipitation measurement. In *Meteorological Applications* (Vol. 18, Issue 3, pp. 334–353). John Wiley & Sons, Ltd. <https://doi.org/10.1002/met.284>
- Kirkby, M. J., Bracken, L. J., & Shannon, J. (2005). The influence of rainfall distribution and morphological factors on runoff delivery from dryland catchments in SE Spain. *Catena*, 62(2–3), 136–156. <https://doi.org/10.1016/j.catena.2005.05.002>
- Knoben, W. J. M., Freer, J. E., & Woods, R. A. (2019). Technical note: Inherent benchmark or not? Comparing Nash-Sutcliffe and Kling-Gupta efficiency scores. *Hydrology and Earth System Sciences*, 23(10), 4323–4331. <https://doi.org/10.5194/hess-23-4323-2019>
- KO, M.-K., & Tarhule, A. (1994). Streamflow droughts of northern Nigerian rivers. *Hydrological Sciences Journal*, 39(1), 19–34.
- Kumar, R., Samaniego, L., & Attinger, S. (2010). The effects of spatial discretization and model parameterization on the prediction of extreme runoff characteristics. *Journal of Hydrology*, 392(1–2), 54–69. <https://doi.org/10.1016/j.jhydrol.2010.07.047>
- Lafaysse, M., Hingray, B., Etchevers, P., Martin, E., & Obled, C. (2011). Influence of spatial discretization, underground water storage and glacier melt on a physically-based hydrological model of the Upper Durance River basin. *Journal of Hydrology*, 403(1–2), 116–129. <https://doi.org/10.1016/J.JHYDROL.2011.03.046>
- Lafon, T., Dadson, S., Buys, G., & Prudhomme, C. (2013). Bias correction of daily precipitation simulated by a regional climate model: A comparison of methods. *International Journal of Climatology*, 33(6), 1367–1381. <https://doi.org/10.1002/joc.3518>
- Lawrence, D. M., Fisher, R. A., Koven, C. D., Oleson, K. W., Swenson, S. C., Bonan, G., Collier, N., Ghimire, B., van Kampenhout, L., Kennedy, D., Kluzek, E., Lawrence, P. J., Li, F., Li, H., Lombardozzi, D., Riley, W. J., Sacks, W. J., Shi, M., Vertenstein, M., ... Zeng, X. (2019). The Community Land Model Version 5: Description of New Features,

- Benchmarking, and Impact of Forcing Uncertainty. *Journal of Advances in Modeling Earth Systems*, 11(12), 4245–4287. <https://doi.org/10.1029/2018MS001583>
- Lawrence, D. M., & Slater, A. G. (2008). Incorporating organic soil into a global climate model. *Climate Dynamics*, 30(2–3), 145–160. <https://doi.org/10.1007/s00382-007-0278-1>
- Lawrence, P. J., Feddema, J. J., Bonan, G. B., Meehl, G. A., O’Neill, B. C., Oleson, K. W., Levis, S., Lawrence, D. M., Kluzek, E., Lindsay, K., & Thornton, P. E. (2012). Simulating the biogeochemical and biogeophysical impacts of transient land cover change and wood harvest in the Community Climate System Model (CCSM4) from 1850 to 2100. *Journal of Climate*, 25(9), 3071–3095. <https://doi.org/10.1175/JCLI-D-11-00256.1>
- Le Moigne, P., Besson, F., Martin, E., Boé, J., Boone, A., Decharme, B., Etchevers, P., Faroux, S., Habets, F., Lafaysse, M., Leroux, D., & Rousset-Regimbeau, F. (2020). The latest improvements with SURFEX v8.0 of the Safran-Isba-Modcou hydrometeorological model for France. *Geoscientific Model Development*, 13(9), 3925–3946. <https://doi.org/10.5194/GMD-13-3925-2020>
- Lehner, B., Döll, P., Alcamo, J., Henrichs, T., & Kaspar, F. (2006). Estimating the Impact of Global Change on Flood and Drought Risks in Europe: A Continental, Integrated Analysis. *Climatic Change 2006 75:3*, 75(3), 273–299. <https://doi.org/10.1007/S10584-006-6338-4>
- Lehner, B., Liermann, C. R., Revenga, C., Vörösmarty, C., Fekete, B., Crouzet, P., Döll, P., Endejan, M., Frenken, K., & Magome, J. (2011). High-resolution mapping of the world’s reservoirs and dams for sustainable river-flow management. *Frontiers in Ecology and the Environment*, 9(9), 494–502.
- Leng, G., Huang, M., Tang, Q., Gao, H., & Leung, L. R. (2014). Modeling the effects of groundwater-fed irrigation on terrestrial hydrology over the conterminous United States. *Journal of Hydrometeorology*, 15(3), 957–972. <https://doi.org/10.1175/JHM-D-13-049.1>
- Leng, G., Huang, M., Tang, Q., & Leung, L. R. (2015). A modeling study of irrigation effects on global surface water and groundwater resources under a changing climate. *Journal of Advances in Modeling Earth Systems*, 7(3), 1285–1304.
- Leroux, D. J., Calvet, J. C., Munier, S., & Albergel, C. (2018). Using satellite-derived vegetation products to evaluate LDAS-Monde over the Euro-Mediterranean Area. *Remote Sensing*, 10(8), 1199. <https://doi.org/10.3390/rs10081199>
- Lewis, S. L., & Maslin, M. A. (2015). Defining the Anthropocene. *Nature*, 519(7542), 171–180. <https://doi.org/10.1038/nature14258>
- Liang, X., Lettenmaier, D. P., & Wood, E. F. (1996). One-dimensional statistical dynamic representation of subgrid spatial variability of precipitation in the two-layer variable infiltration capacity model. *Journal of Geophysical Research: Atmospheres*, 101(D16), 21403–21422.
- Linés, C., Iglesias, A., Garrote, L., Sotés, V., & Werner, M. (2018). Do users benefit from additional information in support of operational drought management decisions in the Ebro basin? *Hydrology and Earth System Sciences*, 22(11), 5901–5917. <https://doi.org/10.5194/hess-22-5901-2018>
- Linés, C., Werner, M., & Bastiaanssen, W. (2017). The predictability of reported drought events and impacts in the Ebro Basin using six different remote sensing data sets. *Hydrology and*

- 
- Earth System Sciences*, 21(9), 4747–4765. <https://doi.org/10.5194/hess-21-4747-2017>
- Liu, J., Zhao, D., Gerbens-Leenes, P. W., & Guan, D. (2015). China's rising hydropower demand challenges water sector. *Scientific Reports*, 5(1), 11446. <https://doi.org/10.1038/srep11446>
- Liu, X., Yang, T., Hsu, K., Liu, C., & Sorooshian, S. (2017). Evaluating the streamflow simulation capability of PERSIANN-CDR daily rainfall products in two river basins on the Tibetan Plateau. *Hydrology and Earth System Sciences*, 21(1), 169–181. <https://doi.org/10.5194/HESS-21-169-2017>
- Liu, Z., Wang, Y., Xu, Z., & Duan, Q. (2019). Conceptual hydrological models. In *Handbook of hydrometeorological ensemble forecasting* (pp. 389–411). Springer.
- Lobell, D., Bala, G., Mirin, A., Phillips, T., Maxwell, R., & Rotman, D. (2009). Regional differences in the influence of irrigation on climate. *Journal of Climate*, 22(8), 2248–2255. <https://doi.org/10.1175/2008JCLI2703.1>
- Lohmann, D. A. G., Nolte-Holube, R., & Raschke, E. (1996). A large-scale horizontal routing model to be coupled to land surface parametrization schemes. *Tellus A*, 48(5), 708–721.
- López-Moreno, J. I., Beniston, M., & García-Ruiz, J. M. (2008). Environmental change and water management in the Pyrenees: Facts and future perspectives for Mediterranean mountains. *Global and Planetary Change*, 61(3–4), 300–312. <https://doi.org/10.1016/J.GLOPLACHA.2007.10.004>
- López-Moreno, J. I., & García-Ruiz, J. M. (2004). Influence of snow accumulation and snowmelt on streamflow in the central Spanish Pyrenees / Influence de l'accumulation et de la fonte de la neige sur les écoulements dans les Pyrénées centrales espagnoles. *Hydrological Sciences Journal*, 49(5). <https://doi.org/10.1623/hysj.49.5.787.55135>
- López-Moreno, J. I., Vicente-Serrano, S. M., Begueria, S., Garcia-Ruiz, J. M., Portela, M. M., & Almeida, A. B. (2009). Dam effects on droughts magnitude and duration in a transboundary basin: The lower river tagus, pain and Portugal. *Water Resources Research*, 45(2), 2405. <https://doi.org/10.1029/2008WR007198>
- López-Moreno, J. I., Vicente-Serrano, S. M., Moran-Tejeda, E., Zabalza, J., Lorenzo-Lacruz, J., & García-Ruiz, J. M. (2011). Impact of climate evolution and land use changes on water yield in the ebro basin. *Hydrology and Earth System Sciences*, 15(1), 311–322. <https://doi.org/10.5194/hess-15-311-2011>
- López, R., & Justribó, C. (2010). The hydrological significance of mountains: a regional case study, the Ebro River basin, northeast Iberian Peninsula. *Hydrological Sciences Journal*, 55(2), 223–233. <https://doi.org/10.1080/02626660903546126>
- Lovat, A., Vincendon, B., & Ducrocq, V. (2019). Assessing the impact of resolution and soil datasets on flash-flood modelling. *Hydrology and Earth System Sciences*, 23(3), 1801–1818. <https://doi.org/10.5194/hess-23-1801-2019>
- Maraun, D. (2016). Bias Correcting Climate Change Simulations - a Critical Review. *Current Climate Change Reports*, 2(4), 211–220. <https://doi.org/10.1007/S40641-016-0050-X/FIGURES/3>
- Mardhel, V., Pinson, S., & Allier, D. (2021). Description of an indirect method (IDPR) to
-

- determine spatial distribution of infiltration and runoff and its hydrogeological applications to the French territory. *Journal of Hydrology*, 592, 125609. <https://doi.org/10.1016/j.jhydrol.2020.125609>
- Marsh, G. P. (2003). *Man and nature*. University of Washington Press.
- Masson, V., Le Moigne, P., Martin, E., Faroux, S., Alias, A., Alkama, R., Belamari, S., Barbu, A., Boone, A., Bouyssel, F., Brousseau, P., Brun, E., Calvet, J. C., Carrer, D., Decharme, B., Delire, C., Donier, S., Essauouini, K., Gibelin, A. L., ... Voldoire, A. (2013). The SURFEXv7.2 land and ocean surface platform for coupled or offline simulation of earth surface variables and fluxes. *Geoscientific Model Development*, 6(4), 929–960. <https://doi.org/10.5194/gmd-6-929-2013>
- Mathevet, T., Michel, C., Andréassian, V., & Perrin, C. (2006). *Large Sample Basin Experiments for Hydrological Model Parameterization: Results of the Model Parameter Experiment-MOPEX A bounded version of the Nash-Sutcliffe criterion for better model assessment on large sets of basins*. 307.
- Maxwell, R. M., & Kollet, S. J. (2008). Interdependence of groundwater dynamics and land-energy feedbacks under climate change. *Nature Geoscience*, 1(10), 665–669. <https://doi.org/10.1038/ngeo315>
- Maxwell, R. M., & Miller, N. L. (2004). On the development of a coupled land surface and groundwater model. *Developments in Water Science*, 55(PART 2), 1503–1510. [https://doi.org/10.1016/S0167-5648\(04\)80161-8](https://doi.org/10.1016/S0167-5648(04)80161-8)
- McFEETERS, S. K. (1996). The use of the Normalized Difference Water Index (NDWI) in the delineation of open water features. *International Journal of Remote Sensing*, 17(7), 1425–1432. <https://doi.org/10.1080/01431169608948714>
- Mckee, T. B., Doesken, N. J., & Kleist, J. (1993). The relationship of drought frequency and duration to time scales. *AMS 8th Conference on Applied Climatology, January*, 179–184. <https://doi.org/citeulike-article-id:10490403>
- McMillan, H., Montanari, A., Cudennec, C., Savenije, H., Kreibich, H., Krueger, T., Liu, J., Mejia, A., Van Loon, A., Aksoy, H., Di Baldassarre, G., Huang, Y., Mazvimavi, D., Rogger, M., Sivakumar, B., Bibikova, T., Castellarin, A., Chen, Y., Finger, D., ... Xia, J. (2016). Panta Rhei 2013-2015: Global perspectives on hydrology, society and change. *Hydrological Sciences Journal*, 61(7), 1174–1191. <https://doi.org/10.1080/02626667.2016.1159308>
- Mega, T., Ushio, T., Kubota, T., Kachi, M., Aonashi, K., & Shige, S. (2014). Gauge adjusted global satellite mapping of precipitation (GSMaP-Gauge). *2014 31th URSI General Assembly and Scientific Symposium, URSI GASS 2014*, 0–3. <https://doi.org/10.1109/URSIGASS.2014.6929683>
- Menne, M. J., Durre, I., Vose, R. S., Gleason, B. E., & Houston, T. G. (2012). An Overview of the Global Historical Climatology Network-Daily Database. *Journal of Atmospheric and Oceanic Technology*, 29(7), 897–910. <https://doi.org/10.1175/JTECH-D-11-00103.1>
- Miguez-Macho, G., & Fan, Y. (2012). The role of groundwater in the Amazon water cycle: 1. Influence on seasonal streamflow, flooding and wetlands. In *Journal of Geophysical Research Atmospheres* (Vol. 117, Issue 15, p. 15113). John Wiley & Sons, Ltd. <https://doi.org/10.1029/2012JD017539>

- Miguez-Macho, G., Fan, Y., Weaver, C. P., Walko, R., & Robock, A. (2007). Incorporating water table dynamics in climate modeling: 2. Formulation, validation, and soil moisture simulation. *Journal of Geophysical Research Atmospheres*, *112*(13), 13108. <https://doi.org/10.1029/2006JD008112>
- Milano, M., Ruelland, D., Dezetter, A., Fabre, J., Ardoin-Bardin, S., & Servat, E. (2013). Modeling the current and future capacity of water resources to meet water demands in the Ebro basin. *Journal of Hydrology*, *500*, 114–126. <https://doi.org/10.1016/j.jhydrol.2013.07.010>
- Mishra, A. K., & Singh, V. P. (2010). A review of drought concepts. *Journal of Hydrology*, *391*(1–2), 202–216.
- Mishra, A. K., & Singh, V. P. (2011). Drought modeling - A review. *Journal of Hydrology*, *403*(1–2), 157–175. <https://doi.org/10.1016/j.jhydrol.2011.03.049>
- Mishra, A. K., Singh, V. P., & Desai, V. R. (2009). Drought characterization: A probabilistic approach. *Stochastic Environmental Research and Risk Assessment*, *23*(1), 41–55. <https://doi.org/10.1007/S00477-007-0194-2/TABLES/13>
- Mo, K. C., & Lettenmaier, D. P. (2014). Objective Drought Classification Using Multiple Land Surface Models. *Journal of Hydrometeorology*, *15*(3), 990–1010. <https://doi.org/10.1175/JHM-D-13-071.1>
- Monreal, T. E., & Amelin, E. V. (2010). Effects of Climate Change on Hydrological Resources in Europe: The Case of Spain. In A. Marquina (Ed.), *Global Warming and Climate Change* (pp. 58–77). Palgrave Macmillan UK. [https://doi.org/10.1057/9780230281257\\_4](https://doi.org/10.1057/9780230281257_4)
- Montanari, A., Young, G., Savenije, H. H. G., Hughes, D., Wagener, T., Ren, L. L., Koutsoyiannis, D., Cudennec, C., Toth, E., Grimaldi, S., Blöschl, G., Sivapalan, M., Beven, K., Gupta, H., Hipsey, M., Schaefli, B., Arheimer, B., Boegh, E., Schymanski, S. J., ... Belyaev, V. (2013). “Panta Rhei-Everything Flows”: Change in hydrology and society-The IAHS Scientific Decade 2013-2022. *Hydrological Sciences Journal*, *58*(6), 1256–1275. <https://doi.org/10.1080/02626667.2013.809088>
- Murphy, B. F., & Timbal, B. (2008). A review of recent climate variability and climate change in Southeastern Australia. In *International Journal of Climatology* (Vol. 28, Issue 7, pp. 859–879). John Wiley & Sons, Ltd. <https://doi.org/10.1002/joc.1627>
- Nabat, P., Somot, S., Cassou, C., Mallet, M., Michou, M., Bouniol, D., Decharme, B., Drugé, T., Roehrig, R., & Saint-Martin, D. (2020). Modulation of radiative aerosols effects by atmospheric circulation over the Euro-Mediterranean region. *Atmospheric Chemistry and Physics*, *20*(14), 8315–8349. <https://doi.org/10.5194/ACP-20-8315-2020>
- Napoly, A., Boone, A., Samuelsson, P., Gollvik, S., Martin, E., Seferian, R., Carrer, D., Decharme, B., & Jarlan, L. (2017). The interactions between soil-biosphere-atmosphere (ISBA) land surface model multi-energy balance (MEB) option in SURFEXv8 - Part 2: Introduction of a litter formulation and model evaluation for local-scale forest sites. *Geoscientific Model Development*, *10*(4), 1621–1644. <https://doi.org/10.5194/gmd-10-1621-2017>
- Narasimhan, B., & Srinivasan, R. (2005). Development and evaluation of Soil Moisture Deficit Index (SMDI) and Evapotranspiration Deficit Index (ETDI) for agricultural drought monitoring. *Agricultural and Forest Meteorology*, *133*(1–4), 69–88.

- <https://doi.org/10.1016/j.agrformet.2005.07.012>
- Nash, J. E., & Sutcliffe, J. V. (1970). River flow forecasting through conceptual models part I— A discussion of principles. *Journal of Hydrology*, *10*(3), 282–290. [https://doi.org/10.1016/0022-1694\(70\)90255-6](https://doi.org/10.1016/0022-1694(70)90255-6)
- Nazemi, A., & Wheeler, H. S. (2015a). On inclusion of water resource management in Earth system models -Part 1: Problem definition and representation of water demand. *Hydrology and Earth System Sciences*, *19*(1), 33–61. <https://doi.org/10.5194/hess-19-33-2015>
- Nazemi, A., & Wheeler, H. S. (2015b). On inclusion of water resource management in Earth system models Part 2: Representation of water supply and allocation and opportunities for improved modeling. *Hydrology and Earth System Sciences*, *19*(1), 63–90. <https://doi.org/10.5194/hess-19-63-2015>
- Nijssen, B., O'Donnell, G. M., Lettenmaier, D. P., Lohmann, D., & Wood, E. F. (2001). Predicting the discharge of global rivers. *Journal of Climate*, *14*(15), 3307–3323. [https://doi.org/10.1175/1520-0442\(2001\)014<3307:PTDOGR>2.0.CO;2](https://doi.org/10.1175/1520-0442(2001)014<3307:PTDOGR>2.0.CO;2)
- Nijssen, B., Shukla, S., Lin, C., Gao, H., Zhou, T., Ishottama, Sheffield, J., Wood, E. F., & Lettenmaier, D. P. (2014). A prototype global drought information system based on multiple land surface models. *Journal of Hydrometeorology*, *15*(4), 1661–1676. <https://doi.org/10.1175/JHM-D-13-090.1>
- Nilsson, C., Reidy, C. A., Dynesius, M., & Revenga, C. (2005). Fragmentation and flow regulation of the world's large river systems. *Science*, *308*(5720), 405–408.
- Noilhan, J., & Mahfouf, J. F. (1996). The ISBA land surface parameterisation scheme. *Global and Planetary Change*, *13*(1–4), 145–159. [https://doi.org/10.1016/0921-8181\(95\)00043-7](https://doi.org/10.1016/0921-8181(95)00043-7)
- Noilhan, J., & Planton, S. (1989). A Simple Parameterization of Land Surface Processes for Meteorological Models. *Monthly Weather Review*, *117*(3), 536–549. [https://doi.org/10.1175/1520-0493\(1989\)117<0536:ASPOLS>2.0.CO;2](https://doi.org/10.1175/1520-0493(1989)117<0536:ASPOLS>2.0.CO;2)
- Oki, T., & Kanae, S. (2006). Global Hydrological Cycles and World Water Resources. *Science*, *313*(5790), 1068–1072. <https://doi.org/10.1126/science.1128845>
- Oki, T., Nishimura, T., & Dirmeyer, P. (1999). Assessment of annual runoff from land surface models using Total Runoff Integrating Pathways (TRIP). *Journal of the Meteorological Society of Japan. Ser. II*, *77*(1B), 235–255.
- Oki, T., & Sud, Y. C. (1998). Design of Total Runoff Integrating Pathways (TRIP)—A Global River Channel Network. *Earth Interactions*, *2*(1), 1–37. [https://doi.org/10.1175/1087-3562\(1998\)002<0001:dotrip>2.3.co;2](https://doi.org/10.1175/1087-3562(1998)002<0001:dotrip>2.3.co;2)
- Onogi, K., Tsutsui, J., Koide, H., Sakamoto, M., Kobayashi, S., Hatsushika, H., Matsumoto, T., Yamazaki, N., Kamahori, H., Takahashi, K., Kadokura, S., Wada, K., Kato, K., Oyama, R., Ose, T., Mannoji, N., & Taira, R. (2007). The JRA-25 reanalysis. *Journal of the Meteorological Society of Japan*, *85*(3), 369–432. <https://doi.org/10.2151/jmsj.85.369>
- Overgaard, J., Rosbjerg, D., & Butts, M. B. (2006). Land-surface modelling in hydrological perspective - A review. In *Biogeosciences* (Vol. 3, Issue 2, pp. 229–241). <https://doi.org/10.5194/bg-3-229-2006>

- Ozdogan, M., Rodell, M., Beaudoin, H. K., & Toll, D. L. (2010). Simulating the effects of irrigation over the united states in a land surface model based on satellite-derived agricultural data. *Journal of Hydrometeorology*, *11*(1), 171–184. <https://doi.org/10.1175/2009JHM1116.1>
- Pal, S., & Sharma, P. (2021). A Review of Machine Learning Applications in Land Surface Modeling. In *Earth (Switzerland)* (Vol. 2, Issue 1, pp. 174–190). Multidisciplinary Digital Publishing Institute. <https://doi.org/10.3390/earth2010011>
- Palmer, M., Bernhardt, E., Chornesky, E., Collins, S., Dobson, A., Duke, C., Gold, B., Jacobson, R., Kingsland, S., & Kranz, R. (2004). Ecology for a crowded planet. In *Science* (Vol. 304, Issue 5675, pp. 1251–1252). American Association for the Advancement of Science.
- Palmer, W. C. (1965). Meteorological droughts. *Weather Bureau Research Paper* 45, 58.
- Panagos, P., Van Liedekerke, M., Jones, A., & Montanarella, L. (2012). European Soil Data Centre: Response to European policy support and public data requirements. *Land Use Policy*, *29*(2), 329–338. <https://doi.org/10.1016/j.landusepol.2011.07.003>
- Pandey, R. P., Mishra, S. K., Singh, R., & Ramasastri, K. S. (2008). Streamflow drought severity analysis of betwa river system (India). *Water Resources Management*, *22*(8), 1127–1141. <https://doi.org/10.1007/s11269-007-9216-6>
- Parry, S., Hannaford, J., Lloyd-Hughes, B., & Prudhomme, C. (2012). Multi-year droughts in Europe: analysis of development and causes. *Hydrology Research*, *43*(5), 689–706. <https://doi.org/10.2166/nh.2012.024>
- Páscoa, P., Gouveia, C. M., Russo, A., & Trigo, R. M. (2017). Drought trends in the Iberian Peninsula over the last 112 years. *Advances in Meteorology*, 2017. <https://doi.org/10.1155/2017/4653126>
- Páscoa, P., Russo, A., Gouveia, C. M., Soares, P. M. M., Cardoso, R. M., Careto, J. A. M., & Ribeiro, A. F. S. (2021). A high-resolution view of the recent drought trends over the Iberian Peninsula. *Weather and Climate Extremes*, *32*, 100320. <https://doi.org/10.1016/j.wace.2021.100320>
- Peel, M. C. (2009). Hydrology: Catchment vegetation and runoff. *Progress in Physical Geography*, *33*(6), 837–844. <https://doi.org/10.1177/0309133309350122>
- Pereira, L. S., Cordery, I., & Iacovides, I. (2002). Coping with water scarcity, Technical Documents in Hydrology. *International Hydrology Programme*, 58.
- Pérez y Pérez, L., & Barreiro-Hurlé, J. (2009). Assessing the socio-economic impacts of drought in the Ebro River Basin. *Spanish Journal of Agricultural Research*, *7*(2 SE-Agricultural economics), 269–280. <https://doi.org/10.5424/sjar/2009072-418>
- Perkins, S. E., Pitman, A. J., Holbrook, N. J., & McAneney, J. (2007). Evaluation of the AR4 Climate Models' Simulated Daily Maximum Temperature, Minimum Temperature, and Precipitation over Australia Using Probability Density Functions. *Journal of Climate*, *20*(17), 4356–4376. <https://doi.org/10.1175/JCLI4253.1>
- Pervez, M. S., & Brown, J. F. (2010). Mapping irrigated lands at 250-m scale by merging MODIS data and national agricultural statistics. *Remote Sensing*, *2*(10), 2388–2412.

- Piani, C., Weedon, G. P., Best, M., Gomes, S. M., Viterbo, P., Hagemann, S., & Haerter, J. O. (2010). Statistical bias correction of global simulated daily precipitation and temperature for the application of hydrological models. *Journal of Hydrology*, 395(3–4), 199–215. <https://doi.org/10.1016/j.jhydrol.2010.10.024>
- Pokhrel, Y. N., Hanasaki, N., Wada, Y., & Kim, H. (2016). Recent progresses in incorporating human land–water management into global land surface models toward their integration into Earth system models. *Wiley Interdisciplinary Reviews: Water*, 3(4), 548–574. <https://doi.org/10.1002/WAT2.1150>
- Pokhrel, Y. N., Koiraala, S., Yeh, P. J. F., Hanasaki, N., Longuevergne, L., Kanae, S., & Oki, T. (2015). Incorporation of groundwater pumping in a global Land Surface Model with the representation of human impacts. *Water Resources Research*, 51(1), 78–96. <https://doi.org/10.1002/2014WR015602>
- Ponce, V. M., Pandey, R. P., & Ercan, S. (2000). Characterization of Drought across Climatic Spectrum. *Journal of Hydrologic Engineering*, 5(2), 222–224. [https://doi.org/10.1061/\(asce\)1084-0699\(2000\)5:2\(222\)](https://doi.org/10.1061/(asce)1084-0699(2000)5:2(222))
- Pongratz, J., Dolman, H., Don, A., Erb, K. H., Fuchs, R., Herold, M., Jones, C., Kuemmerle, T., Luyssaert, S., Meyfroidt, P., & Naudts, K. (2018). Models meet data: Challenges and opportunities in implementing land management in Earth system models. In *Global Change Biology* (Vol. 24, Issue 4, pp. 1470–1487). John Wiley & Sons, Ltd. <https://doi.org/10.1111/gcb.13988>
- Postel, S. L. (2000). Entering an era of water scarcity: The challenges ahead. *Ecological Applications*, 10(4), 941–948. [https://doi.org/10.1890/1051-0761\(2000\)010\[0941:EAEOWS\]2.0.CO;2](https://doi.org/10.1890/1051-0761(2000)010[0941:EAEOWS]2.0.CO;2)
- Postel, S. L., Daily, G. C., & Ehrlich, P. R. (1996). Human appropriation of renewable fresh water. *Science*, 271(5250), 785–788.
- Prein, A. F., & Gobiet, A. (2017). Impacts of uncertainties in European gridded precipitation observations on regional climate analysis. *International Journal of Climatology*, 37(1), 305–327. <https://doi.org/10.1002/JOC.4706>
- Price, K. (2011). Effects of watershed topography, soils, land use, and climate on baseflow hydrology in humid regions: A review. *Progress in Physical Geography*, 35(4), 465–492. <https://doi.org/10.1177/0309133311402714>
- Prudhomme, C., Giuntoli, I., Robinson, E. L., Clark, D. B., Arnell, N. W., Dankers, R., Fekete, B. M., Franssen, W., Gerten, D., Gosling, S. N., Hagemann, S., Hannah, D. M., Kim, H., Masaki, Y., Satoh, Y., Stacke, T., Wada, Y., & Wisser, D. (2014). Hydrological droughts in the 21st century, hotspots and uncertainties from a global multimodel ensemble experiment. *Proceedings of the National Academy of Sciences of the United States of America*, 111(9), 3262–3267. <https://doi.org/10.1073/pnas.1222473110>
- Prudhomme, C., Parry, S., Hannaford, J., Clark, D. B., Hagemann, S., & Voss, F. (2011). How Well Do Large-Scale Models Reproduce Regional Hydrological Extremes in Europe? *Journal of Hydrometeorology*, 12(6), 1181–1204. <https://doi.org/10.1175/2011JHM1387.1>
- Quintana-Seguí, P., Barella-Ortiz, A., Regueiro-Sanfiz, S., & Miguez-Macho, G. (2020). The Utility of Land-Surface Model Simulations to Provide Drought Information in a Water Management Context Using Global and Local Forcing Datasets. *Water Resources*



- Management*, 34(7), 2135–2156. <https://doi.org/10.1007/s11269-018-2160-9>
- Quintana-Seguí, P., Cointe, P. Le, & Team, P.-P. (2022). *PIRAGUA\_atmos\_analysis [Dataset]*. <https://doi.org/https://doi.org/10.20350/digitalCSIC/14665>
- Quintana-Seguí, P., Le Moigne, P., Durand, Y., Martin, E., Habets, F., Baillon, M., Canellas, C., Franchisteguy, L., & Morel, S. (2008). Analysis of near-surface atmospheric variables: Validation of the SAFRAN analysis over France. *Journal of Applied Meteorology and Climatology*, 47(1), 92–107. <https://doi.org/10.1175/2007JAMC1636.1>
- Quintana-Seguí, P., Peral, C., Turco, M., Llasat, M. C., & Martin, E. (2016). Meteorological analysis systems in North-East Spain: Validation of SAFRAN and SPAN. *Journal of Environmental Informatics*, 27(2), 116–130. <https://doi.org/10.3808/jei.201600335>
- Quintana-Seguí, P., Turco, M., Herrera, S., & Miguez-Macho, G. (2017). Validation of a new SAFRAN-based gridded precipitation product for Spain and comparisons to Spain02 and ERA-Interim. *Hydrology and Earth System Sciences*, 21(4), 2187–2201. <https://doi.org/10.5194/hess-21-2187-2017>
- Quintana Seguí, P., Martin, E., Habets, F., & Noilhan, J. (2009). Improvement, calibration and validation of a distributed hydrological model over France. *Hydrology and Earth System Sciences*, 13(2), 163–181. <https://doi.org/10.5194/hess-13-163-2009>
- Raimonet, M., Oudin, L., Thieu, V., Silvestre, M., Vautard, R., Rabouille, C., & Le Moigne, P. (2017). Evaluation of gridded meteorological datasets for hydrological modeling. *Journal of Hydrometeorology*, 18(11), 3027–3041. <https://doi.org/10.1175/JHM-D-17-0018.1>
- Rajczak, J., Pall, P., & Schär, C. (2013). Projections of extreme precipitation events in regional climate simulations for Europe and the Alpine Region. *Journal of Geophysical Research: Atmospheres*, 118(9), 3610–3626. <https://doi.org/10.1002/jgrd.50297>
- Reichle, R. H., Koster, R. D., Dong, J., & Berg, A. A. (2004). Global Soil Moisture from Satellite Observations, Land Surface Models, and Ground Data: Implications for Data Assimilation. *Journal of Hydrometeorology*, 5(3), 430–442. [https://doi.org/https://doi.org/10.1175/1525-7541\(2004\)005<0430:GSMFSO>2.0.CO;2](https://doi.org/https://doi.org/10.1175/1525-7541(2004)005<0430:GSMFSO>2.0.CO;2)
- Rockström, J., Steffen, W., Noone, K., Persson, Å., Chapin, F. S., Lambin, E. F., Lenton, T. M., Scheffer, M., Folke, C., Schellnhuber, H. J., Nykvist, B., de Wit, C. A., Hughes, T., van der Leeuw, S., Rodhe, H., Sörlin, S., Snyder, P. K., Costanza, R., Svedin, U., ... Foley, J. A. (2009). A safe operating space for humanity. *Nature*, 461(7263), 472–475. <https://doi.org/10.1038/461472a>
- Ross, A., & Chang, H. (2020). Socio-hydrology with hydrosocial theory: two sides of the same coin? *Hydrological Sciences Journal*, 65(9), 1443–1457. <https://doi.org/10.1080/02626667.2020.1761023>
- Rost, S., Gerten, D., Bondeau, A., Lucht, W., Rohwer, J., & Schaphoff, S. (2008). Agricultural green and blue water consumption and its influence on the global water system. *Water Resources Research*, 44(9), 9405. <https://doi.org/10.1029/2007WR006331>
- Rummukainen, M. (2016). Added value in regional climate modeling. *Wiley Interdisciplinary Reviews: Climate Change*, 7(1), 145–159. <https://doi.org/10.1002/wcc.378>

- 
- Russo, A., Gouveia, C. M., Dutra, E., Soares, P. M. M., & Trigo, R. M. (2019). The synergy between drought and extremely hot summers in the Mediterranean. *Environmental Research Letters*, *14*(1), 014011. <https://doi.org/10.1088/1748-9326/aaf09e>
- Sacks, W. J., Cook, B. I., Buening, N., Levis, S., & Helkowski, J. H. (2009). Effects of global irrigation on the near-surface climate. *Climate Dynamics*, *33*(2–3), 159–175. <https://doi.org/10.1007/s00382-008-0445-z>
- Sadki, M., Munier, S., Boone, A., & Ricci, S. (2023). Implementation and sensitivity analysis of the Dam-Reservoir OPERATION model (DROP v1.0) over Spain. *Geoscientific Model Development*, *16*(2), 427–448. <https://doi.org/10.5194/gmd-16-427-2023>
- Saeed, F., Hagemann, S., & Jacob, D. (2009). Impact of irrigation on the South Asian summer monsoon. *Geophysical Research Letters*, *36*(20), 20711. <https://doi.org/10.1029/2009GL040625>
- Saleh, F., Flipo, N., Habets, F., Ducharne, A., Oudin, L., Viennot, P., & Ledoux, E. (2011). Modeling the impact of in-stream water level fluctuations on stream-aquifer interactions at the regional scale. *Journal of Hydrology*, *400*(3–4), 490–500. <https://doi.org/10.1016/J.JHYDROL.2011.02.001>
- Samaniego, L., Kumar, R., & Attinger, S. (2010). Multiscale parameter regionalization of a grid-based hydrologic model at the mesoscale. *Water Resources Research*, *46*(5), 5523. <https://doi.org/10.1029/2008WR007327>
- Samaniego, L., Kumar, R., & Zink, M. (2013). Implications of Parameter Uncertainty on Soil Moisture Drought Analysis in Germany. *Journal of Hydrometeorology*, *14*(1), 47–68. <https://doi.org/10.1175/JHM-D-12-075.1>
- Sanderson, E. W., Jaiteh, M., Levy, M. A., Redford, K. H., Wannebo, A. V., & Woolmer, G. (2002). The human footprint and the last of the wild: the human footprint is a global map of human influence on the land surface, which suggests that human beings are stewards of nature, whether we like it or not. *BioScience*, *52*(10), 891–904.
- Santos, L., Thirel, G., & Perrin, C. (2018). Technical note: Pitfalls in using log-transformed flows within the KGE criterion. *Hydrology and Earth System Sciences*, *22*(8), 4583–4591. <https://doi.org/10.5194/hess-22-4583-2018>
- Savenije, H. H. G., Hoekstra, A. Y., & Van Der Zaag, P. (2014). Evolving water science in the Anthropocene. *Hydrology and Earth System Sciences*, *18*(1), 319–332. <https://doi.org/10.5194/HESS-18-319-2014>
- Sawada, Y. (2020). Machine Learning Accelerates Parameter Optimization and Uncertainty Assessment of a Land Surface Model. *Journal of Geophysical Research: Atmospheres*, *125*(20), e2020JD032688. <https://doi.org/10.1029/2020JD032688>
- Scanlon, B. R., Keese, K. E., Flint, A. L., Flint, L. E., Gaye, C. B., Edmunds, W. M., & Simmers, I. (2006). Global synthesis of groundwater recharge in semiarid and arid regions. *Hydrological Processes*, *20*(15), 3335–3370. <https://doi.org/10.1002/hyp.6335>
- Schamm, K., Ziese, M., Becker, A., Finger, P., Meyer-Christoffer, A., Schneider, U., Schröder, M., & Stender, P. (2014). Global gridded precipitation over land: A description of the new GPCP First Guess Daily product. *Earth System Science Data*, *6*(1), 49–60. <https://doi.org/10.5194/ESSD-6-49-2014>
-

- Schewe, J., Heinke, J., Gerten, D., Haddeland, I., Arnell, N. W., Clark, D. B., Dankers, R., Eisner, S., Fekete, B. M., Colón-González, F. J., Gosling, S. N., Kim, H., Liu, X., Masaki, Y., Portmann, F. T., Satoh, Y., Stacke, T., Tang, Q., Wada, Y., ... Kabat, P. (2014). Multimodel assessment of water scarcity under climate change. *Proceedings of the National Academy of Sciences of the United States of America*, 111(9), 3245–3250. <https://doi.org/10.1073/pnas.1222460110>
- Schmidt, L., Heße, F., Attinger, S., & Kumar, R. (2020). Challenges in Applying Machine Learning Models for Hydrological Inference: A Case Study for Flooding Events Across Germany. *Water Resources Research*, 56(5), e2019WR025924. <https://doi.org/10.1029/2019WR025924>
- Schwabe, K., Albiac, J., Connor, J. D., Hassan, R. M., & González, L. M. (2013). Drought in arid and semi-arid regions: A multi-disciplinary and cross-country perspective. In *Drought in Arid and Semi-Arid Regions: A Multi-Disciplinary and Cross-Country Perspective*. Springer Netherlands. <https://doi.org/10.1007/978-94-007-6636-5>
- Schwabe, K., Albiac, J., Connor, J. D., Hassan, R. M., & González, L. M. (2015). *Drought in arid and semi-arid regions*.
- Sellers, P. J., Fennessy, M. J., & Dickinson, R. E. (2007). A numerical approach to calculating soil wetness and evapotranspiration over large grid areas. *Journal of Geophysical Research Atmospheres*, 112(18), 18106. <https://doi.org/10.1029/2007JD008781>
- Sellers, P. J., Mintz, Y., Sud, Y. C., & Dalcher, A. (1986). A Simple Biosphere Model (SIB) for Use within General Circulation Models. *Journal of Atmospheric Sciences*, 43(6), 505–531. [https://doi.org/https://doi.org/10.1175/1520-0469\(1986\)043<0505:ASBMFU>2.0.CO;2](https://doi.org/https://doi.org/10.1175/1520-0469(1986)043<0505:ASBMFU>2.0.CO;2)
- Sellers, P. J., Randall, D. A., Collatz, G. J., Berry, J. A., Field, C. B., Dazlich, D. A., Zhang, C., Collelo, G. D., & Bounoua, L. (1996). A Revised Land Surface Parameterization (SiB2) for Atmospheric GCMs. Part I: Model Formulation. *Journal of Climate*, 9(4), 676–705. [https://doi.org/https://doi.org/10.1175/1520-0442\(1996\)009<0676:ARLSPF>2.0.CO;2](https://doi.org/https://doi.org/10.1175/1520-0442(1996)009<0676:ARLSPF>2.0.CO;2)
- Seneviratne, S., Nicholls, N., Easterling, D., Goodess, C., Kanae, S., Kossin, J., Luo, Y., Marengo, J., McInnes, K., Rahimi, M., Reichstein, M., Sorteberg, A., Vera, C., & Zhang, X. (2012). Changes in climate extremes and their impacts on the natural physical environment. *Managing the Risk of Extreme Events and Disasters to Advance Climate Change Adaptation.*, 109–230. <https://doi.org/10.1017/CBO9781139177245.006>
- Shafer, B. A., & Dezman, L. E. (1982). Development of a surface water supply index (SWSI) to assess the severity of drought conditions in snowpack runoff areas. In *Proceedings of the 50th Annual Western Snow Conference*. <http://www.westernsnowconference.org/node/932>
- Sheffield, J., Goteti, G., Wen, F., & Wood, E. F. (2004). A simulated soil moisture based drought analysis for the United States. *Journal of Geophysical Research D: Atmospheres*, 109(24), 1–19. <https://doi.org/10.1029/2004JD005182>
- Sheffield, J., & Wood, E. F. (2012). *Drought : Past Problems and Future Scenarios*. Taylor and Francis.
- Sheffield, J., Wood, E. F., Chaney, N., Guan, K., Sadri, S., Yuan, X., Olang, L., Amani, A., Ali, A., Demuth, S., & Ogallo, L. (2014). A drought monitoring and forecasting system for sub-sahara african water resources and food security. *Bulletin of the American Meteorological Society*, 95(6), 861–882. <https://doi.org/10.1175/BAMS-D-12-00124.1>

- Sheffield, J., Wood, E. F., & Roderick, M. L. (2012). Little change in global drought over the past 60 years. *Nature*, *491*(7424), 435–438. <https://doi.org/10.1038/nature11575>
- Shen, C. (2018). A Transdisciplinary Review of Deep Learning Research and Its Relevance for Water Resources Scientists. In *Water Resources Research* (Vol. 54, Issue 11, pp. 8558–8593). John Wiley & Sons, Ltd. <https://doi.org/10.1029/2018WR022643>
- Shiau, J.-T., & Shen, H. W. (2001). Recurrence Analysis of Hydrologic Droughts of Differing Severity. *Journal of Water Resources Planning and Management*, *127*(1), 30–40. [https://doi.org/10.1061/\(asce\)0733-9496\(2001\)127:1\(30\)](https://doi.org/10.1061/(asce)0733-9496(2001)127:1(30))
- Shukla, S., & Wood, A. W. (2008). Use of a standardized runoff index for characterizing hydrologic drought. *Geophysical Research Letters*, *35*(2). <https://doi.org/10.1029/2007GL032487>
- Siebert, S., Kummu, M., Porkka, M., Döll, P., Ramankutty, N., & Scanlon, B. R. (2015). A global data set of the extent of irrigated land from 1900 to 2005. *Hydrology and Earth System Sciences*, *19*(3), 1521–1545.
- Singh, R., Archfield, S. A., & Wagener, T. (2014). Identifying dominant controls on hydrologic parameter transfer from gauged to ungauged catchments - A comparative hydrology approach. *Journal of Hydrology*, *517*, 985–996. <https://doi.org/10.1016/j.jhydrol.2014.06.030>
- Sivapalan, M. (2015). Debates - Perspectives on socio-hydrology: Changing water systems and the “tyranny of small problems” - Socio-hydrology. *Water Resources Research*, *51*(6), 4795–4805. <https://doi.org/10.1002/2015WR017080>
- Sivapalan, M., Konar, M., Srinivasan, V., Chhatre, A., Wutich, A., Scott, C. A., Wescoat, J. L., & Rodríguez-Iturbe, I. (2014). Socio-hydrology: Use-inspired water sustainability science for the Anthropocene. *Earth's Future*, *2*(4), 225–230. <https://doi.org/10.1002/2013ef000164>
- Sivapalan, M., Savenije, H. H. G., & Blöschl, G. (2012). Socio-hydrology: A new science of people and water. In *Hydrological Processes* (Vol. 26, Issue 8, pp. 1270–1276). John Wiley & Sons, Ltd. <https://doi.org/10.1002/hyp.8426>
- Slowik, A., & Kwasnicka, H. (2020). Evolutionary algorithms and their applications to engineering problems. In *Neural Computing and Applications* (Vol. 32, Issue 16, pp. 12363–12379). Springer. <https://doi.org/10.1007/s00521-020-04832-8>
- Smakhtin, V. U. (2001). Low flow hydrology: A review. *Journal of Hydrology*, *240*(3–4), 147–186. [https://doi.org/10.1016/S0022-1694\(00\)00340-1](https://doi.org/10.1016/S0022-1694(00)00340-1)
- Smakhtin, V. Y., Sami, K., & Hughes, D. A. (1998). Evaluating the performance of a deterministic daily rainfall-runoff model in a low-flow context. *Hydrological Processes*, *12*(5), 797–812. [https://doi.org/10.1002/\(SICI\)1099-1085\(19980430\)12:5<797::AID-HYP632>3.0.CO;2-S](https://doi.org/10.1002/(SICI)1099-1085(19980430)12:5<797::AID-HYP632>3.0.CO;2-S)
- Somers, L. D., & McKenzie, J. M. (2020). A review of groundwater in high mountain environments. *Wiley Interdisciplinary Reviews: Water*, *7*(6), e1475. <https://doi.org/10.1002/WAT2.1475>
- Sood, A., & Smakhtin, V. (2015). Revue des modèles hydrologiques globaux. *Hydrological*

- Sciences Journal*, 60(4), 549–565. <https://doi.org/10.1080/02626667.2014.950580>
- Sordo-Ward, Á., Bejarano, M. D., Granados, I., & Garrote, L. (2020). Facing Future Water Scarcity in the Duero-Douro Basin: Comparative Effect of Policy Measures on Irrigation Water Availability. *Journal of Water Resources Planning and Management*, 146(4), 1–12. [https://doi.org/10.1061/\(asce\)wr.1943-5452.0001183](https://doi.org/10.1061/(asce)wr.1943-5452.0001183)
- Sordo-Ward, Á., Granados, A., Iglesias, A., Garrote, L., & Bejarano, M. D. (2019). Adaptation effort and performance of water management strategies to face climate change impacts in six representative basins of Southern Europe. *Water (Switzerland)*, 11(5). <https://doi.org/10.3390/w11051078>
- Sorooshian, S., Li, J., Hsu, K. L., & Gao, X. (2012). Influence of irrigation schemes used in regional climate models on evapotranspiration estimation: Results and comparative studies from California's Central Valley agricultural regions. *Journal of Geophysical Research Atmospheres*, 117(6), 6107. <https://doi.org/10.1029/2011JD016978>
- Sousa, P. M., Trigo, R. M., Aizpurua, P., Nieto, R., Gimeno, L., & Garcia-Herrera, R. (2011). Trends and extremes of drought indices throughout the 20th century in the Mediterranean. *Natural Hazards and Earth System Science*, 11(1), 33–51. <https://doi.org/10.5194/nhess-11-33-2011>
- Spinoni, J., Naumann, G., Vogt, J. V., & Barbosa, P. (2015). The biggest drought events in Europe from 1950 to 2012. *Journal of Hydrology: Regional Studies*, 3, 509–524. <https://doi.org/10.1016/j.ejrh.2015.01.001>
- Stahl, K. (2001). *Hydrological Drought - a Study across Europe*. PhD thesis (Vol. 15). Freiburger Schriften zur Hydrologie.
- Stahl, K., & Hisdal, H. (2004). Hydroclimatology. In L. M. Tallaksen & H. A. J. Van Lanen (Eds.), *Hydrological drought: processes and estimation methods for streamflow and groundwater* (1. ed., pp. 19–51). Elsevier.
- Stahl, K., Hisdal, H., Hannaford, J., Tallaksen, L. M., van Lanen, H. A. J., Sauquet, E., Demuth, S., Fendekova, M., & Jódar, J. (2010). Streamflow trends in Europe: evidence from a dataset of near-natural catchments. *Hydrology and Earth System Sciences*, 14(12), 2367–2382. <https://doi.org/10.5194/hess-14-2367-2010>
- Stahl, K., Kohn, I., Blauhut, V., Urquijo, J., De Stefano, L., Acácio, V., Dias, S., Stagge, J. H., Tallaksen, L. M., Kampragou, E., Van Loon, A. F., Barker, L. J., Melsen, L. A., Bifulco, C., Musolino, D., de Carli, A., Massarutto, A., Assimacopoulos, D., & Van Lanen, H. A. J. (2016). Impacts of European drought events: insights from an international database of text-based reports. *Natural Hazards and Earth System Sciences*, 16(3), 801–819. <https://doi.org/10.5194/nhess-16-801-2016>
- Stahl, K., Tallaksen, L. M., Gudmundsson, L., & Christensen, J. H. (2011). Streamflow data from small basins: A challenging test to high-resolution regional climate modeling. *Journal of Hydrometeorology*, 12(5), 900–912. <https://doi.org/10.1175/2011JHM1356.1>
- Stahl, K., Tallaksen, L. M., Hannaford, J., & Van Lanen, H. A. J. (2012). Filling the white space on maps of European runoff trends: Estimates from a multi-model ensemble. *Hydrology and Earth System Sciences*, 16(7), 2035–2047. <https://doi.org/10.5194/hess-16-2035-2012>
- Staudinger, M., Stahl, K., Seibert, J., Clark, M. P., & Tallaksen, L. M. (2011). Comparison of

- hydrological model structures based on recession and low flow simulations. *Hydrology and Earth System Sciences*, 15(11), 3447–3459. <https://doi.org/10.5194/hess-15-3447-2011>
- Sterling, S. M., Ducharne, A., & Polcher, J. (2013). The impact of global land-cover change on the terrestrial water cycle. *Nature Climate Change*, 3(4), 385–390. <https://doi.org/10.1038/nclimate1690>
- Sun, Q., Miao, C., Duan, Q., Ashouri, H., Sorooshian, S., & Hsu, K. L. (2018). A Review of Global Precipitation Data Sets: Data Sources, Estimation, and Intercomparisons. *Reviews of Geophysics*, 56(1), 79–107. <https://doi.org/10.1002/2017RG000574>
- Sutanudjaja, E. H., Van Beek, L. P. H., De Jong, S. M., Van Geer, F. C., & Bierkens, M. F. P. (2011). Large-scale groundwater modeling using global datasets: A test case for the Rhine-Meuse basin. *Hydrology and Earth System Sciences*, 15(9), 2913–2935. <https://doi.org/10.5194/HESS-15-2913-2011>
- Takata, K., Emori, S., & Watanabe, T. (2003). Development of the minimal advanced treatments of surface interaction and runoff. *Global and Planetary Change*, 38(1–2), 209–222. [https://doi.org/10.1016/S0921-8181\(03\)00030-4](https://doi.org/10.1016/S0921-8181(03)00030-4)
- Tallaksen, L. M., Hisdal, H., & Lanen, H. A. J. V. (2009). Space-time modelling of catchment scale drought characteristics. *Journal of Hydrology*, 375(3–4), 363–372. <https://doi.org/10.1016/j.jhydrol.2009.06.032>
- Tallaksen, L. M., & Van Lanen, H. A. J. (2004). Hydrological Drought: Processes and Estimation Methods for Streamflow and Groundwater. In *Development in Water Science* (Vol. 48). Elsevier B.V. <http://www.amazon.com/dp/0444516883>
- Tang, Q., Oki, T., Kanae, S., & Hu, H. (2007). The influence of precipitation variability and partial irrigation within grid cells on a hydrological simulation. *Journal of Hydrometeorology*, 8(3), 499–512. <https://doi.org/10.1175/JHM589.1>
- Tapiador, F. J., Turk, F. J., Petersen, W., Hou, A. Y., García-Ortega, E., Machado, L. A. T., Angelis, C. F., Salio, P., Kidd, C., Huffman, G. J., & de Castro, M. (2012). Global precipitation measurement: Methods, datasets and applications. In *Atmospheric Research* (Vols. 104–105, pp. 70–97). Elsevier. <https://doi.org/10.1016/j.atmosres.2011.10.021>
- TATE, E. L., & FREEMAN, S. N. (2000). Three modelling approaches for seasonal streamflow droughts in southern Africa: the use of censored data. *Hydrological Sciences Journal*, 45(1), 27–42. <https://doi.org/10.1080/02626660009492304>
- Tejedor, E., Saz, M. A., Esper, J., Cuadrat, J. M., & de Luis, M. (2017). Summer drought reconstruction in northeastern Spain inferred from a tree ring latewood network since 1734. *Geophysical Research Letters*, 44(16), 8492–8500. <https://doi.org/10.1002/2017GL074748>
- Tesfa, T. K., Tarboton, D. G., Chandler, D. G., & McNamara, J. P. (2009). Modeling soil depth from topographic and land cover attributes. *Water Resources Research*, 45(10), 1–16. <https://doi.org/10.1029/2008WR007474>
- Teutschbein, C., & Seibert, J. (2010). Regional climate models for hydrological impact studies at the catchment scale: A review of recent modeling strategies. In *Geography Compass* (Vol. 4, Issue 7, pp. 834–860). John Wiley & Sons, Ltd. <https://doi.org/10.1111/j.1749-8198.2010.00357.x>

- Themeßl, M. J., Gobiet, A., & Heinrich, G. (2012). Empirical-statistical downscaling and error correction of regional climate models and its impact on the climate change signal. *Climatic Change*, *112*(2), 449–468. <https://doi.org/10.1007/s10584-011-0224-4>
- Thober, S., Kumar, R., Sheffield, J., Mai, J., Schäfer, D., & Samaniego, L. (2015). Seasonal Soil Moisture Drought Prediction over Europe Using the North American Multi-Model Ensemble (NMME). *Journal of Hydrometeorology*, *16*(6), 2329–2344. <https://doi.org/10.1175/JHM-D-15-0053.1>
- Thompson, S. E., Sivapalan, M., Harman, C. J., Srinivasan, V., Hipsey, M. R., Reed, P., Montanari, A., & Blöschl, G. (2013). Developing predictive insight into changing water systems: Use-inspired hydrologic science for the anthropocene. *Hydrology and Earth System Sciences*, *17*(12), 5013–5039. <https://doi.org/10.5194/hess-17-5013-2013>
- Tian, W., Li, X., Cheng, G. D., Wang, X. S., & Hu, B. X. (2012). Coupling a groundwater model with a land surface model to improve water and energy cycle simulation. *Hydrology and Earth System Sciences*, *16*(12), 4707–4723. <https://doi.org/10.5194/hess-16-4707-2012>
- Tijdeman, E., Hannaford, J., & Stahl, K. (2018). Human influences on streamflow drought characteristics in England and Wales. *Hydrology and Earth System Sciences*, *22*(2), 1051–1064. <https://doi.org/10.5194/hess-22-1051-2018>
- Todini, E. (1996). The ARNO rainfall-runoff model. *Journal of Hydrology*, *175*(1–4), 339–382. [https://doi.org/10.1016/S0022-1694\(96\)80016-3](https://doi.org/10.1016/S0022-1694(96)80016-3)
- Torma, C., Giorgi, F., & Coppola, E. (2015). Added value of regional climate modeling over areas characterized by complex terrain-precipitation over the Alps. *Journal of Geophysical Research*, *120*(9), 3957–3972. <https://doi.org/10.1002/2014JD022781>
- Tramblay, Y., Koutroulis, A., Samaniego, L., Vicente-Serrano, S. M., Volaire, F., Boone, A., Le Page, M., Llasat, M. C., Albergel, C., Burak, S., Cailleret, M., Kalin, K. C., Davi, H., Dupuy, J. L., Greve, P., Grillakis, M., Hanich, L., Jarlan, L., Martin-StPaul, N., ... Polcher, J. (2020). Challenges for drought assessment in the Mediterranean region under future climate scenarios. *Earth-Science Reviews*, *210*(August), 103348. <https://doi.org/10.1016/j.earscirev.2020.103348>
- Trenberth, K. E., Zhang, Y., & Gehne, M. (2017). Intermittency in Precipitation: Duration, Frequency, Intensity, and Amounts Using Hourly Data. *Journal of Hydrometeorology*, *18*(5), 1393–1412. <https://doi.org/10.1175/JHM-D-16-0263.1>
- Troch, P. A., Carrillo, G., Sivapalan, M., Wagener, T., & Sawicz, K. (2013). Climate-vegetation-soil interactions and long-term hydrologic partitioning: Signatures of catchment co-evolution. *Hydrology and Earth System Sciences*, *17*(6), 2209–2217. <https://doi.org/10.5194/hess-17-2209-2013>
- Troy, T. J., Konar, M., Srinivasan, V., & Thompson, S. (2015). Moving sociohydrology forward: a synthesis across studies. *Hydrol. Earth Syst. Sci.*, *19*(8), 3667–3679. <https://doi.org/10.5194/hess-19-3667-2015>
- Tuinenburg, O. A., Hutjes, R. W. A., Stacke, T., Wiltshire, A., & Lucas-Picher, P. (2014). Effects of irrigation in India on the atmospheric water budget. *Journal of Hydrometeorology*, *15*(3), 1028–1050. <https://doi.org/10.1175/JHM-D-13-078.1>
- Van Beek, L. P. H., Wada, Y., & Bierkens, M. F. P. (2011). Global monthly water stress: 1. Water

- balance and water availability. *Water Resources Research*, 47(7), 7517. <https://doi.org/10.1029/2010WR009791>
- Van Loon, A. F. (2013). *On the Propagation of Drought.: How Climate and Catchment Characteristics Influence Hydrological Drought Development and Recovery*. Wageningen University and Research.
- Van Loon, A. F. (2015). Hydrological drought explained. *WIREs Water*, 2(4), 359–392. <https://doi.org/10.1002/wat2.1085>
- Van Loon, A. F., Gleeson, T., Clark, J., J M Van Dijk, A. I., Stahl, K., Hannaford, J., Di Baldassarre, G., Teuling, A. J., Tallaksen, L. M., Uijlenhoet, R., Hannah, D. M., Sheffield, J., Svoboda, M., Verbeiren, B., Wagener, T., Rangelcroft, S., Wanders, N., & J Van Lanen, H. A. (2016). Drought in the Anthropocene. *Nature Publishing Group*, 9. <https://doi.org/10.1038/ngeo2646>
- Van Loon, A. F., Rangelcroft, S., Coxon, G., Werner, M., Wanders, N., Di Baldassarre, G., Tjeldeman, E., Bosman, M., Gleeson, T., Nauditt, A., Aghakouchak, A., Breña-Naranjo, J. A., Cenobio-Cruz, O., Costa, A. C., Fendekova, M., Jewitt, G., Kingston, D. G., Loft, J., Mager, S. M., ... Van Lanen, H. A. J. (2022). Streamflow droughts aggravated by human activities despite management. *Environmental Research Letters*, 17(4), 044059. <https://doi.org/10.1088/1748-9326/ac5def>
- Van Loon, A. F., Van Huijgevoort, M. H. J., & Van Lanen, H. A. J. (2012). Evaluation of drought propagation in an ensemble mean of large-scale hydrological models. *Hydrology and Earth System Sciences*, 16(11), 4057–4078. <https://doi.org/10.5194/hess-16-4057-2012>
- Verburg, P. H., Dearing, J. A., Dyke, J. G., Leeuw, S. van der, Seitzinger, S., Steffen, W., & Syvitski, J. (2016). Methods and approaches to modelling the Anthropocene. *Global Environmental Change*, 39, 328–340. <https://doi.org/10.1016/j.gloenvcha.2015.08.007>
- Vergnes, J. P., Decharme, B., Alkama, R., Martin, E., Habets, F., & Douville, H. (2012). A Simple Groundwater Scheme for Hydrological and Climate Applications: Description and Offline Evaluation over France. *Journal of Hydrometeorology*, 13(4), 1149–1171. <https://doi.org/10.1175/JHM-D-11-0149.1>
- Vergnes, J. P., & Habets, F. (2018). Impact of river water levels on the simulation of stream–aquifer exchanges over the Upper Rhine alluvial aquifer (France/Germany). *Hydrogeology Journal*, 26(7), 2443–2457. <https://doi.org/10.1007/S10040-018-1788-0/FIGURES/13>
- Vergnes, J. P., Roux, N., Habets, F., Ackerer, P., Amraoui, N., Besson, F., Caballero, Y., Courtois, Q., De Dreuzy, J. R., Etchevers, P., Gallois, N., Leroux, D. J., Longuevergne, L., Le Moigne, P., Morel, T., Munier, S., Regimbeau, F., Thiéry, D., & Viennot, P. (2020). The AquiFR hydrometeorological modelling platform as a tool for improving groundwater resource monitoring over France: Evaluation over a 60-year period. *Hydrology and Earth System Sciences*, 24(2), 633–654. <https://doi.org/10.5194/HESS-24-633-2020>
- Vicente-Serrano, S. M. (2006). Spatial and temporal analysis of droughts in the Iberian Peninsula (1910–2000). *Hydrological Sciences Journal*, 51(1), 83–97. <https://doi.org/10.1623/hysj.51.1.83>
- Vicente-Serrano, S. M., Beguería, S., & López-Moreno, J. I. (2010). A multiscalar drought index sensitive to global warming: The standardized precipitation evapotranspiration index. *Journal of Climate*, 23(7), 1696–1718. <https://doi.org/10.1175/2009JCLI2909.1>



- Vicente-Serrano, S. M., Lopez-Moreno, J. I., Beguería, S., Lorenzo-Lacruz, J., Sanchez-Lorenzo, A., García-Ruiz, J. M., Azorin-Molina, C., Morán-Tejeda, E., Revuelto, J., Trigo, R., Coelho, F., & Espejo, F. (2014). Evidence of increasing drought severity caused by temperature rise in southern Europe. *Environmental Research Letters*, *9*(4), 044001. <https://doi.org/10.1088/1748-9326/9/4/044001>
- Vicente-Serrano, S. M., López-Moreno, J. I., Drumond, A., Gimeno, L., Nieto, R., Morán-Tejeda, E., Lorenzo-Lacruz, J., Beguería, S., & Zabalza, J. (2011). Effects of warming processes on droughts and water resources in the NW Iberian Peninsula (1930-2006). *Climate Research*, *48*(2–3), 203–212. <https://doi.org/10.3354/cr01002>
- Vidal, J.-P., Martin, E., Franchistéguy, L., Habets, F., Soubeyroux, J.-M., Blanchard, M., & Baillon, M. (2010). Multilevel and multiscale drought reanalysis over France with the Safran-Isba-Modcou hydrometeorological suite. *Hydrology and Earth System Sciences*, *14*(3), 459–478. <https://doi.org/10.5194/hess-14-459-2010>
- Viste, E., Korecha, D., & Sorteberg, A. (2013). Recent drought and precipitation tendencies in Ethiopia. *Theoretical and Applied Climatology*, *112*(3–4), 535–551. <https://doi.org/10.1007/s00704-012-0746-3>
- Vitousek, P. M., Mooney, H. A., Lubchenco, J., & Melillo, J. M. (1997). Human domination of Earth's ecosystems. *Science*, *277*(5325), 494–499.
- Vörösmarty, C. J., Green, P., Salisbury, J., & Lammers, R. B. (2000). Global Water Resources: Vulnerability from Climate Change and Population Growth. *Science*, *289*(5477), 284–288. <https://doi.org/10.1126/science.289.5477.284>
- Vörösmarty, C. J., Hoekstra, A. Y., Bunn, S. E., Conway, D., & Gupta, J. (2015). Fresh water goes global. In *Science* (Vol. 349, Issue 6247, pp. 478–479). American Association for the Advancement of Science. <https://doi.org/10.1126/science.aac6009>
- Vörösmarty, C. J., McIntyre, P. B., Gessner, M. O., Dudgeon, D., Prusevich, A., Green, P., Glidden, S., Bunn, S. E., Sullivan, C. A., & Liermann, C. R. (2010). Global threats to human water security and river biodiversity. *Nature*, *467*(7315), 555–561.
- Vörösmarty, C. J., & Sahagian, D. (2000). Anthropogenic Disturbance of the Terrestrial Water Cycle. *BioScience*, *50*(9), 753–765. [https://doi.org/10.1641/0006-3568\(2000\)050\[0753:ADOTTW\]2.0.CO;2](https://doi.org/10.1641/0006-3568(2000)050[0753:ADOTTW]2.0.CO;2)
- Wada, Y., Bierkens, M. F. P., De Roo, A., Dirmeyer, P. A., Famiglietti, J. S., Hanasaki, N., Konar, M., Liu, J., Schmied, H. M., Oki, T., Pokhrel, Y., Sivapalan, M., Troy, T. J., Van Dijk, A. I. J. M., Van Emmerik, T., Van Huijgevoort, M. H. J., Van Lanen, H. A. J., Vörösmarty, C. J., Wanders, N., & Wheeler, H. (2017). Human-water interface in hydrological modelling: Current status and future directions. *Hydrology and Earth System Sciences*, *21*(8), 4169–4193. <https://doi.org/10.5194/hess-21-4169-2017>
- Wada, Y., de Graaf, I. E. M., & van Beek, L. P. H. (2016). High-resolution modeling of human and climate impacts on global water resources. *Journal of Advances in Modeling Earth Systems*, *8*(2), 735–763. <https://doi.org/10.1002/2015MS000618>
- Wada, Y., van Beek, L. P. H., & Bierkens, M. F. P. (2011). Modelling global water stress of the recent past: on the relative importance of trends in water demand and climate variability. *Hydrology and Earth System Sciences Discussions*, *8*(4), 7399–7460. <https://doi.org/10.5194/hessd-8-7399-2011>

- Wada, Y., Van Beek, L. P. H., Wanders, N., & Bierkens, M. F. P. (2013). Human water consumption intensifies hydrological drought worldwide. *Environmental Research Letters*, 8(3). <https://doi.org/10.1088/1748-9326/8/3/034036>
- Wada, Y., Wisser, D., & Bierkens, M. F. P. (2014). Global modeling of withdrawal, allocation and consumptive use of surface water and groundwater resources. *Earth System Dynamics*, 5(1), 15–40. <https://doi.org/10.5194/esd-5-15-2014>
- Walker, A. P., Ye, M., Lu, D., De Kauwe, M. G., Gu, L., Medlyn, B. E., Rogers, A., & Serbin, S. P. (2018). The multi-assumption architecture and testbed (MAAT v1.0): R code for generating ensembles with dynamic model structure and analysis of epistemic uncertainty from multiple sources. *Geoscientific Model Development*, 11(8), 3159–3185. <https://doi.org/10.5194/gmd-11-3159-2018>
- Wanders, N., Van Lanen, H. A. J., & Van Loon, A. F. (2010). *WATCH Technical Report No. 24: Indicators for drought characterization on a global scale* (Issue 24).
- Wanders, N., & Wada, Y. (2015). Human and climate impacts on the 21st century hydrological drought. *Journal of Hydrology*, 526, 208–220. <https://doi.org/10.1016/j.jhydrol.2014.10.047>
- Wang, P. L., & Feddema, J. J. (2020). Linking Global Land Use/Land Cover to Hydrologic Soil Groups From 850 to 2015. *Global Biogeochemical Cycles*, 34(3), e2019GB006356. <https://doi.org/10.1029/2019GB006356>
- Wang, Y. P., & Leuning, R. (1998). A two-leaf model for canopy conductance, photosynthesis and partitioning of available energy I: Model description and comparison with a multi-layered model. *Agricultural and Forest Meteorology*, 91(1–2), 89–111. [https://doi.org/10.1016/S0168-1923\(98\)00061-6](https://doi.org/10.1016/S0168-1923(98)00061-6)
- Weihermüller, L., Lehmann, P., Herbst, M., Rahmati, M., Verhoef, A., Or, D., Jacques, D., & Vereecken, H. (2021). Choice of Pedotransfer Functions Matters when Simulating Soil Water Balance Fluxes. *Journal of Advances in Modeling Earth Systems*, 13(3), e2020MS002404. <https://doi.org/10.1029/2020MS002404>
- Wilhite, D. A. (2000). Drought as a natural hazard: Concepts and definitions. *Drought: A Global Assessment*, 3–18.
- Wilhite, D. A., & Glantz, M. H. (1985). Understanding: the Drought Phenomenon: The Role of Definitions. *Water International*, 10(3), 111–120. <https://doi.org/10.1080/02508068508686328>
- Wilhite, D. A., & Hayes, M. J. (1998). *Chapter 2 Drought Planning in the United States : Status and Future Directions Drought Planning in the United States : Status and Future Directions*.
- Wilhite, D. A., Svoboda, M. D., & Hayes, M. J. (2007). Understanding the complex impacts of drought: A key to enhancing drought mitigation and preparedness. *Water Resources Management*, 21(5), 763–774. <https://doi.org/10.1007/s11269-006-9076-5>
- Winsemius, H. C., Schaeffli, B., Montanari, A., & Savenije, H. H. G. (2009). On the calibration of hydrological models in ungauged basins: A framework for integrating hard and soft hydrological information. *Water Resources Research*, 45(1), 12422. <https://doi.org/10.1029/2009WR007706>

- WMO. (2018). Guide to Instruments and Methods of Observation Volume III – Observing systems. In *Guide to instruments and methods of observation: Vol. III* (2018 Editi, Issue 8). World Meteorological Organization. [https://library.wmo.int/index.php?lvl=notice\\_display&id=12407%0Ahttps://library.wmo.int/index.php?lvl=notice\\_display&id=12407#.YkdSz3XMLio](https://library.wmo.int/index.php?lvl=notice_display&id=12407%0Ahttps://library.wmo.int/index.php?lvl=notice_display&id=12407#.YkdSz3XMLio)
- Wong, G., van Lanen, H. A. J., & Torfs, P. J. J. F. (2013). Probabilistic analysis of hydrological drought characteristics using meteorological drought. *Hydrological Sciences Journal*, *58*(2), 253–270. <https://doi.org/10.1080/02626667.2012.753147>
- Wood, E. F., Lettenmaier, D. P., & Zartarian, V. G. (1992). A land-surface hydrology parameterization with subgrid variability for general circulation models. *Journal of Geophysical Research*, *97*(D3), 2717–2728. <https://doi.org/10.1029/91JD01786>
- Wood, E. F., Roundy, J. K., Troy, T. J., Beek, L. P. H. van, Bierkens, M. F. P., Blyth, E., Roo, A. de, Döll, P., Ek, M., Famiglietti, J., Gochis, D., Giesen, N. van de, Houser, P., Jaffé, P. R., Kollet, S., Lehner, B., Lettenmaier, D. P., Peters-Lidard, C., Sivapalan, M., ... Whitehead, P. (2011). Hyperresolution global land surface modeling: Meeting a grand challenge for monitoring Earth's terrestrial water. *Water Resources Research*, *47*(5). <https://doi.org/10.1029/2010WR010090>
- Wood, E. F., Schubert, S. D., Wood, A. W., Peters-Lidard, C. D., Mo, K. C., Mariotti, A., & Pulwarty, R. S. (2015). Prospects for advancing drought understanding, monitoring, and prediction. *Journal of Hydrometeorology*, *16*(4), 1636–1657. <https://doi.org/10.1175/JHM-D-14-0164.1>
- Wood, P. J., Hannah, D. M., & Sadler, J. P. (2008). *Hydroecology and ecohydrology: past, present and future*. John Wiley & Sons.
- Xia, Y., Ek, M. B., Mocko, D., Peters-Lidard, C. D., Sheffield, J., Dong, J., & Wood, E. F. (2014). Uncertainties, Correlations, and Optimal Blends of Drought Indices from the NLDAS Multiple Land Surface Model Ensemble. *Journal of Hydrometeorology*, *15*(4), 1636–1650. <https://doi.org/10.1175/JHM-D-13-058.1>
- Yang, Y., Donohue, R. J., & McVicar, T. R. (2016). Global estimation of effective plant rooting depth: Implications for hydrological modeling. *Water Resources Research*, *52*(10), 8260–8276. <https://doi.org/10.1002/2016WR019392>
- Yevjevich, V. M. (1967). An objective approach to definitions and investigations of continental hydrologic droughts. *Hydrology Papers* *23*, 23, 25. [https://doi.org/10.1016/0022-1694\(69\)90110-3](https://doi.org/10.1016/0022-1694(69)90110-3)
- Yokohata, T., Kinoshita, T., Sakurai, G., Pokhrel, Y., Ito, A., Okada, M., Satoh, Y., Kato, E., Nitta, T., Fujimori, S., Felfelani, F., Masaki, Y., Iizumi, T., Nishimori, M., Hanasaki, N., Takahashi, K., Yamagata, Y., & Emori, S. (2020). MIROC-INTEG-LAND version 1: A global biogeochemical land surface model with human water management, crop growth, and land-use change. *Geoscientific Model Development*, *13*(10), 4713–4747. <https://doi.org/10.5194/gmd-13-4713-2020>
- York, J. P., Person, M., Gutowski, W. J., & Winter, T. C. (2002). Putting aquifers into atmospheric simulation models: An example from the Mill Creek Watershed, Northeastern Kansas. *Advances in Water Resources*, *25*(2), 221–238. [https://doi.org/10.1016/S0309-1708\(01\)00021-5](https://doi.org/10.1016/S0309-1708(01)00021-5)

- Yue, C., Ciais, P., Luyssaert, S., Li, W., McGrath, M. J., Chang, J., & Peng, S. (2018). Representing anthropogenic gross land use change, wood harvest, and forest age dynamics in a global vegetation model ORCHIDEE-MICT v8.4.2. *Geoscientific Model Development*, *11*(1), 409–428. <https://doi.org/10.5194/gmd-11-409-2018>
- Zabaleta, A., Beguería, S., Antigüedad, I., Lambán, J., Hakoun, V., Jung, M., Le Cointe, P., Caballero, Y., & POCTEFA-PIRAGUA, T. (2022). *PIRAGUA\_indicators [Dataset]*. CSIC - Estación Experimental de Aula Dei (EEAD). <https://doi.org/10.20350/digitalCSIC/14658>
- Zargar, A., Sadiq, R., Naser, B., & Khan, F. I. (2011). A review of drought indices. *Environmental Reviews*, *19*(NA), 333–349. <https://doi.org/10.1139/a11-013>
- Zhang, L., Dawes, W. R., & Walker, G. R. (2001). Response of mean annual evapotranspiration to vegetation changes at catchment scale. *Water Resources Research*, *37*(3), 701–708. <https://doi.org/10.1029/2000WR900325>
- Zhang, X., Hao, Z., Singh, V. P., Zhang, Y., Feng, S., Xu, Y., & Hao, F. (2022). Drought propagation under global warming: Characteristics, approaches, processes, and controlling factors. *Science of the Total Environment*, *838*(19), 156021. <https://doi.org/10.1016/j.scitotenv.2022.156021>
- Zhao, T., & Dai, A. (2015). The magnitude and causes of global drought changes in the twenty-first century under a low-moderate emissions scenario. *Journal of Climate*, *28*(11), 4490–4512. <https://doi.org/10.1175/JCLI-D-14-00363.1>
- Zolina, O., Simmer, C., Kapala, A., Shabanov, P., Becker, P., Mächel, H., Gulev, S., & Groisman, P. (2014). Precipitation Variability and Extremes in Central Europe: New View from STAMMEX Results. *Bulletin of the American Meteorological Society*, *95*(7), 995–1002. <https://doi.org/10.1175/BAMS-D-12-00134.1>
- Zou, X., Zhai, P., & Zhang, Q. (2005). Variations in droughts over China: 1951-2003. *Geophysical Research Letters*, *32*(4), 1–4. <https://doi.org/10.1029/2004GL021853>



---

## List of figures

Figure 2-1 Diagram of the water cycle considering human components.....	6
Figure 2-2 Schematic representation of drought categories and their development (Van Loon, 2015). .....	7
Figure 2-3 Schematic representation of natural and human-induced drivers and their corresponding interactions (AghaKouchak et al., 2021). .....	9
Figure 2-4 Drought duration from historical observations (E-OBS) during the period 1960–2014 and with RCP 2.6, 6.0, and 8.5 for three periods: near future (2010–2030), mid-century (2031–2060), and end of the century (2061–2090) for the Mediterranean region (Tramblay et al., 2020). .....	12
Figure 2-5 Chronological overview of the development of land surface models (Fisher & Koven, 2020). .....	18
Figure 2-6 Schematic representation of the LSMs’ components and their exchanges between them (Blyth et al., 2021). .....	19
Figure 2-7 Schematic illustrating the interconnections and impact pathways between human land-water management practices and the simulated land-atmosphere-ocean processes within Earth System Models (Pokhrel et al., 2016). .....	26
Figure 2-8 Schematic representation of exchange between water and main human systems (Blyth et al., 2021). .....	27
Figure 3-1 Location of the study area and domain used for simulations. ....	30
Figure 3-2. Location of the CAyC and the two reservoirs that supply this irrigated area.....	32
Figure 3-3 Location of the selected rain gauge stations, in yellow circles; the streamflow stations, in red; stations in black circles are defined as near-natural. The river network is depicted in blue. ....	34
Figure 3-4 Selected outlet gauging stations of near-natural basins. ....	36
Figure 3-5 SURFEX (Surface Externalisée, in French) modelling platform (source: <a href="http://www.umr-cnrm.fr/surfex/">http://www.umr-cnrm.fr/surfex/</a> ). .....	40

---

Figure 3-6 Overview of the new irrigation algorithm illustrating the sequential steps involved in its implementation (Druel et al., 2022). .....	41
Figure 4-1 Pathway used to improve the hydrologic modeling. ....	44
Figure 4-2 Schematic representation of Perkins Skill Score. ....	48
Figure 5-1 Flow chart of the methodology proposed to correct the hourly precipitation distribution and evaluate the hydrological response. ....	53
Figure 5-2 Comparison of frequency from different precipitation intensities for observed data in gray (saih), precipitation simulated by SAFRAN in red (sfrn), and corrected precipitation (7 days) in blue (corrected). The horizontal line in each box represents the median, top and bottom box edges represent the interquartile range. ....	56
Figure 5-3 Time series comparison for the Tortosa-Ebro station (only the last 3 years for better visualization). ....	57
Figure 5-4 Relative frequencies of precipitation for observations (in black), SAFRAN (in red), CNRM-ALADIN (in gray), and correction (in blue) from different correction windows. Probabilities are computed for the period (2005 - 2014) hourly precipitation to the Ebro-Tortosa station. PSS number corresponds to Perkins Skill Score for corrected precipitation. The vertical dotted line represents the 99 <sup>th</sup> percentile of the observation. ....	58
Figure 5-5 Same as Figure 5-4 but only for the 7 days correction for each station. ....	60
Figure 5-6 Composite of the 6 highest hourly events in the Ebro-Tortosa station. Mean precipitation is plotted in gray bars (the improved precipitation) and red bars (SAFRAN's precipitation). Solid lines represent the mean variables (accumulated) from the new simulation. The dashed lines represent the variables of the default simulation. In blue, the runoff; in green, the evaporation and in black the drainage. ....	62
Figure 5-7 Same as Figure 5-6 but for each selected station. ....	63
Figure 5-8 Relative frequencies of water balance variables (runoff, drainage, evapotranspiration) for the Ebro-Tortosa station. Solid lines represent the simulation driven by corrected precipitation; dashed lines correspond to the default simulation (SAFRAN). Frequencies are computed with the hourly simulation for the last 3 years (2011-2014) ....	64
Figure 5-9 Same as figure 5-7 for each station. ....	65
Figure 5-10. Comparison of different hourly percentiles (R=runoff, D=drainage, and E=evaporation) for simulation driven by SAFRAN (default, light colors) and by improved precipitation forcing (improved, darker colors). The horizontal line in each box represents the median, and the box represents the interquartile range. The whiskers extend a maximum of 1.5 times the interquartile range. ....	66
Figure 6-1 Accumulated distribution of the KGE from the different simulations varying the <i>runoff b</i> parameter. The left panel shows the KGE calculated on discharges and the right panel shows the KGE calculated on root-square transformed discharges. ....	73

- Figure 6-2 Accumulated distribution of KGE scores. The dashed line represents the default simulation and the solid line represents the IDPR terciles simulation. .... 74
- Figure 6-3 Histograms of the KGE values on the selected station. The left panel shows the default simulation (PIR1) and the right panel shows the simulation using improved soil information (PIR1ESDACGDRD) ..... 75
- Figure 6-4 General framework used in this analysis. The left panel show steps used during the local calibration and the right panel detailed the steps of the regionalization approach. .... 78
- Figure 6-5 Diagram of the conceptual reservoir implementation, in the SASER modeling chain. .... 79
- Figure 6-6 Scheme of the main steps of the regionalization approach. For each time that the algorithm is run, the steps (parameter maps and hydrological modeling) are repeated in each iteration for the optimization process..... 82
- Figure 6-7  $KGE(Q^{1/2})$  scores between observed data and the default simulation, for the whole period (1979-2014). Larger circles with a black border indicate stations defined as natural or near-natural. The other stations are considered as influenced..... 84
- Figure 6-8 Comparison of different daily runoff percentiles for observed data (OBS) and simulated streamflow (default simulation in red and simulation with reservoir scheme in blue). The horizontal line in each box represents the median, the box represents the interquartile range. The whiskers extend a maximum of 1.5 times the interquartile range..... 85
- Figure 6-9 Distribution of the 53 catchments used in the local calibration (catchment by catchment). Panels (a) and (c) show each catchment's calibrated values of the  $k$  [-] and  $L_{max}$  [mm] parameters, respectively. Lower panels, (b) and (c), show the histograms of each parameter. .. 86
- Figure 6-10 Accumulated distribution of KGE scores: a) for the calibration period (1979-1997), b) for the validation period (1997-2014), and c) the comparison between KGE obtained in both periods for local calibration..... 87
- Figure 6-11 Daily time series comparison of two stations, for two hydrological years of the calibration (a and b) and validation (c and d) periods, respectively. Observed streamflow (black line), simulated streamflow without reservoir scheme (red line), and simulated streamflow adding a conceptual reservoir (blue line).  $KGE(Q^{1/2})$  is calculated over each complete period (1979-1997 to calibration and 1997-2014 to validation, respectively). .... 88
- Figure 6-12 Evolution of performance metric (median  $KGE(Q^{1/2})$  and  $KGE_B$ ) in each iteration for one experiment ..... 89
- Figure 6-13 Boxplot of KGE scores for the validation period using the local calibration (adding conceptual reservoir), the regionalization (cross-validation), and default simulation (without conceptual reservoir)..... 89
- Figure 6-14 Box plot of KGE for streamflow of the local calibration, using the genetic algorithm (run 01 to 08), the median of simulated streamflow (median runs), the median of eight parameter



maps (median params), and simulation using fixed parameter values over the full domain. Streamflow validation period from 1997 to 2014. ....	90
Figure 6-15 Comparison of the observed (black line), simulated by SASER without adding the reservoir (red dashed line), and the median values of the eight simulations (blue line) of daily streamflow for a catchment; shaded area represents the percentile 90th and 5 <sup>th</sup> of the eight simulations. Y-axis is the discharge root square. ....	91
Figure 6-16 a) KGE scores obtained to calculate the streamflow with the routing scheme using the regionalization approach against the observed streamflow. (b) Improvement in KGE after regionalization (difference between Figure 6 4 and Figure 6 13(a)). ....	92
Figure 6-17 Same as Figure 6-10, comparing KGE from local calibration (blue) and KGE by the regionalization (green) against to default simulation (red) for calibration (solid line) and validation (dashed line) period. ....	93
Figure 6-18 Median of the eight maps of the two parameters ( $k$ and $L_{max}$ ) of the reservoir obtained applying the regionalization approach. The map set was obtained by cross-validation. ....	94
Figure 6-19 Comparison of relative bias [%] for low flow indices for the default simulation and for the two approaches. The left panel shows the ratio $Q_{90}/Q_{50}$ and the right panel the QMNA(5). The line in each box represents the median and the box the interquartile range. The whiskers extend a maximum of 1.5 times the interquartile range. ....	95
Figure 6-20 Mean monthly streamflow time series at Tortosa station (main Ebro River) from observations and different models. ....	96
Figure 7-1 Scheme used to implement the reservoir simulation to SASER modeling chain. ....	106
Figure 7-2 Operation scheme of the high-resolution Water Availability and Adaptation Policy Assessment (WAAPA) model (Sordo-Ward et al., 2019). ....	107
Figure 7-3 Schematic representation of the reservoir model as implemented in the area of study. Dams are represented by triangles; inflows and outflows are represented by arrows. Light triangles represent dams not considered in the simulation. ....	109
Figure 7-4 Total irrigation amount simulated by SURFEX for the hydrological year 2013-2014. ....	111
Figure 7-5 Scheme of drought characteristics using the run theory, from (Mishra & Singh, 2010). ....	112
Figure 7-6 Illustration of the threshold level method, with a) constant and seasonally constant threshold, b) monthly-varying threshold, and c) daily-varying threshold (Stahl, 2001). ....	113
Figure 7-7 Panel (a) shows the FDC for each month and (b) the variable threshold level scheme based on the 80 <sup>th</sup> percentile from the FDC. ....	115

Figure 7-8 Irrigation demands estimated by SURFEX for both areas supplied by (a) Barasona and (b) Santa Ana. Gray lines represent each year and the green line represents the mean. The black solid line represents the irrigated demand derived from the CHE data.....	117
Figure 7-9 Performance evaluation results of the reservoir operation scheme. KGE metric for the naturalized scenario and the human-influenced scenarios (S1 to S4). Panel (a) for Barasona and (b) for Santa Ana reservoir.....	118
Figure 7-10 Simulated storage and releases (blue solid lines) for the S1 (observed data as input) scenario for the Barasona reservoir.....	119
Figure 7-11 Same as Figure 7-10 but for Santa Ana reservoir.....	120
Figure 7-12 Time series comparison for Barasona reservoir. ....	122
Figure 7-13. Monthly deficits for precipitation, streamflow, and ET for the Barasona case study. The upper panels represent the natural situation and the lower panels represent the human situation. ....	123
Figure 7-14 Deficits in downstream flow simulated by the reservoir scheme, for the S4 scenario. ....	124
Figure 7-15 Time series comparison for Santa Ana reservoir.....	125
Figure 7-16. Monthly deficits for precipitation, streamflow, and ET for the Santa Ana case study. Upper panels represent the natural situation and lower panels represent the human situation. ....	127
Figure 7-17 Deficits in downstream flow simulated by the reservoir scheme, for the S4 scenario. ....	128
Figure 7-18. Drought boxplot results for natural and human influenced droughts in the (a) Barasona and (b) Santa Ana case studies. The y-axis shows different scales. The horizontal line in each box represents the median, the box represents the interquartile range. The whiskers extend a maximum of 1.5 times the interquartile range.....	130
Figure A 1-1 Scheme of the variable infiltration model at sub-grid runoff. The right panel shows the variation of the saturated proportion of the grid cell to different values of the parameter $b$ . ....	143
Figure A 1-2 Histograms of the KGE calculated on root-squared transformed discharge for the different simulations.....	144
Figure A 1-3 Histogram of the selected stations with KGE values above -0.5, to each B value ....	145

Figure A 1-4 Comparison between the SIMPA (reference) model and the SASER model for the Ebro-Tortosa station.....	146
Figure A 1-5 IDPR table's guide (Mardhel et al., 2021). .....	147
Figure A 1-6 Relationship between the median IPDR value and the <i>runoff</i> <i>b</i> parameter. Each data point represents a catchment selected as near-natural or natural. ....	147
Figure A 1-7 Map of IDPR and the best <i>runoff</i> <i>b</i> parameter for near-natural stations.....	148
Figure A 1-8 (a) IDPR at 25 m (original) spatial resolution over the whole domain, and (b) classification of IDPR terciles used for simulation.....	149
Figure A 1-9 Selected station (natural and near-natural), in black circles, in the initial database of the PIRAGUA project.....	150
Figure A 2-1 Improved soil depth map used in PIR1ESDACGDRD simulation .....	153
Figure A 2-2 Daily time series comparison for two stations, for five hydrological years (to make the plots easy to read). Observed streamflow (dashed black line), simulated streamflow using ESDAC soil database (blue line), and simulated streamflow using default configuration (red line). The $KGE(Q^{1/2})$ is calculated over the complete period (1979-2014).....	154
Figure B 1-1 Example of the determination of reservoir area for different time steps .....	155
Figure B 1-2 Area-Volume curves determined for Barasona and Santa Ana. ....	156
Figure B 2-1 Reservoir simulation results to Barasona case study for S1 scenario. The upper panel shows the input data used in this simulation. Middle panels show the storage and releases ( $Hm^3$ ), respectively. The lower panel depicts the percentage of deficit.....	157
Figure B 2-2 Same as Figure B 2-1 but for the S2 scenario.....	158
Figure B 2-3 Same as Figure B 2-1 but for the S3 scenario.....	159
Figure B 2-4 Same as Figure B 2-1 but for the S4 scenario.....	160
Figure B 2-5 Reservoir simulation results to Santa Ana case study for S1 scenario. The upper panel shows the input data used in this simulation. Middle panels show the storage and releases ( $Hm^3$ ), respectively. The lower panel depicts the percentage of deficit.....	161
Figure B 2-6 Same as Figure B 2-5 but for the S2 scenario.....	162
Figure B 2-7 Same as Figure B 2-5 but for the S3 scenario.....	163
Figure B 2-8 Same as Figure B 2-5 but for the S4 scenario.....	164

Figure B 3-1 Example of some monthly fitted distribution for both variables (streamflow and ET) at different time scales. Blue and green bars represent the natural distribution of streamflow and ET, respectively. Red bars show the shift in these variables due to human influences. .... 166

Figure B 3-2 Standardized drought indices (a) SPI-12 (precipitation), (b) SRI-12 (streamflow), and (c) SEI-12 (evapotranspiration) for the Barasona case study. Blue and Green lines represent the natural situation. Black lines in each respective panel represent the standardized index considering the human influences based on natural data distribution. .... 167



---

## List of tables

Table 2-1 Nature and causes of the different phenomena related to water availability (adapted from Pereira et al., 2002).....	9
Table 3-1. Location of the selected stations .....	34
Table 3-2 Thresholds of short-term scarcity for Barasona reservoir (volume stored in Hm <sup>3</sup> )....	38
Table 3-3 Thresholds of short-term scarcity for Santa Ana, Canelles, and Escales reservoir (cumulative volume stored in Hm <sup>3</sup> ) .....	38
Table 3-4 Monthly environmental flows (in Hm <sup>3</sup> ).....	38
Table 5-1. PSS values for different time-step and each selected station.....	59
Table 5-2. PSS obtained for precipitation amounts above different percentiles for each station. Corresponding percentile values were calculated from the observed data (SAIH) for the whole period. The PSS value of the improved precipitation is indicated in bold in the third column for each percentile.....	61
Table 5-3 Water budget per year over the Ebro basin.....	66
Table 7-1 Monthly distribution of irrigation demands for each irrigated area (Hm <sup>3</sup> ).....	110
Table 7-2 Drought metrics results from naturalized and human-influenced data, respectively.	129
Table 7-3 Percentage change results from naturalized to human-induced data .....	131

---

